Special Publication SJ 90-SP10

TWO- AND THREE-DIMENSIONAL NUMERICAL ANALYSIS OF THE EFFECTS OF GROUNDWATER DEVELOPMENT IN THE GENEVA AREA, SEMINOLE COUNTY, FLORIDA: FINAL REPORT

Prepared for

St. Johns River Water Management District
Palatka, Florida

by

Sorab Panday, Peter S. Huyakorn
and John B. Robertson

HydroGeoLogic, Inc.
Herndon, Virginia

September 28, 1990

ACKNOWLEDGEMENTS

The authors wish to acknowledge the contributions of Scott Randall, Debra Johnston and Sue Heinrich and thank them for their participation in this project.

TABLE OF CONTENTS

LIST OF FIGURES

LIST OF TABLES

1. EXECUTIVE SUMMARY

The St. Johns River Water Management District (The District) contracted HydroGeoLogic Inc. to conduct a modeling study of the Geneva freshwater lens system in the upper Floridan aquifer, Seminole County, Florida. The objectives were to adopt and calibrate a two-dimensional cross-sectional, and a three-dimensional density-dependent model for simulating groundwater flow and chloride transport in the system.

The Geneva freshwater lens consists of an isolated lens of freshwater surrounded on all sides and the bottom by brackish water. The lens, which is about 22 mi^2 in area, exists because of a unique set of hydrogeologic and recharge conditions which occur in the area. The lens is within the upper Floridan aquifer. A zone of relative high recharge associated with a topographically high area and a more permeable zone in the Miocene aquitard units overlying the Floridan aquifer provides the recharge neccessary to maintain the lens.

The key issue of concern is how much additional pumping can be allowed at various areas of the lens without adversely impacting water quality by inducing the invasion or upconing of salty water. Also of interest are the potential impacts of recharge decreases caused by climatic changes or other influences.

The finite-element DSTRAM numerical code was selected for cross-sectional and the fully three-dimensional modeling. A cross-section oriented along the north-south axis of the lens, parallel

to the regional flow pattern in the Floridan aquifer, was selected. Boundary conditions and material properties for model input were selected from numerous sources including previously published data and file data supplied by the District. Key input data included the following:

- The southern upgradient boundary at the Econlockhatchee River was assigned a constant fluid influx and chloride concentration.
- The northern discharge boundary near the St. Johns River was defined as a no flux boundary since a hydraulic divide in the aquifer is observed there.
- The lateral boundaries along Lake Jessup and Lake Harney were assigned no-flux conditions because they lie approximately parallel to the ambient flow direction.
- A 450 ft zone of the Floridan aquifer was modeled as a confined system with prescribed recharge rates over the central recharge zone of the lens and with discharge zones on the periphery.
- The bottom boundary was treated as a prescribed head and prescribed salt concentration boundary. Simulations under various assumed conditions were made in which the lens size and shape and associated

chloride distributions were allowed to equilibrate or respond to imposed conditions.

A series of steady-state calibration simulations were followed by steady-state sensitivity runs. Finally, the calibrated model was used to explore a variety of transient scenarios in which recharge rates were decreased and pumping rates were increased. This procedure was followed for both two-dimensional cross-sectional, and the fully three-dimensional analyses of the Geneva lens system.

The most significant results and conclusions are the following:

1. The DSTRAM code performed well for this application.
2. Steady-state verification simulations produced good match with field data regarding lens width and depth.
3. The three-dimensional simulations required re-calibrating the material parameters because the effects of the third dimension (which were neglected in the two-dimensional cross-sectional scenarios) are significant. The steady-state three-dimensional lens obtained using the 2-D simulation material parameters was unrealistically small.
4. The lens is stable under current recharge and pumping conditions and could probably sustain

considerably more pumping without adverse impact.

5. Simulations assuming zero recharge over large time periods indicate that the lens would degrade over a period of 100 years or more. Short-term decreases in recharge are therefore an insignificant factor in transient behavior of the lens, provided the average recharge rates are maintained over long time periods. Hydraulic head distributions, however, respond much more rapidly and reach equilibrium within days. The two-dimensional cross-sectional simulations produced a lens which sustained itself for much longer periods of no recharge than the three-dimensional simulations. This was due to the different discharge rates in the two models, and the effects of the transverse flow direction on the lens.
6. Impacts of increased future pumping effects were somewhat sensitive to the position and distribution of pumping wells. Spacing wells over a larger area appears to be better than concentrating pumping in one central location.
7. The lens is moderately sensitive to a number of other variables or uncertain factors such as discharge rates at the northern end,

chloride concentrations at the southern boundary, and transverse dispersivity.

8. Two-dimensional cross-sectional modeling cannot be used for quantitative predictions of the actual dynamic behavior of the lens under field conditions, due to three-dimensional flow and geometrical considerations. However, the two-dimensional model is an effective screening tool for conceptual model refinement, sensitivity analyses, development of efficient finite element nodal grid designs, initial conditions for other two-and three-dimensional simulations and for a quick qualitative analysis of various scenarios of interest.

9. Fully three-dimensional modeling of the Geneva lens is essential for any quantitative assessment of the behavior of the groundwater system and its response to various impulses. The three-dimensional model developed herein is a tool which the District can effectively utilize in planning and managing appropriate water development approaches for the Geneva area.

Additional data needs which could help reduce uncertainty and strengthen confidence in predictive model simulations include the following:

- Better definition of vertical chloride and head distributions is needed over the area underlying and surrounding the lens. The lack of sufficient field data on vertical head distribution leads to large limitations and uncertainty in the calibration of the model flow parameters. However, this constraint does not have a major impact on simulated chloride distribution patterns because of their slow response to head changes. On the other hand, the scarcity of field data on vertical chloride distributions does impose a significant uncertainty in the accuracy of the chloride transport calibration.
- Additional head data in the deeper portions of the lens are needed to confirm Phelps and Rohrer's (1987) estimates of horizontal head gradients and further confirm that approximately the same gradients may be assumed to occur at the bottom of the modeled region.
- More definitive data on discharge rates and patterns along the northern portion and the

Lake Jessup and Lake Harney sides of the lens is necessary. The lens was not very sensitive however, to discharges near the Econlockhatchee River.

- It might be useful to conduct additional sensitivity analysis of anisotropy in hydraulic conductivity of the Floridan aquifer under high pumping conditions and varying leakance factors that control recharge through the Miocene aquitard units.

water (water containing more than 250 mg/l chloride) into the production zones of the lens.

A three-dimensional model is needed by the District in which boundary conditions can be varied or adjusted and pumping stresses can be varied in time and by location. The model should be capable of simulating groundwater flow and solute transport, including the effects of variable density, under various imposed steady-state and transient conditions. The intended uses of the model include determining cause and effect relationships between groundwater withdrawals and chloride invasions, and categorizing areas according to potential water development suitability. After completion of the model, an additional objective will be to train District personnel to use the model independently for simulating various situations of interest.

The objective of Phase 1 of the study was to construct and calibrate a two-dimensional cross-sectional model to simulate the approximate flow and transport of the freshwater lens and the diffuse salinity zone surrounding it under steady-state and transient conditions. This task also included sensitivity and transient test simulations. This was intended as a preliminary step and feasibility assessment for the development of the more complex three dimensional model, which was the objective of Phase 2 in this project.

2.3 GENERAL APPROACH

The general approach used for this study consisted of the following steps:

1. Assemble and review existing data and reports relating to the area and problem, including discussions with District personnel.
2. Develop a conceptual model for flow and transport of the system based on available data and professional judgement.
3. Set up a two-dimensional cross-sectional numerical model to simulate steady-state freshwater/brackish water distribution.
4. Calibrate a cross-sectional model so that simulated chloride concentrations match field data to a reasonably acceptable degree.
5. Use the calibrated cross-sectional model to conduct sensitivity and transient analyses by changing key variables such as recharge rates, pumping rates and locations, and anisotropic hydraulic conductivities.
6. Based on results of Phase 1, assess feasibility, limitations, and potential usefulness of a fully three-dimensional, variable-density flow and transport model.
7. Prepare a report describing the model and results of Phase 1.

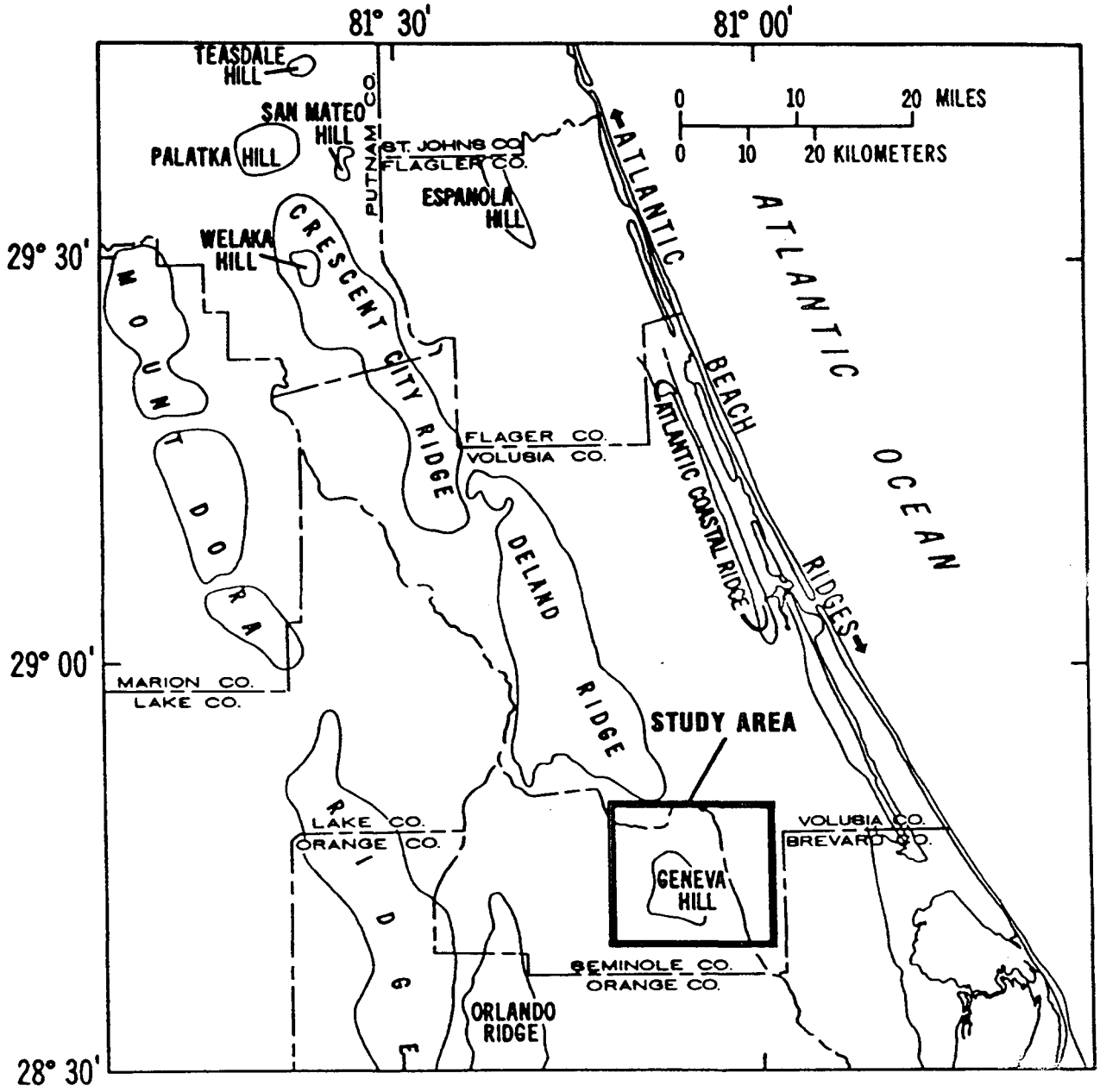

Figure 2.1. Physiographic map of part of central Florida (from Phelps and Rohrer, 1987, p.7).

of the interrelated processes and properties controlling the system, a numerical modeling approach is the only feasible method of assessing effects of various groundwater development scenarios on the system.

The study area consists of about 70 mi^2 in northeast Seminole County as shown in Figure 2.1 (Phelps and Rohrer, 1987). A map showing a typical areal extent of the lens, based on the pattern of chloride content in groundwater, is shown in Figure 2.2. The position and shape of the lens is controlled in part by an isolated zone of relatively high-elevation land where recharge rates are much greater than in surrounding areas of lower elevations (Phelps and Rohrer, 1987).

HydroGeoLogic, Inc., of Herndon, Virginia, was contracted by St. Johns River Water Management District (The District) of Palatka, Florida to develop a numerical modeling method for assessing the development potential of the Geneva freshwater lens and the potential impact from saltwater encroachment and upconing that might result from additional pumping.

2.2 STUDY OBJECTIVES

The overall principal objective of this study is to develop a numerical model which the St. Johns River Water Management District staff can use to evaluate potential water quantity and quality impacts due to current and future consumptive withdrawals of freshwater from the Geneva lens. Of primary interest is the potential lateral flow and vertical upconing of brackish

2. INTRODUCTION

2.1 BACKGROUND AND NATURE OF THE PROBLEM

The northeast part of Seminole County, Florida, in the vicinity of the City of Geneva, is underlain by a lens of fresh groundwater in the Floridan aquifer which overlies and is surrounded by brackish or saline water. This freshwater lens serves as the water supply for Geneva and other nearby communities and households. There is considerable interest in additional development of this water resource to serve the expanding needs of Geneva and its surrounding area, and to protect the water wells in adjacent areas which have a limited amount of fresh groundwater available.

Because of the limited size and recharge rate of the freshwater lens, combined with the rather delicate equilibrium between the freshwater and the brackish water surrounding it, excessive freshwater withdrawal could induce the invasion of brackish water into freshwater production wells. It is therefore necessary to develop some quantitative understanding of three-dimensional dynamics of this freshwater/saltwater system to provide a basis for sound development strategies and decisions.

Although considerable information and understanding has been developed on the geometry, hydrogeology, hydraulic head, and water quality of this system, additional work is needed in order to predict dynamic responses of the system to various hydraulic stress scenarios. Because of the dimensional and parametric complexities

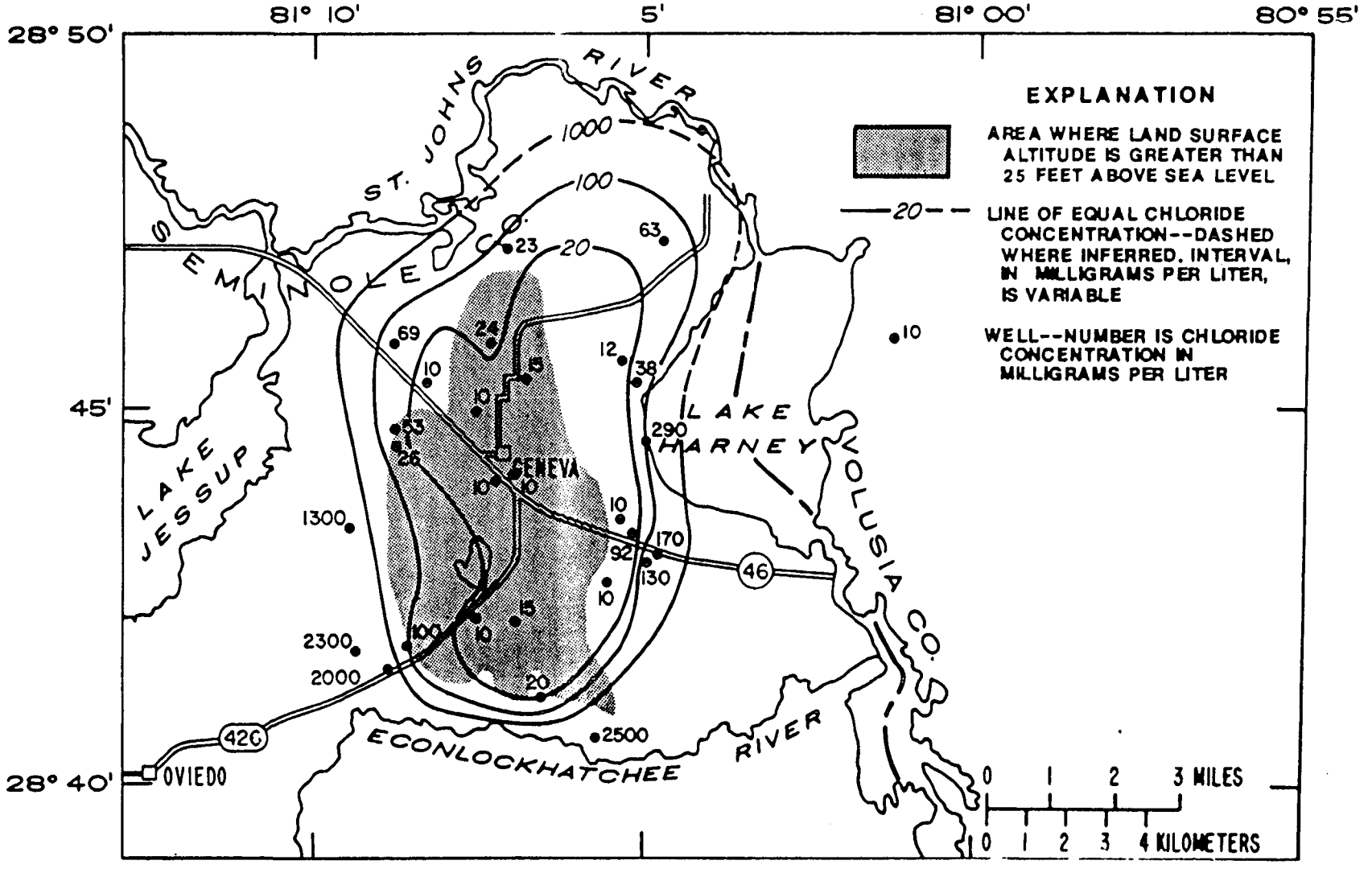

Figure 2.2 Chloride concentration of water from the upper part of the system, October 1982, wet conditions (from Phelps and Rohrer, 1987, p.49).

8. Review existing data and reports pertaining to the three-dimensional model, including discussions with District personnel.
9. Develop a three-dimensional conceptual model of the system based on available data and professional judgement.
10. Set up and calibrate a three-dimensional steady-state model to simulate chloride concentrations that match field data.
11. Use the calibrated model to conduct transient analyses of various scenarios of interest.
12. Prepare a report of entire modeling effort.

2.4 PREVIOUS STUDIES

Florida has established an early and prominent reputation as a leader in developing quantitative data for analyses of its groundwater resources. Consequently, there is an abundance of published technical reports and long-term data records on many aspects of Florida hydrogeology and water resources. The relatively small area of northeast Seminole County which is the subject of this study is no exception. The limited availability of fresh (non-brackish) groundwater or surface water in the study area, together with increasing water demands, has prompted several important previous studies which have contributed to a substantial data base and conceptual understanding of the freshwater lens in

the Geneva area. Some of the most significant and useful studies include the following.

There are some important published groundwater and hydrogeology studies in the Seminole County area as early as 1913. (Matson and Sanford, 1913, and Sellards and Gunter, 1913). Stubbs conducted one of the earliest and more comprehensive regional groundwater studies in the area (Stubbs, 1937). He described potentiometric head distribution and changes in head since 1913, zones of artesian pressure, chloride distributions, general relationships between freshwater and saltwater, water uses, numbers and locations of wells, aquifer properties and geology. Barraclough (1962) conducted a more extensive and comprehensive assessment of groundwater resources in Seminole County. He clearly identified the oval-shaped freshwater lens in the Geneva area and related it to recharge, piezometric head distributions and land surface elevations in the area. He also provided a detailed geological and stratigraphic description of Eocene units comprising the upper Floridan aquifer, the aquitard units overlying the Floridan aquifer and the surficial aquifer units. Barraclough's studies included quantitative assessments of aquifer hydraulic properties.

Another important study was published in 1977 by the U.S. Geological Survey (Tibbals, 1977). That study was focused on the greatly increasing water demands due to a rapid population growth in Seminole County. The report provides an assessment of the water resources currently available and potential impacts on water

quantity and quality caused by increasing ground-water withdrawals. Tibbals pointed out that groundwater in the Geneva freshwater lens should be developed cautiously because of the potential for brackish water intrusion due to lowered piezometric head. That report includes many useful maps and illustrations pertaining to groundwater conditions in Geneva and the surrounding areas. In an earlier study, Tibbals (1975) describes areas of the Floridan aquifer in Seminole County.

One of the most important and definitive studies on the area was a recent cooperative effort by the St. Johns River Water Management District and the U.S. Geological Survey (Phelps and Rohrer, 1987). That study was focused specifically on the fresh groundwater lens in the Geneva area and describes geology; hydraulic properties of the aquifer and aquitard units; well data; recharge, discharge, and other components of the water budget; three-dimensional water quality variations; and geochemical mixing. The principal purpose of that study was to delineate the vertical and lateral extent of the freshwater lens and to evaluate groundwater potentials. They concluded that the freshwater lens is the result of local rainfall and recharge flushing out preexisting sea water from the Floridan aquifer system. Data from that study indicate that the maximum thickness of the freshwater lens is approximately 250 to 300 ft near the center. Phelps and Rohrer (1987) estimated that annual recharge to the lens ranges from 5 inches to 13 inches for a two year period studied and averaged 11 inches per year over a 30 year period. They concluded that if

natural groundwater outflow from the lens (not including pumpage withdrawals) is reduced to less than 10 inches per year, deterioration of the water quality will eventually occur.

Although present groundwater withdrawals from the lens are less than five percent of recharge, increase in groundwater development could cause a reduction in natural outflow to less than 10 inches per year and a potential for deteriorative groundwater quality. The Phelps and Rohrer study serves as the principal foundation on which the modeling analysis described in this report is based. The data in their report is the principal source used to formulate the conceptual model, along with initial conditions, boundary conditions and material properties of the model.

Another recent and significant study was that by Skipp (1988) which involves a regional numerical groundwater flow model of a large area including Brevard, Indian River, Orange, Osceola, and Seminole Counties. Skipp's results indicate that the hydraulic response of the Floridan aquifer system is sensitive to uncertainties in irrigation well withdrawal rates and storage in confining layers. Although that model did not consider water quality and density effects, it provided useful information on water budget, material hydraulic properties, and sensitivity analyses.

Another important modeling study was conducted by Planert and Aucott (1985). Although their study area did not include Seminole County, it provides considerable insight into regional hydrogeologic conditions immediately south of the Geneva study

area. That information has proven useful in establishing the conceptual model and southern boundary conditions for the Geneva area modeling.

2.5 DESCRIPTION OF NUMERICAL CODE, DSTRAM

2.5.1 General

The numerical code selected for modeling the Geneva freshwater lens system is DSTRAM (Density-dependent Flow and Solute Transport Analysis Model). DSTRAM is a three-dimensional finite element code that simulates density-dependent, single-phase fluid flow and solute transport in saturated porous media. The code is designed to deal specifically with a complex situation where the flow of fluid (groundwater) is influenced significantly by variations in solute concentration. DSTRAM can perform steady-state and transient simulations in a cross-section, an axisymmetric configuration, or a fully three-dimensional mode. A wide range of boundary conditions can be accommodated including those involving water table conditions, infiltration, aquitard leakages, and pumping and injection wells. For contaminant transport simulation, DSTRAM can account for advection, hydrodynamic dispersion, linear equilibrium sorption, and first-order degradation.

DSTRAM was developed by HydroGeoLogic, Inc. and is based on an earlier code, SWICHA (Huyakorn et al., 1986). The DSTRAM code was selected for this study because of the following reasons:

- The code has been documented and successfully applied to problems of similar complexity. It has been verified against problems with known solutions.
- DSTRAM employs the most advanced finite element and matrix computation techniques available. The code has robust (Preconditioned Conjugate Gradient and ORTHOMIN) matrix solvers unavailable in other standard codes which made it more efficient and versatile.
- The DSTRAM code can easily be applied in a variety of configurations (i.e., areal two-dimensional, cross-sectional, axisymmetric, and fully three-dimensional regions). The code was specifically designed to analyze problems of lateral sea-water intrusion and/or upconing in complex hydrogeologic settings.

2.5.2 Method of Analysis and Simulation Options

The finite element method is used to approximate the governing equations of flow and transport. A sequential solution strategy is used to handle coupled flow and transport problems. Spatial discretization is performed using brick elements with Cartesian or orthogonal curvilinear coordinate geometry. Such elements are simple to deal with and their matrices can be readily computed using efficient influence-coefficient formulas. Nonlinearity resulting from density differences is handled via a Picard algorithm. An upstream-weighting procedure is used when needed to circumvent numerical oscillations. Matrix equations are solved

using Preconditioned Conjugate Gradient (PCG) and ORTHOMIN accelerated iterative techniques. The PCG and ORTHOMIN matrix solvers are not subject to convergence difficulties like Slice Successive Relaxation (SSR) and Line Successive Relaxation (LSR) methods and can outperform SSR and LSR by as much as an order of magnitude for typical field-scale problems.

Several types of analyses can be performed. These include groundwater flow analysis, trace concentration solute transport analysis, and density-dependent coupled flow and solute transport analysis. The groundwater flow and the transport equations can be solved independently or concurrently. Velocity output from groundwater flow simulations is in the form required for input into transport analyses.

DSTRAM has a capability to perform automatic generation of a rectangular mesh for a regular geometry. For a three-dimensional problem, the region may be discretized using either a vertical slicing approach or a horizontal layering approach. Although the code is designed for three-dimensional Cartesian or orthogonal curvilinear coordinate systems, for many applications a simpler, two-dimensional or axisymmetric cylindrical coordinate system is sufficient. An axisymmetric analysis is readily accomplished in a simple manner by revolving the chosen slice about its axis of revolution. For areal problems, one horizontal slice is specified and gravity is set to zero.

2.5.3 Material Properties and Boundary Conditions

Heterogeneous and anisotropic properties are readily handled by DSTRAM in the flow and transport analyses. Layering, lateral discontinuities, and heterogeneities in material properties can be accommodated in a simple manner. When a rectangular grid is used, the code allows the user to obtain a stepped approximation of irregular boundaries and lateral discontinuities by blocking out certain unwanted elements. For a transport analysis, a velocity dependent dispersion tensor, as well as sorption and decay are permitted. The velocity field may be steady or transient.

Boundary conditions for the flow equation include prescribed nodal values of the equivalent fresh-water (reference) hydraulic head or prescribed integrated nodal values of fluid volumetric fluxes. Head-dependent fluxes due to induced infiltration and vertical leakage through an aquitard overlain by a surficial aquifer can also be accommodated. Boundary conditions for the solute transport equation include prescribed nodal values of concentrations, and solute mass fluxes. Transient boundary conditions can be readily accommodated by using a continuous or discontinuous (stepped) representation of the boundary value versus time.

2.5.4 Input Data and Simulation Output

Input organization for DSTRAM is similar to that of its predecessor, SWICHA. An input file for DSTRAM can be prepared using the input guide in the DSTRAM code documentation.

Outputs of flow analyses are nodal values of the reference (or equivalent fresh-water) hydraulic head. If required, Darcy velocities and flow rates can also be obtained. A print-option that provides relationships of simulated head versus time is also available for certain specified nodes. Outputs of the solute transport analysis are nodal values of concentration. For certain specified nodes, the relationships of concentration versus time are also printed. Information on volumetric fluid and solute mass fluxes can also be printed if desired. Back-up data files that may be used for restarting the simulation or plotting numerical results can also be created. These files can be readily interfaced with plotting packages such as Surfer, Grapher, Disspla, Contur, Plot88, Plotmatic, and Grafmatic.

3. HYDROGEOLOGIC SETTING

3.1 GEOLOGIC FRAMEWORK

The geologic history, and descriptions of the geologic structure of the stratigraphic units were summarized by Phelps and Rohrer (1987). Details of the regional geology are described by Chen (1965). The principal geologic units of interest are shown in the northeast-southwest cross-section through the Geneva area given in Figure 3.1. The areal location of the cross-section is shown in Figure 3.2.

The stratigraphic units, in descending order, consist of:

1. Surficial post-Miocene (undifferentiated Pliocene to Holocene) unconsolidated sands, sandy clays, and silt and clays, ranging in thickness from 10 to 70 feet.
2. Miocene deposits, 20 to 60 feet thick consisting of the middle Miocene Hawthorn formation or undifferentiated upper Miocene deposits. These deposits are predominantly shell and clayey sand and contain some sandy phosphatic limestone.
3. Limestones of Eocene and Oligocene age extending to a depth of about 1500 feet below sea level. These include the Eocene Ocala Limestone (10 to about 200 ft thick) and the Eocene Avon Park Formation (estimated to be about 1000 to 1400 feet thick; apparently no wells in the study area have penetrated the entire thickness of the Avon

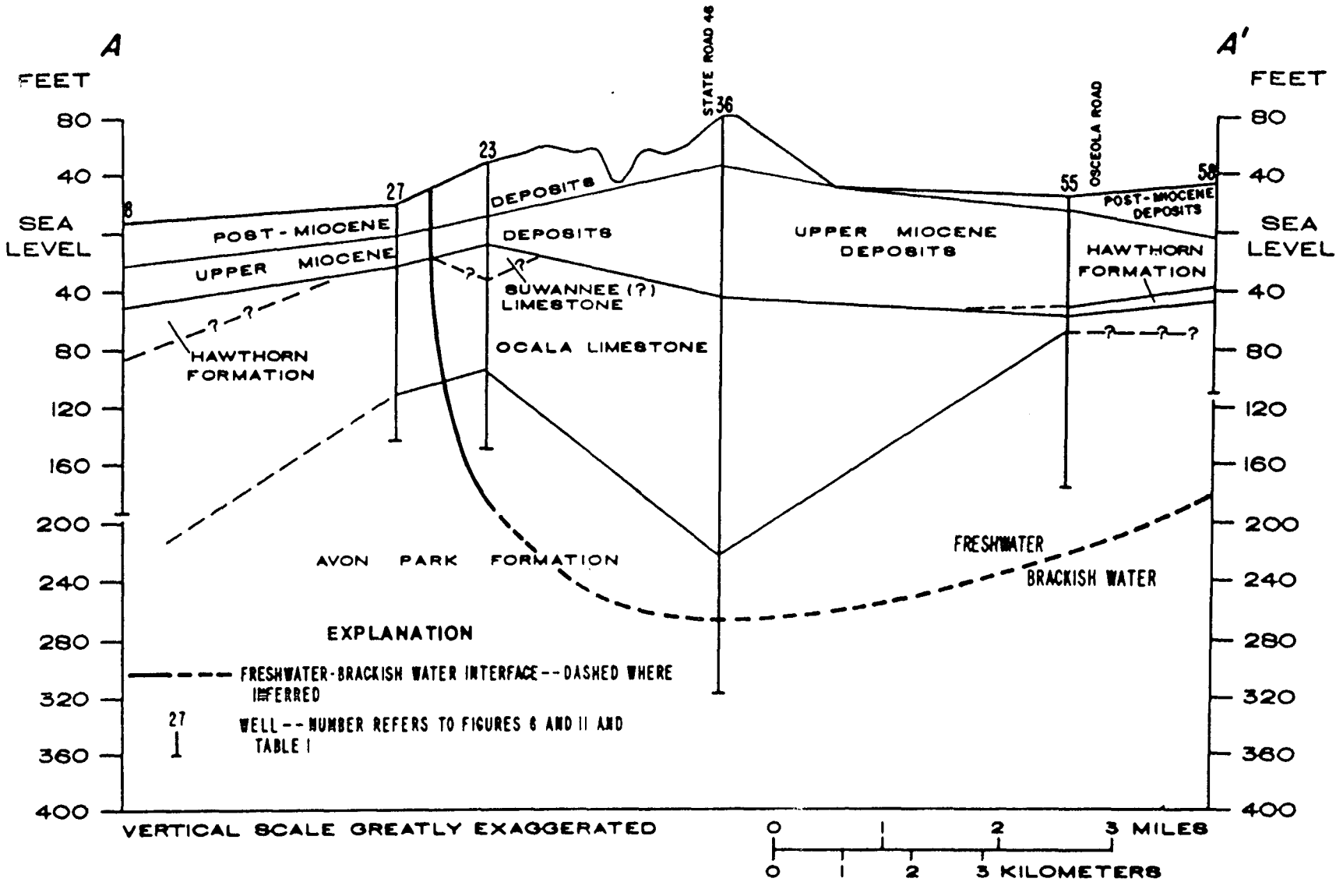

Figure 3.1 Geologic section A-A' and approximate location of freshwater-brackish water interface (from Phelps and Rohrer, 1987, p.36).

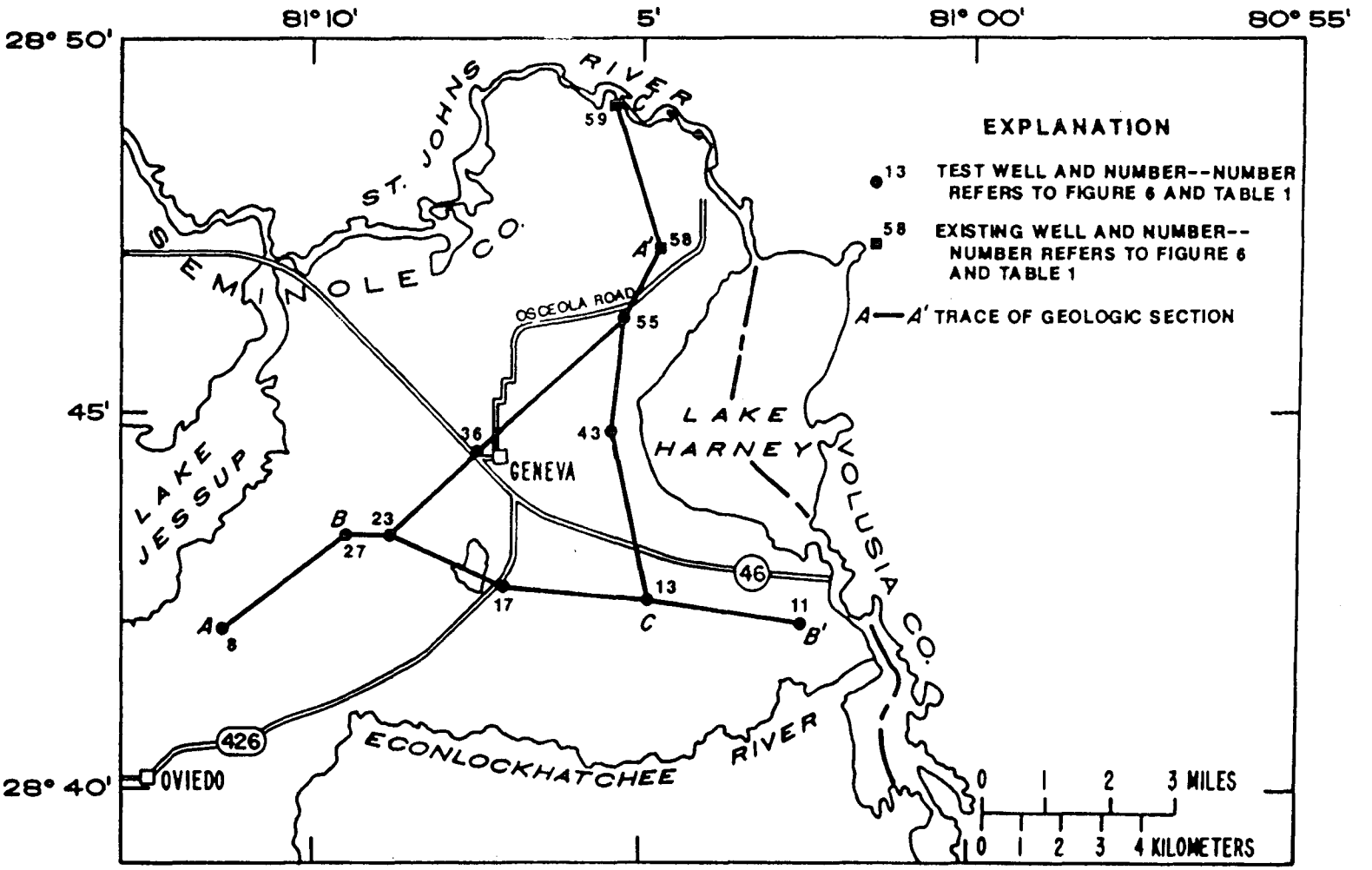

Figure 3.2 Locations of test wells and geologic sections (from Phelps and Rohrer, 1987, p.25).

Park). These units comprise the hydrogeologic unit referred to as the Floridan aquifer.

3.2 HYDROGEOLOGIC CHARACTERISTICS

The uppermost post-Miocene sediments comprise the surficial unconfined aquifer which contains the water table, generally at a depth of 10 to 20 feet below land surface. This is a relatively thin aquifer. In the Geneva area, the surficial aquifer has limited use for domestic water supply and irrigation (Phelps and Rohrer, 1987).

Between the surficial aquifer and the deeper Eocene limestones forming the Floridan aquifer are Miocene sediments which generally act as a confining unit or aquitard. These units are quite variable in thickness and clay content, factors which control their rate of a vertical leakage and confinement effects. The Geneva area is situated on a topographic high where the confining units are sandy clay beds with relatively high vertical permeability which promote vertical recharge to the underlying Floridan aquifer. In the topographically lower areas surrounding the Geneva recharge zone, the Miocene units have thicker clay layers (up to 20 ft) which impede recharge and cause greater confinement of the Floridan aquifer.

The thick permeable Eocene or Oligocene limestones and dolomites (principally the Ocala and Avon Park) form the Floridan aquifer system which is the principal source of water in the Geneva area. The thickness of the Ocala formation may be estimated over

the area of interest, from Figures 4 and 5 of Barraclough (1962) which map the altitude of the top of the Ocala and the Avon Park formations respectively. Furthermore, Figures 13-15 of Phelps and Rohrer (1987) supply a limited amount of recent data and estimates for the Ocala thickness. The regional direction of flow in that area of the State is to the northeast; from the central Florida recharge areas to the principal discharge areas along the St. Johns river.

A unique hydrologic feature occurs in the Geneva area which is superimposed on the regional hydrologic system. This feature is the presence of a localized recharge zone associated with the Geneva topographic high area, and the resulting lens of fresh groundwater which is surrounded by, and floats upon the saline water. The zones of recharge to the upper Floridan aquifer have been mapped by Phelps and Rohrer (Figure 10, 1987), as the area where land surface altitude is greater than 25 ft above sea level. Recharge/discharge zones at the top of the upper Floridan aquifer are also mapped by Tibbals (Figure 3, 1977). The freshwater lens is maintained by the unique combination of hydrogeologic characteristics in the area and the balance of dynamic forces of gravity-driven flowing water and buoyancy effects due to density differences between saline and fresh-water. Other factors which influence this delicate balance are seasonal and climatic variations in recharge and changes in the quantity of water being pumped from the system. The areal pattern of the lens is shown in Figure 2.2 and the approximate vertical shape is shown in Figure

3.1. The lowest point in the base of the freshwater lens is estimated to occur at an elevation of about 270 ft below sea level (about 300 to 350 ft below land surface). According to Tibbals (1977) the configuration of the lens has shown little change since it was first mapped in the early 1950's (Barraclough 1962).

Estimated transmissivities of the upper Floridan aquifer based on model calibration, range from 35,000 ft^2/day to 100,000 ft^2/day for the Geneva area (Tibbals, 1981, Figure 6). A recent pump test conducted by the District (SJRWMD) during construction of monitoring well S-0200 yielded an estimated transmissivity of approximately 14,000 ft^2/day for the uppermost 50 ft of the upper Floridan. This well is located at the Seminole County Landfill near the northern end of the modeled cross-section (near site 58 of Figure 3.2). The probable cause of model-based transmissivities being higher than values based on field tests is that the models used represent the entire thickness of the upper Floridan aquifer, whereas wells used for aquifer tests are open to only a limited portion of the thickness.

Phelps and Rohrer (1987) estimate that as many as 100 wells tap the Floridan aquifer within the Geneva freshwater lens. Because of relatively rapid population growth in the area, numerous new wells are being constructed each year. There are several municipal supply wells and many irrigation wells in the general area.

The potentiometric surface of the Floridan aquifer in the Geneva Area has been mapped (Phelps and Rohrer, 1987) for two different periods. Potentiometric water levels range from about 30

feet above sea level in the southwest to about 10 feet above sea level in the northeast portion of the area (see Figure 3.3). Additional data on the potentiometric surface is supplied by Barraclough (Figures 7 and 8, 1962) and Tibbals (Figures 3 and 7, 1977). Table 3.1 summarizes the available data at the site.

3.3 WATER BUDGET

The configuration and stability of the Geneva freshwater lens is controlled by the hydraulic properties of the hydrogeologic units and the inputs and outputs of water from the system (water budget). Because of the rather delicate balance among dynamic and buoyant forces which support the fresh water lens, relatively small changes in the water balance can eventually lead to large changes in the size and shape of the lens. For example, significant increases in pumping or decreases in recharge can lead to lateral intrusion or vertical upconing of saline water into formerly freshwater zones and can thus render supply wells useless.

In order to assess these potential effects through the use of numerical models (which is the motivating purpose of this study) the most reliable estimate of all key components of the water budget are used as model input. Phelps and Rohrer (1987) provide a water budget analysis which was used as a basis for model input to this study. A summary of their estimate is provided below.

For the upper Floridan aquifer, they used the equation:

$$R_e + GI = P_u + GU_F + \Delta S_F$$

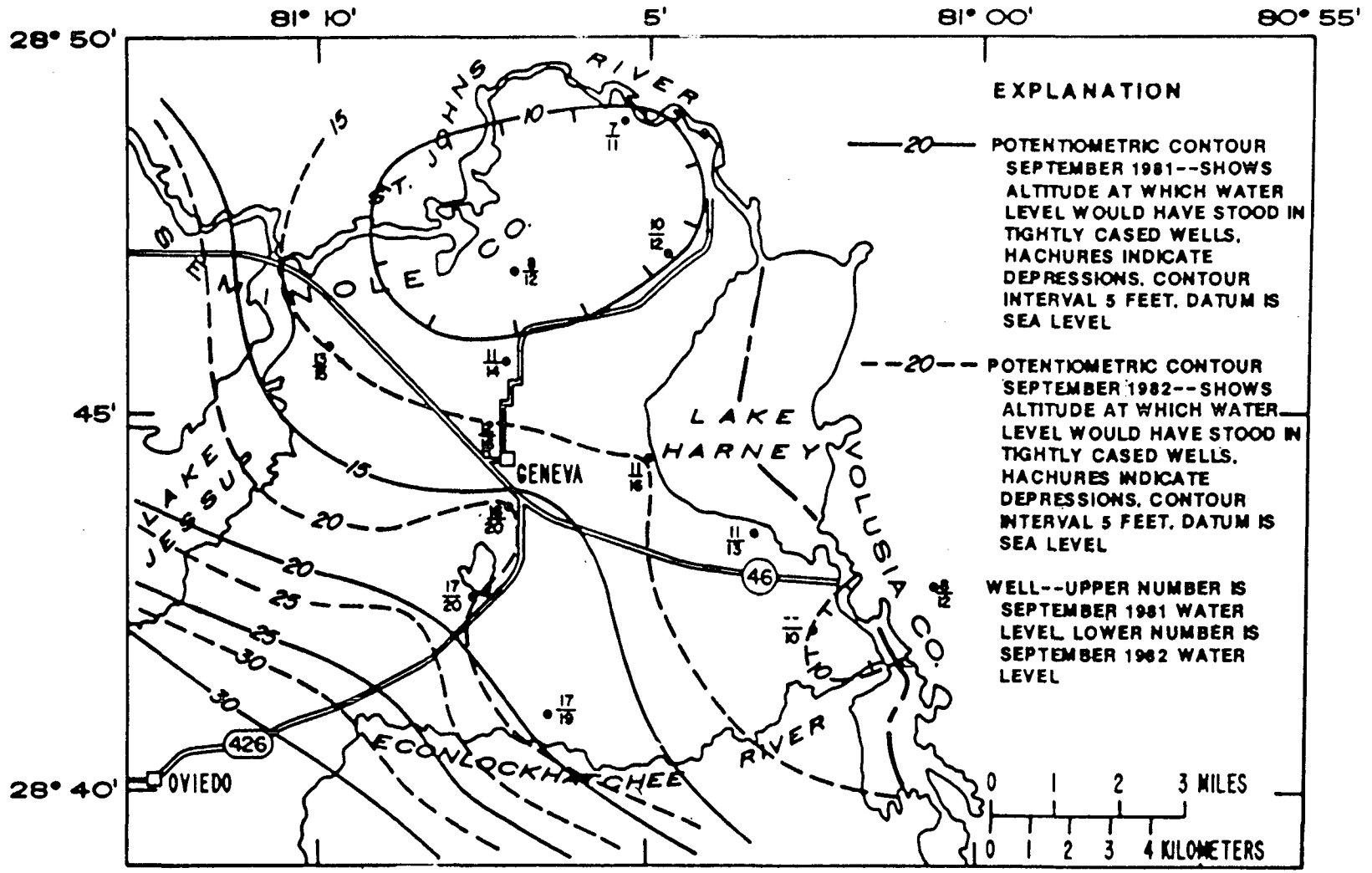

Figure 3.3. Potentiometric surface of the upper part of the Floridan aquifer system, September 1981 and 1982 (from Phelps and Rohrer, 1987, p.23).

TABLE 3.1 SOURCES OF DATA FOR THE UPPER FLORIDAN AQUIFER IN THE GENEVA AREA.

Data	Reference of Data Source
Active recharge zones	Phelps and Rohrer (1987); Figure 1. (Within 25 ft altitude contour) Tibbals (1977); Figure 3.
Discharge zones	Phelps and Rohrer (1987); Figure 1. Tibbals (1977); Figure 3. Barraclough (1962); Figure 9.
Chloride distribution	Phelps and Rohrer (1987); Figures 4, 5, 16 and 17. Tibbals (1977); Figure 11. Barraclough (1962); Figure 36.
Potentiometric surface	Phelps and Rohrer (1987); Figures 9 and 10. Tibbals (1977); Figures 3 and 7. Barraclough (1962); Figures 7 and 8. Several wells sampled by the District. Personal communication.
Material zone thickness and extent	Phelps and Rohrer (1987); Figures 13, 14 and 15. Barraclough (1962); Figures 4 and 5. Personal communication with District personnel.
Material Parameters	Phelps and Rohrer (1987): Storage coefficient, p. 64; Transmissivities, p. 68. Remaining material properties obtained from personal communication and previous modeling efforts at the District by Dave Skipp (unpublished).

3-9

where

R_e = recharge from the surficial aquifer

GI = groundwater inflow

P_u = pumpage

GU_F = groundwater outflow (Floridan)

ΔS_F = change in water stored in the Floridan.

Phelps and Rohrer first calculated the water balance of the surficial aquifer in order to estimate recharge rates to the Floridan aquifer. Key components in the surficial portion of the budget are:

Rainfall:	53.32 inches (30-yr average). In 1981 and 1982 annual precipitation ranged from 41.84 inches to 73.06 inches, respectively.
Evapotranspiration:	estimated at 42 inches per year (30 year average)
Runoff, withdrawals, and changes in storage:	negligible
Water available for recharge to the Floridan aquifer:	10.8 inches (30 yr average)

For the upper Floridan aquifer their water budget estimates include the following results, based on the thirty-year average data for the area within the 25-foot altitude, topographic contour (Figure 2.2, shaded area)

Recharge available : 10.8

Groundwater inflow : 0

Withdrawals : 0.37

Groundwater outflow: 10.4

Change in storage : 0

Based on their budget analysis (which indicates that long-term groundwater outflow from the lens is about 10 inches per year), Phelps and Rohrer concluded that if additional groundwater withdrawals (or reductions in recharge) cause the annual recharge rates (or natural outflow rates) to decline below 10 inches/year over a period of many years, the equilibrium between the freshwater and saltwater will be disturbed. This can potentially cause intrusion or upconing of saltwater into freshwater zones being pumped.

3.4 WATER QUALITY AND FRESHWATER, SALTWATER RELATIONSHIPS

Water samples from numerous wells have been analyzed in several previous studies in order to characterize the groundwater quality of the Floridan aquifer in the Geneva area (Phelps and Rohrer, 1987). Chloride is the most significant constituent of interest in this region. A typical areal distribution of chloride concentration in the upper part of the upper Floridan aquifer in the Geneva area is shown in Figure 2.2. The recommended drinking water limit for chloride is 250 mg/l (ppm). That criterion is frequently used to delineate the bounding surface of the freshwater lens. In the Geneva and surrounding area, chloride concentrations in groundwater range from less than 10 mg/l in the central part of the recharge area to greater than 5000 mg/l in the eastern discharge regions.

As suggested by Figure 3.1, the chloride concentration generally increases with depth. The deepest portion of the fresh water lens with chloride concentrations less than 250 mg/l is about 270 ft below sea level.

Other water quality parameters of interest are iron, sulphate, hydrogen sulfide and hardness. These aspects of groundwater quality are discussed in more detail by Phelps and Rohrer (1987). Chloride distribution is the only significant factor, however, for the purpose of this study.

Phelps and Rohrer also use geochemical data to support their conclusion that the zone of high recharge in the Geneva area is responsible for the existence of the freshwater lens and that recharge has, over recent geologic time, displaced the pre-existing seawater formerly in the aquifer, to form the lens. The recharge water flows in all three directions within the upper Floridan aquifer where it mixes with the brackish water near the fringe of the lens. A schematic representation of this system is shown in Figure 3.4. The seasonal variations of recharge and discharge are averaged, and uniform fluxes are prescribed to the model. Transport of solutes is affected only slightly by averaging the associated flow problem (Duguid and Reeves, 1977). The conceptual models developed from this understanding of the processes occurring beneath the Geneva area are explained in greater detail in Chapters 4 and 7 for the two and three-dimensional approaches, respectively.

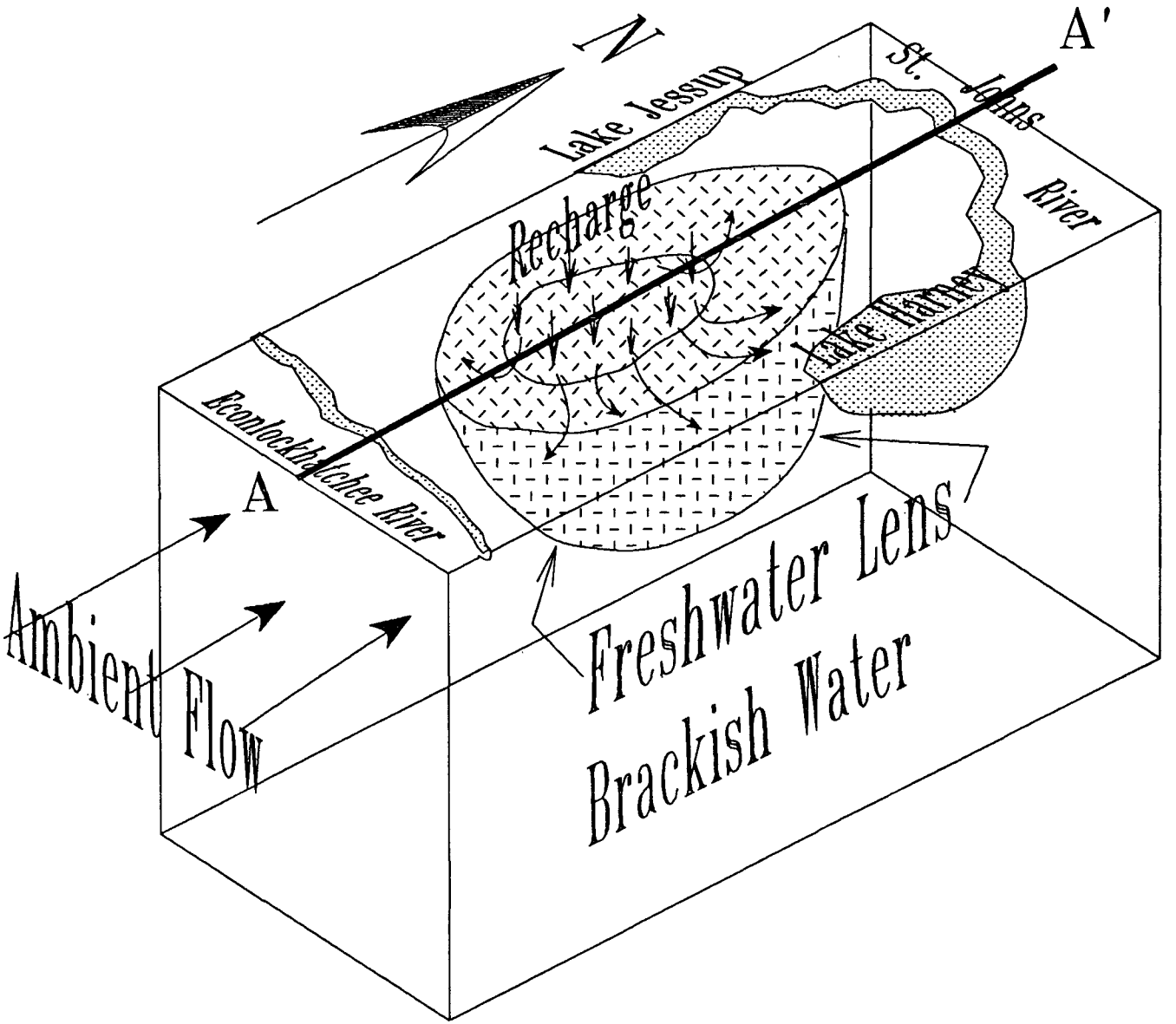

Figure 3.4. Schematic representation of the Geneva freshwater lens.

4. TWO-DIMENSIONAL CROSS-SECTIONAL ANALYSIS

4.1 CROSS-SECTIONAL CONCEPTUAL MODEL

Before proceeding to fully three-dimensional (3-D) modeling, it is useful and desirable to conduct simpler two-dimensional (2-D) simulations. Insight and conclusions developed from the cross-sectional modeling approach can help refine the conceptual model of the system, calibrate key boundary conditions and material properties, identify particular sensitive parameters of the system, determine appropriate responses of the system to a range of imposed stress scenarios, and help optimize the finite element mesh design. Results of the two-dimensional modeling effort further provide general guidelines for a three-dimensional simulation. The cross-sectional modeling analysis thus serves as a preliminary step which facilitates a subsequent three-dimensional modeling analysis.

A number of different orientations of a cross-sectional model are feasible. An appropriate representative cross-section can be selected based on general consideration of three-dimensional geometry, boundary conditions, and groundwater flow patterns determined from previous field investigations.

Based on information provided by Phelps and Rohrer (1987), the selected cross-section was oriented approximately ten degrees clockwise from north-south. This selected orientation, shown in Figure 4.1, is approximately parallel to the general dominant regional groundwater flow direction to the northeast which is a

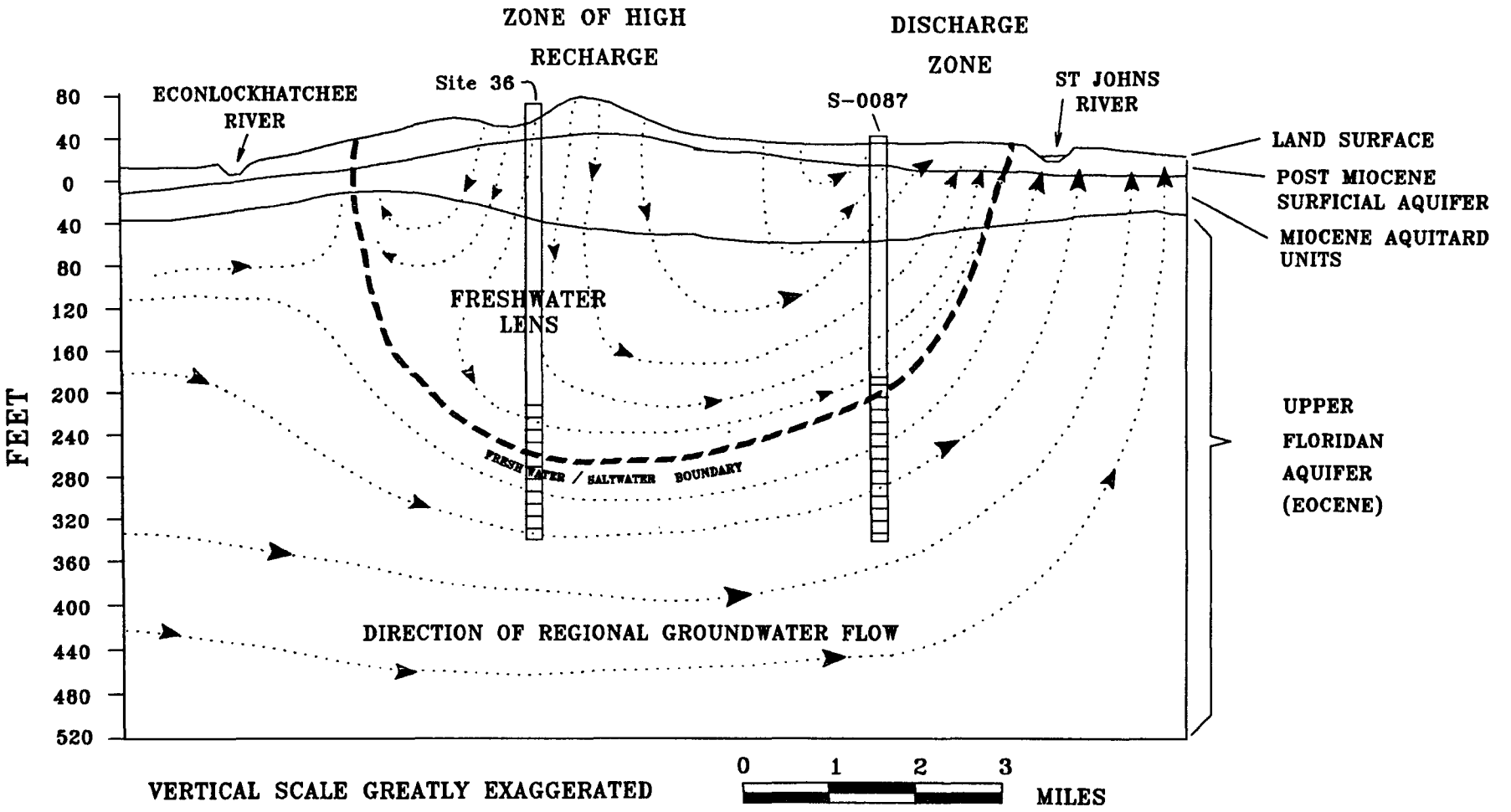

Figure 4.1. Cross-sectional conceptual model of Geneva area freshwater lens in the Floridan aquifer system.

desirable characteristic of a cross-sectional model (Figure 4.2). The orientation accommodates the approximate symmetry plane of the lens, which is also important. Based on three-dimensional problem considerations, the cross-sectional orientation selected is also consistent with the orientation of the three-dimensional grid region to be adopted in the fully three-dimensional simulations.

The configuration and key features of the modeled cross section, AA', are shown in Figure 4.3. The length of the section is 12 miles. The ends of the cross-sectional model correspond to the south and north boundaries of the 3-D model area. The section intercepts the Econlockhatchee and the St. Johns Rivers near the north and the south ends, respectively. The aquifer system that will be discretized using a finite element mesh comprises the upper Floridan aquifer, and extends from a depth of 30 ft to 480 ft. It is represented as a three-zone system comprising the Ocala formation, the Avon Park formation and a lower portion of the Avon Park formation. Evidence for separating the Avon Park into two layers is provided by geophysical logs of SJRWMD observation wells at the Seminole County landfill (site 58 of Figure 3.2). Within each zone, the material properties are treated as homogeneous.

4.2 BOUNDARY CONDITIONS

The selected cross section intersects the recharge area of the groundwater system at distances of 2 and 9 miles from the southern side (left boundary) of the modeled section. Thus a prescribed recharge rate of freshwater is applied to the corresponding central

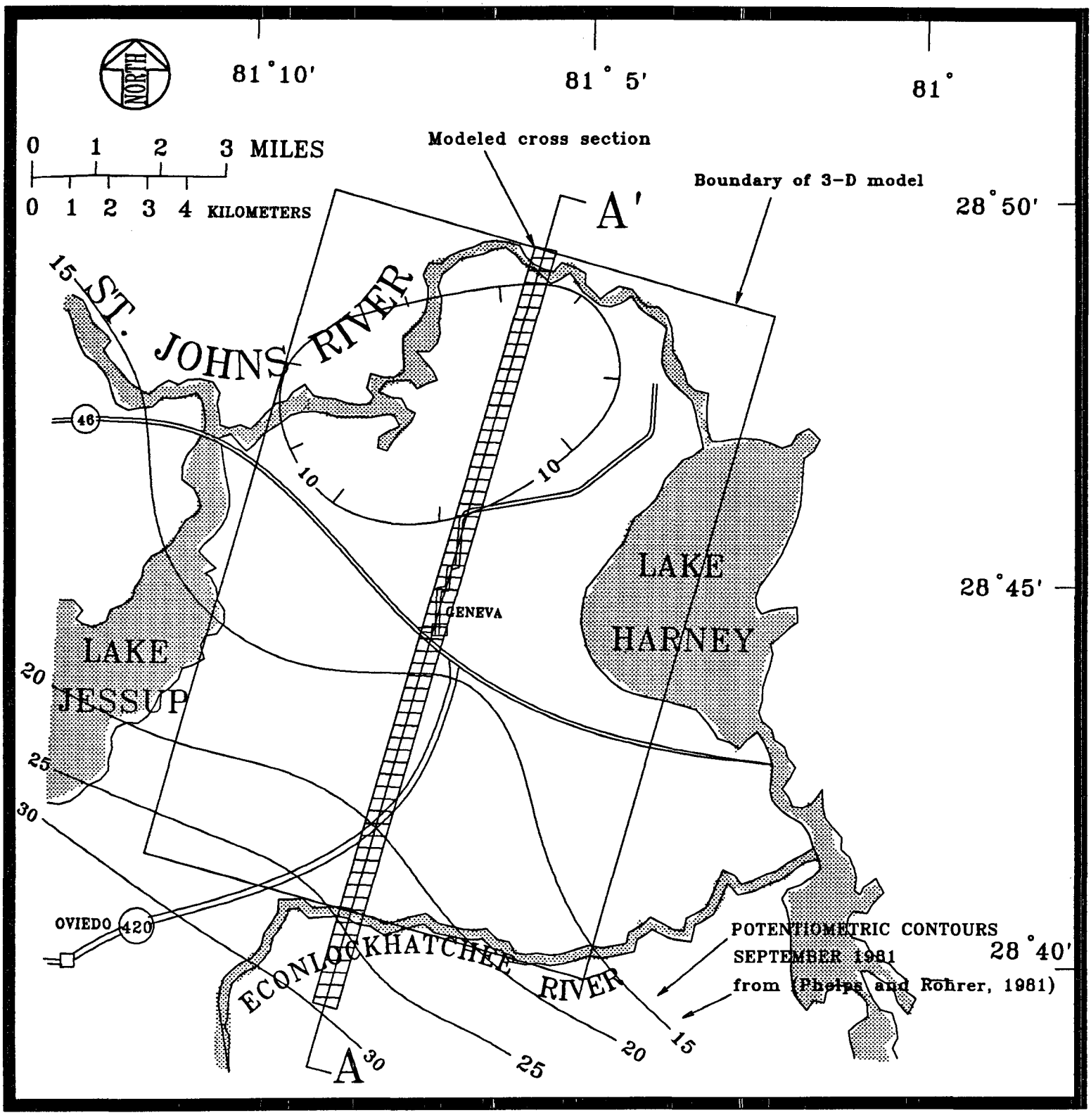

Figure 4.2. Selected cross-section and proposed boundary of a three-dimensional model.

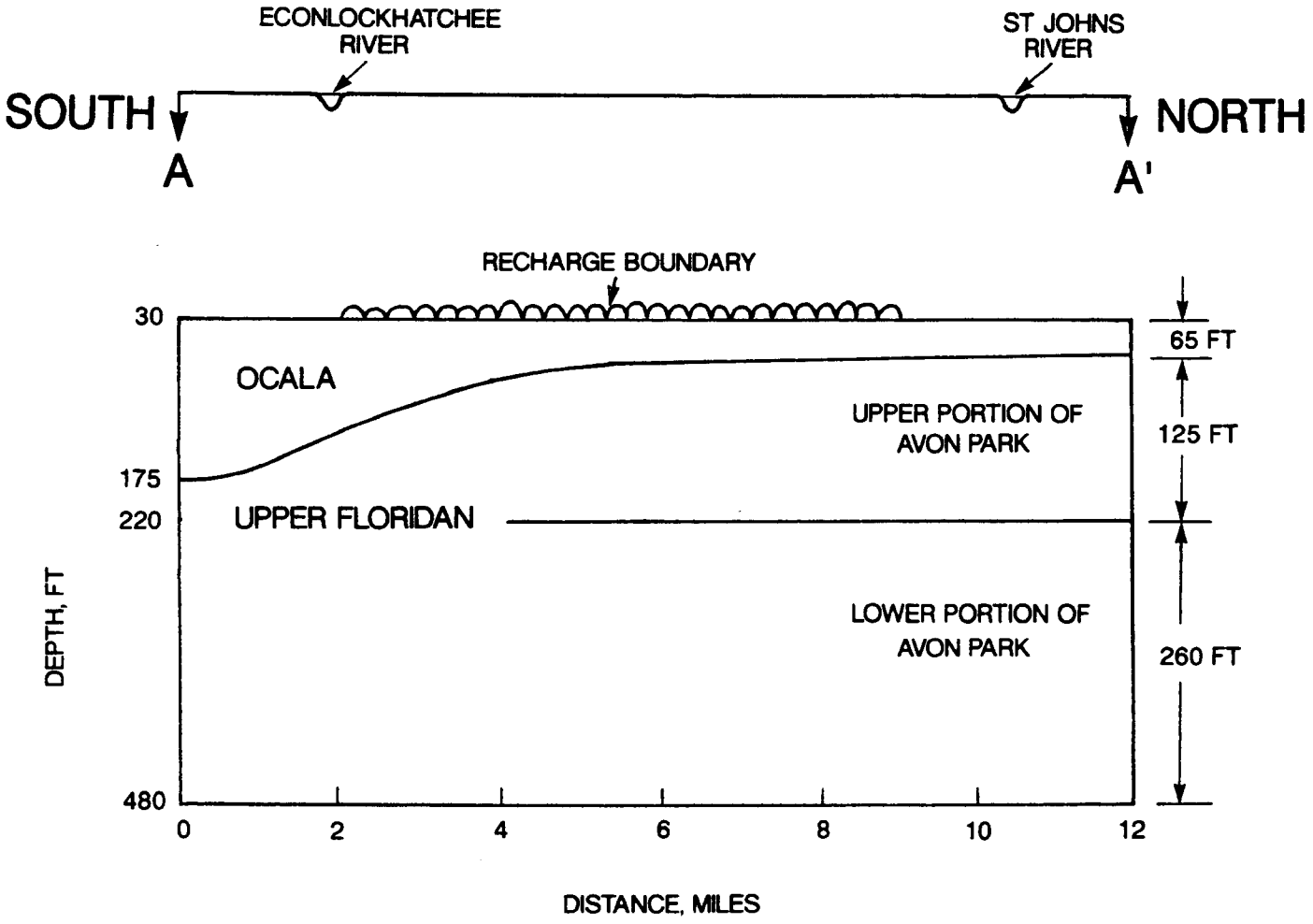

Figure 4.3. Configuration of the modeled cross-section, A-A'.

portion of the top boundary (see Figure 4.3). The remaining two portions of the top boundary are regarded as groundwater discharge boundaries. Both recharge and discharge of the regional flow system occur as leakages through a semipermeable confining clay unit which is overlain by the surficial aquifer.

Field evidence indicates that ambient groundwater flow is from south to north. Consequently, groundwater inflow is conceived to occur at the left hand side boundary portions intercepting the Ocala and Avon Park formation. The ambient flow rate can be computed using the potentiometric contour map shown in Figure 4.2, and reported transmissivity values of all formations. The net flow into the domain through the lower Avon Park formation is approximately 25 times lower than that calculated for the upper layers, and may hence be neglected. The groundwater inflow is assumed to have a chloride concentration of 3000 ppm. This assumption is based on an extrapolation of observed concentration data in well no. 1 (see Tables 1 and 4 in Phelps and Rohrer, 1987) located in the immediate vicinity of the Econlockhatchee River.

Lateral outflow of groundwater is also conceived to occur, and a prescribed outflow rate is applied to the right-hand-side boundary portion that intercepts the Ocala formation. As the observed potentiometric head data near the St. Johns river is rather limited, an appropriate value of the outflow rate needs to be determined from model calibration.

The bottom boundary of the model is treated as a prescribed head boundary. The head distribution that will be incorporated in

the numerical model is shown in Figure 4.4a (this is based on the average observed heads in the upper Floridan, and has been used in previous modeling efforts by the District due to lack of information at the required depth). Chloride concentration at the base of the modeled section is also prescribed. The concentration value is assumed to be 10,000 ppm. The assumption is based on an extrapolation of maximum concentration values reported for deep observation wells (e.g. bottom hole sample from well S-0200 at site 58 of Figure 3.2 is approximately 10,000 mg/l). Well S-0200 has an open-hole completion in an interval corresponding to the bottom of the model domain.

For numerical solution of the groundwater flow equation, the remaining (lower) portions of the left and right hand side boundaries are treated as no-flow boundaries. This assumption is a reasonable one to make for a deep groundwater system strongly driven by recharge. For numerical solution of the solute transport equation, zero normal gradients of concentration are applied to discharge and outflow boundaries.

In a situation where well pumping of the Floridan aquifer is considered, a total anticipated withdrawal rate of groundwater in the Geneva lens area is considered in the numerical simulation. Since a cross-sectional analysis is to be performed, the total withdrawal rate per unit width of the freshwater lens is applied to the two-dimensional model. The pumping area is assumed to be located within the central part of the lens between distances of 5 and 8 miles from the upstream inflow boundary.

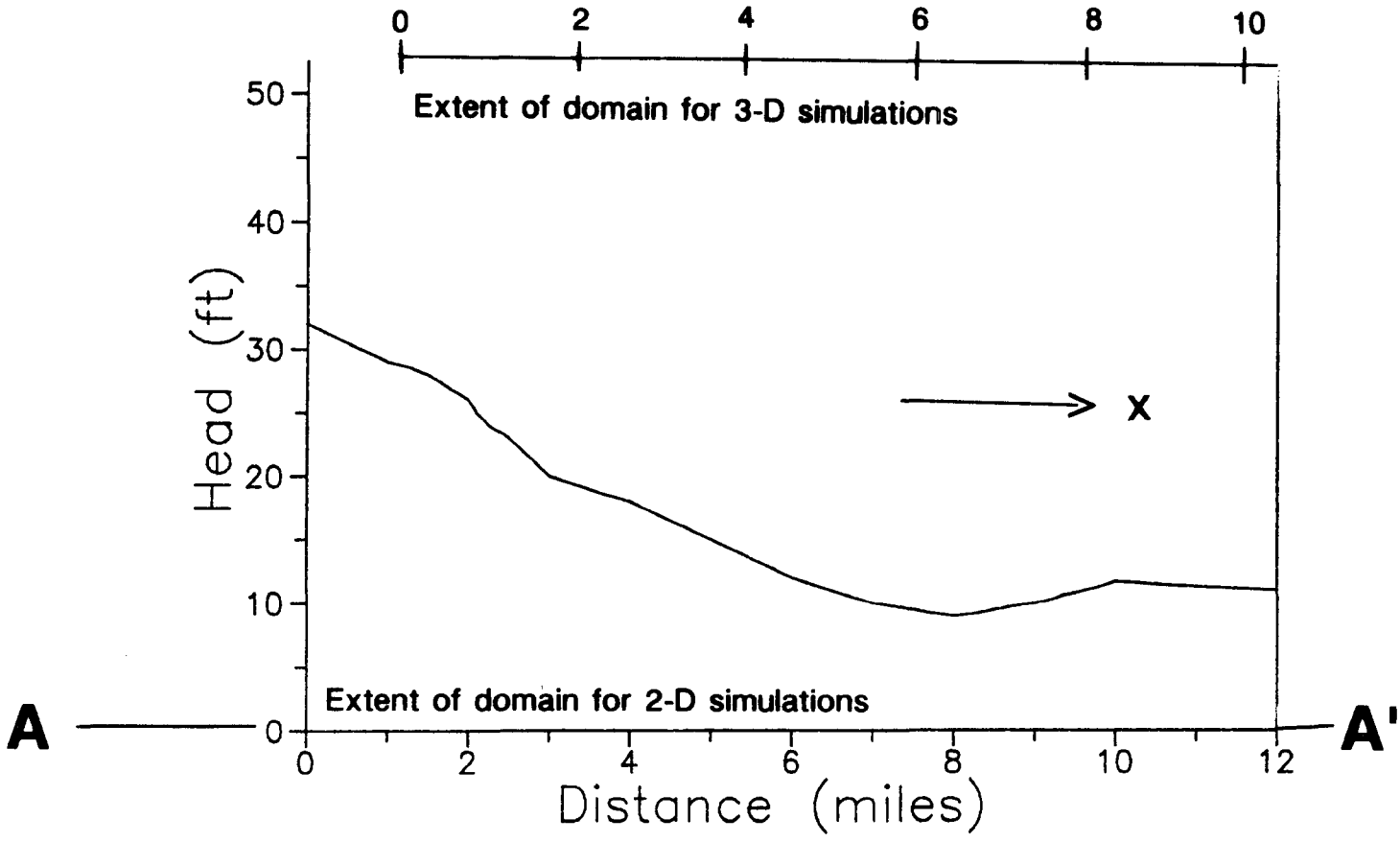

Figure 4.4a. Equivalent Freshwater Hydraulic head at the base of the upper Floridan aquifer.

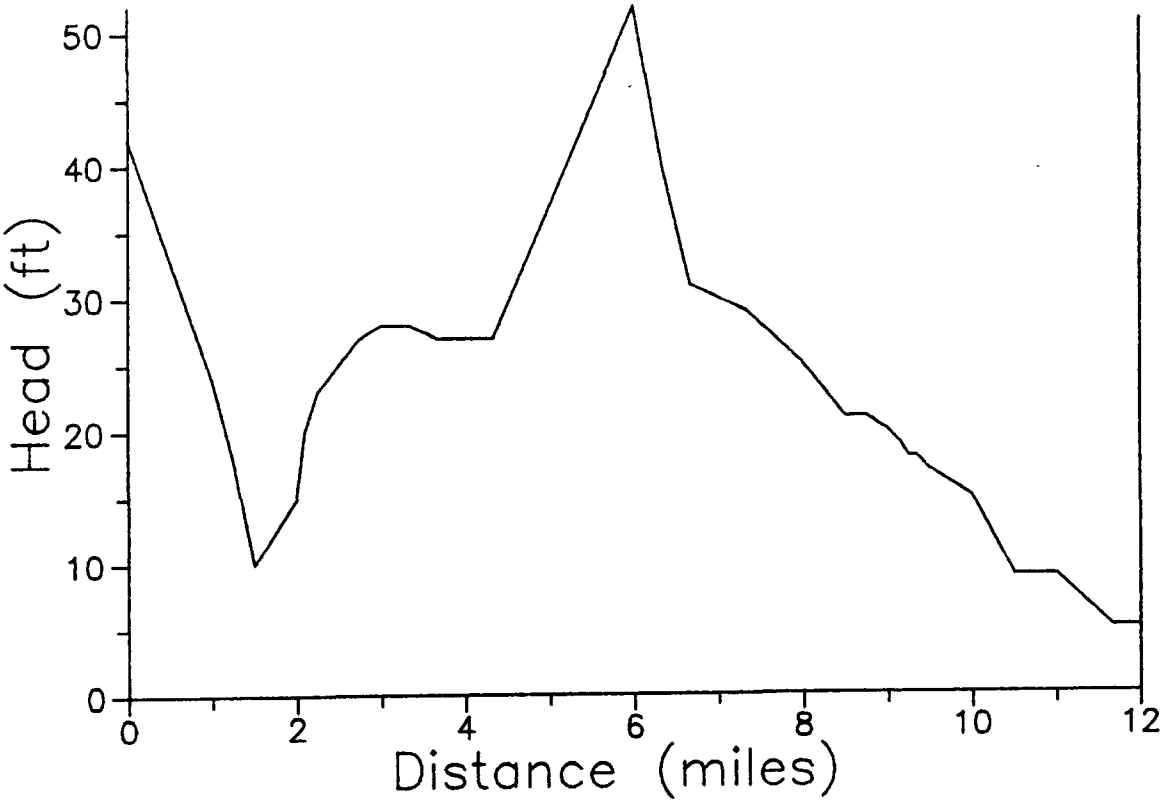

Figure 4.4b. Equivalent Freshwater Hydraulic head in the surficial aquifer.

The boundary conditions described above are adopted for simulations of steady-state and transient responses of the system under non-pumping and pumping conditions. The cross-sectional model is calibrated under a steady-state non-pumping condition using field data reported by Phelps and Rohrer (1987), for chloride concentrations of water from the upper part of the Floridan aquifer system. Based on the steady-state model calibration result, an estimation of leakance coefficient of the confining clay bed overlying the Ocala unit can be made. The leakance calculation assumes a prescribed head distribution in the surficial aquifer as shown in Figure 4.4b. This is useful for actual scenarios where temporal variations in piezometric heads of the surficial aquifer are known.

4.3 MESH DESIGN CONSIDERATIONS

Mesh design is an important task of the numerical modeling procedure particularly when dealing with the advective-dispersive solute transport equation. Caution needs to be exercised to avoid using an inappropriate mesh that leads to inaccurate numerical solutions with unacceptable numerical oscillations or excessive numerical dispersion.

We elect to discretize the modeled region shown in Figure 4.3 using a rectangular finite element mesh with variable nodal spacings but a constant number of nodes along each grid line. This type of mesh is automatically generated by the DSTRAM code with user-supplied values of grid spacings or coordinates of row and

column grid lines. Zonal identification is accomplished via specification of element material numbers. Two separate meshes are adopted for steady-state and transient simulation runs, respectively. Because the steady-state study involves model calibration as well as aquifer parameter sensitivity analysis, it is desirable to use a refined mesh with conservative values of nodal spacings that meet stringent Peclet number criteria throughout the flow region. This gives us confidence that numerical results obtained will be accurate for a wide range of parameters that is expected in the sensitivity analysis. For subsequent transient simulations, a coarser mesh may be used once we have developed a good understanding of the expected pattern of concentration distribution, for the calibrated set of aquifer parameter values. This mesh has been designed such that much larger nodal spacings are used, thereby possibly violating the Peclet number criteria in parts of the region where concentration gradients are small. To ensure that the coarser mesh is adequate, its numerical solution needs to be calibrated against that of the refined mesh. We will elaborate on this mesh calibration in Section 6.4.1.

4.4 MODEL ASSUMPTIONS AND LIMITATIONS

A number of assumptions have been made in the development of the conceptual model for cross-sectional analyses. These assumptions and additional assumptions used in the DSTRAM variable density simulations are summarized as follows:

- The concentration distribution in the vertical plane of the selected cross-section is governed by two-dimensional flow of water and chloride transport in that plane. The effects of advection and dispersion across the plane on chloride concentrations may be neglected. Flow and transport are assumed to occur under an isothermal condition.

- The rates of groundwater recharge and discharge on the top boundary of the model may be treated as uniformly distributed. Likewise the lateral inflow and outflow at the left and right hand side boundary portions (Figure 4.3) may be treated as uniformly distributed. The remaining boundary conditions are assumed to be those described in Section 4.3.

- Material properties within each zone of the modeled region may be regarded as constant.

- Hydraulic conductivities of aquifer materials may be regarded as unaffected by changes in fluid density and viscosity due to variability of chloride concentration.

Most of the above assumptions are fairly appropriate and consistent with the reported field conditions and available site information except for one that neglects the transverse horizontal flow and transport components. Consequently, a major limitation of the cross-sectional modeling approach is the inability of the model to account for flow and transport out of the plane of the cross section. For situations involving well pumping, the transverse flow and transport components are likely to be important. Another limitation of the cross-sectional model is the disregarding of

areal distributions of groundwater recharge and discharge as well as of lateral boundary conditions of the three-dimensional flow system. In view of these limitations, the fully three-dimensional model described in Chapter 7 is more appropriate for quantitative descriptions of the lens system.

5. TWO-DIMENSIONAL STEADY STATE SIMULATIONS

5.1 GENERAL APPROACH

Steady-state simulations of groundwater flow and chloride transport were performed for the selected cross-section of the upper Floridan aquifer system. The main objectives of the steady-state analyses were to enhance overall understanding of the system characteristics, and to identify the roles of key parameters controlling flow patterns, chloride distributions, and the configuration and extent of the freshwater lens. Additionally, the optimal steady-state solution obtained from the model calibration provides a rational starting point (or initial condition) for subsequent transient simulations.

The steady-state simulation study was conducted in three stages. In the first stage, test simulation runs were performed in order to verify the DSTRAM code using the input data and mesh supplied by the District. Mesh refinement was made to test convergence of the numerical solution. Following the code verification, a series of model calibration runs was performed during the second stage of the steady-state simulations. Optimal values of material parameters and boundary conditions were determined for the system under study. The parameter range supplied by the District was used as a starting point for calibration. Model results were compared with observed chloride concentration data for 1982. In the third stage, sensitivity runs were made by varying the values of key parameters from those used in the model calibration.

The steady-state model calibration described in this chapter provides a sound basis for determining if the two-dimensional conceptualization gives results consistent with field observations. Although the steady-state cross-sectional modeling approach neglects three-dimensional effects and transient behavior, it is highly useful for gaining a preliminary understanding of the system under study. Furthermore, data gaps can also be identified. The significance of the overall response of the modeled system to data uncertainty can be determined via a sensitivity analysis. A carefully designed sensitivity analysis helps enhance our understanding of the system, and provides an indication of the level of confidence that can be placed on the simulation results. A refinement of the conceptualization of the system is needed if the sensitivity analysis produces results contrary to physical behavior, even though calibrated results match field data.

5.2 BOUNDARY CONDITIONS AND MATERIAL PROPERTIES

The location of the selected vertical cross-section is shown in Figure 5.1. As mentioned previously in Chapter 4, cross-section A-A′ was selected because groundwater flow is predominantly parallel to its orientation and because it passes through the central portion of the freshwater lens. A schematic representation of the modeled region is shown in Figure 5.2. The length of the region along the x-axis is approximately twelve miles. The modeled section is intercepted by the Econlockhatchee River and the St. Johns River near the south and north ends, respectively.

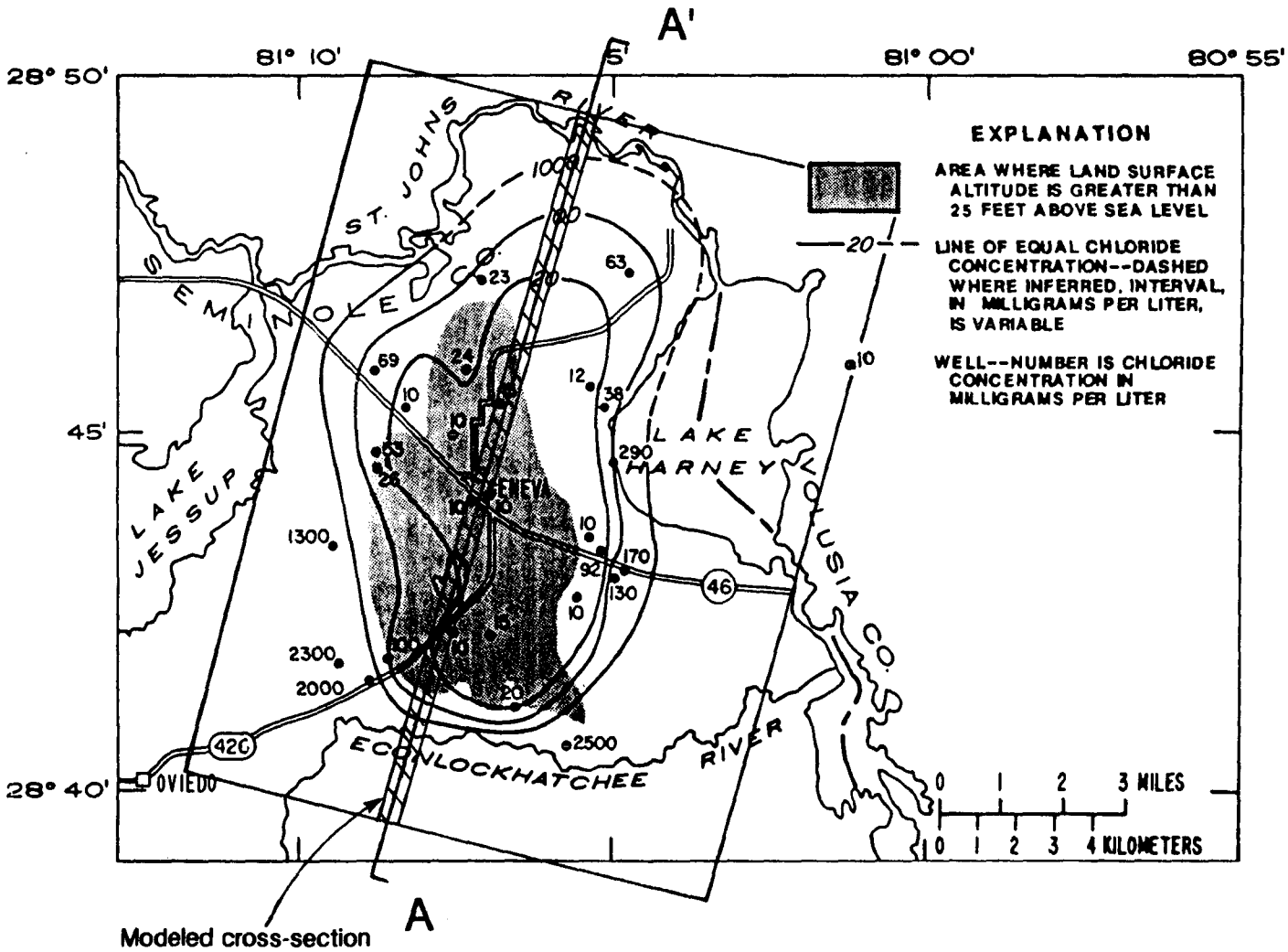

Figure 5.1. Modeling area of saltwater intrusion in the upper Floridan aquifer of Northeast Seminole County.

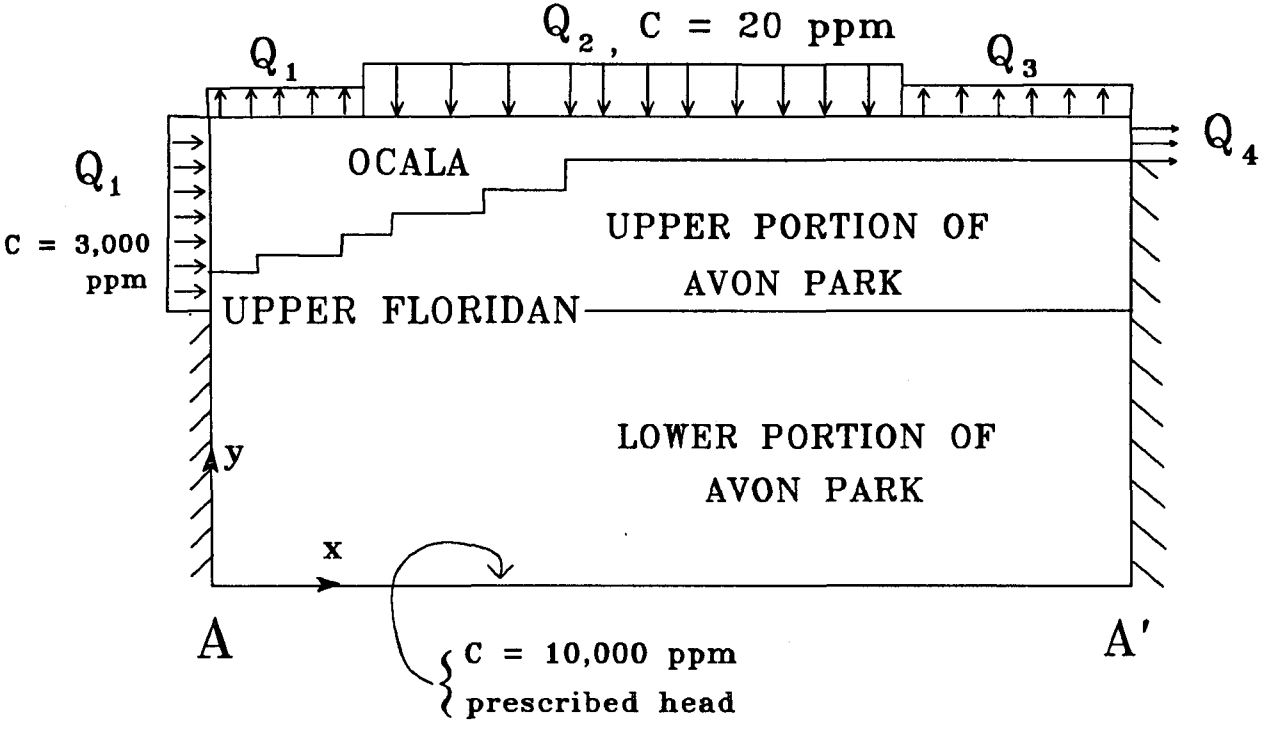

Figure 5.2. Schematic representation of modeled cross-section.

Lateral inflow at the southern boundary near the Econlockhatchee River was estimated from the regional potentiometric surface (Phelps and Rohrer, 1987, p. 23) and transmissivity of the aquifer in the region. A unit flux of Q_1 = 0.11 ft/d is thus prescribed on the upper 190 ft of the Econlockhatchee River boundary. The net inflow through the lower 260 ft of the boundary is over an order of magnitude lower, and is hence neglected. Chloride concentrations at this boundary are approximately 3000 ppm under both wet and dry seasonal conditions (Phelps, and Rohrer 1987, p. 48 and p. 49). The bottom boundary of the modeled region lies at a depth of 480 ft (below Mean Sea Level) in the zone of brackish water at the bottom of the upper Floridan aquifer. Chloride concentrations of 10,000 ppm were prescribed at this base. The hydraulic head along the bottom was prescribed as an equivalent freshwater value, according to data supplied by the District. This information is extrapolated by the District from the average piezometric heads available at observation wells and does not necessarily represent the heads at the bottom boundary. Fortunately, however, these heads act as a datum for the conceptual model described herein and their absolute values do not signifi-cantly affect the flow field or concentration patterns. Informa-tion on the boundary conditions at the north side of the cross-section near the St. Johns River is also scarce. This boundary was treated as a no-flow, zero-concentration gradient boundary below the base of the Ocala, and an outflow boundary with zero concentration gradient was applied near the surface. The upper Floridan system is overlain by an aquitard, with an

unconfined (surficial) aquifer above it. The leakance of the aquitard (K'/b'), and hydraulic head difference between the two aquifers determines the vertical leakage (i.e. groundwater recharge and discharge) through the aquitard. Recharge and discharge zones are delineated by the sign of the head difference. The average recharge into the upper Floridan system was estimated to be 10 in/yr (Phelps and Rohrer, 1987, p. 1). The discharge through portions of the top boundary were chosen such that the field behavior is adequately represented by the model. With head differences between the two aquifers known, the leakance for the aquitard can be estimated for the given fluxes using Darcy's law.

5.3 SELECTED MESH AND RATIONALE FOR SELECTION

The mesh used in the cross-sectional steady-state simulations of model calibration and parameter sensitivity is illustrated in Figure 5.3. It is a refined mesh consisting of 5852 rectangular elements and 6180 nodes. Nodal spacings of the mesh were graded gradually in both the horizontal and the vertical directions. The horizontal spacing varied from 150 to 400 ft, and the vertical spacing varied from 15 to 30 ft. Extremely fine elements were placed in the outer zones of the region where high concentration gradients could occur. Coarser elements were placed in the central portion of the freshwater lens.

No. of nodes = 6180
No. of elements = 5852

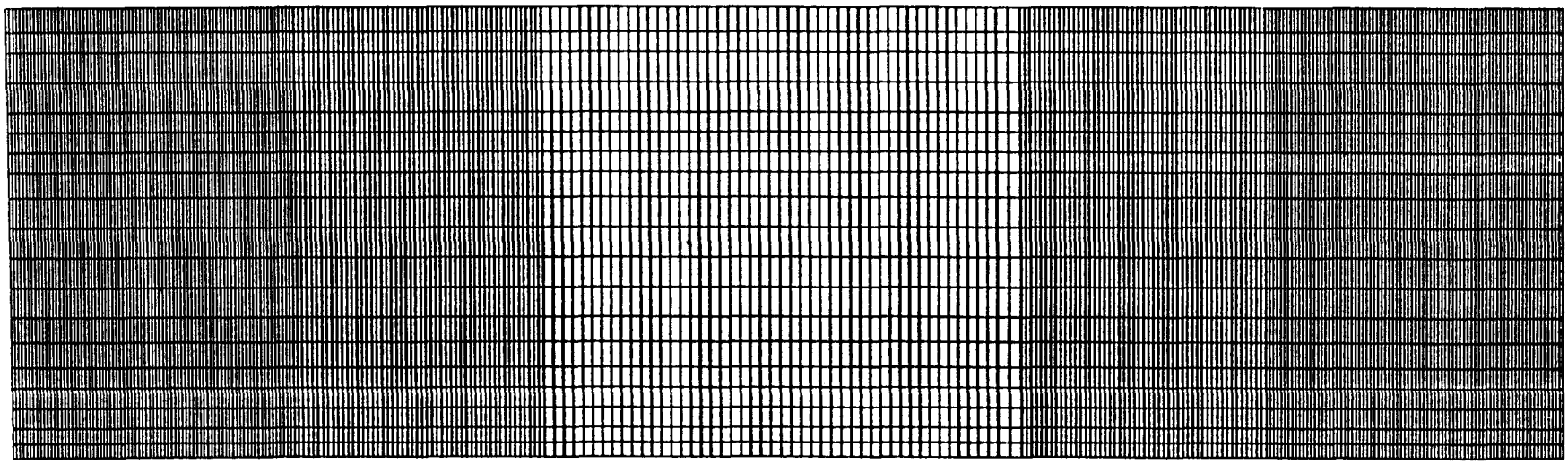

Figure 5.3. Domain discretization for steady-state simulations

Our reasons for adopting such a fine mesh are two-fold. Firstly, it is desirable to ensure accurate numerical solutions for the full range of parameter values used in the sensitivity study to avoid incorrect interpretation of the model response to parameter variation. Secondly, we take advantage of the fact that the DSTRAM code provides an inexpensive steady-state analysis even with a grid having over 6000 nodes.

5.4 MODEL VERIFICATION AND CALIBRATION

5.4.1 Verification test

A number of test simulation runs were first conducted using parameter values, boundary conditions and a coarse grid supplied by the District. The grid consisted of 912 elements and 980 nodes. Two situations, referred to hereafter as scenarios A and B, were considered. Scenario A was one where the recharge and discharge fluxes for the nodes on the top of the Ocala formation were prescribed (or assigned directly) to the code. Consequently, the properties (i.e. leakance) of the overlying aquitard and the head data for the surficial aquifer were not needed. Scenario B was one where aquitard leakage corresponding to the groundwater recharge and discharge of Scenario A was computed by using the aquitard leakance coefficient and prescribed freshwater head in the surficial aquifer. Scenarios A and B were analyzed using the material properties depicted in Tables 5.1 and 5.2 respectively, using the coarse grid supplied by the District, and the fine grid designed for the steady-state simulations depicted in Figure 5.3.

TABLE 5.1 MATERIAL PARAMETERS OF SCENARIO A

Parameter	(Units)	Parameter Value		
		Ocala	Avon Park	Bottom Layer
Hydraulic conductivity	K_{xx}(ft/d)	160	50	5
Hydraulic conductivity	K_{yy}(ft/d)	16	5	0.05
Longitudnal dispersivity	α_L(ft)	100	100	50
Tranverse dispersivity	α_T(ft)	50	50	25

TABLE 5.2 MATERIAL PARAMETERS OF SCENARIO B

Parameter	(Units)	Parameter Value		
		Ocala	Avon Park	Bottom Layer
Hydraulic conductivity	K_{xx}(ft/d)	100	50	10
Hydraulic conductivity	K_{yy}(ft/d)	10	5	0.1
Longitudnal dispersivity	α_L(ft)	100	100	50
Tranverse dispersivity	α_T(ft)	50	50	25

OVERLYING AQUITARD PARAMETERS

(Units)	ZONE 1	ZONE 2	ZONE 3	ZONE 4
Leakance factor L'=K'/b' (ft/d)/ft)	0.56E-04	0.7E-04	0.9333E-04	1.4E-04
Extent of Zones (miles)	0 - 2	2 - 3	3 - 5 9 - 12	5 - 9

For both scenarios, the chloride concentration at the inlet lateral flow boundary was prescribed as 100 ppm. Isochlor contours produced by the DSTRAM code are plotted in Figures 5.4a and 5.5a for scenarios A and B, respectively, using the fine grid. Corresponding simulation results obtained by the Districts modeling staff using the SWICHA code (Huyakorn et al., 1986) are shown in Figures 5.4b and 5.5b respectively for scenarios A and B. The depicted isochlor values are normalized values relative to the maximum concentration of 10,000 ppm at the base of the model region. The results of the DSTRAM code were found to be in excellent agreement with results obtained previously by the District using the original SWICHA code. This verified the expected performance of DSTRAM and of the fine grid considered. A careful examination of Figures 5.4 and 5.5 versus observed chloride distribution data indicates that model predictions of the freshwater lens disagree with the field conditions reported by Phelps and Rohrer (Figures 4, 5, 16, 17; 1987). The predicted maximum thickness of the freshwater lens (i.e. the depth to the lowest part of the 250 ppm isochlor) is approximately 200 ft whereas the observed maximum is approximately 280 ft. Furthermore, the simulated lens is considerably narrower than the observed lens.

The misprediction of the freshwater lens was due mainly to the use of an inappropriate value for the transverse dispersivity. The next set of simulations was thus performed with transverse dispersivity values, α_T, reduced by a factor of 10 (i.e., the Ocala and Avon Park had a transverse dispersivity of 5 ft, and the bottom

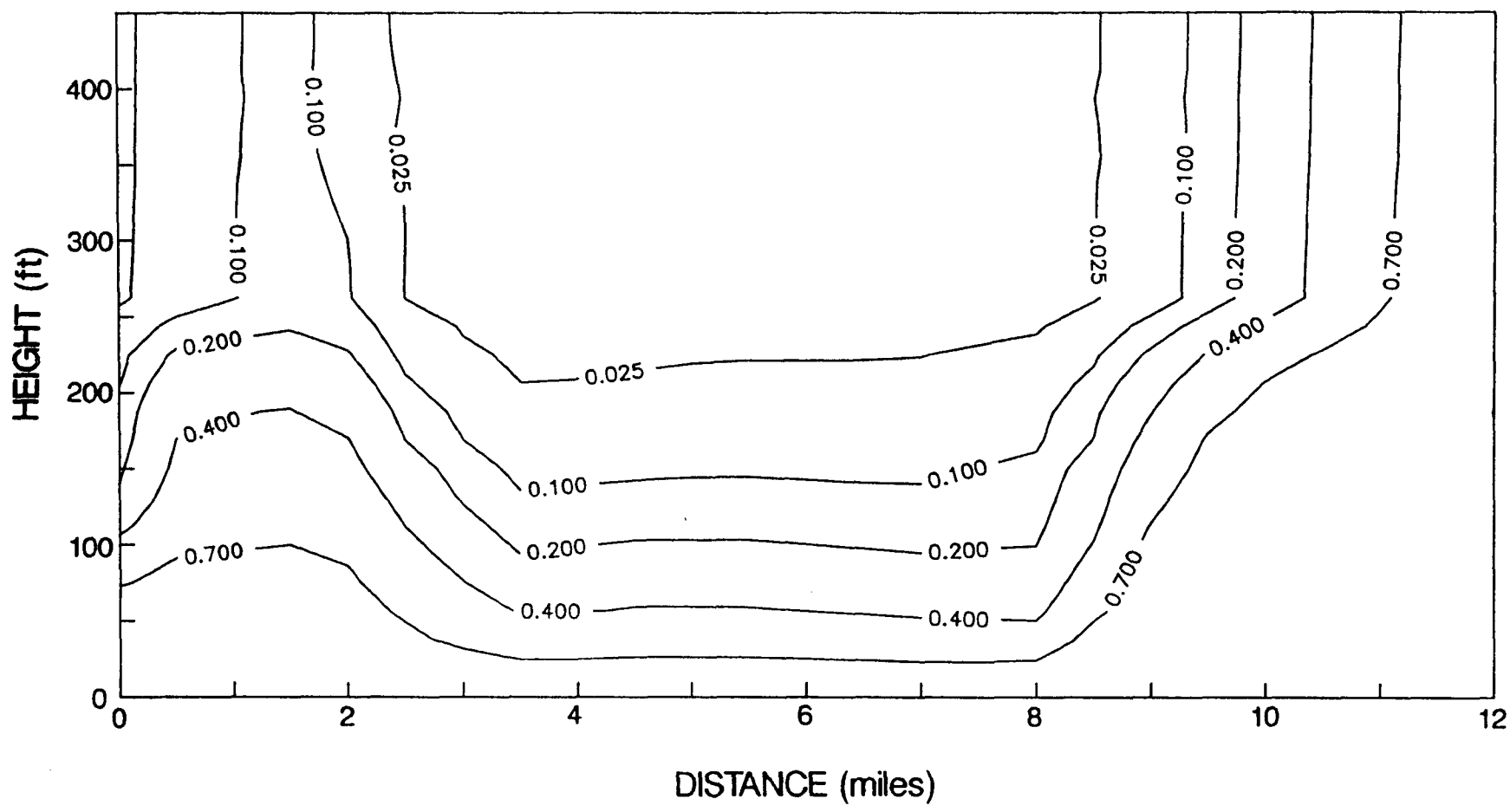

Figure 5.4a. Relative concentration contours of a grid verification simulation - no aquitard case.

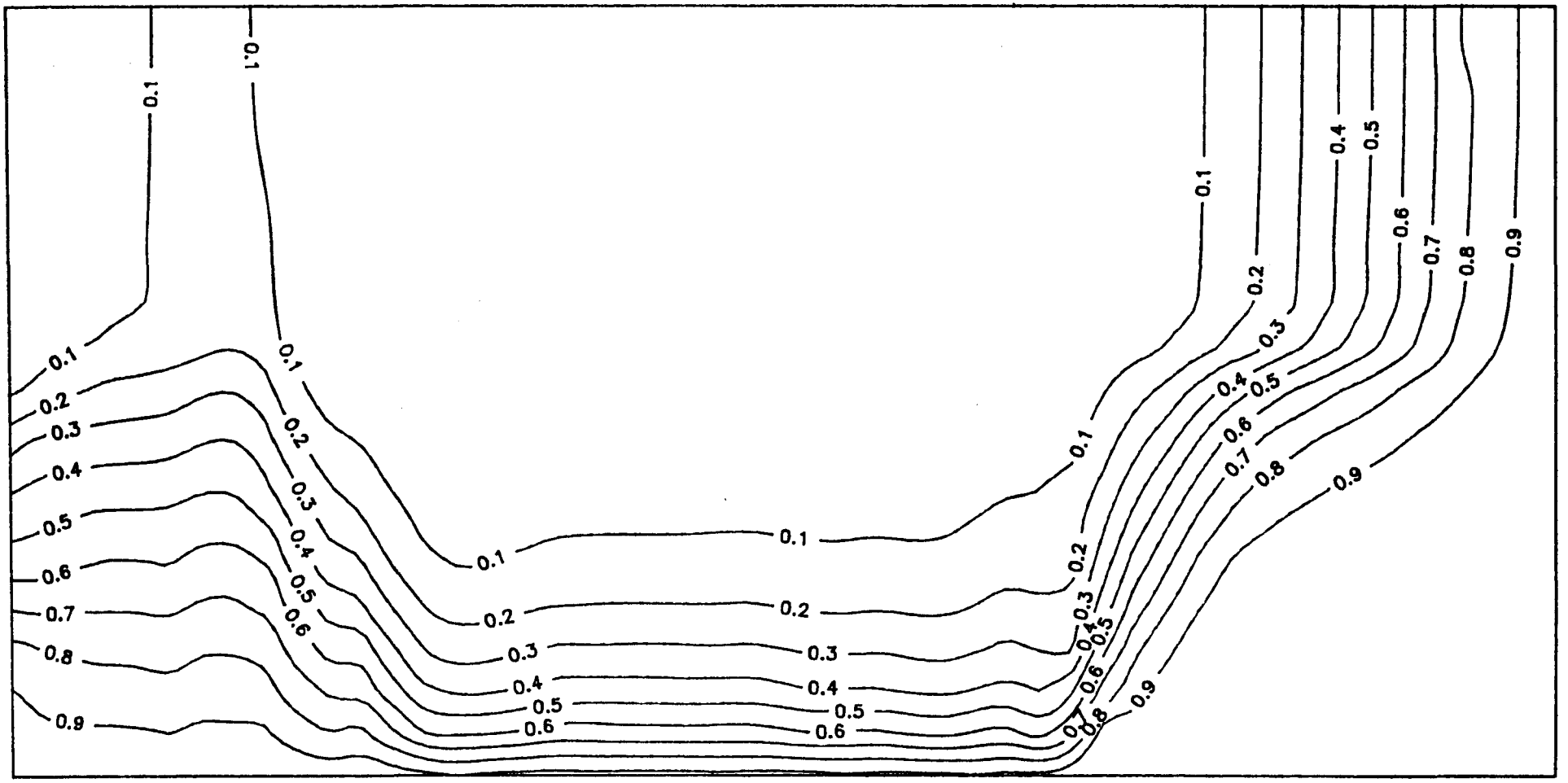

Figure 5.4b. Relative concentration contours for the no aquitard case as modeled by the District.

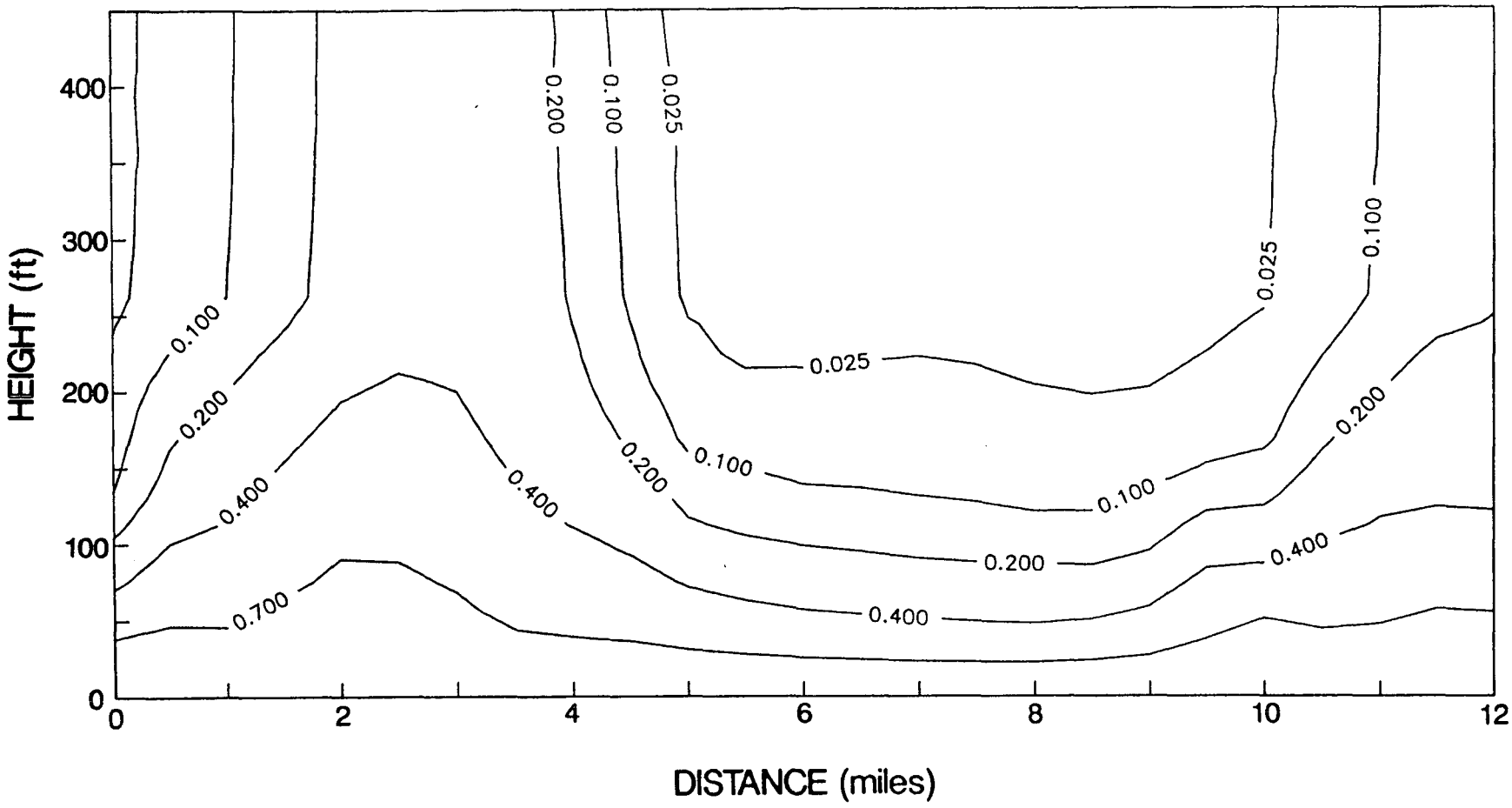

Figure 5.5a. Relative concentration contour of a grid verification simulation - overlying aquitard case.

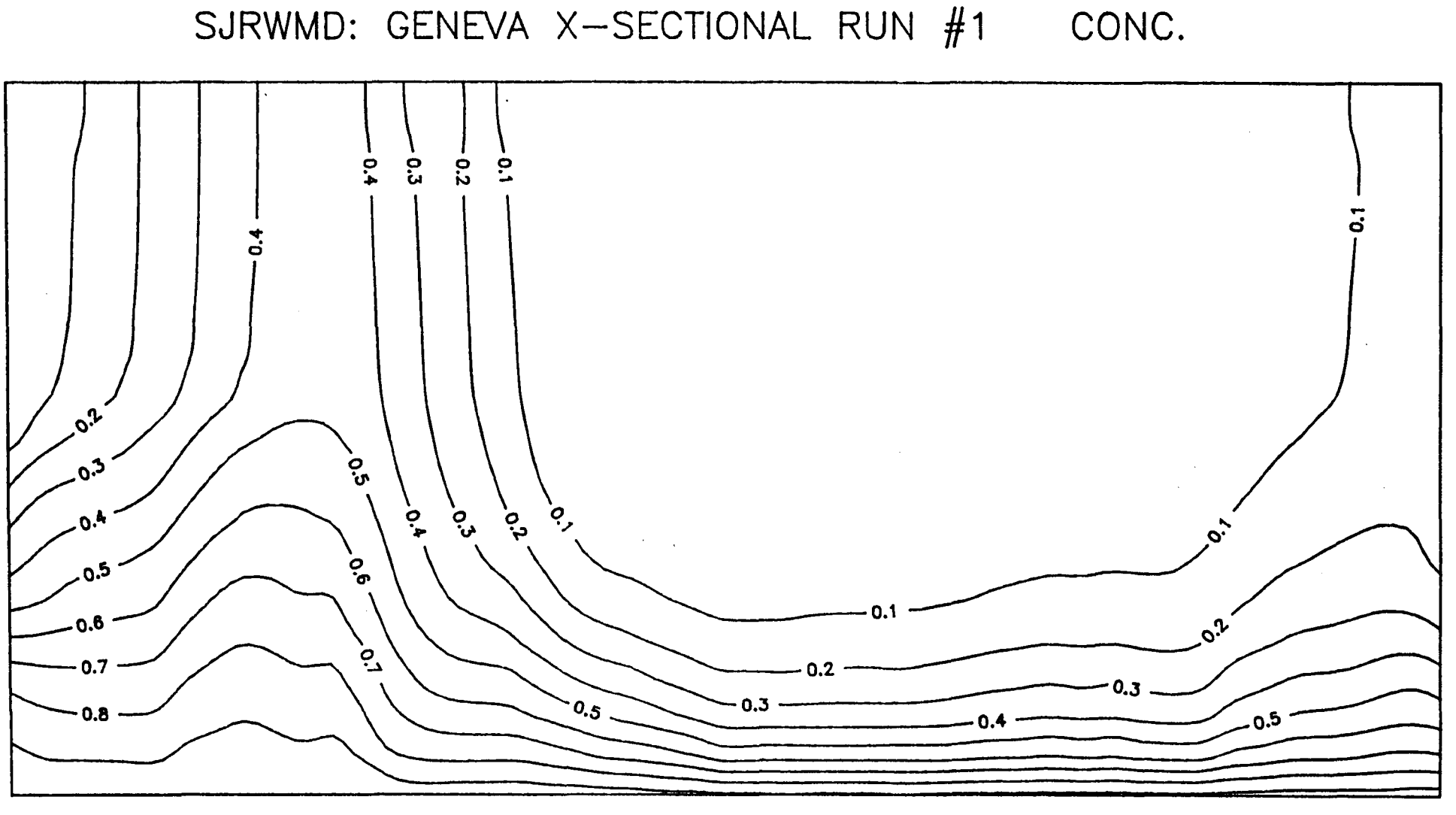

Figure 5.5b Relative concentration contours for the overlying aquitard case as modeled by the District.

layer transverse dispersivity was reduced to 2.5 ft. Note that the values of 50 ft and 25 ft used previously seem rather large for the 450 ft thick system being modeled. Consequently it produces excessive upward spreading of the brackish water). To obtain accurate numerical results for the cases of smaller dispersivity values (α_T = 5 ft and 2.5 ft) we elected to use the fine grid described in Section 5.3. The numerical results for Scenarios A and B are displayed in Figures 5.6 and 5.7, respectively. As can be seen, there is a substantial change in the configuration and size of the freshwater lens. Note that the response to an order of magnitude decrease in transverse dispersivity is more dramatic for Scenario B than Scenario A, and the concentration distributions for the two scenarios are substantially different. This suggests that the two scenarios are hydraulically dissimilar. There is a significant difference in the fluid flux distributions at the top boundary of the discretized system for the two scenarios (i.e. the leakage fluxes calculated at the top boundary for Scenario B are considerably different from the prescribed values of recharge and discharge used in Scenario A). Net fluxes for Scenario A are Q_1 = 20.8 ft^2/d, Q_2 = 85 ft^2/d, and Q_3 = 85 ft^2/d, (see figure 5.2), while those calculated for Scenario B are Q_1 = 8.5 ft^2/d, Q_2 = 47.8 ft^2/d, and Q_3 = 3.2 ft^2/d. Note, however, that despite their different flux distributions, the two scenarios give similar concentration patterns for large transverse dispersivities (Figures 5.4 and 5.5), because chloride migration towards the surface is dominated by dispersive rather than hydraulic effects.

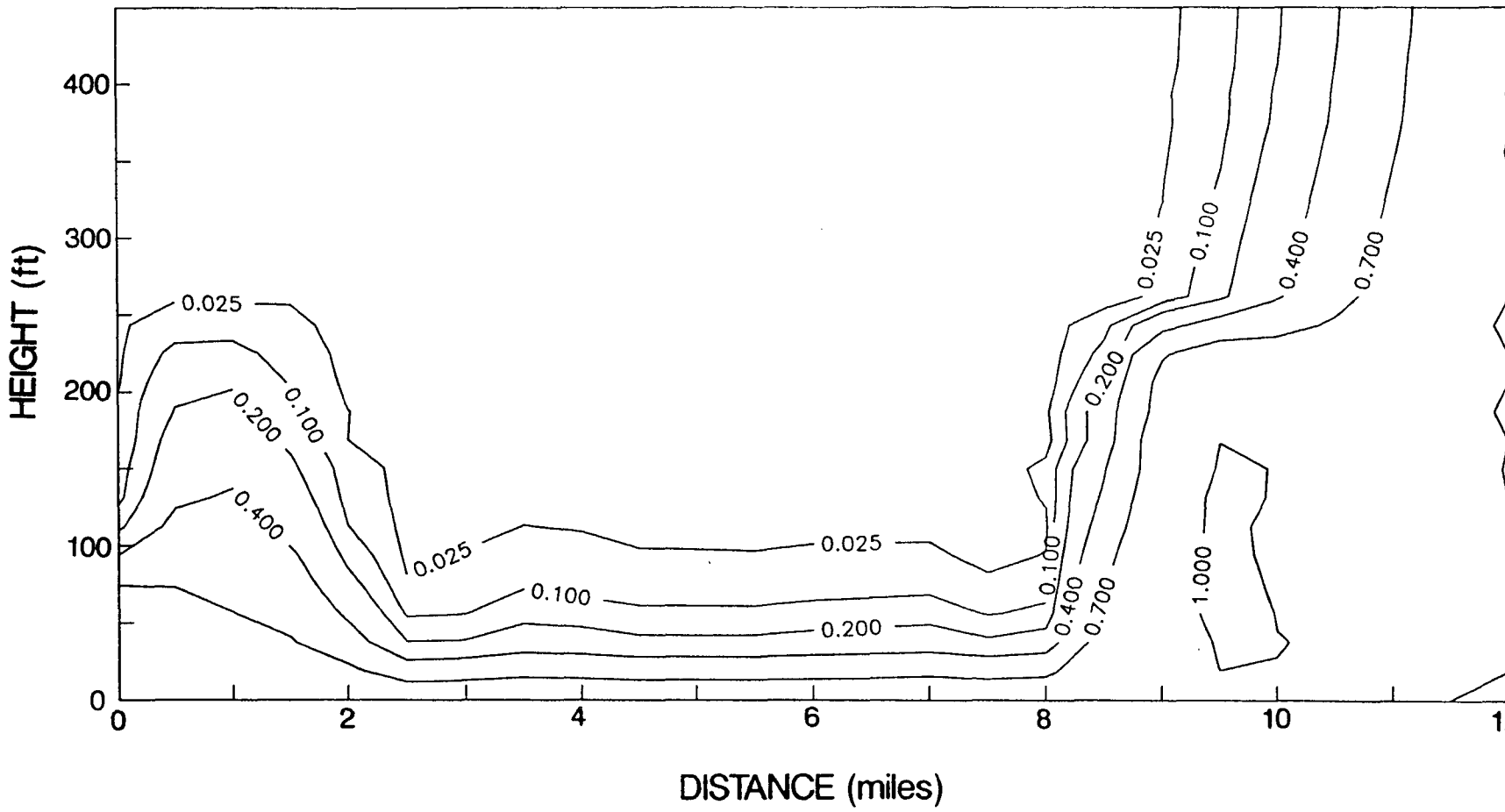

Figure 5.6. Relative concentration contours for simulation with low dispersivity values - no aquitard case (Scenario A).

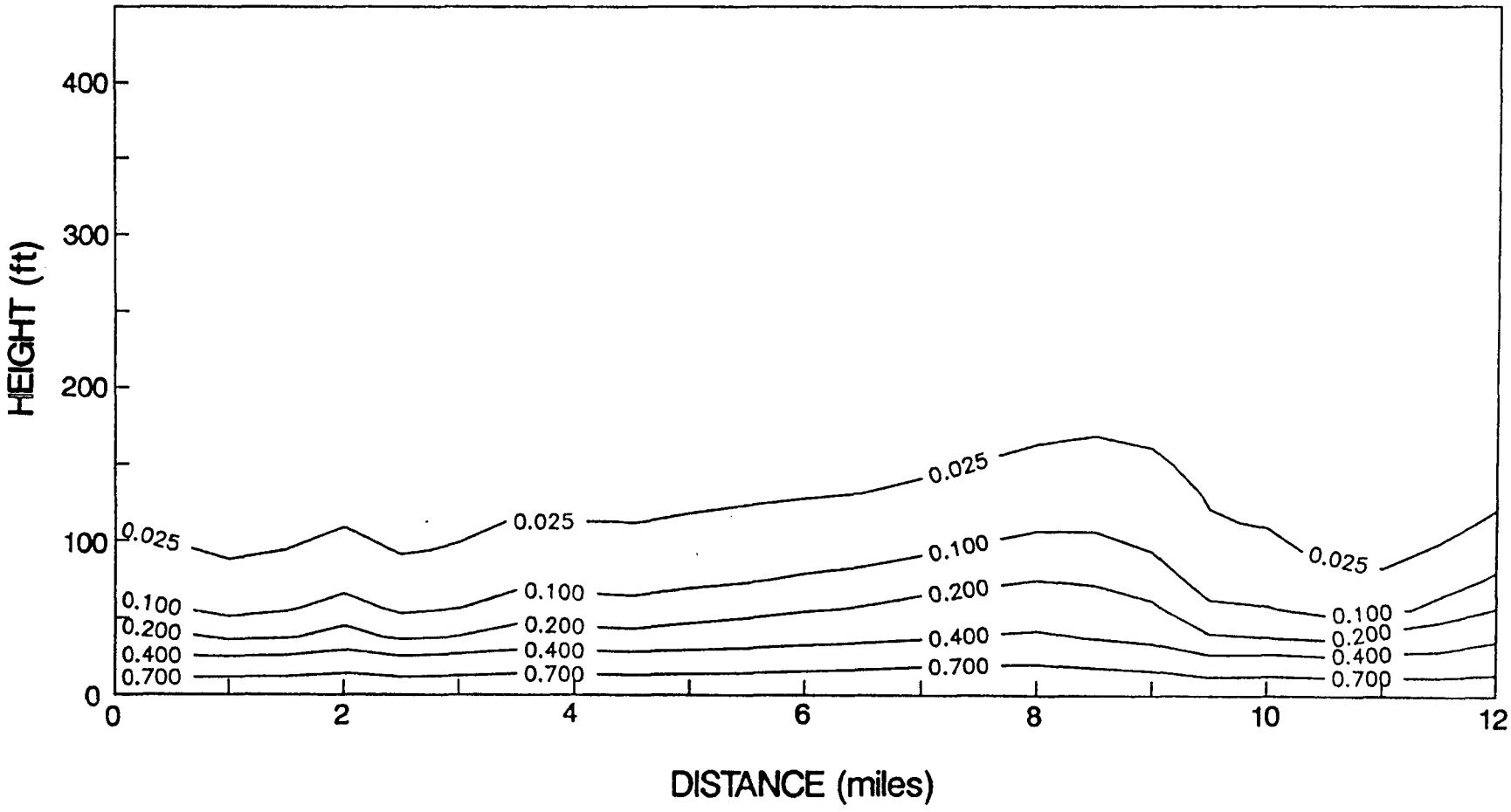

Figure 5.7. Relative concentration contours for simulation with low dispersivity values - overlying aquitard case (Scenario B).

The code verification exercise enabled us to identify major limitations and potential problems associated with the first-cut simulation runs. These may be summarized as follows:

1) Large grid Peclet numbers associated with the coarse grid caused numerical difficulties.

2) Gross underprediction of freshwater lens thickness resulted from unrealistically large transverse (vertical) dispersivities.

3) Inlet concentration boundary conditions near the Econlockhatchee River (c=100 ppm) are inconsistent with field values (c=3000 ppm) reported by Phelps and Rohrer (1987).

4) Discharge flux boundary conditions in the vicinity of the St. Johns River are too high. As a result, outlet concentrations are considerably larger than reported field values due to upward migration of brackish water from the base.

5.4.2 Model Calibration

Having developed a preliminary understanding of the behavior of the freshwater lens, we then proceeded to perform model calibration. We elected to calibrate the steady-state cross-sectional model based on Scenario-A-type simulations. The reason for selecting Scenario A in preference to Scenario B is the fact that it is more convenient to deal directly with the prescribed recharge and discharge fluxes than to incorporate aquitard leakage

boundary conditions. Furthermore, a Scenario-B-type simulation would be sensitive to the prescribed head values in the surficial aquifer and at the bottom of the domain since the net flux would be determined by the potential gradient across the top and bottom of the system. In selecting Scenario-A-type simulations, the prescribed heads at the bottom of the domain act only as a datum. Additionally, advantage is taken of the fact that the two scenarios are equivalent if the same flux distribution is applied at the top of the modeled region (i.e. the top of the Ocala portion of the Floridan aquifer).

A series of model calibration runs were made using the fine grid shown in Figure 5.3. Simulation results were compared with observed chloride concentration data for the wet condition of 1982. Successive adjustments of key parameters and boundary conditions were made using a standard trial-and-error procedure. Shown in Figure 5.8 are the calibrated model parameter values and boundary conditions. The boundary inflows and outflows for calibrated flow simulation are Q_1 = 20.8 ft^2/d, Q_2 = 85 ft^2/d, Q_3 = 10 ft^2/d, and Q_4 = 10 ft^2/d. The outflow quantity Q_4 was distributed over 160 ft of the upper portion of the boundary near the St. Johns River (Figure 5.8). Prescribed head values along the bottom boundary were interpolated onto each of the nodes along the base using the head distribution supplied by the District (Figure 4.4a). Contours of relative concentration obtained from this simulation are shown in Figure 5.9a. The predicted length and thickness of the fresh-water lens is reasonably consistent with the field observations

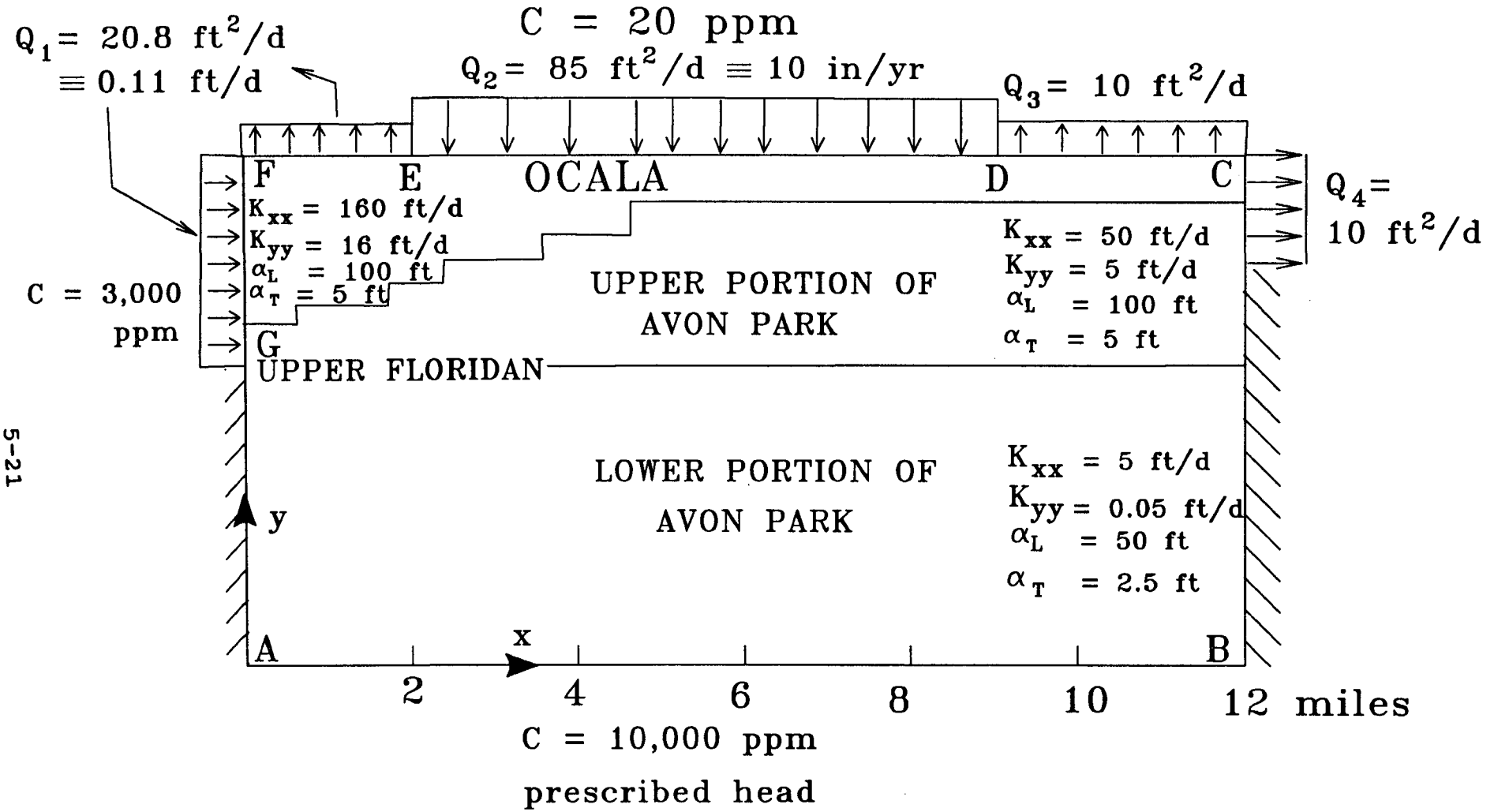

Figure 5.8. Calibrated model parameters.

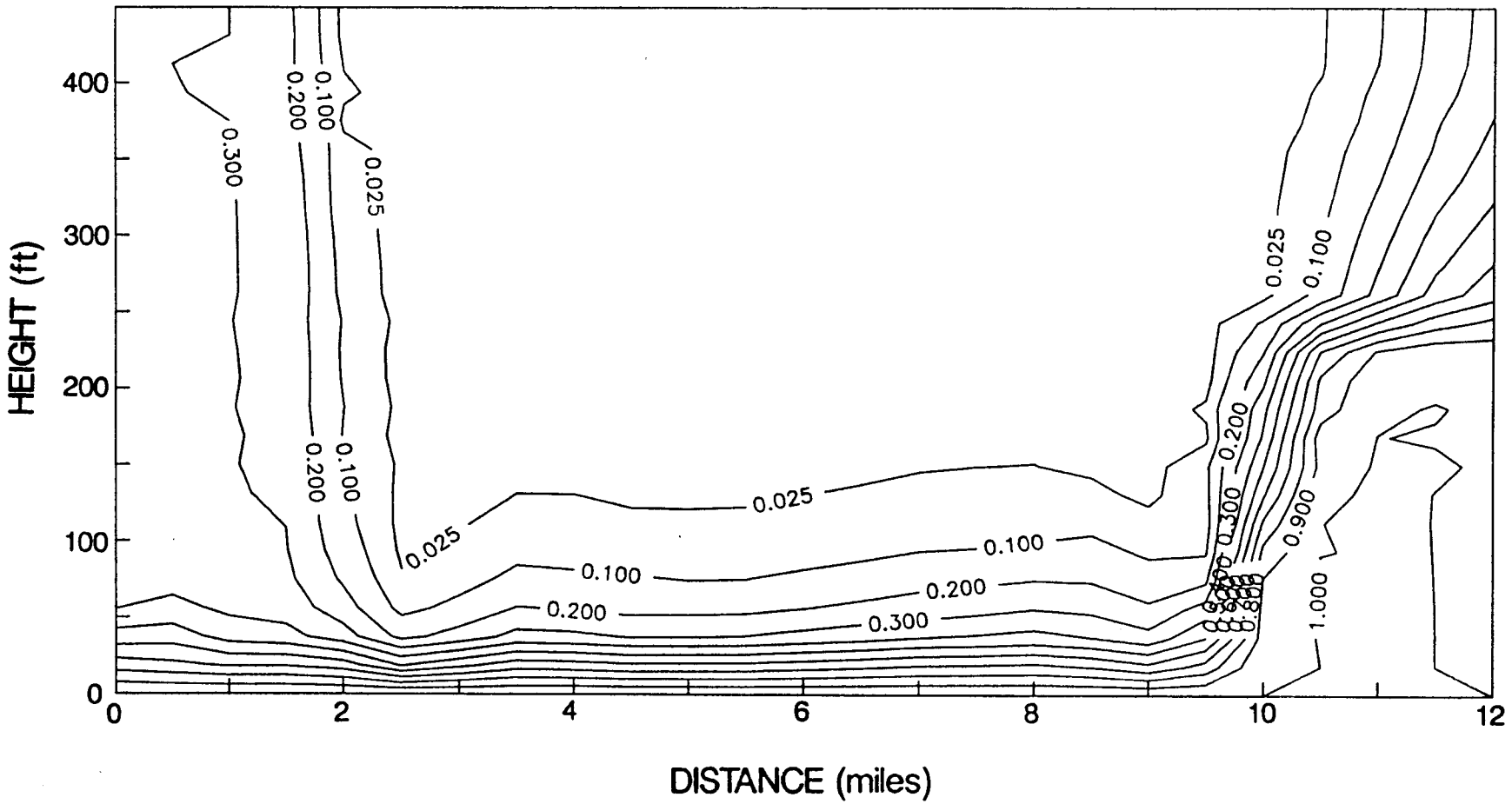

Figure 5.9 a. Relative concentration contours for calibrated simulation.

described in Figures 16, and 17 of Phelps and Rohrer (1987) for the 1982 period. The maximum thickness of the simulated freshwater lens (i.e. maximum depth to 0.025 relative concentration or 250 ppm isochlor) is approximately 300 ft, at the center of the lens. A zone of brackish water with concentration equal to about 3000 ppm extends approximately one and a half miles into the domain from the Econlockhatchee River boundary. The 1000 ppm concentration value extends approximately 2 miles into the domain from both the left (i.e. south) and the right (i.e. north) boundaries, in the upper regions of the modeled system. Figure 5.9b shows chloride concentrations along the surface of the upper Floridan aquifer. The field observed values depicted in the figure were measured at different levels in the different wells, and this could account for the discrepancies between observed and calculated values. Furthermore, the well depth and casing depth of several wells are unknown and hence the level of sampling is not completely determined. Calibration of the model is, therefore, a difficult task. The general agreement however, is reasonable considering the substantial degree of uncertainty involved.

5.5 SENSITIVITY ANALYSIS

A sensitivity analysis was performed to quantify the effect of uncertainties in boundary conditions and parameter values on the size and shape of the freshwater lens. The key factors varied from the calibrated base-case condition, and likely to be the most important ones, include the recharge and discharge fluxes of fresh

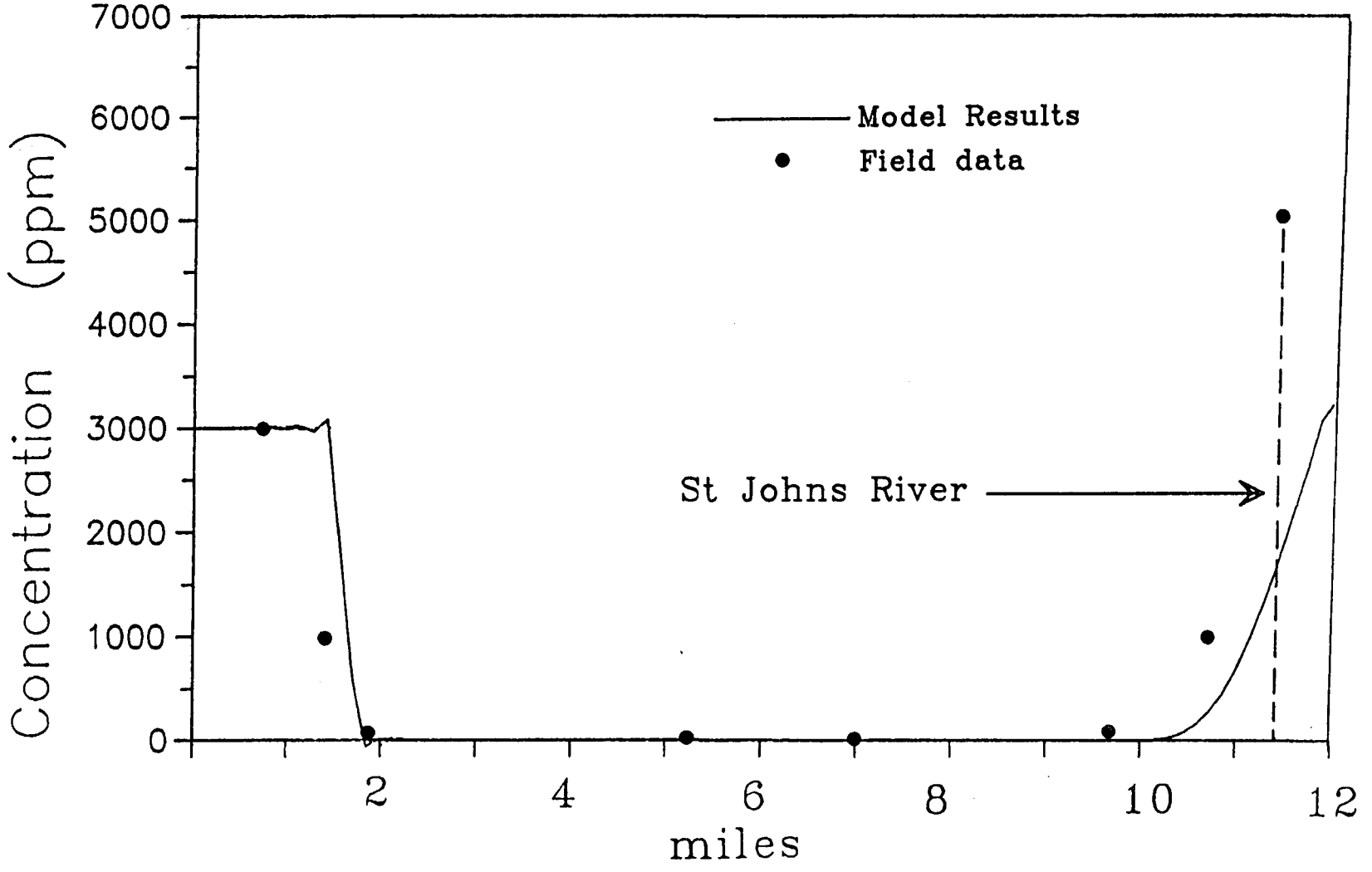

Figure 5.9b. Comparison of field data with model results along the surface of the upper Floridan aquifer.

and brackish groundwater on the boundaries of the domain, anisotropy of the hydraulic conductivity, head distribution at the domain bottom, and well pumping. For the sake of convenience, a summary of the key elements of the sensitivity analysis is provided in Table 5.3.

The first sensitivity simulation involved the case where the input concentration on the left (i.e. south) boundary was reduced from 3000 ppm to 1000 ppm (see Figure 5.8). The results are presented in Figure 5.10. The lateral extent of the freshwater lens is larger for this case, compared to the calibrated base case, with the 1000 ppm concentration contour extending only about a mile into the domain from the Econlockhatchee River boundary. The concentration results were not affected in the remainder of the domain and the freshwater lens thickness remains at 300 ft.

For the next two simulations, the net discharge from the top of the aquifer near the St. Johns River was increased from 10 ft^2/d to 20 ft^2/d and 50 ft^2/d, respectively. Concentration patterns for these sensitivity runs are shown in Figures 5.11 and 5.12, respectively. In both cases, the freshwater lens is seen to be smaller in lateral extent compared to that for the calibration run (Figure 5.9), with a brackish water concentration of 1000 ppm (0.1 relative concentration isochlor) extending 3 miles into the domain from the St. Johns river boundary. A concentration value equal to 9000 ppm (0.9 relative concentration isochlor) extends about half a mile into the domain for the 50 ft^2/d discharge case (Figure 5.12). The remainder of the domain is mostly unaffected by these

TABLE 5.3 SUMMARY OF KEY ELEMENTS OF THE 2-D SENSITIVITY ANALYSIS

Case	Key Factor	Figure	Remarks
0 (Base case)	Calibration run. See Fig. 5.8 for B.C.'s and material parameters	5.9	Lens thickness approx. 300 ft., areal extent approx. 7-8 miles. Concentration under Econlockhatchee river ≈ 1000 ppm, and under St. Johns river ≈ 3000 ppm.
1	South side input con. reduced to 1000 ppm	5.10	Lens size increased laterally by approx. 1-5 mi. near South end. Rest of lens unaffected.
2	Discharge into St. Johns River increased to 20 ft^2/d	5.11	Lens size decreases laterally by 0.5 mi to 1 mi. Rest of lens unaffected.
3	Discharge into St. Johns River increased to 50 ft^2/d	5.12	Lens size decreases laterally by approx. 2 mi. Rest of lens unaffected.
4	Discharge at North side boundary increased to 20 ft^2/d and into St. Johns River increased to 20 ft^2/d	5.13	Increasing discharge into St. Johns River tends to decrease lens size. Increasing discharge out of North side tends to increase lens size.
5	Discharge at North side boundary increased to 20 ft^2/d and into St. Johns River increased to 50 ft^2/d	5.14	For high discharge into St. Johns River, increasing discharge out of North side does not affect lens size as in Scenario 9, but spreads out the concentration contours.
6	Anisotropy of all materials increased to 50:1 (K_y changed)	Not plotted	No effect on lens.
7	Discharge into Econlockhatchee River reduced to zero	5.15	Lens is shifted to the north by about a mile. Lateral extent of lens extends beyond St. Johns River boundary.
8	Well pumping 25 ft^2/d (5 Mgal/d)	5.16	Lens reduced laterally about half a mile.
9	Well pumping 50 ft^2/d (10 Mgal/d)	5.17	Lens reduced laterally about a mile. Upconing of brackish water under well location. 250 ppm salt concentration incipient in bottom well node.
10	Ocala thickness increased to 190 ft throughout domain	5.18	Entire upper formation lateral conductivity is therefore larger, increasing lateral flow of freshwater, which extends to right edge of domain in the upper formation.

TABLE 5.3 CONTINUED

Case	Key Factor	Figure	Remarks
11	Side boundary at North is no flow; Discharge into St. John's river increased to 20 ft^2/d. Note: This is the initial condition for transient simulations.	5.19 5.20 5.21	Lens size decreases by less than half a mile laterally. Almost the same lens as base case lens of Figure 5.9.
12	All bottom heads decreased by 20 ft from values of Figure 4.4a (to be compared with case 11 above)	5.22 5.23 5.24	Lens is identical. Head profiles are also identical to that of case 11, all head values being 20 ft lower. Velocity field is also identical.
13	Prescribed heads at bottom boundary changed from values of Figure 4.4a to constant value of 20 ft freshwater head (to be compared with case 11 above)	5.25 5.26 5.27	Lens almost unchanged. True head distribution affected significantly. Velocity field affected considerably. Flow directions are however not affected greatly in the upper part of the domain where the lens develops.

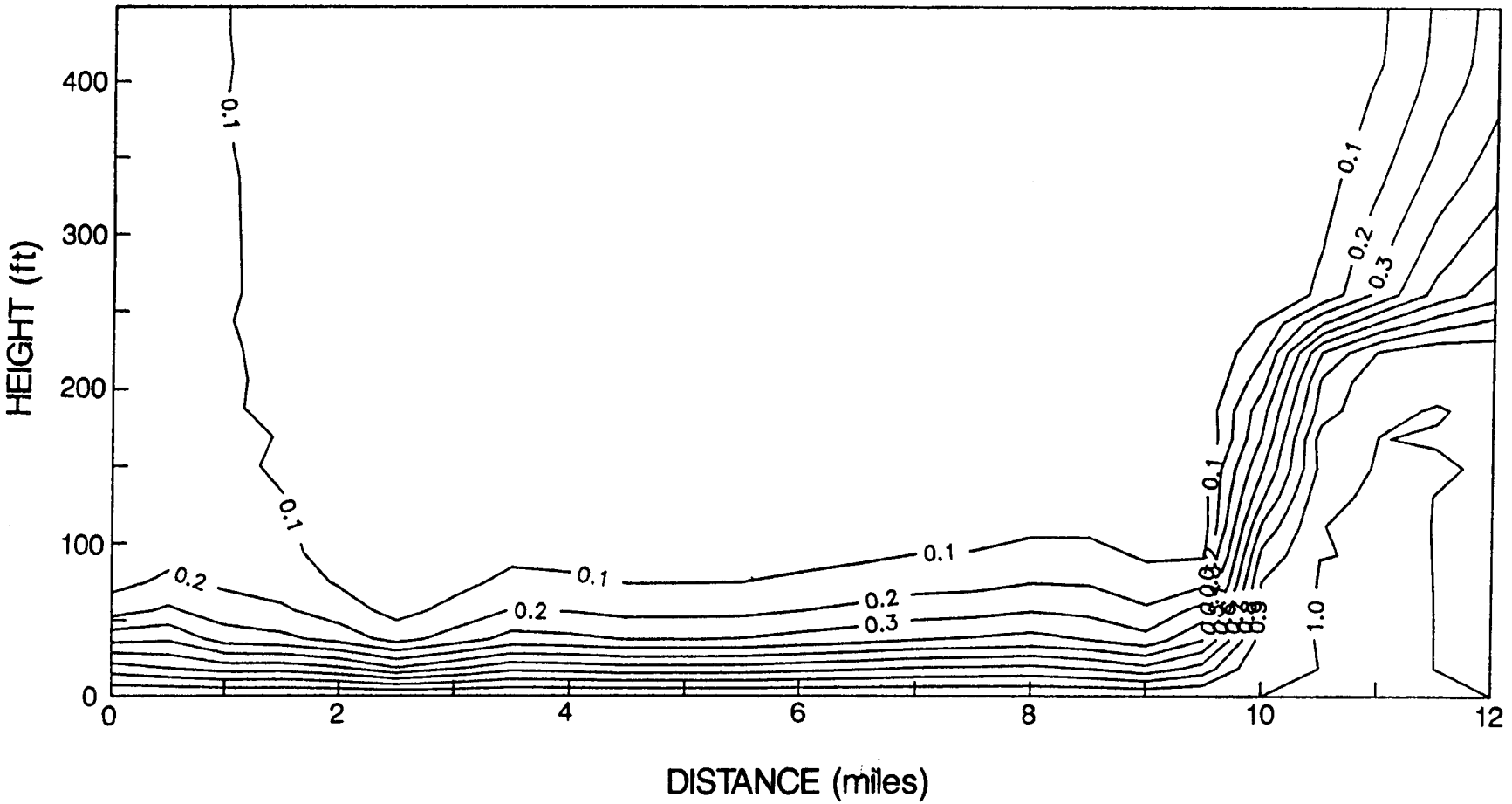

Figure 5.10. Sensitivity of predicted concentration to input concentration on the south-side of flow domain (c = 1000 ppm) [case 1, Table 5.3]

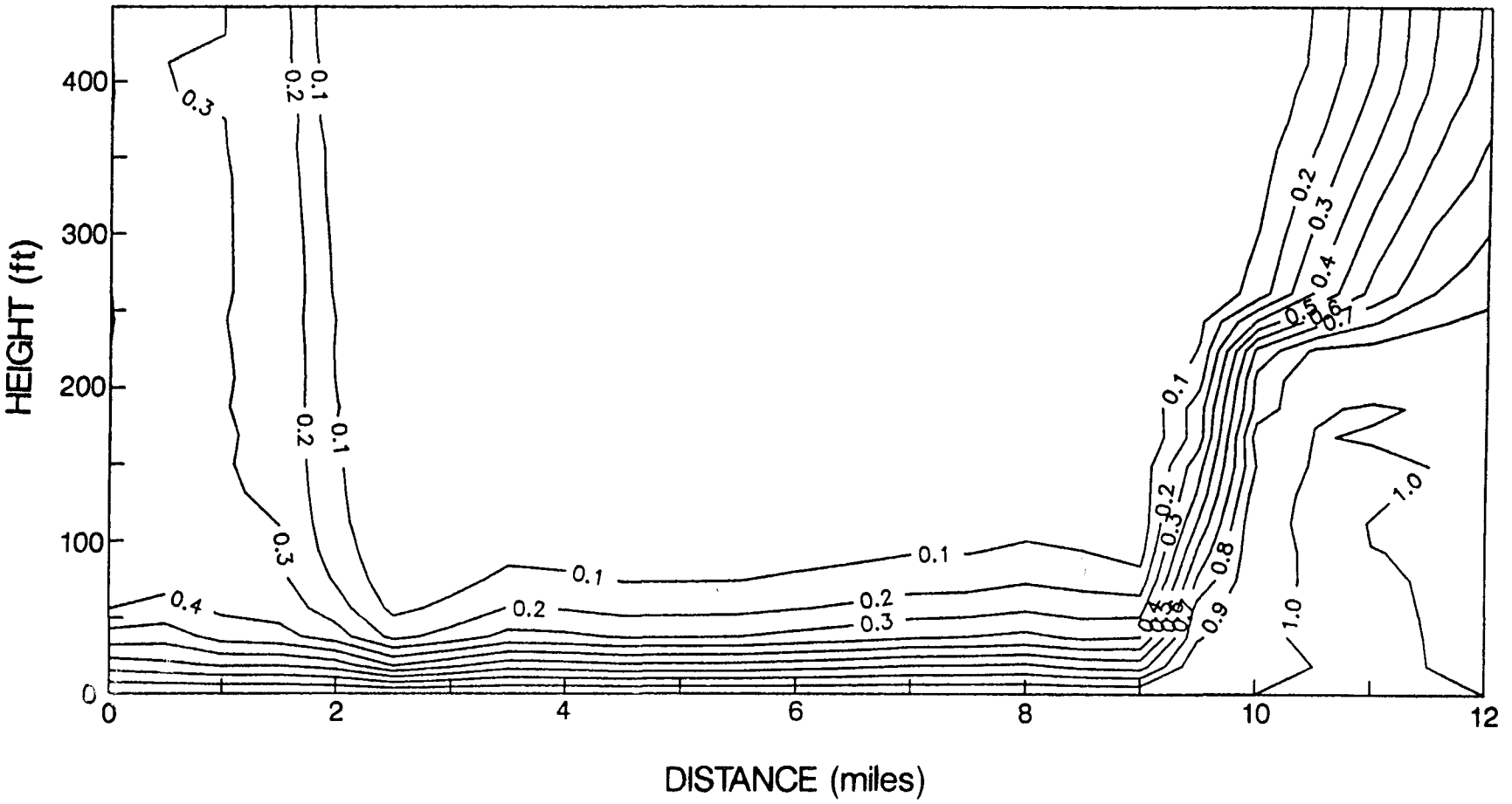

Figure 5.11. Sensitivity of predicted concentration to discharge into St. Johns River (20 ft^2/d) [case 2, Table 5.3].

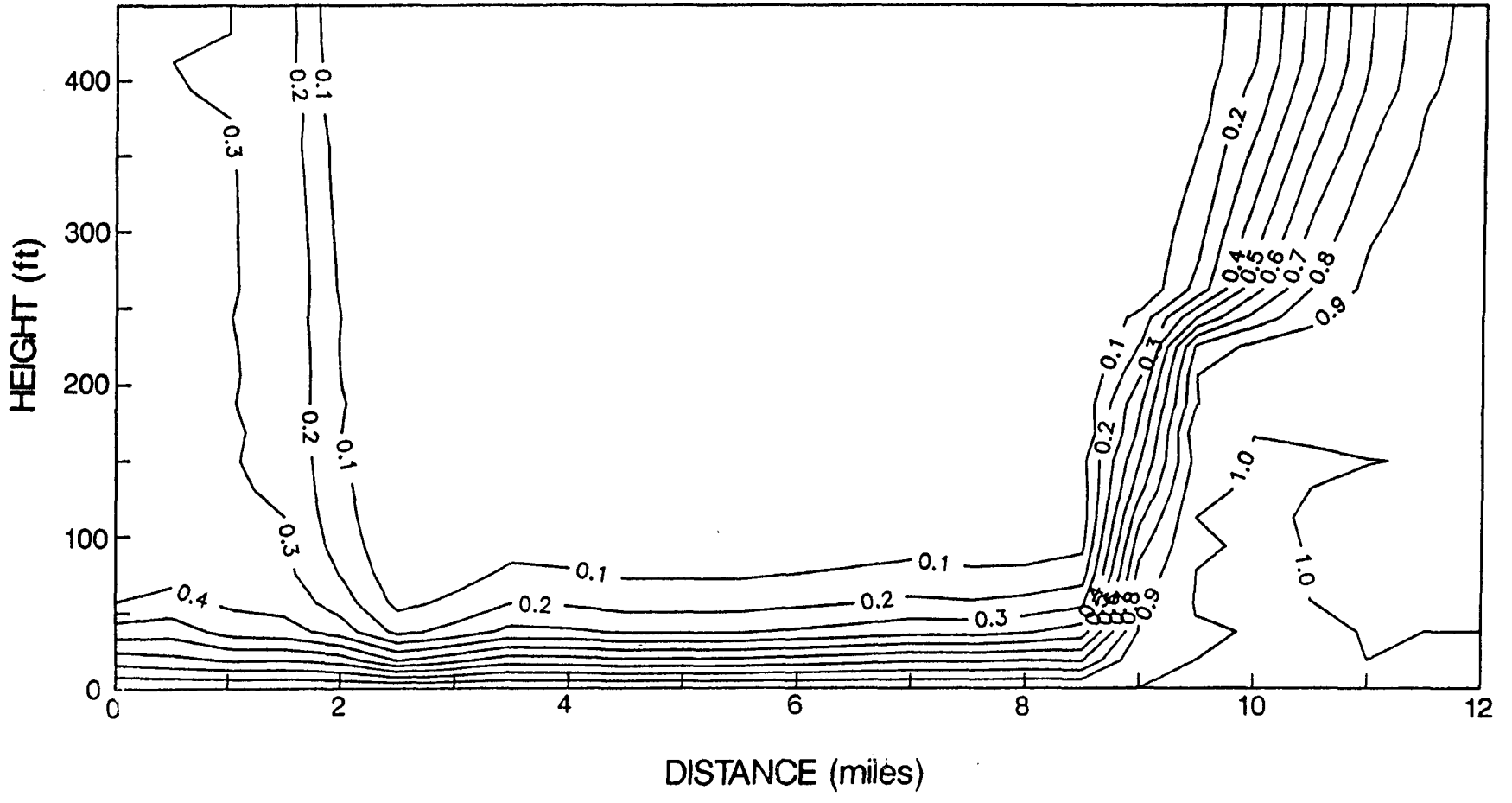

Figure 5.12. Sensitivity of predicted concentration to discharge into St. Johns River (50 ft^2/d) [case 3, Table 5.3].

different boundary discharge conditions imposed on the right-hand-side of the system.

The next simulation set considers the effect of higher discharge rates imposed along both the top and the side boundaries near the St. Johns River. This set also consists of two simulations. The discharge values used along the right-hand portion of the top boundary were 20 ft^2/d and 50 ft^2/d, and in each simulation, the discharge through the side was increased to 20 ft^2/d. Isochlors for both simulations are shown in Figures 5.13 and 5.14. The effect of an increase in the discharge flux through the right-hand side portion of the top surface is to reduce the size of the freshwater lens. This occurs primarily because of induced upward migration of the brackish water from the base of the system. An increase in the discharge through the right side tends to draw brackish water entering through the bottom boundary towards the right boundary of the domain, thus increasing the size of the freshwater lens provided that the vertical discharge through the top is not overly dominant. This can be seen by comparing Figures 5.13 and 5.11 for the case where 20 ft^2/d exits through the top near the St. Johns River boundary. For the case in which 50 ft^2/d discharges through the top (Figure 5.14), the effect of the side efflux is not dominant, and the lateral extent of the lens remains approximately the same as that of Figure 5.12. Some spreading of the concentration profiles is noticed, however, when the discharge at the side is increased. (See Figures 5.12 and 5.14) The extent of the freshwater lens in the vicinity of the St. Johns River

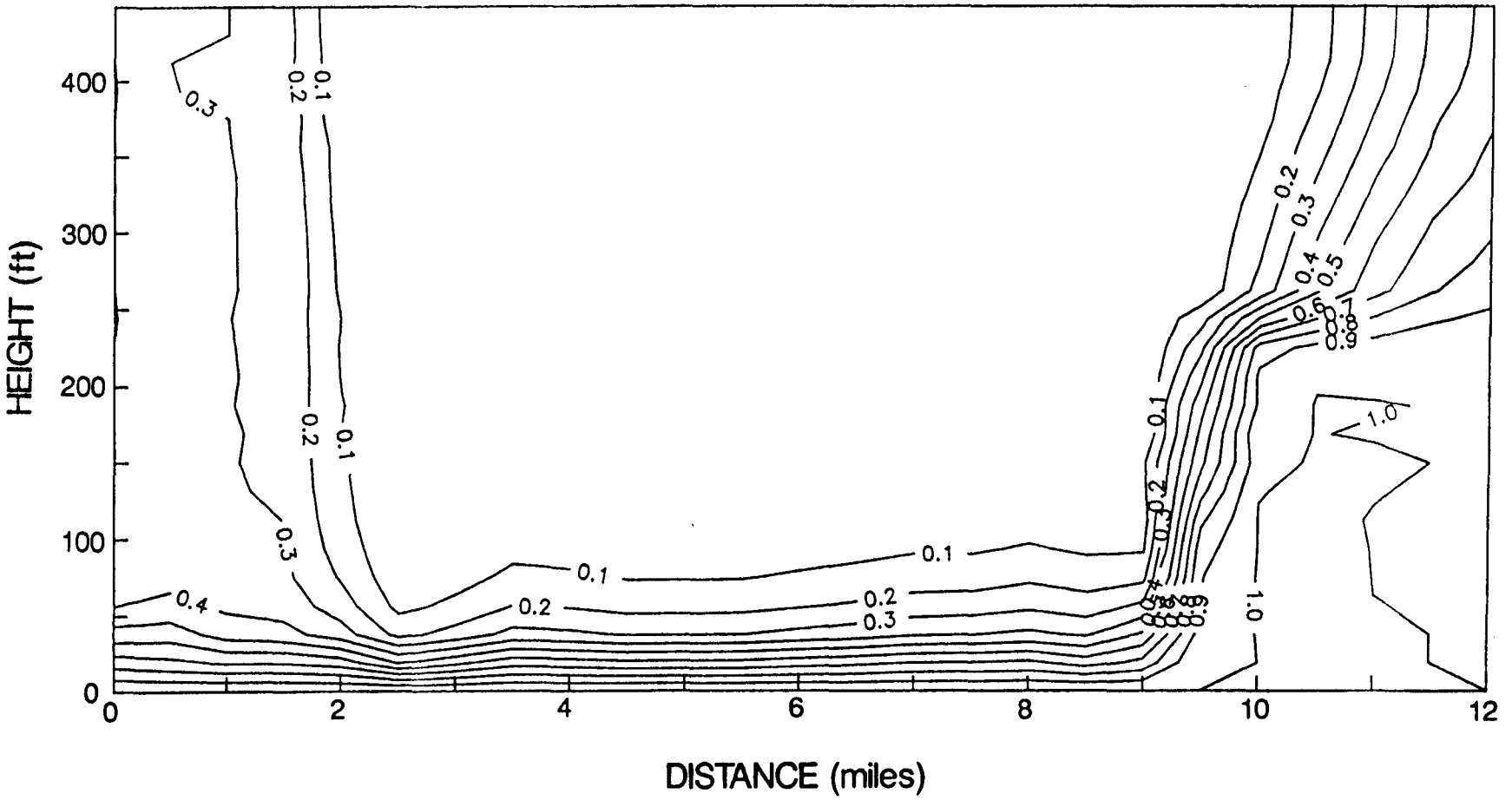

Figure 5.13. Sensitivity of predicted concentration to discharge into St. Johns river (20 ft^2/d) and discharge off North end (20 ft^2/d) [case 4, Table 5.3].

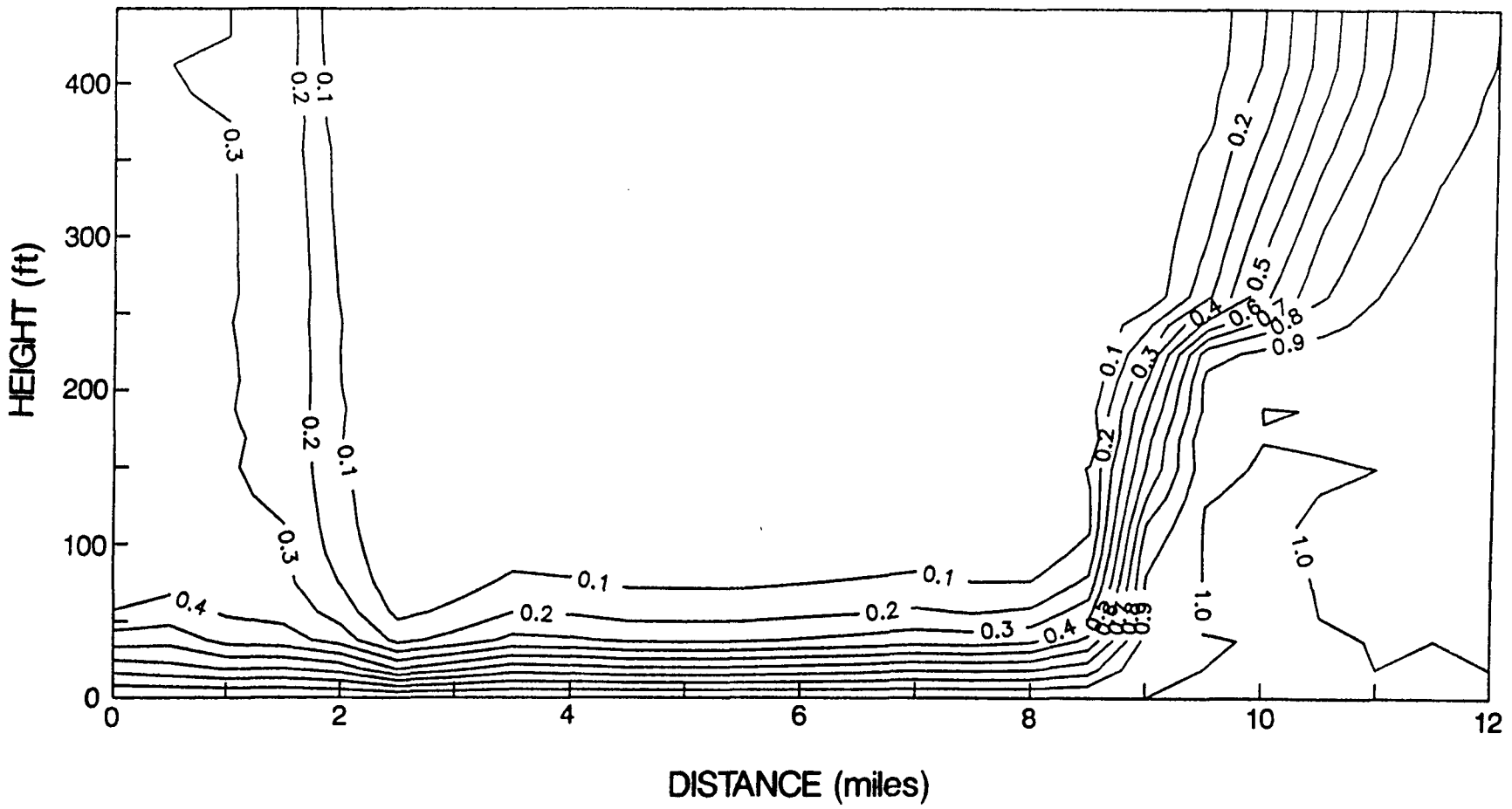

Figure 5.14. Sensitivity of predicted concentration to discharge into St. Johns river (50 ft^2/d) and discharge off North end (20 ft^2/d) [case 5, Table 5.3].

therefore depends on the discharge in this region and its spatial distribution.

Conceivably, different recharge and discharge rates or different spatial distributions of boundary fluxes (including a non-uniform discharge distribution not examined here) can produce similar chloride concentration patterns in the aquifer. Thus, additional field observations of flow patterns and chloride concentrations are required in order to represent the hydraulic and chemical response of the system more uniquely. This need becomes more critical if, for example, the response to pumping effect occurs at a specified recharge or discharge boundary. Model results may then be adversely affected by the improper representation of such a boundary condition.

The next sensitivity simulation was designed to examine the effect of a reduction in discharge across the upper surface near the left (Econlockhatchee River) boundary. An extreme case was simulated wherein the discharge across the top left portion of the boundary was zero. The result is shown in Figure 5.15. It can be seen that the freshwater lens has shifted approximately one mile towards the St. Johns River for this case. Thus, groundwater discharge through the top boundary of the Floridan aquifer in the vicinity of the Econlockhatchee River, as represented in the calibrated system, acts to prevent the encroachment of the brackish water into the domain.

The effect of anisotropy of hydraulic conductivity was examined next. The horizontal to vertical conductivity ratio of

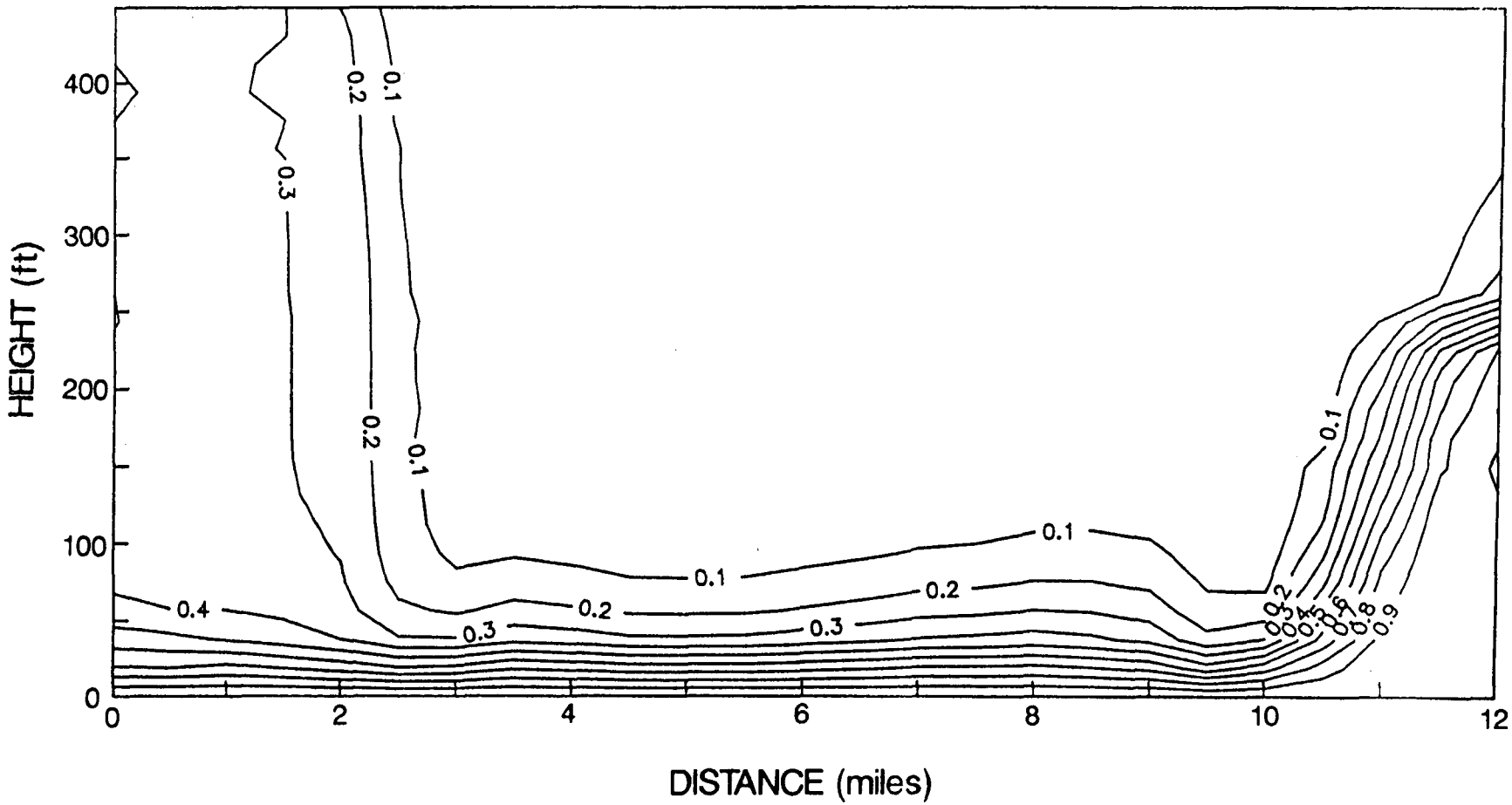

Figure 5.15. Sensitivity of predicted concentration to discharge into Econlockhatchee river (0 ft^2/d) [case 7, Table 5.3].

all hydrogeological units was increased from 10:1 to 50:1. The shape and size of the fresh-water lens were found to be essentially unchanged compared to the calibrated base case given in Figure 5.9.

The effect of steady-state pumping was studied, by first applying a recent overall withdrawal rate equal to 0.44 Mgal/d, which translates to approximately 2.2 ft^2/d per unit dimension normal to the plane of the cross-section, for an average fresh-water lens width of 5 miles. This rate of withdrawal was applied as a line sink representing a line of wells located five miles to the north of the Econlockhatchee river (i.e. left) boundary. For the sake of convenience, we will refer to this line sink as "a model well". The model well was assumed to be screened from an elevation of 325 to 375 ft. from the bottom of the simulation domain. A pumping rate of 2.2 ft^2/d (equivalent to 0.44 Mgal/d) had no apparent effect on the system compared to the calibrated results shown in Figure 5.9. A pumping rate of 25 ft^2/d (5.0 Mgal/d) reduces the freshwater areal extent by approximately half a mile, without significant effect on the lens thickness (Figure 5.16). A pumping rate of 50 ft^2/d (10 Mgal/d), however, decreases the lateral extent of the lens by more than a mile. Furthermore, significant upconing of the brackish water from the base also occurs (Figure 5.17), and the well has intercepted the 50 ppm isochlor.

It should be emphasized once again that the assumed pumping rates for the two-dimensional simulations do not accurately represent actual pumping effects because of three-dimensional flow

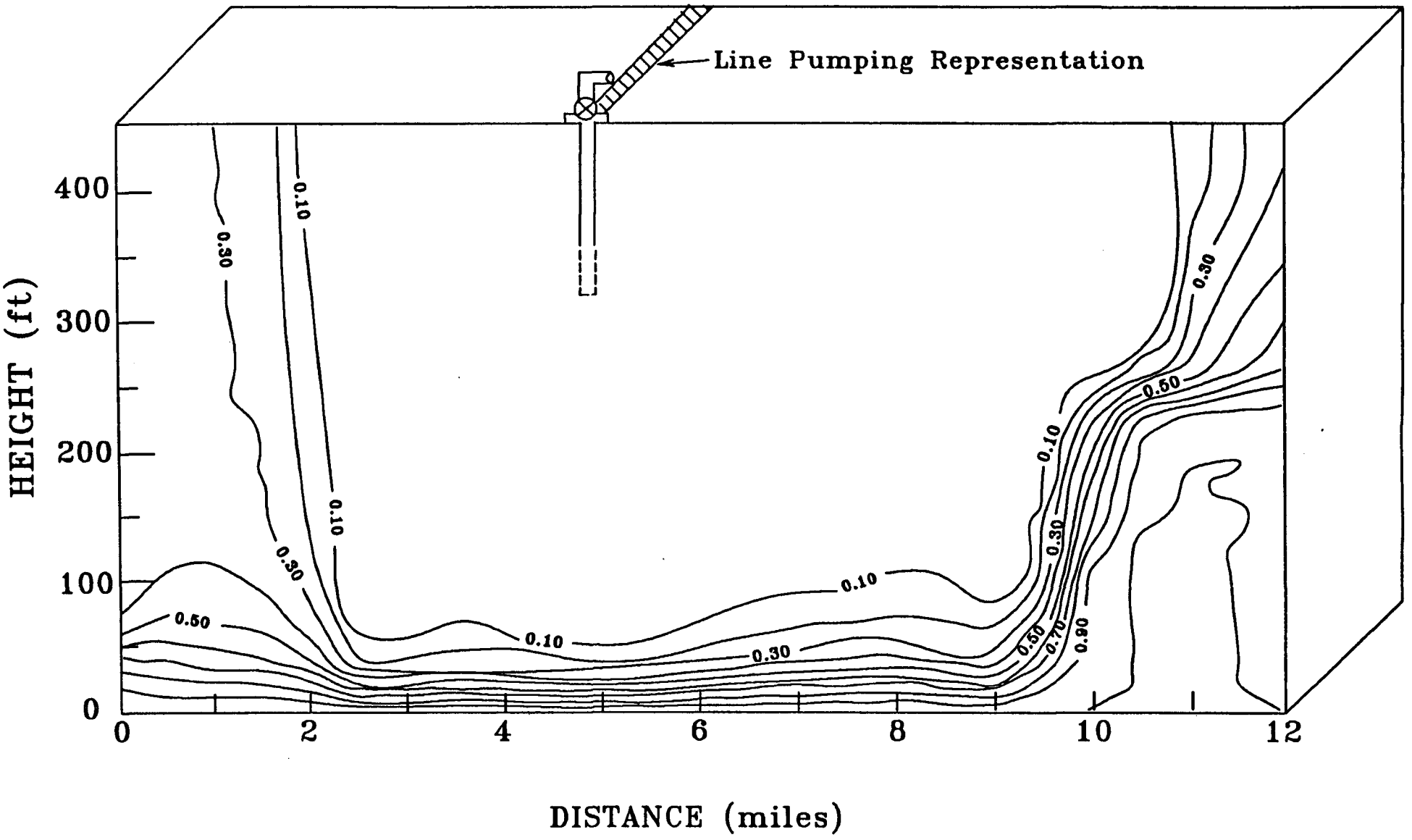

Figure 5.16. Sensitivity of predicted concentration to pumping (withdrawal rate 25 ft^2/d, pumping location = 5 mi from south edge) [case 8, Table 5.3].

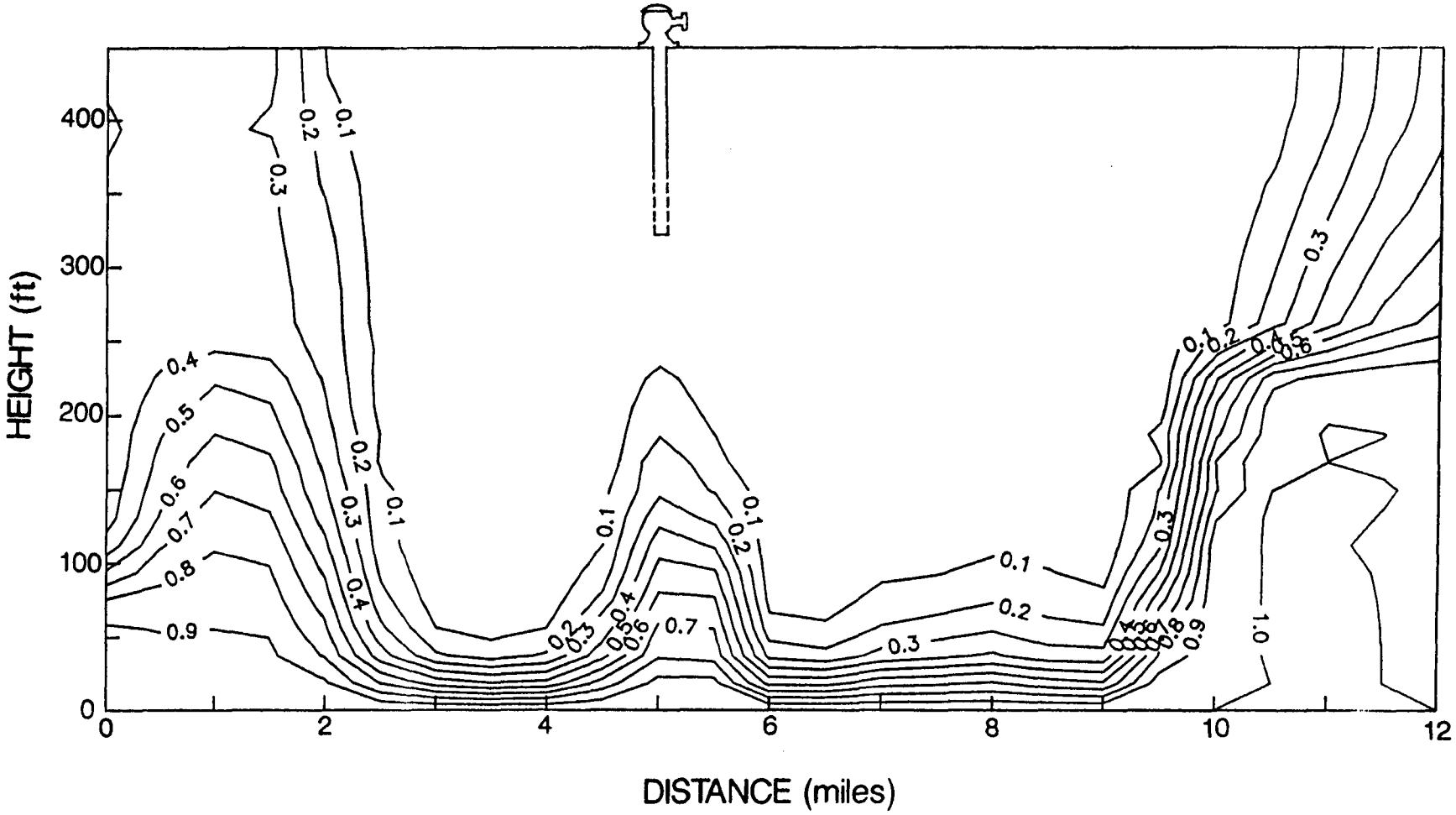

Figure 5.17. Sensitivity of predicted concentration to pumping (withdrawal rate 50 ft^2/d, pumping location = 5 mi from south edge) [case 9, Table 5.3].

effects and areal distribution of the well locations. These withdrawals are indicative of a line-pumping situation, in the direction normal to the plane of simulation(see Figure 5.16). Despite this drawback, the two-dimensional, cross-sectional simulations can show relative importance of various parameters and model sensitivity to parameter variations quite effectively.

The next sensitivity simulation was to investigate the effect of a larger Ocala formation. The Ocala formation (of higher permeability than the Avon Park formation) is 190 ft thick and extends to the lower portion of the Avon Park formation for this simulation (Figure 4.3). Concentration profiles for this simulation (Figure 5.18) show the potable lens to extend beyond the boundary of the St. Johns river for this case.

The next steady-state simulation (case 11) considers the vertical boundary near the St. Johns River to be a hydraulic divide and is hence a no flow boundary, as suggested by the District technical staff. The outflow into the St. Johns river area is however increased to 20 ft^2/d, thus maintaining a constant total outflow from the south boundary. Concentration profiles for this simulation are shown in Figure 5.19. The areal size of the potable lens decreases by less than half a mile for this scenario, from the calibrated case. The true head contours for the cross-section are plotted in Figure 5.20 for this situation (Note that the term "true head" is used in this report to refer to the actual piezometric head measured in the field). The plot in Figure 5.20 displays relatively large vertical head gradients near the base of

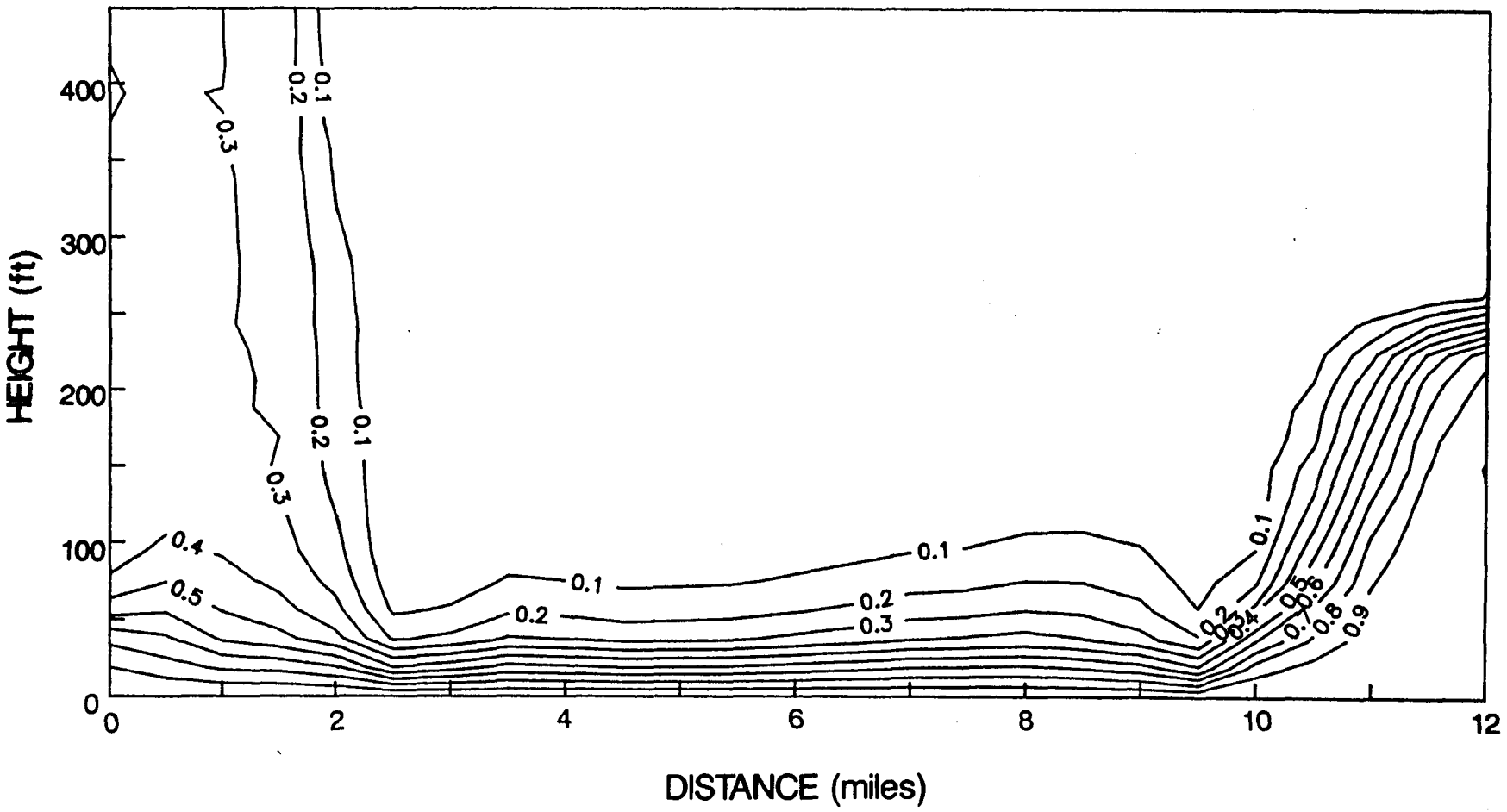

Figure 5.18. Sensitivity of predicted concentration to increase in thickness of Ocala formation [case 10, Table 5.3].

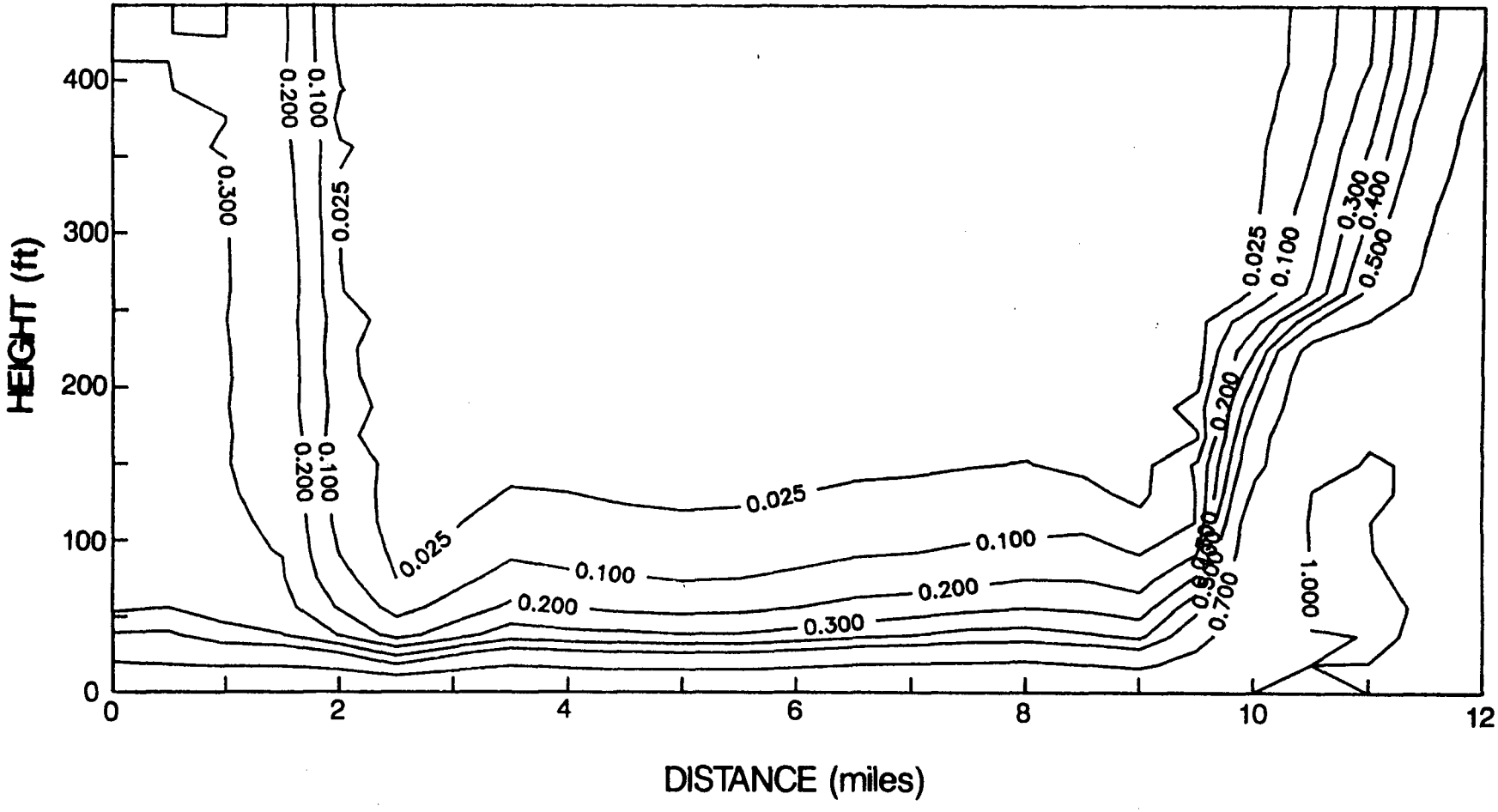

Figure 5.19. Sensitivity of predicted concentration to discharge into St. Johns river (20 ft^2/d) with hydraulic divide (i.e., no flow) at North end [case 11, Table 5.3]. Note: This is the initial condition for transient simulations that follow in Section 6.

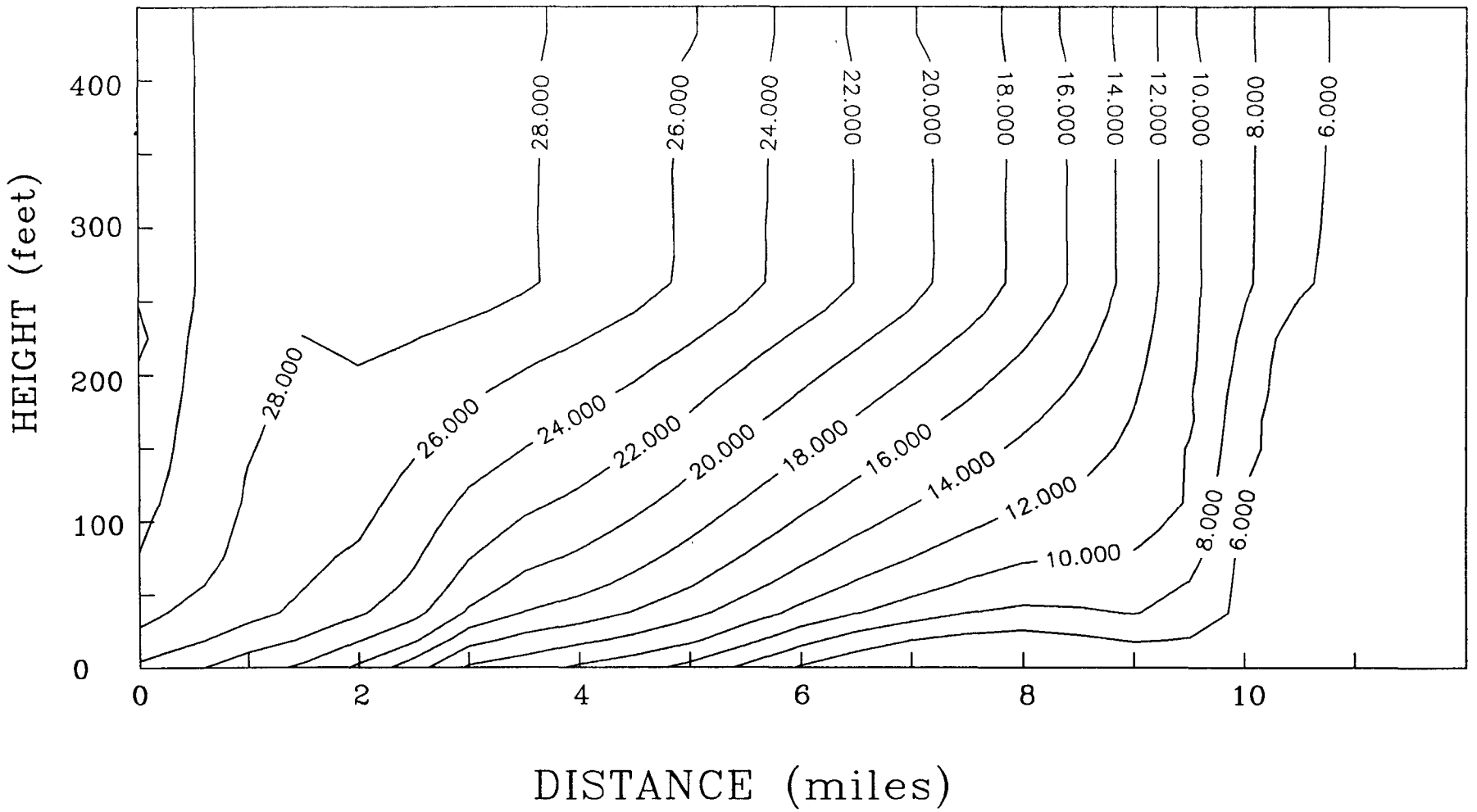

Figure 5.20. True head distribution for cross-sectional simulation of case 11 [Table 5.3].

the flow region as indicated by the manner in which the contour lines approach the bottom boundary. Generally, the head value decreases with depth and increases from left to right as expected. The flow pattern is shown by the velocity vector plot in Figure 5.21. Dominant horizontal velocity components are present in the upper portions of the system. Zones of mixing of fresh and saltwater can be noticed at locations marked a and b on the figure. Mixing occurs mainly in these zones where recharge water encounters the saline water entering the domain from the Econlockhatchee River side boundary and near the bottom right corner of the domain where freshwater interferes with saline water discharging upwards into the St. Johns River. The scenario of Figure 5.19 will be considered as the initial configuration for subsequent transient simulations discussed in Chapter 6. Tables 5.4 and 5.5 summarize the material parameter values and boundary conditions that create this steady-state lens, and briefly discuss the rationale for their selection.

The next sensitivity run is designed to examine the effects of the bottom head boundary prescription on the freshwater lens system. Data for this boundary are unknown in the system and only a rough estimate of its range can be made from the average piezometric data available at the site. For this simulation, the prescribed head values at the base of the domain are reduced uniformly by 20 ft from those shown in Figure 4.4a. The remaining parameters are identical to those used for Figures 5.19-5.21 (case 10 of Table 5.3).

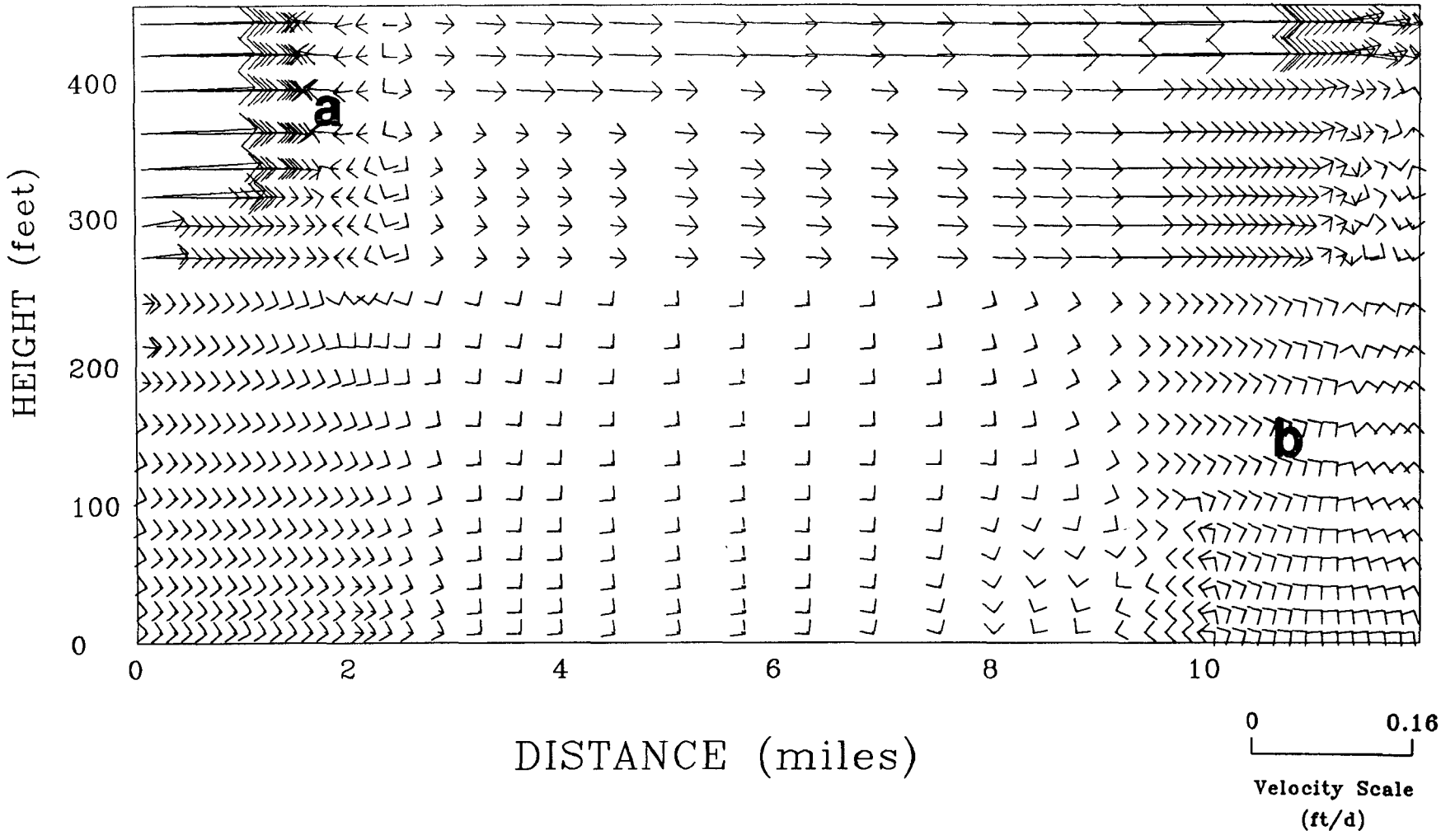

Figure 5.21. Velocity field in the cross-section for case 11 [Table 5.3]. Note that a and b in the figure denote zones of mixing.

TABLE 5.4 MATERIAL PARAMETERS FOR 2-D CROSS-SECTIONAL STEADY-STATE ANALYSIS.

MATERIAL	PARAMETER	VALUE	BASIS OR SOURCE FOR SELECTION (NOTE: EXACT VALUE FALLS WITHIN A REASONABLE RANGE)
Ocala	K_{xx} (ft/d)	160	Skipp's modeling effort (unpublished). Corroborates with Phelps and Rohrer (1987) estimates.
	K_{yy} (ft/d)	16	Skipp's modeling effort (unpublished). Within range of anisotropy values estimated by the District.
	α_L (ft)	100	Skipp's modeling effort (unpublished). Corroborates with values used for Ocala in similar locations.
	α_T (ft)	5	Value determined from model calibration by comparing predicted and observed lens shapes and chloride concentrations.
	areal extent and thickness	see Figure 5.8	Skipp's modeling effort (unpublished). Corroborates with Figures 4 and 5 of Barraclough (1962).
Upper Avon Park	K_{xx} (ft/d)	50	Same basis as for K_{xx} of Ocala above.
	K_{yy} (ft/d)	5	Same basis as for K_{yy} of Ocala above.
	α_L (ft)	100	Same basis as for α_L of Ocala above.
	α_T (ft)	5	Same basis as for α_T of Ocala above.
	areal extent and thickness	see Figure 5.8	Skipp's modeling effort (unpublished). Confirmed by communication with District personnel.
Lower Avon Park	K_{xx} (ft/d)	5	Same basis as for K_{xx} of Ocala above.
	K_{yy} (ft/d)	0.05	Same basis as for K_{yy} of Ocala above.
	α_L (ft)	50	Same basis as for α_L of Ocala above.
	α_T (ft)	2.5	Same basis as for α_T of Ocala above.
	areal extent and thickness	see Figure 5.8	Skipp's modeling effort (unpublished). Confirmed by communication with District personnel.
Salt (chlorides)	water density	1 g/cm^3	Standard value.
	max-solution density	1.013 g/cc	Standard value corresponding to chloride concentration of 10,000 ppm.
	Diffusion	0.001(ft^2/d)	Selected value based on information in the literature

TABLE 5.5 BOUNDARY CONDITIONS FOR 2-D CROSS-SECTIONAL STEADY-STATE ANALYSIS.

BOUNDARY	SECTION (SEE FIGURE 5.8)	PARAMETER	VALUE	BASIS OR SOURCE FOR SELECTION
Bottom	A - B	head	See Fig 4.4a	Skipp's simulation (unpublished). Corroborates with reported values of Phelps & Rohrer (1987) for the average piezometric head. It is the best estimate possible with available data. See sensitivity to this parameter in Section 5.5.
		conc.	10,000 ppm.	Skipp's simulation (unpublished). Most wells show this value at this depth.
Right side	B - C	fluid flux	0	Hydraulic divide estimated here by District.
		$\partial c/\partial x$	0	Natural condition of zero concentration gradient for no-flux boundary.
Top	C - D length of zone determined from Phelps & Rohrer (1987). Also Skipp's simulations	Q_3 (Fig 5.8)	20 ft^2/d	Estimate of this value. See sensitivity of lens to this parameter in Section 5.5. Due to 3-D nature of flow, this parameter needs to be calibrated for the 2-D simulations.
		$\partial c/\partial x$	0	Natural condition of zero concentration gradient for outflow boundary.
	D - E length of zone determined from Phelps & Rohrer (1987). Also Skipp's simulations.	Q_2 (Fig 5.8)	85 ft^2/d	Equivalent to 10 in/yr recharge estimated by Phelps and Rohrer (1987).
		conc.	0	Recharge water does not contain chlorides.
	E - F length of zone determined from Phelps & Rohrer (1987) altitude below 25 ft. contour	Q_1 (Fig 5.8)	20.8 ft^2/d	Discharges an equivalent quantity, as enters the domain from left side boundary. See sensitivity to this parameter in section 5.5.
		$\partial c/\partial x$	0	Natural condition of zero concentration gradient for outflow boundary.
Left side	F - G zone bounds upper two topographic layers	Q_1 (Fig 5.8)	20.8 ft^2/d	Conductivity of this zone and ambient potential gradient as estimated by Phelps and Rohrer (1987) are used to calculate flux by Darcy's Law.
		conc.	3000 ppm	Phelps and Rohrer (1987) estimate for this location.
	G - A zone bounds lower Avon Park	fluid flux	0	Negligible compared to flux across F - G, using Darcy's Law calculation for this zone.
		$\partial c/\partial x$	0	Natural condition of zero concentration gradient for no-flow boundary.

Chloride concentration contours, true head contours and the velocity field are shown in Figures 5.22, 5.23 and 5.24 respectively for this simulation. The chloride distribution and velocity field are unchanged from those shown in Figures 5.19 and 5.21. The pattern of head distribution is virtually identical to that of Figure 5.20, with all absolute values being reduced by 20 ft. This is to be expected since the prescribed heads at the bottom serve only as a datum for the flow calculation, and all absolute magnitudes are adjusted to provide the same flow field.

The next sensitivity run was performed to investigate the effect of a different head field applied at the bottom boundary. All bottom boundary heads are prescribed at 20 ft., instead of the nonuniform values presented in Figure 4.4a. Horizontal head gradients are therefore zero, and the flow component in the horizontal direction at the bottom is negligible. The remaining parameters are identical to those of cases 10 and 11 of Table 5.3. Chloride concentration profiles, true head plots and the velocity field for the cross-section are shown in Figures 5.25, 5.26 and 5.27 respectively. It is interesting to note that the freshwater lens is not significantly affected for this situation even though the true head distribution is markedly different throughout the domain. This is because the freshwater lens is controlled mainly by surface recharge and discharge patterns. The velocity field is also seen to be different from that of Figure 5.21. However, the flow directions in the upper part of the domain (where the freshwater lens is situated) are not affected greatly thus

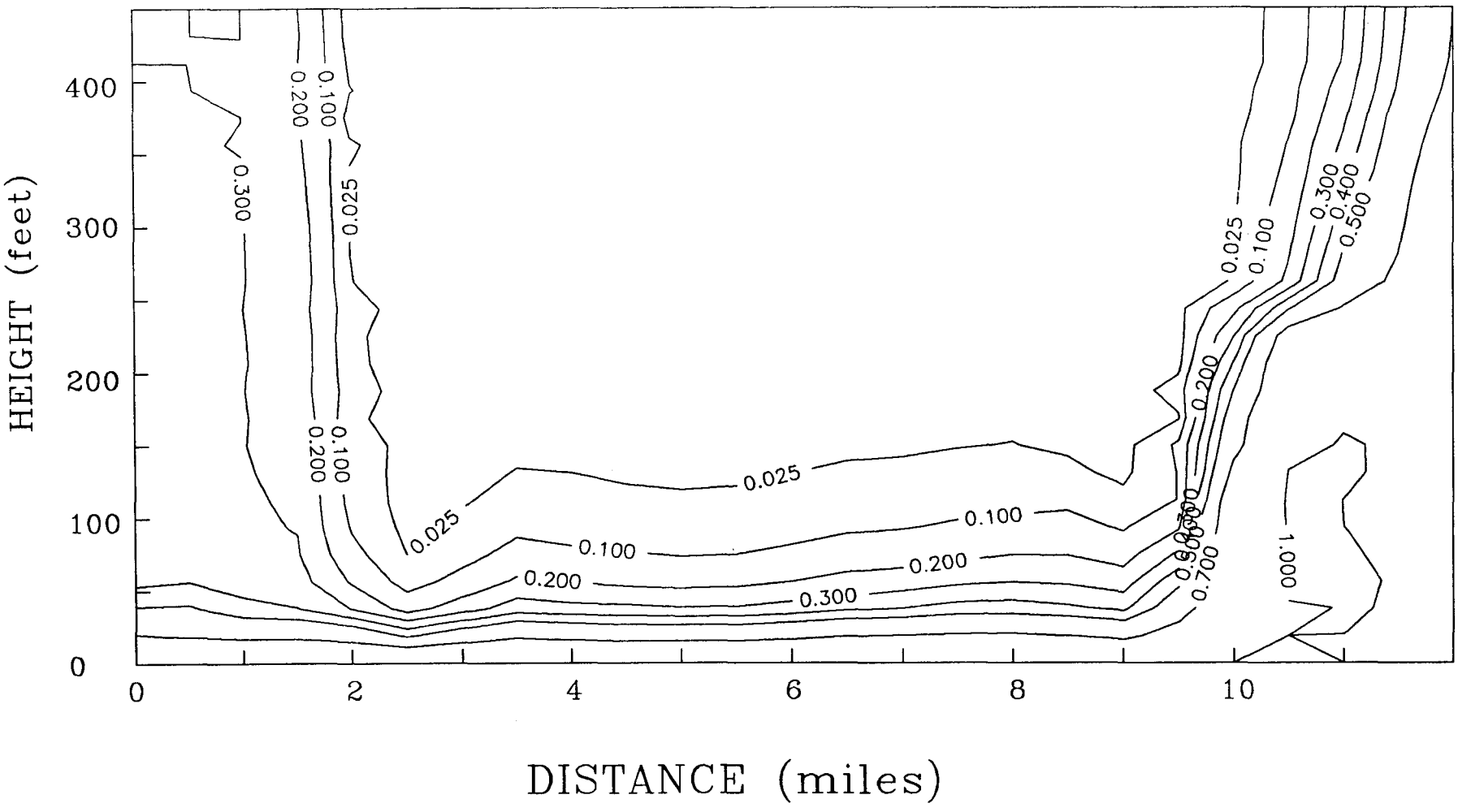

Figure 5.22. Sensitivity of concentration distribution to bottom boundary head prescription (all head values lowered by 20 ft from those of Figure 4.4a) [case 12, Table 5.3].

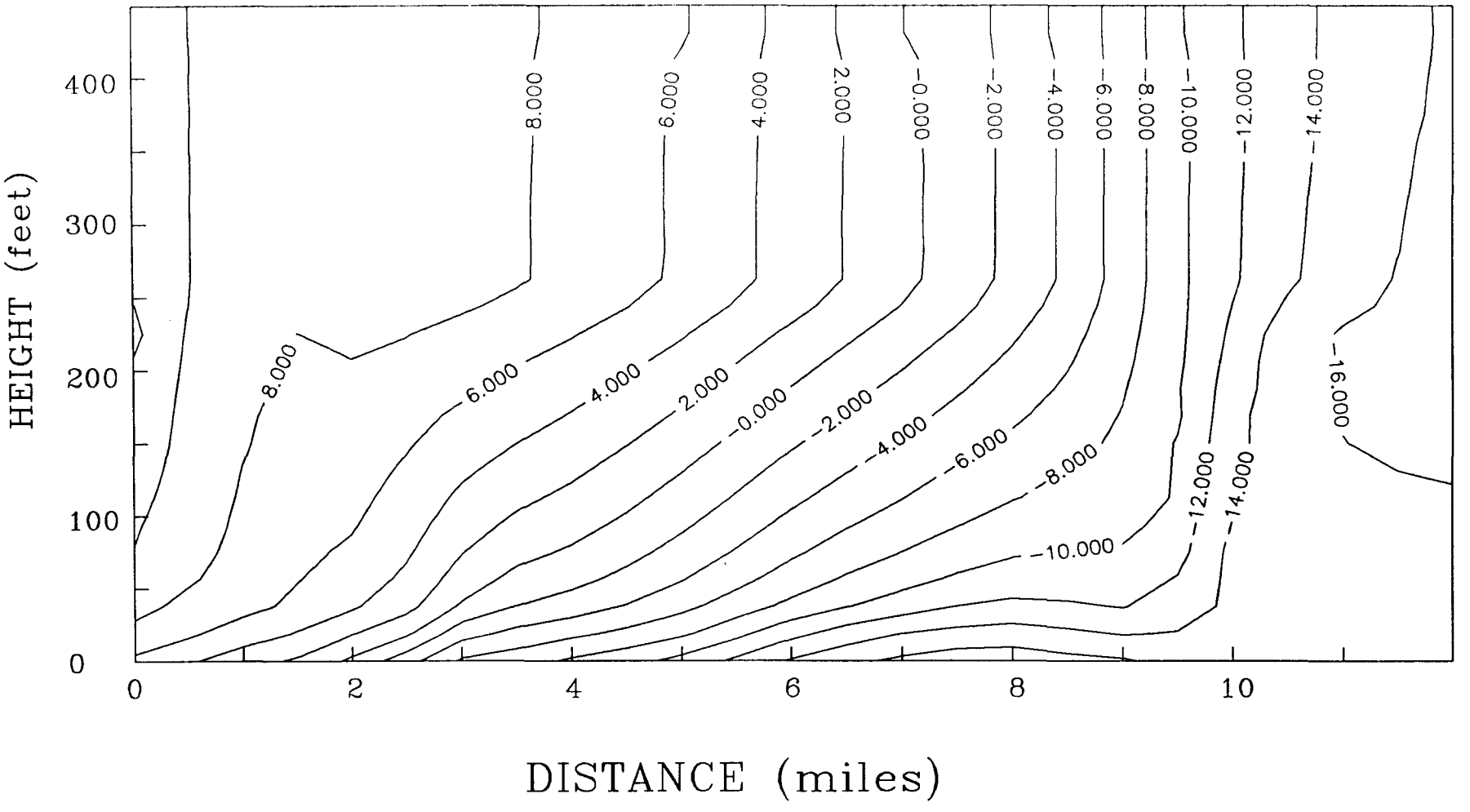

Figure 5.23. Sensitivity of true head distribution to bottom boundary head prescription (all head values lowered by 20 ft from those of Figure 4.4a) [case 12, Table 5.3].

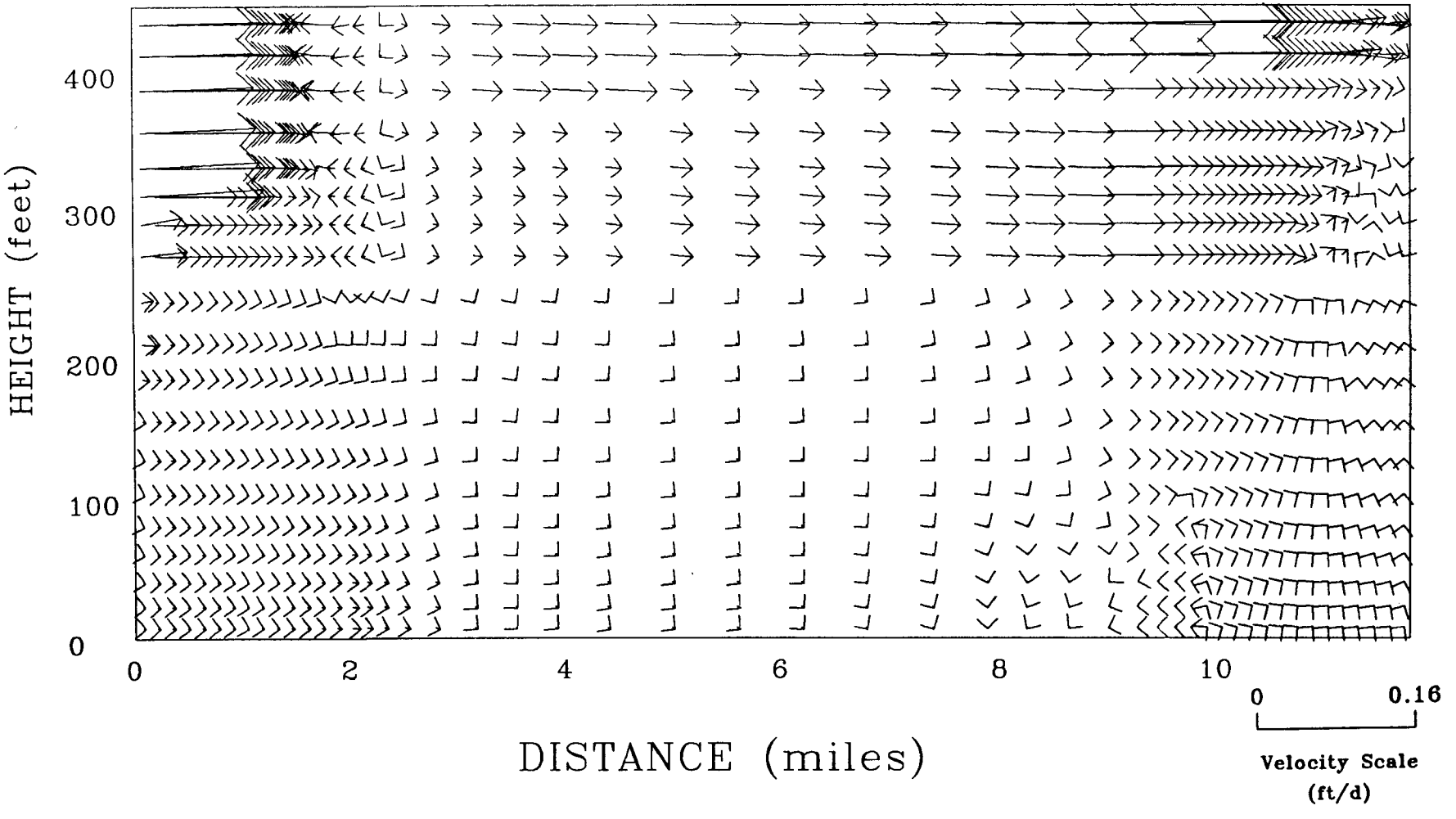

Figure 5.24. Sensitivity of velocity field to bottom boundary head prescription (all head values lowered by 20 ft from those of Figure 4.4a) [case 12, Table 5.3].

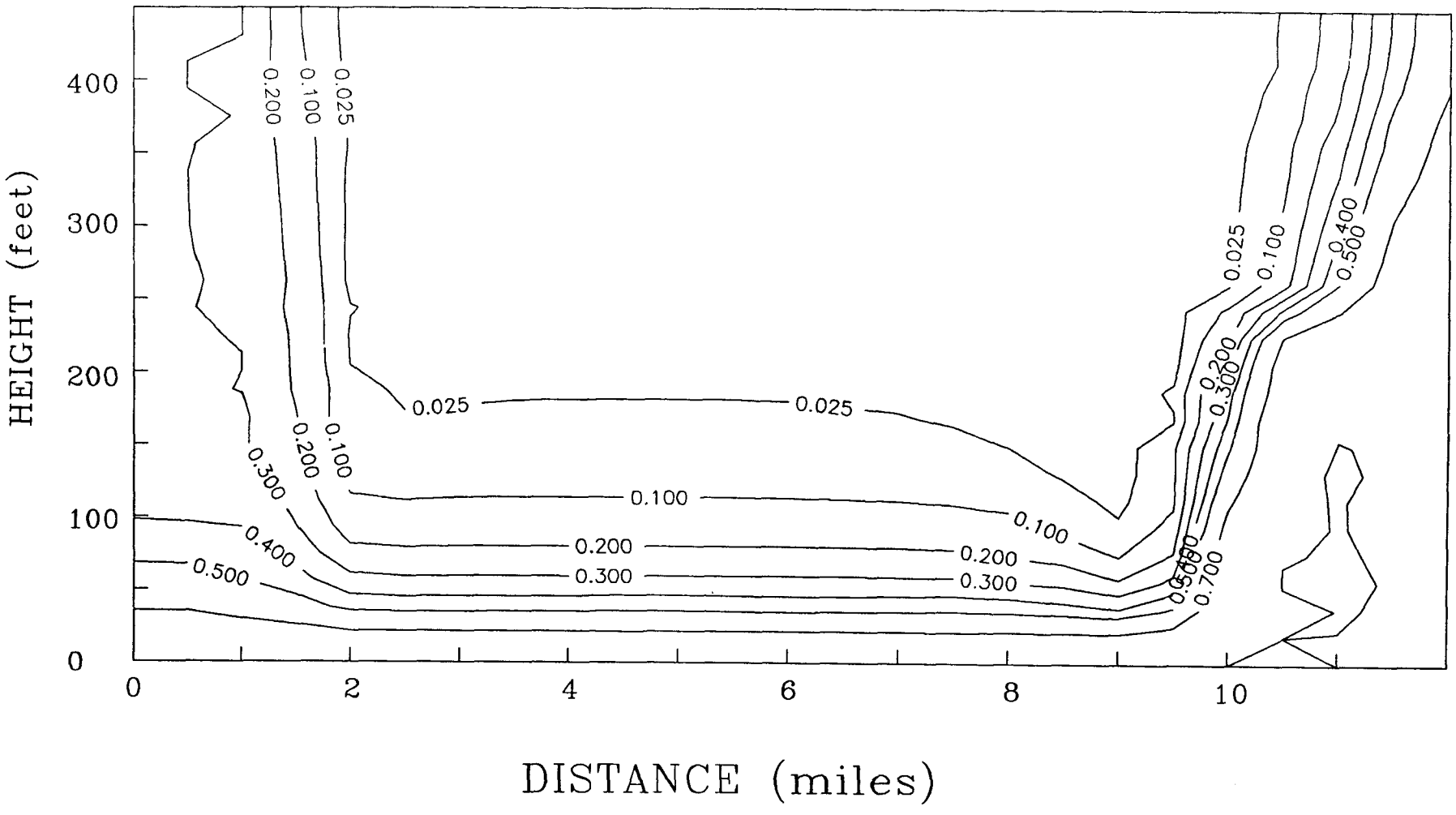

Figure 5.25. Sensitivity of concentration distribution to bottom boundary head prescription (bottom boundary head values are uniform at 20 ft) [case 13, Table 5.3].

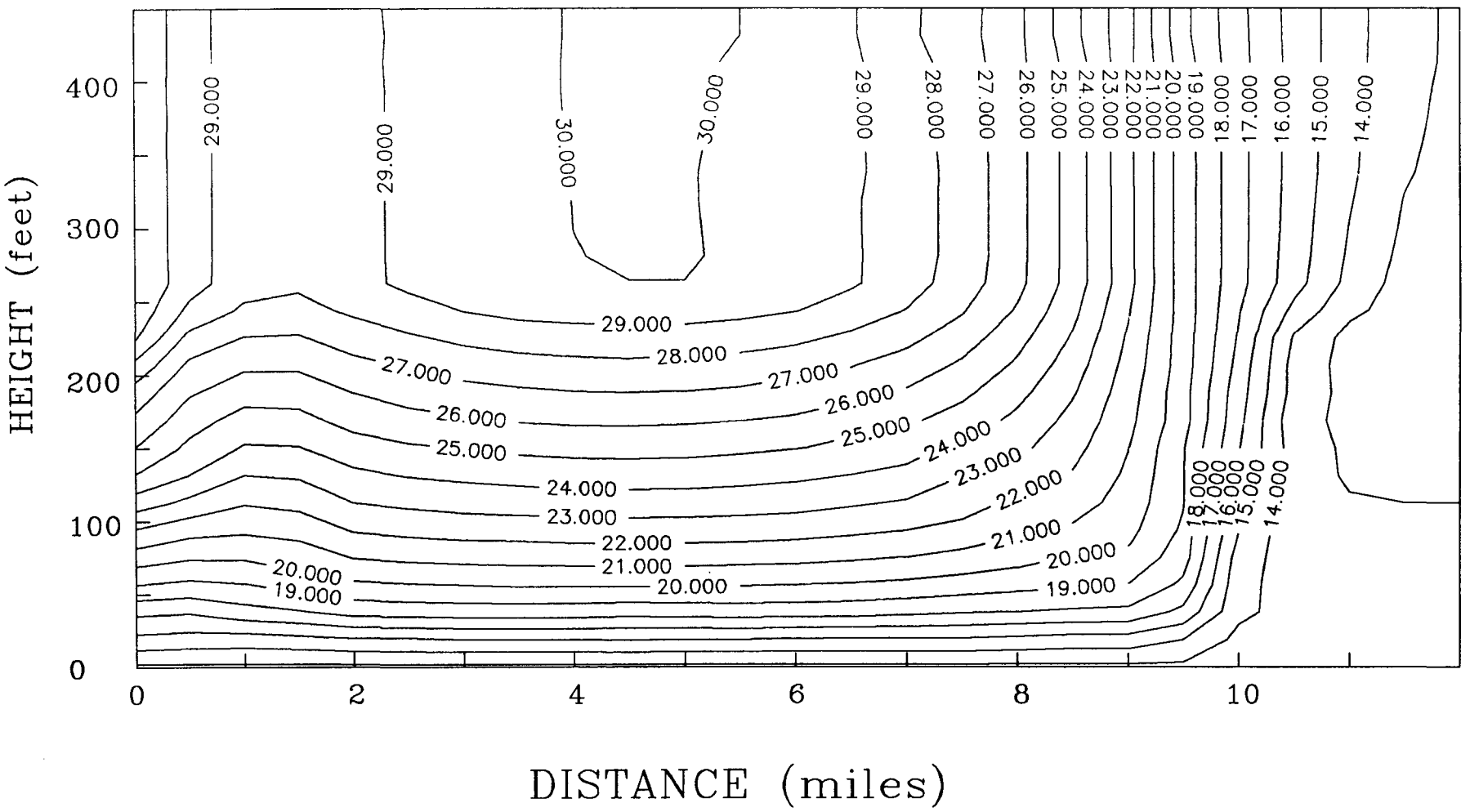

Figure 5.26. **Sensitivity of true head distribution to bottom boundary head prescription (bottom boundary head values are uniform at 20 ft) [case 13, Table 5.3].**

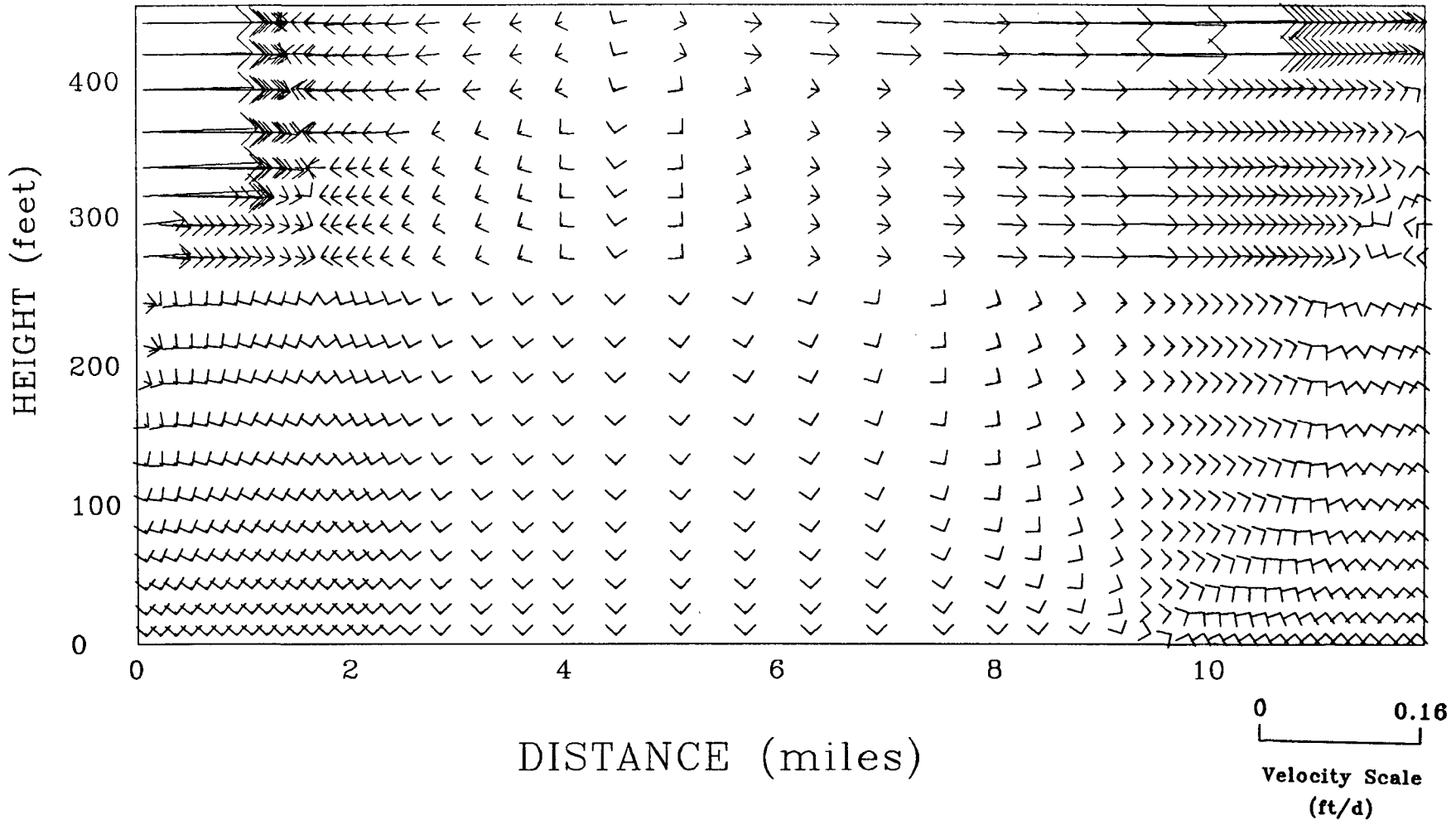

Figure 5.27. Sensitivity of velocity field bottom boundary head prescription (bottom boundary head values are uniform at 20 ft) [case 13, Table 5.3].

distributing the freshwater in a similar fashion. The low sensitivity of the freshwater lens to bottom head variations thus provides us with increased confidence in the predicted lens pattern. On the other hand, the head values within the flow domain are, however, highly sensitive to the prescribed head condition at the base. Bottom head values of the model are thus the most important information needed to obtain an accurate prediction of a steady-state head distribution within the system. Field measurements using multilevel and deeper observation wells are required to obtain a better assessment of the bottom head as well as vertical head profiles. Head at the bottom of the domain is known at only one location (well #S-0200 near site 58, Figure 3.2). Fortunately, predictions of the freshwater lens behavior and chloride distributions are of greater interest in this study, and the chloride concentration distributions are fairly insensitive to the bottom-head prescription.

5.6 SUMMARY AND CONCLUSIONS OF STEADY-STATE TWO-DIMENSIONAL CROSS-SECTIONAL ANALYSES

The two-dimensional cross-sectional simulations of the Geneva lens system have been performed. The cross-section A-A′ shown in Figure 4.2 was selected for these simulations. The section approximately passes through the center of the lens system, and is oriented approximately parallel to the main direction of ambient groundwater flow indicated by the potentiometric map of the area. Necessary modeling data for the region were assimilated from numerous sources summarized in Table 3.1. Aquifer material

parameters and boundary conditions used for the calibrated steady-state lens are shown in Figure 5.8 and are fairly representative of the available field data (Tables 5.4 and 5.5). The calibrated steady-state lens (Figure 5.9) is approximately 300 ft thick, and extends 7 to 8 mi along the top of the upper Floridan. Chloride concentrations at observation wells in the area are reasonably duplicated by the model. Depth of sampling is undetermined for most observation wells, thus increasing the difficulty of calibrating the model.

The sensitivity of the system behavior to various parameters was also studied and is summarized in Table 5.3. Key uncertainties of the model were varied to observe the system response. The lens was insensitive to varying the anisotropy ratio of all materials, and to fairly low values of pumping stresses applied on the system. High pumping stresses, however, greatly affect chloride distribution. The areal distribution of chloride is moderately responsive to discharge rates at the Econlockhatchee and St. Johns Rivers. Lens thickness is, however, unaffected by discharge rates at these locations, for the various cases examined. Further data collection should focus on quantifying discharge rates at various locations within the domain. Data obtained from the standard technique of staging the river at various locations is of limited use for this study, since random flux patterns develop in the karst system beneath the Geneva area. In addition, any additional information on vertical variation of piezometric head is essential in quantifying the absolute head distribution in the region. If

attention is only focused on, the prediction of the chloride distribution and general behavior of freshwater lens, the availability of the desirable head data is not critical. The simulated chloride concentration distribution is insensitive to imposed variations of the uncertain head at the bottom of the model.

6. TWO-DIMENSIONAL TRANSIENT SIMULATIONS

6.1 OBJECTIVES

Transient simulations of groundwater flow and chloride transport were performed for the selected cross-section of the upper Floridan system. The main objective of the transient analysis was to examine various 'worst case' scenarios. Lens responses to distribution of withdrawals and reduced recharge were described in this chapter. The response to reducing recharge was noted to be extremely slow, and hence the transients of varying recharge need not be considered. The selected conceptual model imposed recharge/discharge rates at the surface, in preference to considering an overlying aquitard with prescribed head conditions in the surficial aquifer. All cases investigated in this chapter consider a lens initially developed by a steady-state recharge of 10 in/yr. This situation has been examined in greater detail in Chapter 5 (see Figure 5.19).

Numerous scenarios were simulated in the transient study. First, the effects of reducing the freshwater recharge to the upper Floridan aquifer were examined, without pumping imposed on the system. The objectives here were to determine system response to reduced recharge rates, and how long the lens system could sustain itself during periods of low recharge. Next, pumping stresses were applied to the lens system at different locations in order to assess the impact of well placement and distribution on the position and lateral extent of the lens, on upconing of the

underlying brackish water, and on the quality of the pumped water. Two-dimensional, cross-sectional pumping scenarios are indicative of line sink or strip withdrawal. The pumping rate modeled thus corresponds to the volume of groundwater extracted per unit time per unit width normal to the plane of the simulation. Hence, results of these cross-sectional simulations should be viewed qualitatively.

One of the primary shortcomings of a cross-sectional analysis is that it neglects the effects of the transverse dimension. Furthermore, well placement and its effects and interactions are restricted to being within the simulation plane and hence optimal well field design and operation cannot be studied. However, a cross-sectional analysis can provide invaluable insight on the essential characteristics of the system, and on the general behavioral trends that can be expected from the situation under study. Furthermore, the cross-sectional model is useful as a stepping stone to fully three-dimensional modeling.

6.2 SELECTED MESH

The grid used for the steady-state analyses in Chapter 5, is exceedingly fine and will demand substantial computational effort when performing further transient analyses. It was designed to study the effects of large perturbations in the values of various parameters, with a high degree of confidence that numerical difficulties will not be encountered in zones where steep gradients and/or sharp fronts may exist. A clearer picture of system

behavior was developed from the steady-state analyses, and a more efficient yet robust grid was generated for the subsequent transient simulation study such that zones with low gradients are discretized with larger grid blocks. The new grid design, is shown in Figure 6.1. It contains 51 columns and 20 rows of nodes comprising a total of 1020 nodes and 950 elements. The mesh is finer near the edges of the domain where concentration gradients are expected to be high. Horizontal grid spacings range from 750 ft to 3200 ft, and vertical spacings range from 15 to 30 ft. To ensure satisfactory performance of this new mesh, it was calibrated against the fine mesh used previously in the steady-state analysis.

6.3 BOUNDARY CONDITIONS AND MATERIAL PROPERTIES

Material properties for the transient simulations are the same as those for the calibrated steady-state model. Boundary conditions used are also the same unless otherwise specified. These values have been presented in Figure 5.8 and Tables 5.4 and 5.5. The fluxes Q_2 = 85 ft^2/d, and Q_1 = 20.8 ft^2/d have been maintained throughout these simulations. However, the flux Q_4 has been set to zero, and Q_3 = 20 ft^2/d, since a hydraulic barrier is reported to be present at the St. Johns river edge of the domain. The transient simulations require knowledge of the specific storage and effective porosity values of each of the material types. The chosen values of specific storage are 6.6×10^{-4}, 4.4×10^{-4} and 2.2×10^{-4} ft^{-1} for the Ocala, Avon Park and the lower layer, respectively. The corresponding values of effective porosity are

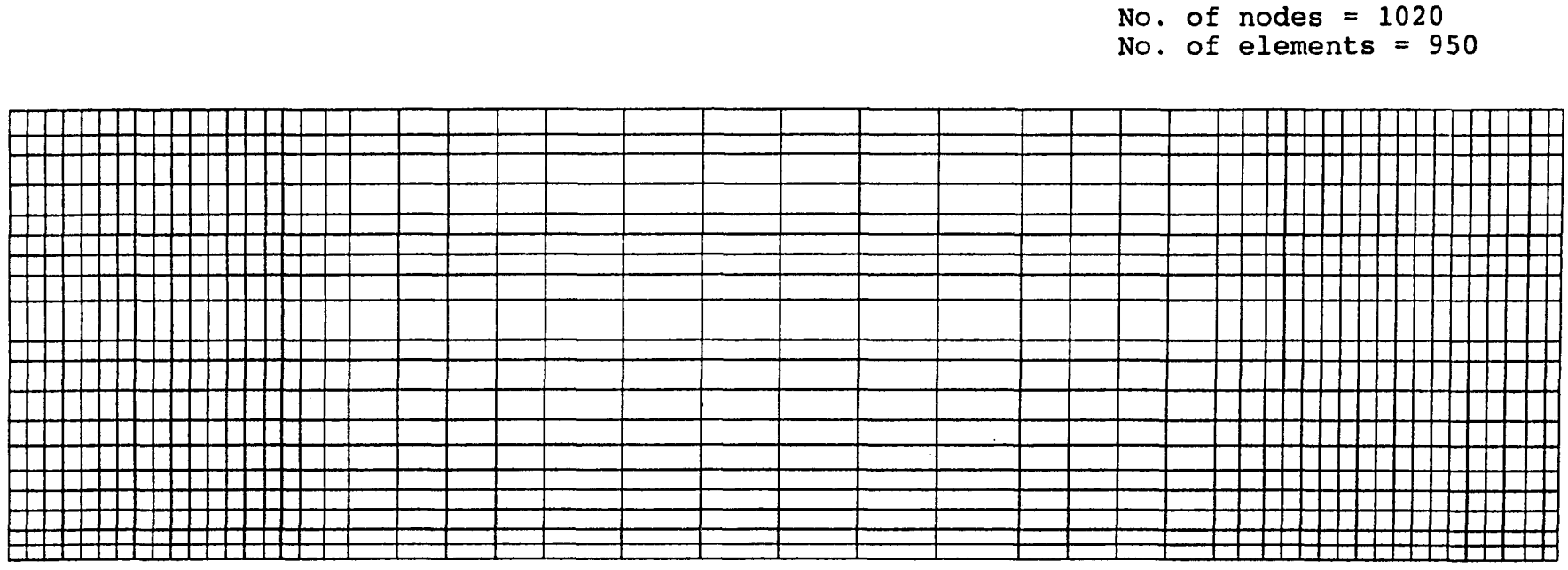

Figure 6.1. Domain discretization for transient simulations

0.3, 0.2 and 0.1, respectively. The case where the top boundary fluxes are prescribed (as opposed to the case where the heads above an overlying aquitard are prescribed) was used in the transient simulations in order to clearly relate the predicted lens behavior to the different values of pumping rates and to the recharge and discharge that were imposed. The initial condition for each transient simulation was assumed to correspond to the steady-state result of the calibrated model shown in Figure 5.19.

6.4 MESH CALIBRATION SCENARIO SIMULATIONS

6.4.1 Mesh Calibration Run

The newly designed grid for the transient simulations was first tested by performing a steady-state simulation identical to that of the calibration run described in Section 5.4. For this case, the ambient brackish water inflow of 20.8 ft^2/d and concentration equal to 3000 ppm is supplied at the left (i.e. south) boundary. Along the upper boundary, the outflow is specified as 20.8 ft^2/d over a two-mile distance (i.e., Q_1 = 20.8 ft^2/d, Figure 5.8). The next seven miles along the upper Floridan has a recharge of Q_2 = 85 ft^2/d, which is the only source sustaining the fresh-water lens. A discharge of Q_3 = 10 ft^2/d is specified along the next three miles of the upper boundary near the St. Johns River, and a discharge of Q_4 = 10 ft^2/d is prescribed along the upper portion of the right boundary. The bottom of the simulation domain comprises brackish water at a concentration equal

to 10,000 ppm. The hydraulic heads along the bottom boundary are as prescribed for the steady-state simulation. Figure 6.2a depicts the steady-state concentration contours obtained from the newly designed grid, and Figure 6.2b shows a comparison of results from the two grids. The solid lines indicate concentration profiles from the fine grid, while the dashed lines represent concentration profiles obtained using the new coarser grid. Because the results of the two simulations are almost the same, it can be concluded that the coarser grid shown in Figure 6.1 is suitable for the transient simulations. The slight differences can be attributed to both the grid design and the interpolation routines used by the contouring software.

6.4.2 Initial Condition for Transient Simulations

The initial lens profile for transient simulations is shown in Figure 5.19. This is the sensitivity case where $Q_4 = 0$, and $Q_3 = 20$ ft^2/d. The lateral flow is set to zero for this case, since the district estimates that a hydraulic divide occurs at the boundary near the St. Johns River.

6.4.3 Decreasing Recharge and Pumping Scenarios

Transient response to various scenarios were sought in the next set of simulations. The first simulation examined lens response to the extreme case of zero recharge to the system, over long time periods. The remaining transient simulation examined the effects of well placement in the Geneva lens system. These

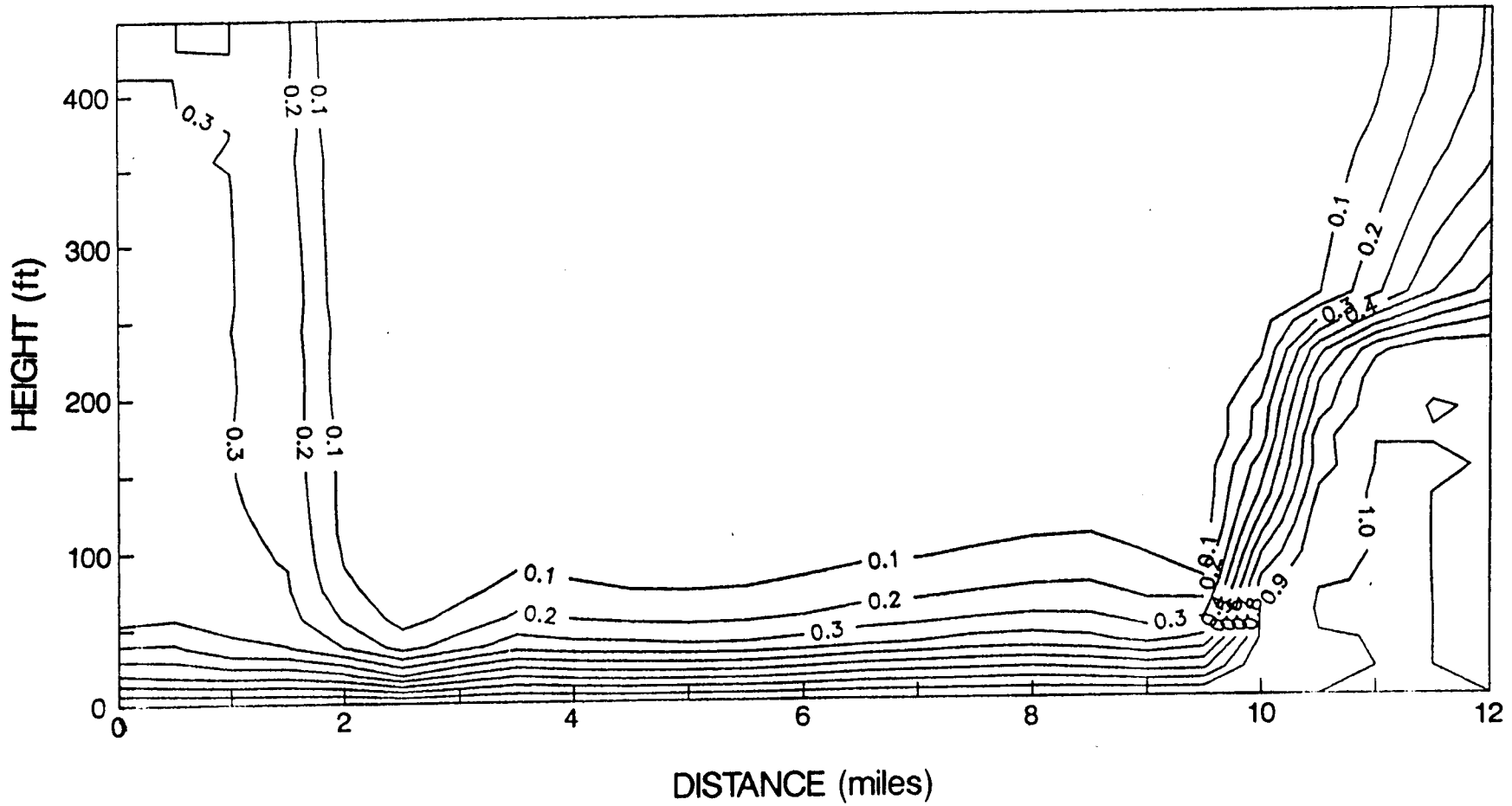

Figure 6.2a. Calibrated steady-state chloride concentration contours of new grid; initial condition for transient simulations.

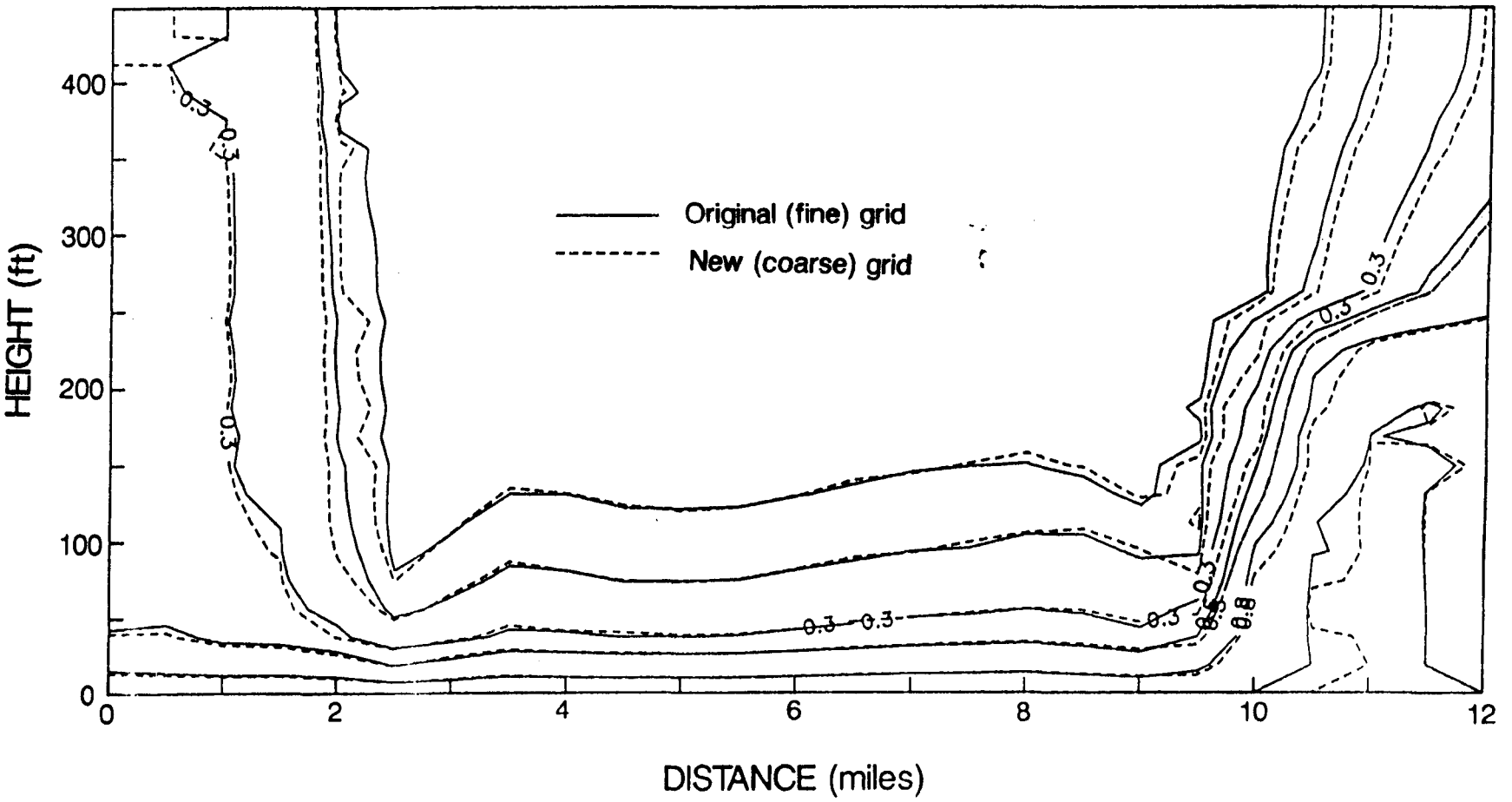

Figure 6.2b. Comparison of steady-state concentration contours for the two grids.

simulations should be analyzed qualitatively since the true system is three-dimensional.

The first transient scenario simulation was performed to examine the effects of a reduced recharge on the shape and size of the freshwater lens. The lateral discharge at the right-hand-side boundary, Q_2, in Figure 5.8, was set to zero for this simulation. All other conditions were kept identical to the steady state scenario mentioned above. The concentration contours at 25, 50, 100, and 150 years are plotted in Figures 6.3, 6.4, 6.5, and 6.6 respectively. The lateral extent of the lens is seen to decrease at an extremely slow rate. Outflow from the top of the upper Floridan near the Econlockhatchee River causes the brackish water to migrate upward from the bottom boundary. The 250-ppm isochlors at 0, 25, 50, 100, and 150 years are shown in Figure 6.7. The lens reduces by 3½ miles in lateral extent over a period of 150 years of no recharge. The 250-ppm concentration value has encroached approximately 2 miles further into the pre-existing lens on the Econlockhatchee River side, and approximately 1.5 miles on the St. Johns river side over this period, demonstrating the extremely slow response of the lens to reduced recharge. Further simulations, therefore, need not focus on the effects of varying recharge to the lens system, since it is of little practical concern. The following set of simulations, therefore examines the effects of pumping distribution from the Geneva fresh-water lens system. The pumping scenarios consider a withdrawal of 75 cubic feet per day per unit dimension normal to the cross-section, from the lens.

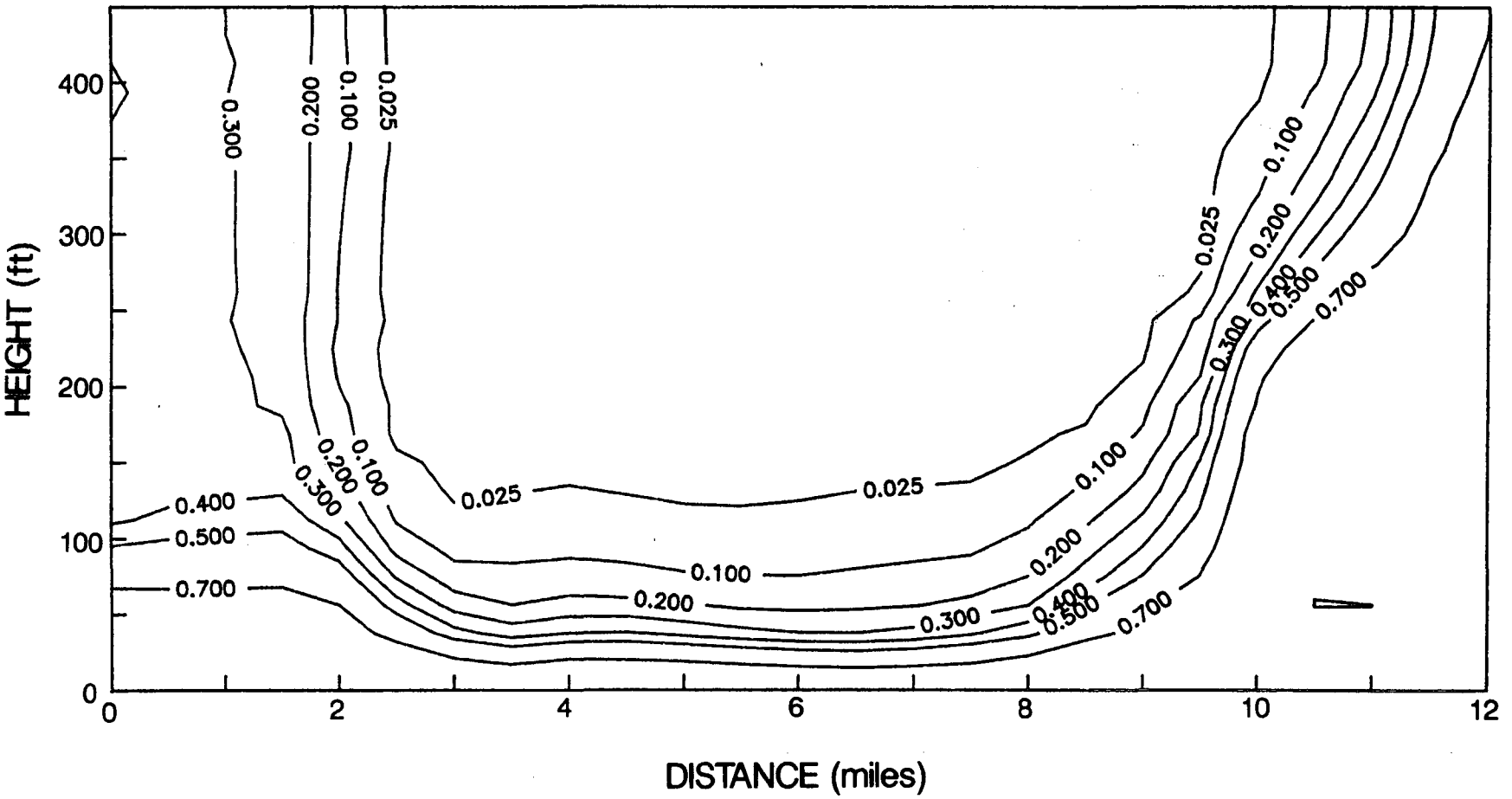

Figure 6.3. Relative concentration contours at 25 years for zero recharge.

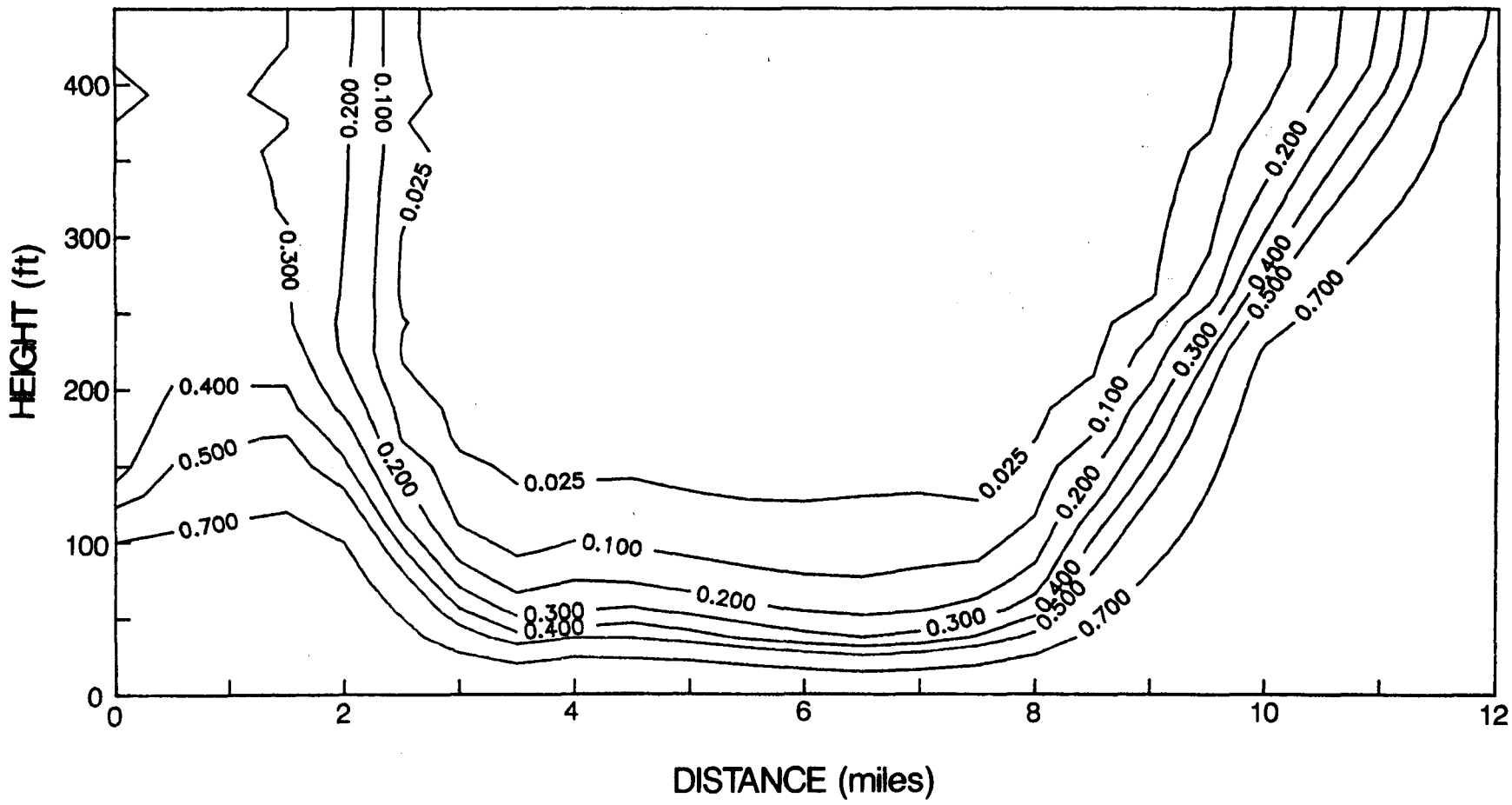

Figure 6.4. Relative concentration contours at 50 years for zero recharge.

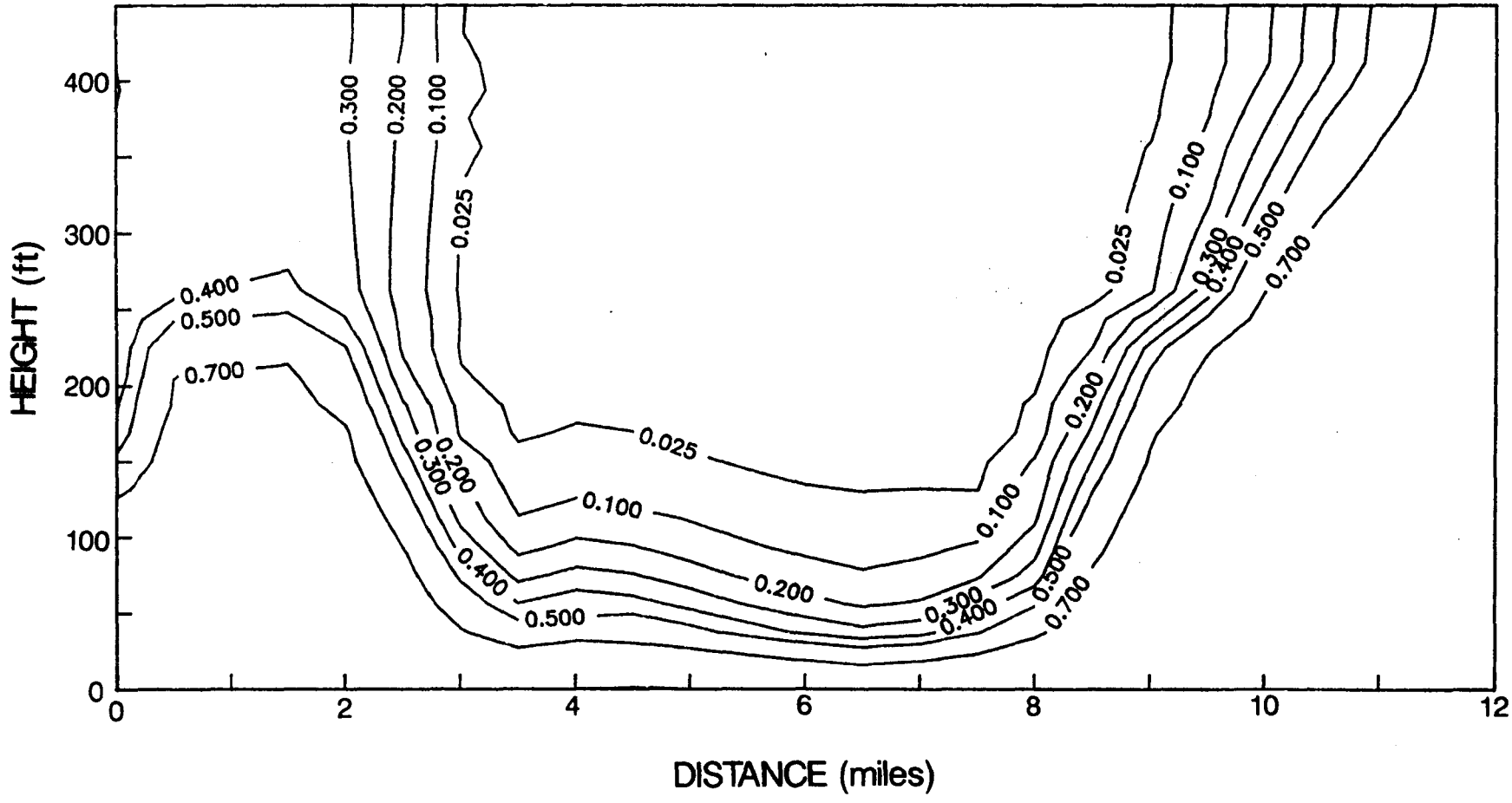

Figure 6.5. Relative concentration contours at 100 years for zero recharge.

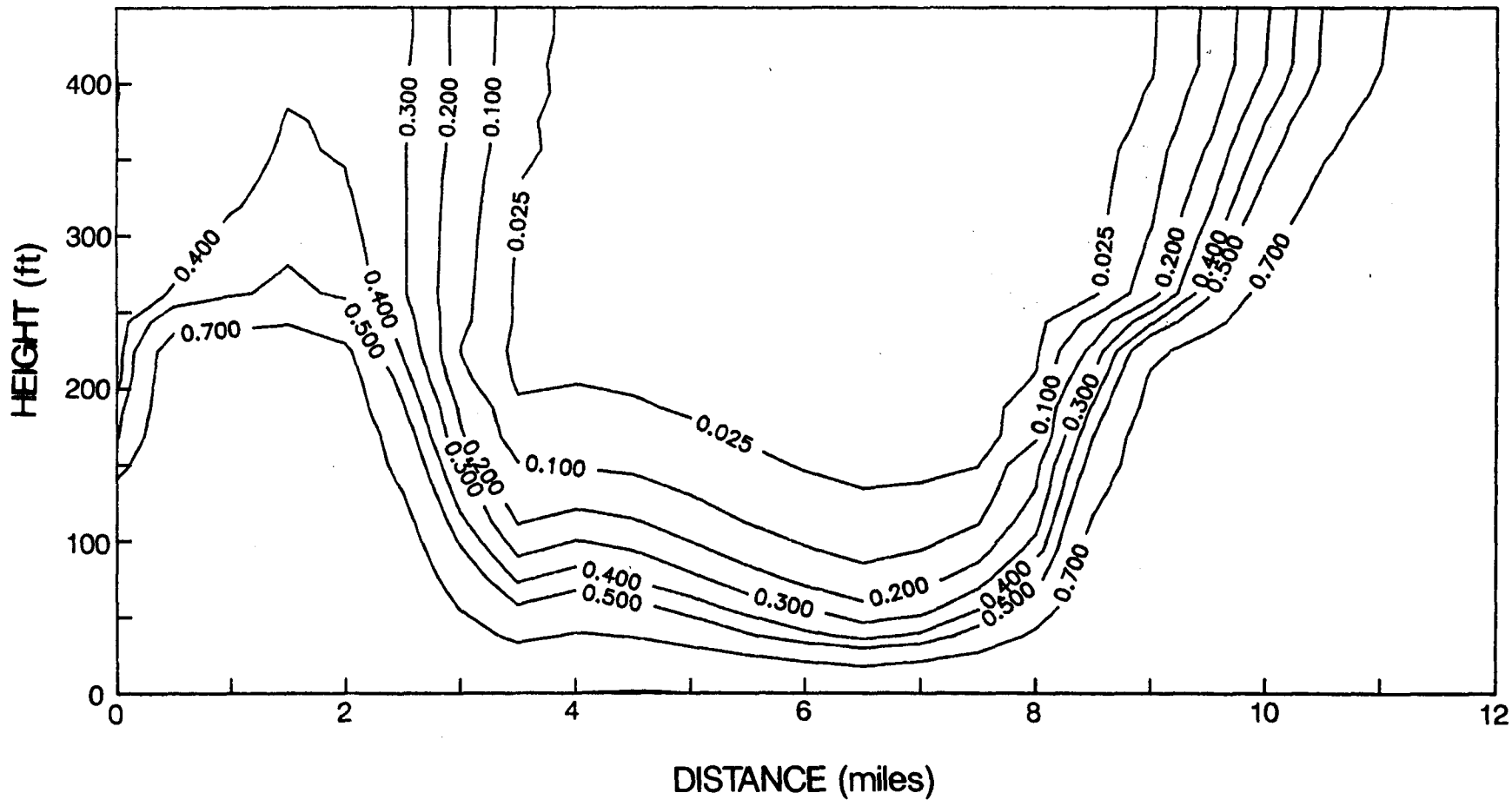

Figure 6.6. Relative concentration contours at 150 years for zero recharge.

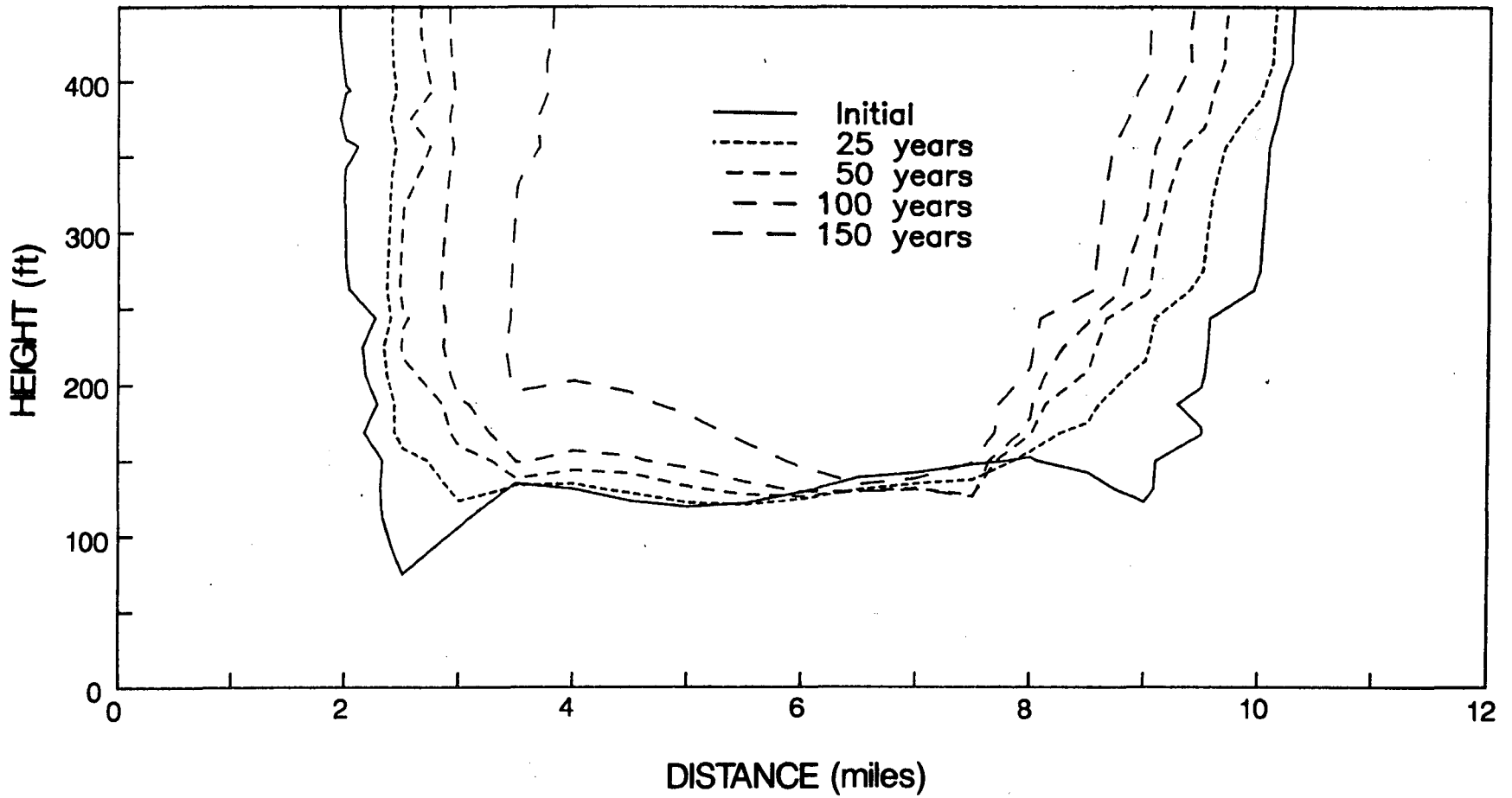

Figure 6.7. Propagation of 250-ppm isochlor for the zero recharge simulation.

The first scenario considers a strip of withdrawal, 5.4 mi from the left edge of the domain. The second scenario considers two such pumping locations at 3.8 and 6 mi from the left edge, with equal withdrawals. Finally, 8 pumping locations of equal withdrawal rate are considered between 3.8 and 7.8 mi from the left boundary. The progression of chlorides into the domain and chloride levels reaching the pumping wells are noted for all scenarios.

The first pumping scenario considers a withdrawal of 75 ft^2/d (equivalent to 15 Mgal/d being withdrawn from the 5 mile wide lens over the width of the lens) from a well located 5.38 mi into the simulation domain from the Econlockhatchee River side boundary. The model well, representing a pumping strip or line sink (see Figure 5.16 for representation), is assumed to be screened between 325 and 375 ft above the bottom of the simulation domain. Concentration profiles at 10, 20, 50, 100, and 150 years from the start of simulation are plotted in Figures 6.8, 6.9, 6.10, 6.11, and 6.12, respectively. The lens responds fairly quickly to this pumping rate, and upconing of brackish water is significant. Effects of pumping on the lens are noticed within 10 years and the upconing of chlorides is seen to rapidly increase. Figure 6.13 shows the 250-ppm isochlors at 0, 10, 20, 25, 50, 100, and 150 years, respectively. By 150 years, the areal extent of the lens is reduced by over a mile, and upconing effects are felt over a three mile region near the base of the lens. The breakthrough curve of Figure 6.14 shows the invasion of brackish water at the well. By 30 years, the 250-ppm isochlor has invaded the well, and the well

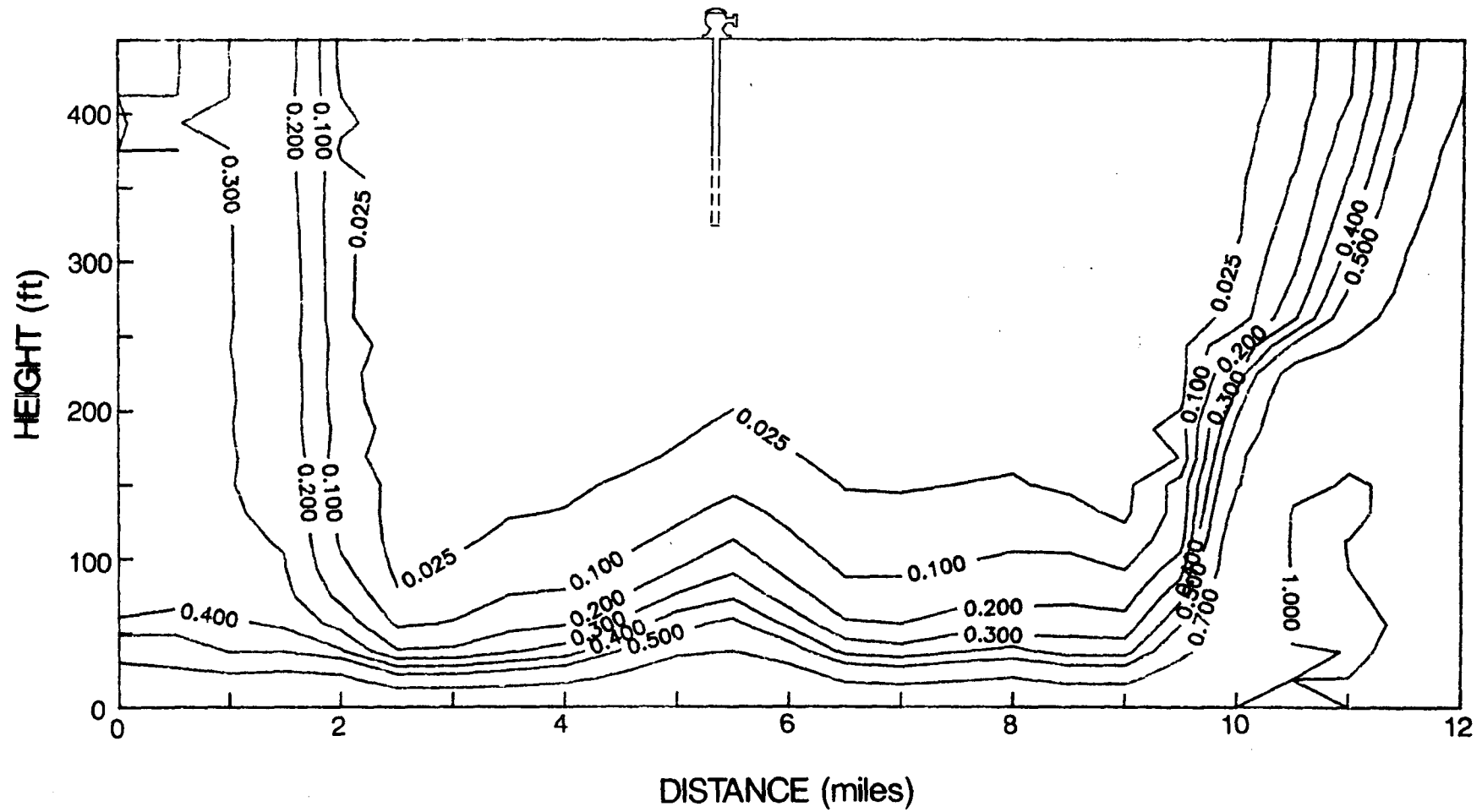

Figure 6.8. Relative concentration contours at 10 years for pumping of 75 ft^2/d at 5.4 miles.

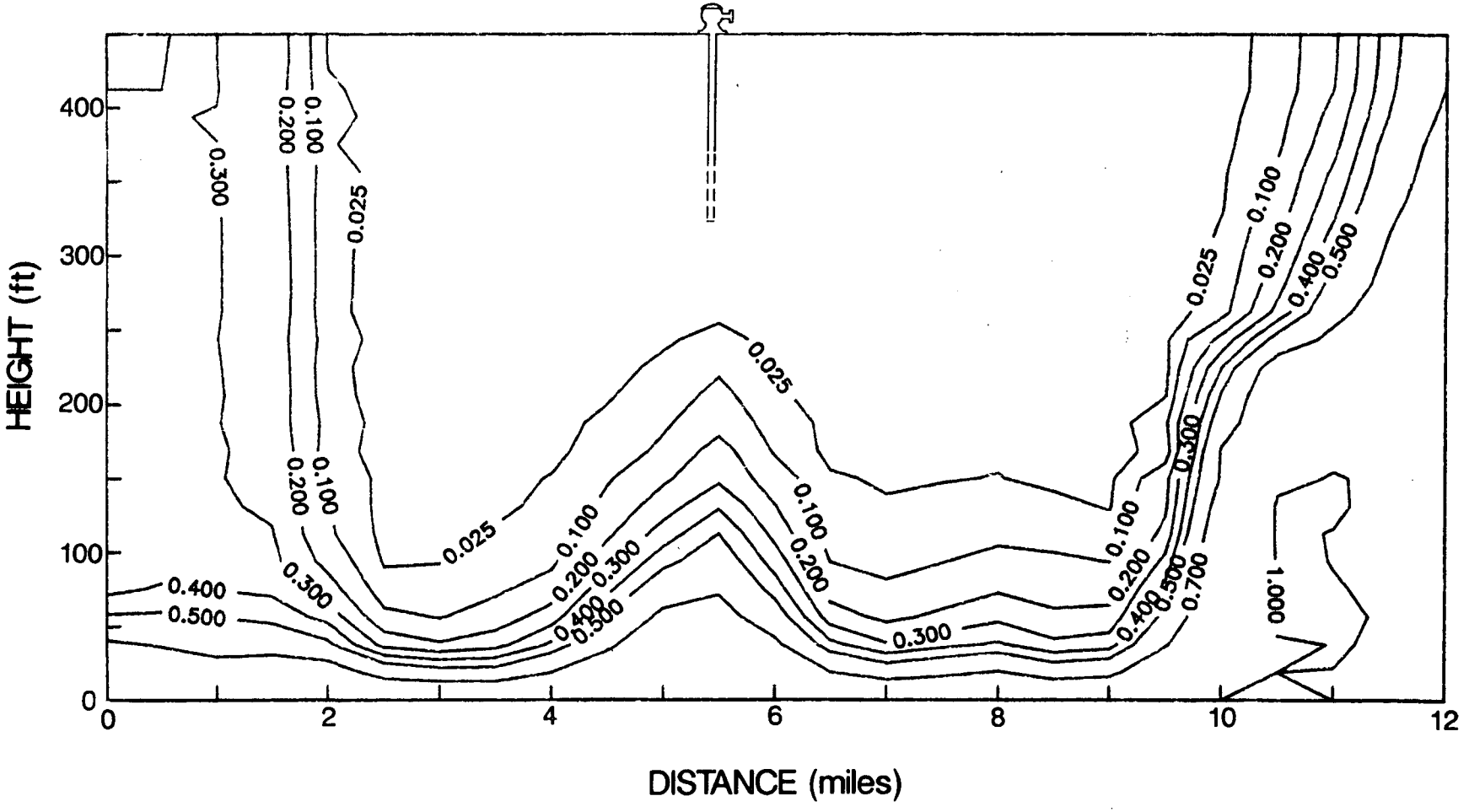

Figure 6.9. Relative concentration contours at 20 years for pumping of 75 ft^2/d at 5.4 miles.

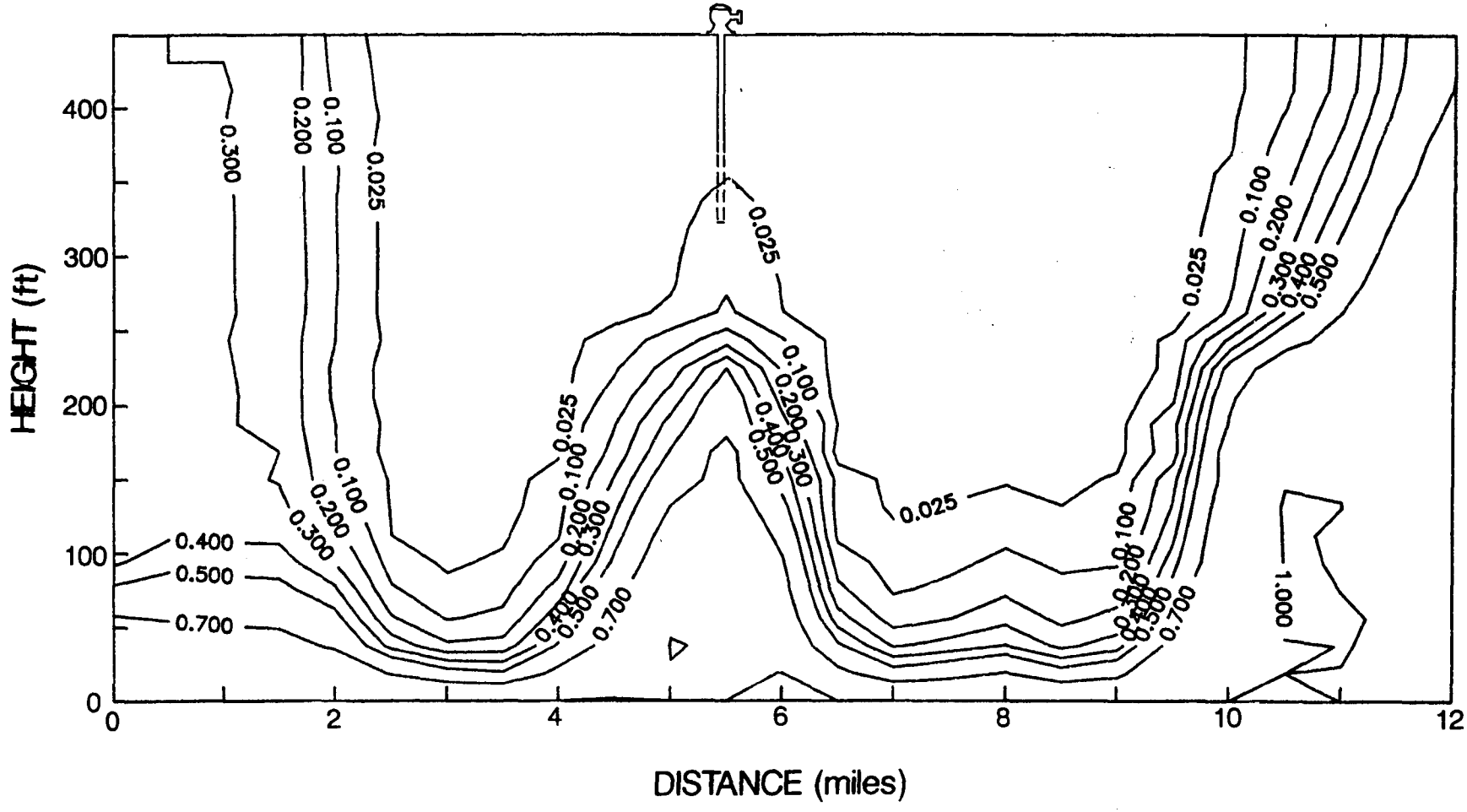

Figure 6.10. Relative concentration contours at 50 years for pumping of 75 ft^2/d at 5.4 miles.

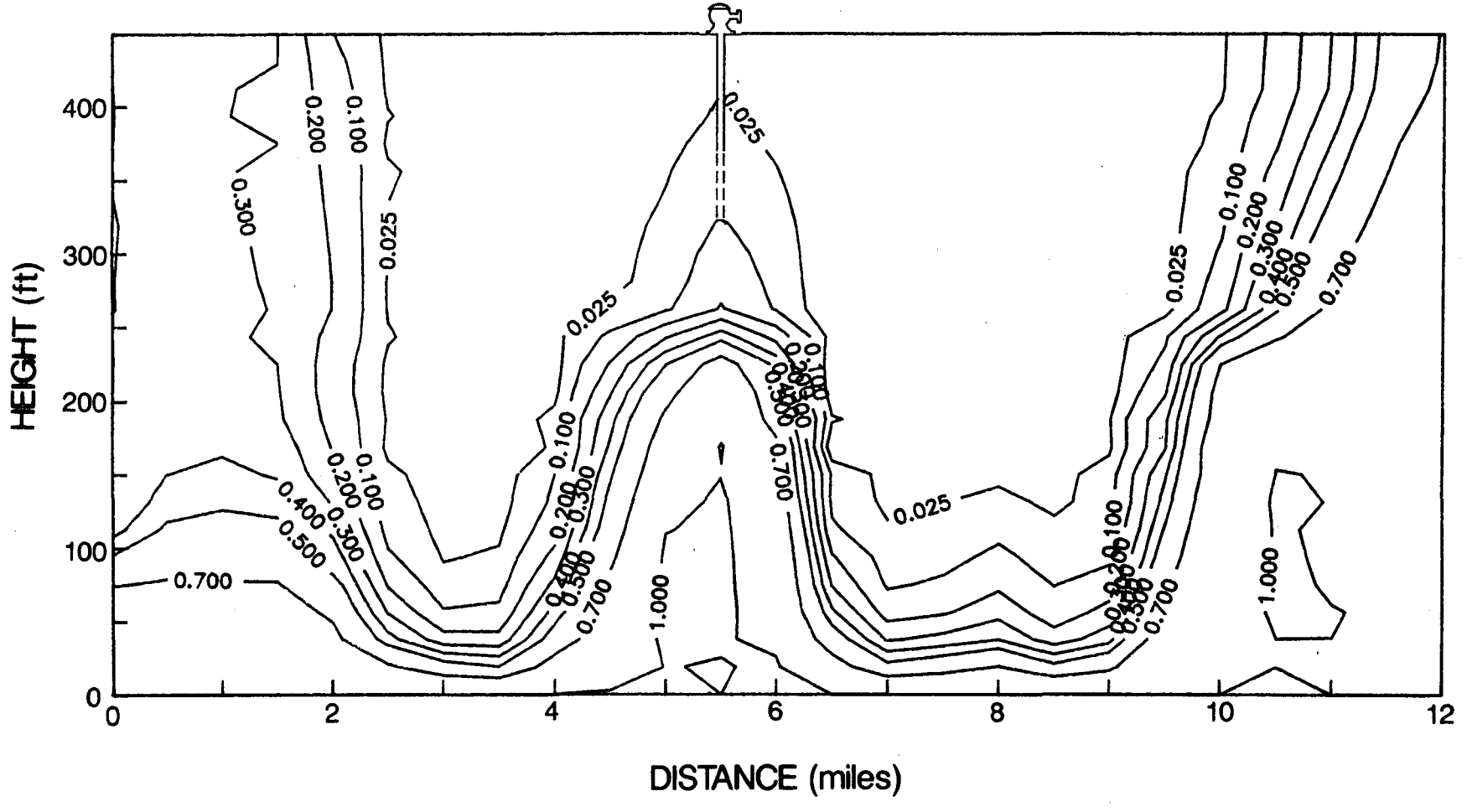

Figure 6.11. Relative concentration contours at 100 years for pumping of 75 ft^2/d at 5.4 miles.

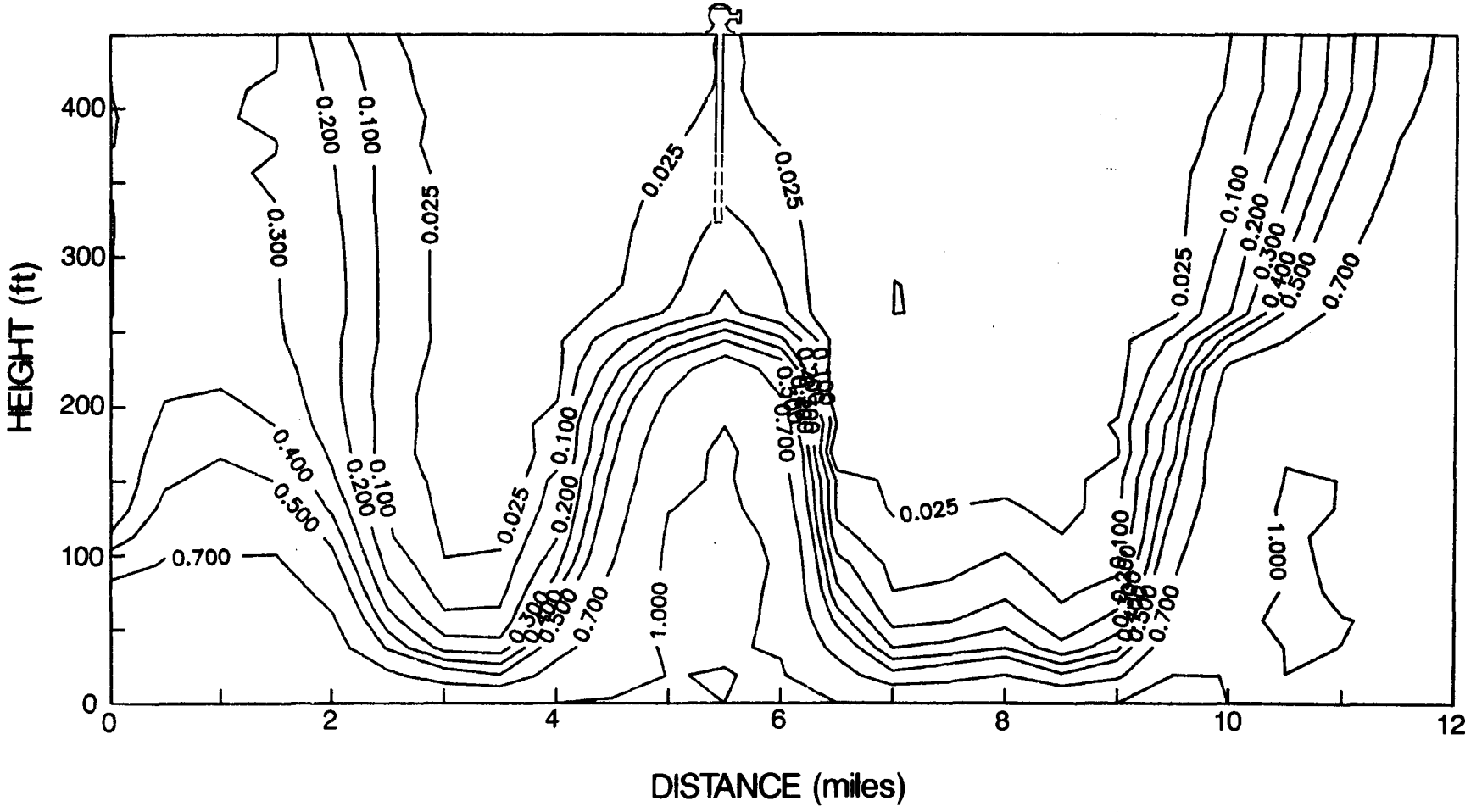

Figure 6.12. Relative concentration contours at 150 years for pumping of 75 ft^2/d at 5.4 miles.

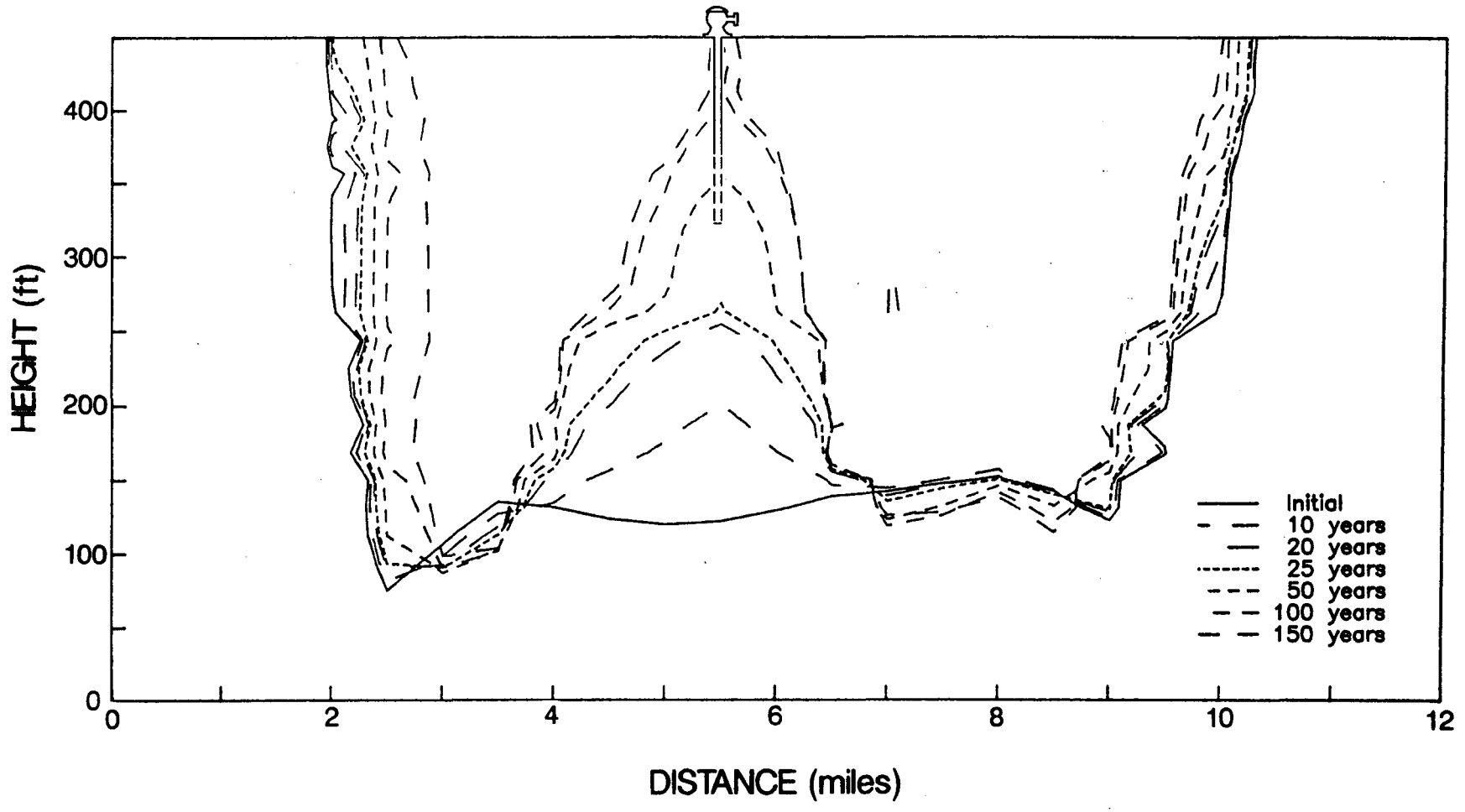

Figure 6.13. Propagation of the 250-ppm isochlor for pumping of 75 ft^2/d at 5.4 miles.

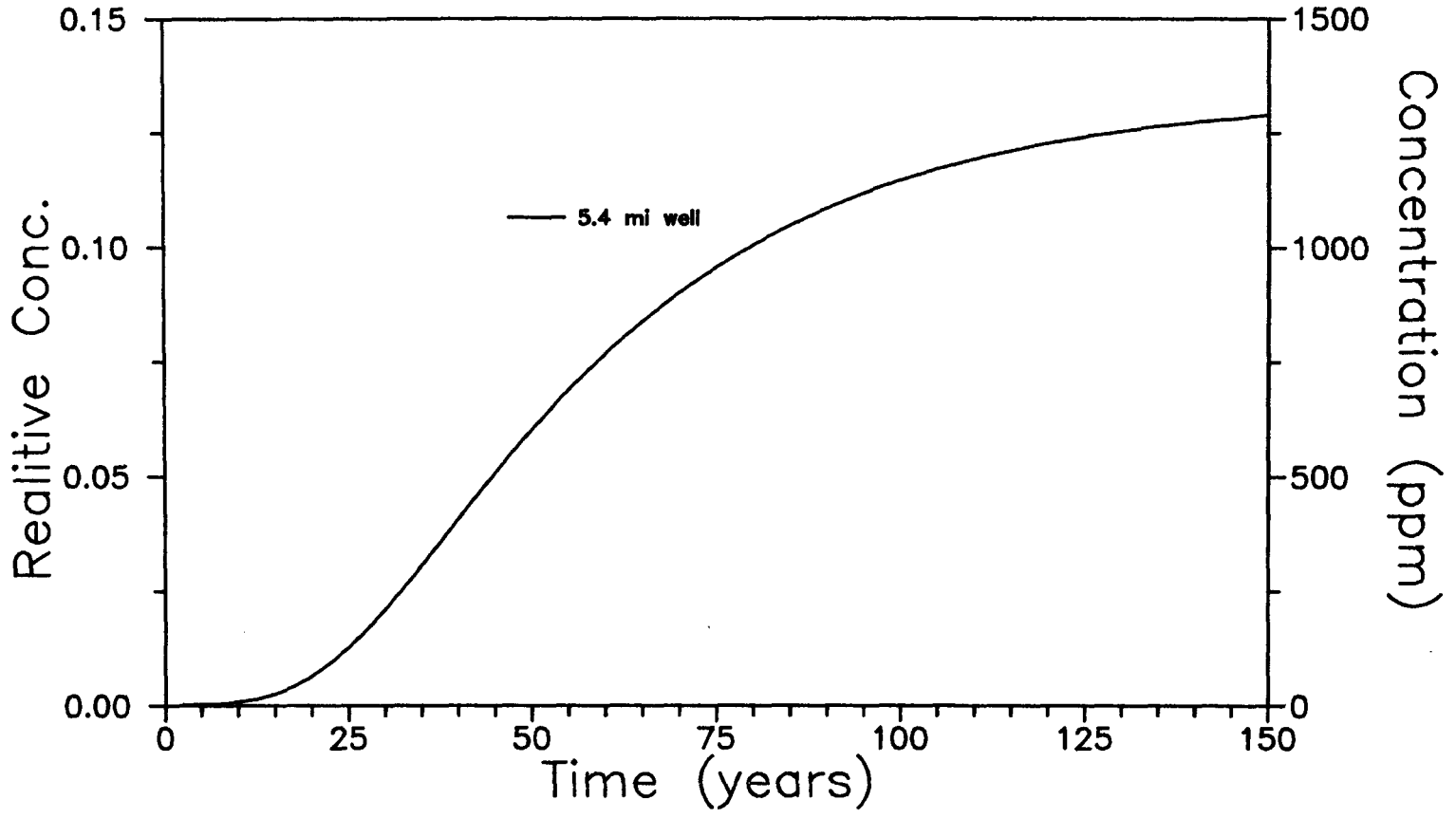

Figure 6.14. Chloride breakthrough curve at the pumping well for pumping of 75 ft^2/d at 5.4 miles.

would be considered contaminated. Figures 6.15 and 6.16 show the true head distribution and velocity field after 2.5 years of simulation. The potential field is affected significantly by this pumping, lowering the heads in the region of the well. The change is significant considering the high storativity values used in these simulations. Figure 6.17 shows the head distribution after 10 years of simulation. The head pattern has reached steady-state by this time.

The next simulation is a sensitivity of the transient behavior to the specific storativity values of the formations. All specific storativity values are lowered by an order of magnitude. The transport of chlorides is not affected by this parameter as seen in Figure 6.18 which shows the intrusion of the 250-ppm isochlor at 0, 10, 20, 25, 50 and 100 years. The head distribution is however affected more rapidly as seen in Figure 6.19 which plots the head pattern after 2.5 years of simulation. The head pattern is the same as that of Figure 6.17, and steady state of the flow field is achieved. The flow equation equilibrates extremely quickly to the existing conditions, as compared to the transport equation. Depending on the storage, the flow equation equilibrates within 2 to 10 years for the high storage values used. The chlorides have barely begun to move within this period of time.

The next simulation considers withdrawals of 75 ft^2/d, evenly distributed over two locations at 3.8 miles and 6 miles from the Econlockhatchee river edge of the simulation domain. Upconing of brackish water is noticed again at both wells. Figure 6.20 shows

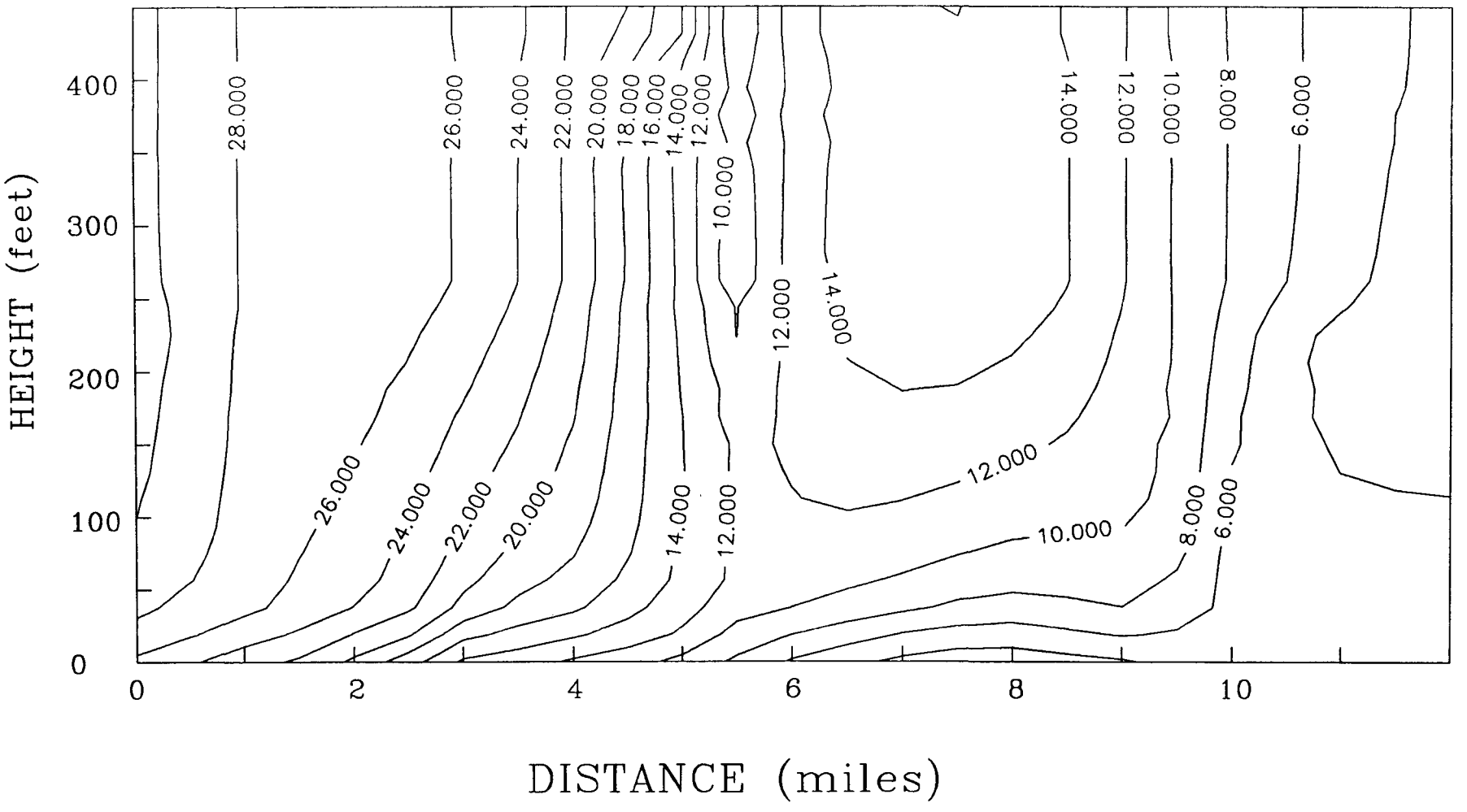

Figure 6.15. True head distribution after 2.5 years of pumping 75 ft^2/d at 5.4 mi.

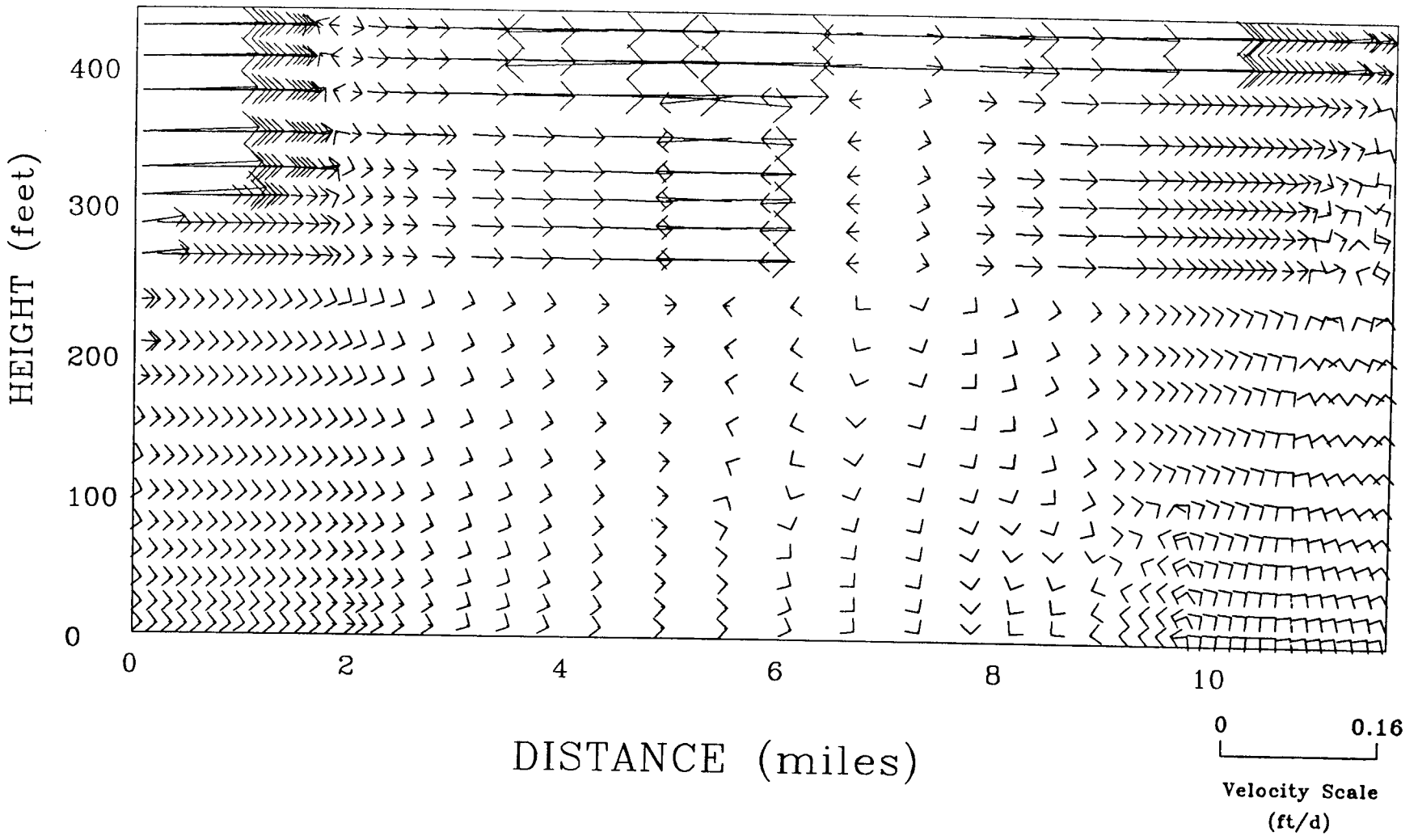

Figure 6.16. Groundwater velocity field after 2.5 years of pumping 75 ft^2/d at 5.4 mi.

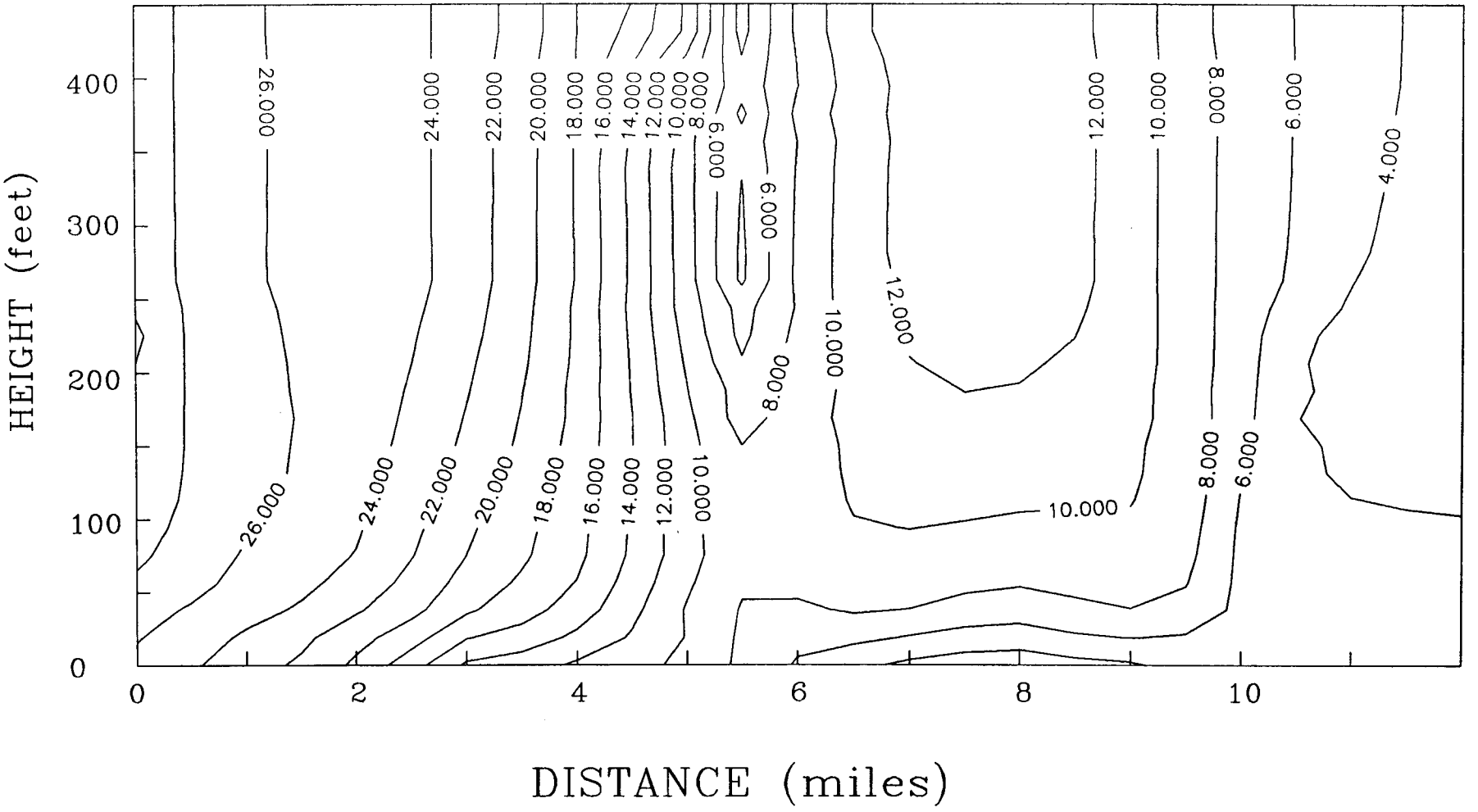

Figure 6.17. True head distribution after 10 years of pumping 75 ft^2/d at 5.4 mi.

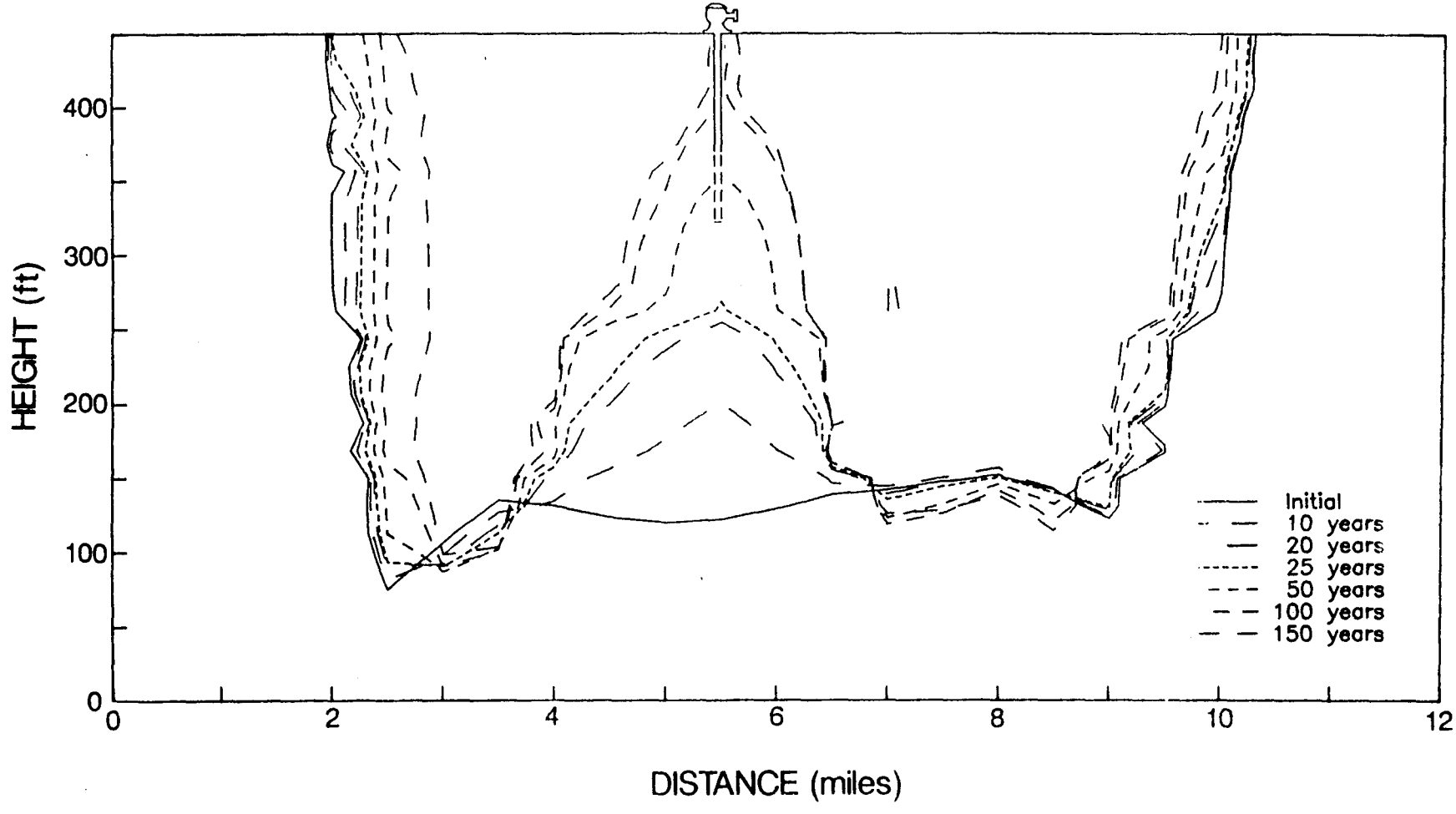

Figure 6.18. Sensitivity of transient simulations to specific storage of materials (reduced by order of magnitude). Figure shows the propagation of 250-ppm isochlors at 0, 10, 20, 25, 50 and 100 years of pumping 75 ft^2/d at 5.4 mi.

6-27

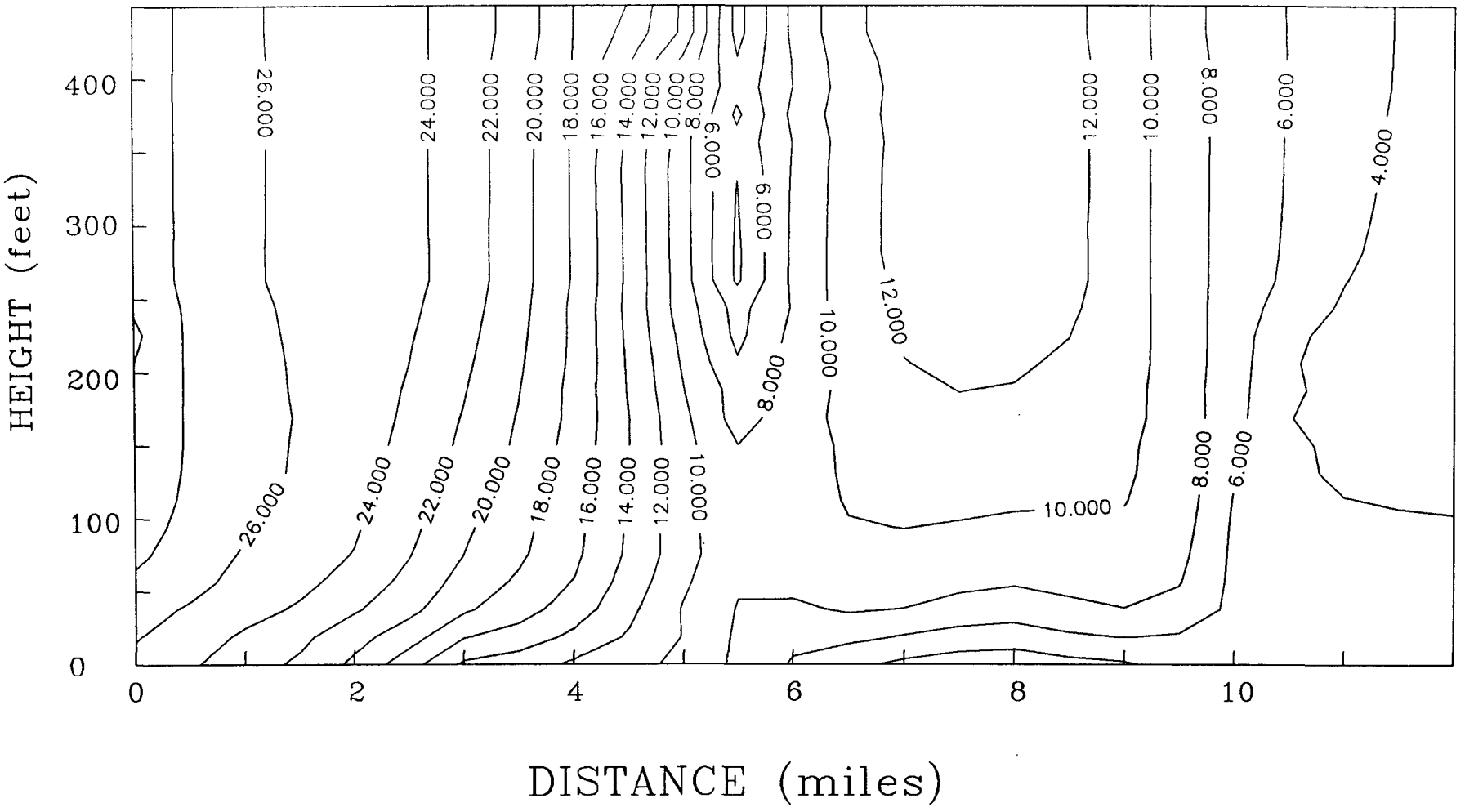

Figure 6.19. Sensitivity of transient simulations to specific storage of materials (reduced by order of magnitude). Figure shows the true head distribution after 2.5 years of pumping 75 ft^2/d at 5.4 mi.

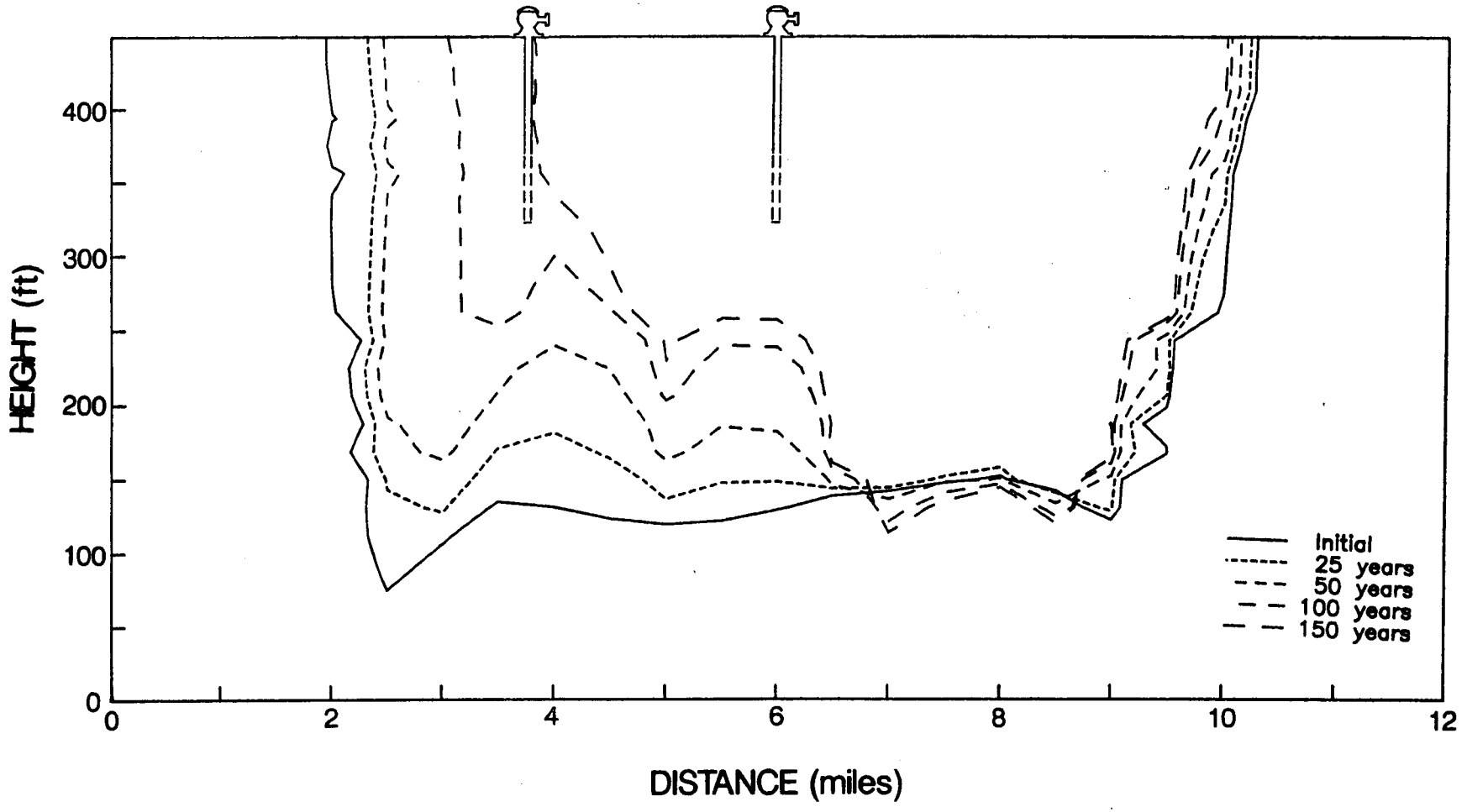

Figure 6.20. Propagation of the 250-ppm isochlor for total pumping of 75 ft^2/d from 2 wells at 3.8 miles and 6.0 miles.

the 250-ppm isochlor at 0, 20, 50, 100, and 150 years for this case. Upconing of brackish water is again noticed at both wells. The well at 3.8 miles has a significant impact on the areal extent of the lens near the Econlockhatchee River by 150 years of simulation. The 250-ppm isochlor has encroached approximately 2 miles into the original freshwater lens on this side alone. (Note that for the case of a single pumping location at the lens center, the encroachment upon the lens was approximately 1.5 miles by 150 years.) The well at 6 miles was not contaminated throughout the course of this simulation as seen in the breakthrough curves of Figure 6.21. The well at 3.8 miles extracted freshwater for 100 years after the start of simulation.

The next simulation evenly distributes the total withdrawal of 75 ft^2/d over 8 pumping locations at 3.8, 4.2, 4.8, 5.4, 6.0, 6.6, 7.2, and 7.8 miles from the Econlockhatchee River edge of the domain. The 250-ppm isochlors at 25, 50, 100 and 150 years from the start of simulation are depicted in Figure 6.22. Significantly reduced upconing of brackish water occurs for this case, than for the previous cases. In fact, none of the wells were invaded by the 250-ppm isochlor by 150 years. The lens was evenly diminished areally by over 1.5 miles during this period of time.

6.5 SUMMARY AND CONCLUSIONS

In summarizing the transient pumping simulations, we note that the freshwater lens and the pumping wells can be utilized effectively, if the rates of withdrawal from the lens are below a

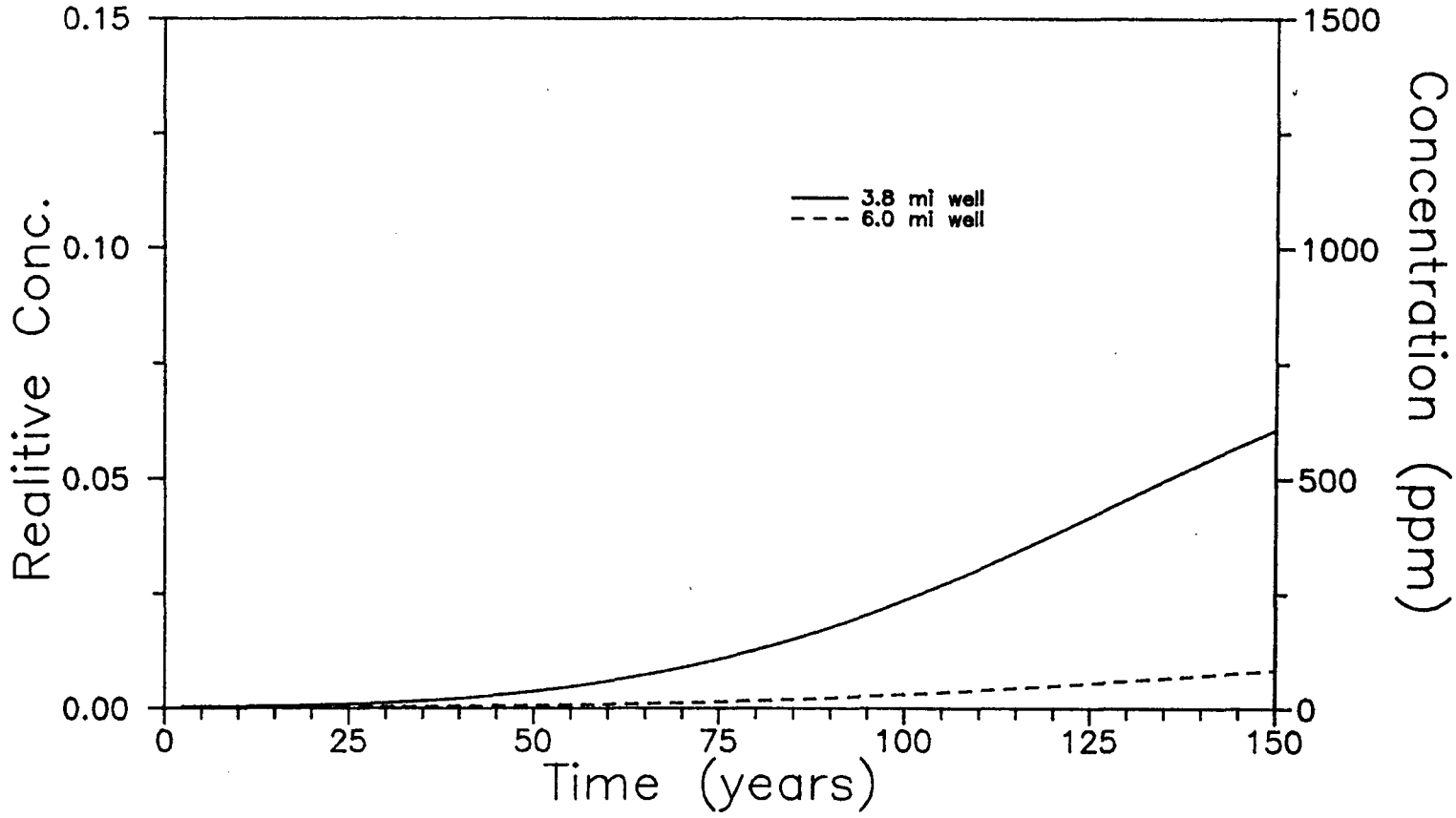

Figure 6.21. Chloride breakthrough curves at pumping wells for total pumping of 75 ft^2/d from 2 wells at 3.8 miles and 6.0 miles.

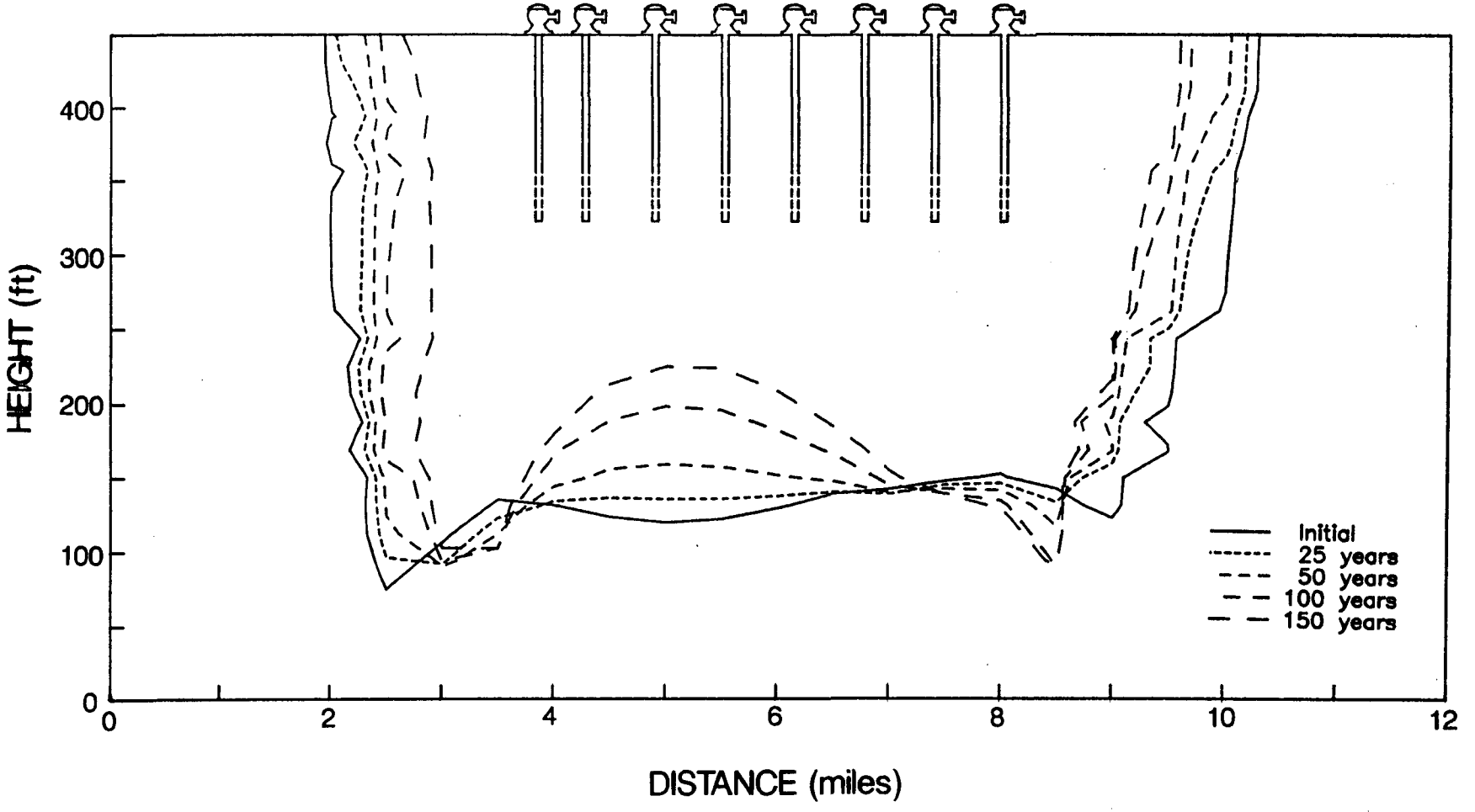

Figure 6.22. Propagation of the 250-ppm isochlor for total pumping of 75 ft^2/d from 8 wells at 3.8, 4.2, 4.8, 5.4, 6.0, 6.6, 7.2 and 7.8 miles.

certain maximum value. Steady-state withdrawals at the rates of 25 and 50 ft^3/d per unit width from the lens (Figures 5.21 and 5.22) do not affect long term practical use of the lens for potable water supply when the well is screened from 25 to 75 ft below the top of the upper Floridan (Note that for the two-dimensional analyses performed, a withdrawal rate of 25 ft^2/d is equivalent to 5 Mgal/d being withdrawn from a 5-mile wide lens over the width dimension normal to the plane of simulation). For a withdrawal rate of 75 ft^2/d, the model well would be contaminated within 30 years.

The results of the two-dimensional cross-sectional analysis show that a total withdrawal rate of 75 ft^2/d evenly distributed over two pumping locations allowed for approximately 100 years before one of the model wells was contaminated. Additionally, an even distribution of the total withdrawal rate over 8 pumping locations was required to control the quality of groundwater withdrawn from the Geneva lens over a period of 150 years. T h e transient simulations are insensitive to the specific storage of the aquifer materials. The time scale for equilibration of the groundwater flow, which is in terms of days, is much smaller than time scales for chloride transport, which is in terms of years. Therefore, with the exception of early time values at the start of simulation, the role of aquifer specific storage is insignificant in the transient transport analysis.

It should be mentioned once again that 2-D simulations with groundwater withdrawals can only give general guidelines for water management. The 2-D nature of the problem invokes the assumption

that pumping is applied uniformly over the entire width of the lens, and hence only strip (line sink) withdrawals can be examined. Effects of the third direction with respect to flow due to individual wells and well interferences are neglected. Furthermore, effects of dispersion in the third direction, and the lens boundary in the third direction are also neglected. The modeled cross-section passes through the center of the lens and is probably the largest cross-section of freshwater in the domain, not representative of the entire lens system. Upconing, lateral encroachment, and breakthrough of the 250-ppm isochlor may be grossly underpredicted with respect to sections closer to the edge of the lens. Thus, fully three-dimensional analyses are essential for a better quantitative assessment of the Geneva freshwater lens system.

7. THREE-DIMENSIONAL CONCEPTUAL MODEL

7.1 GENERAL

The conceptual model for three dimensional (3-D) simulations is an extension of the approach used for the cross-sectional 2-D simulations. A plan view of the rectangular domain for 3-D simulations is shown in Figure 4.2. The cross-section A-A' simulated in the 2-D analyses passes through the center of this domain. The extent of the domain is, however, reduced from that of the cross-sectional analyses by 1½ miles at the south-west end, where it passes through the discharge area at the Econlockhatchee River. The model boundary encompasses the freshwater lens system entirely, and hence the reduction in the domain length will reduce the size of the problem without significant loss of information. The length of the domain is 10.5 miles, intersecting the Econlockhatchee River at the south end, and the St. Johns River near the north. The domain width is 7 miles, between Lake Jessup and Lake Harney. The rectangular domain is oriented approximately ten degrees clockwise from north-south such that its length is parallel to that of the cross-sectional model studied earlier.

The Geneva freshwater lens sits in the upper 350 ft of the Upper Floridan aquifer, and is surrounded laterally and underlain by brackish water. The simulation domain is 450 ft deep, and intercepts the Ocala formation and the upper and lower portions of the Avon Park formation. Little data is available on the thickness and hydraulic characteristics of these zones, and their variations

within the simulation domain. Material properties within each zone are hence treated as homogeneous. The thickness of the Ocala formation can be estimated from Figures 4 and 5 of Barraclough (1962) which depict the configuration and altitude of the top of the Ocala and Avon Park respectively. Phelps and Rohrer (1987) further provide geologic and geophysical logs at various test holes (Figures 11 and 12 of Phelps and Rohrer) and extrapolate the stratigraphy of the system in the Geneva area from this and other available data (see Figures 13, 14 and 15 of Phelps and Rohrer). The estimates of Phelps and Rohrer are more accurate than the predictions of Barraclough due to the availability of more data, as seen at the recent wells logged by the district. In case of data discrepancies, the Phelps and Rohrer (1987) estimates will be used in the simulations, since they appear to represent the system more accurately. Sketchy information is available on the division between the upper and lower portions of the Avon Park formation. Hence, the thickness of the lower Avon Park formation is kept constant throughout the domain.

The exchange of water between the surficial aquifer and the upper Floridan is treated as a recharge-discharge condition. The land surface area surrounding Geneva which has an altitude greater than 25 ft is considered a recharge area (Phelps and Rohrer, 1987). The regions along the St. Johns River, and the Econlockhatchee River are discharge zones, as have been mapped by Barraclough (1962, Figure 9). Tibbals (1977) maps the most effective recharge zones, discharge zones, and zones of moderate or low recharge.

Seasonal recharge/discharge has been documented at certain Phelps and Rohrer's observation well sites and is corroborated by further monitoring of these sites by District personnel. Average steady-state recharge/discharge conditions are used for the current modeling effort, since the errors introduced in the solute transport calculations by considering time averaged flow are small (Duguid and Reeves, 1977). The two-dimensional modeling efforts of Chapter 5, however, treat all recharge zones uniformly in order to facilitate quick qualitative assessments of the lens system and its sensitivity to various parameters. Further refinement of the conceptual model herein, provides for a more reliable quantitative description of the Geneva lens system. Current withdrawals from the lens are small, and will hence be neglected in the steady-state simulations.

7.2 BOUNDARY CONDITIONS

The areal extent of the 3-D simulation domain is shown in Figure 4.2. The boundary along the Econlockhatchee River is a prescribed flux boundary, with flow rates computed from the potentiometric contour map shown in Figure 4.2, and estimated conductivities of the formations. The concentration of solutes is estimated at 1000 ppm - 4000 ppm in this region (Figure 36 of Barraclough, 1962, Figure 11 of Tibbals, 1977, Figures 16, and 17 of Phelps and Rohrer, 1987). The lateral boundary along the St. Johns River is a no flux boundary where a hydraulic barrier is reported to occur. The two lateral boundaries crossing Lake Jessup

and Lake Harney are also treated as no-flow boundaries, since they are approximately parallel to the ambient groundwater flow. Zero advective flux of solute occurs across these no-flow boundaries. The top surface of the upper Floridan is a prescribed recharge/ discharge boundary with values estimated from Phelps and Rohrer (1987) and Tibbals (1977). A prescribed value of freshwater recharge rate is applied to the main recharge zone, and a smaller recharge value is used for the moderate to low recharge zones. Discharge zones are estimated from data of Stubbs (1938), Phelps & Rohrer (1987), Tibbals (1977), and Barraclough (1962). Discharges to the surface near the Econlockhatchee River boundary are assumed to be equal to the lateral influx from the side boundary. A constant discharge rate is used along the St. Johns River, and at the discharge zones around Lake Jessup and Lake Harney. The discharge rate is estimated such that net influx to the system (from the Econlockhatchee River end of the domain, and from recharge) is approximately balanced by net discharge through the top. Discharge boundaries are given zero normal-concentration-gradient conditions, in solving the transport equation. The bottom of the domain lies in the brackish water zone at a depth of 450 ft below the top of the upper Floridan aquifer. Chloride concentrations and head distributions at this base are prescribed. A uniform chloride concentration of 10,000 ppm is supplied at the bottom, since all deep wells, penetrating to this level show chloride concentrations close to this value. The ambient potentiometric surface, and data available from the few wells

monitored by the District are used to determine the head distributions at the base. Available field data depict the average potentiometric heads over the screened intervals of the observation wells. These head values are adopted as a basis for specifying the bottom-head boundary condition due to lack of better field information. Another reason for this is the fact that the bottom head condition serves merely as a datum for calculating the flow field and the flow pattern is governed by the gradients of the bottom heads rather than their absolute values.

The boundary conditions described above are used for simulations of steady-state and transient conditions. The model is calibrated under a steady-state non-pumping condition using field data reported by Phelps and Rohrer (1987) and Tibbals (1977), for chloride concentrations of water in the upper part of the Floridan aquifer. The availability and uncertainty of data on material properties and boundary conditions required for modeling the Geneva lens system has been summarized in Table 3.1 of chapter 3.

7.3 MESH DESIGN CONSIDERATIONS

A rectangular finite element mesh with a variable nodal spacing is used to discretize the domain. The mesh is automatically generated by the DSTRAM code with user supplied values of the coordinate grid lines.

The modeled region is discretized into 20 vertical slices uniformly spaced at a distance of 1945 ft in the z-direction, as shown in Figure 7.1. Each vertical slice is discretized into 15

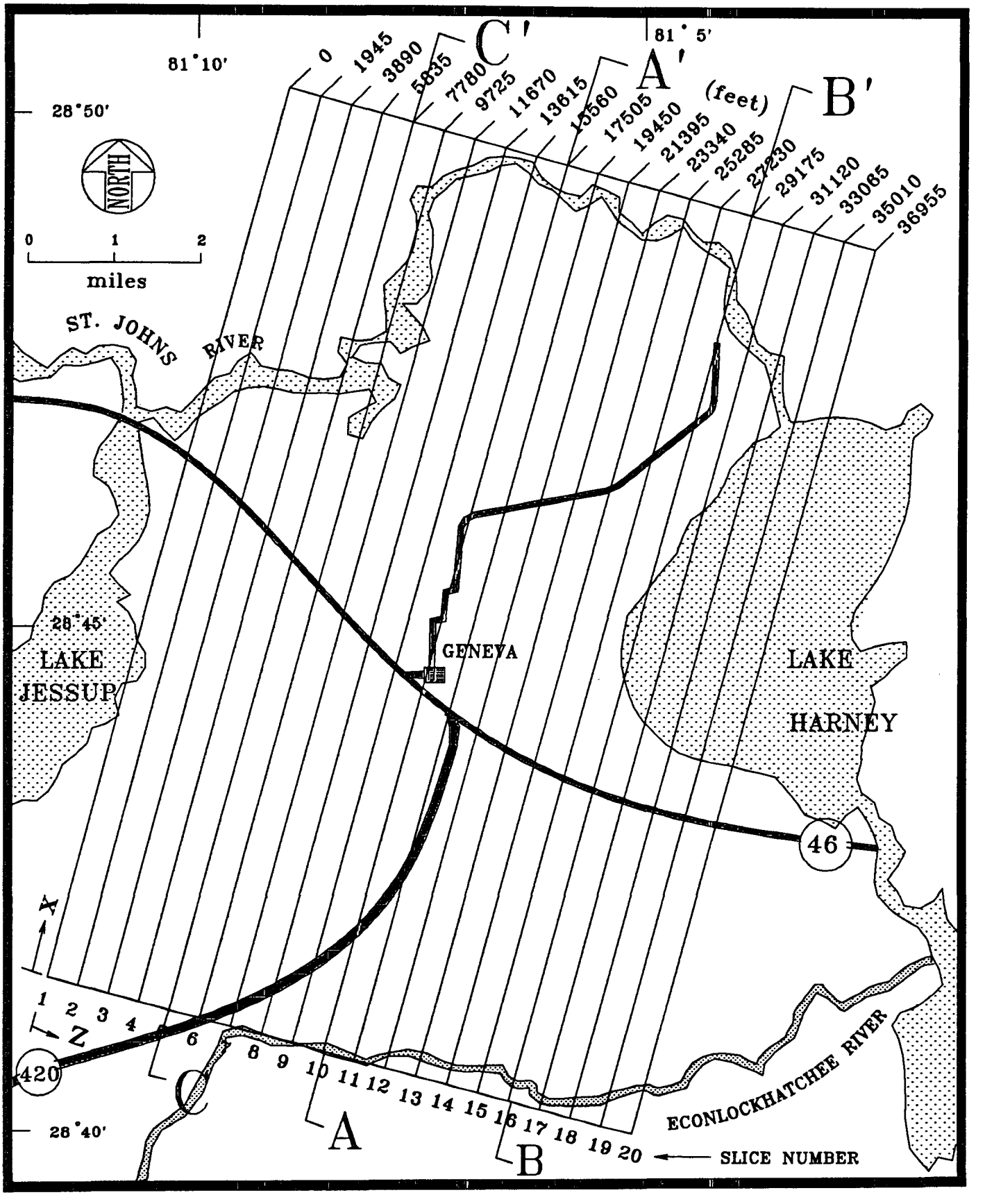

Figure 7.1. Plan view of simulation domain showing locations of slices for a three-dimensional analysis of the Geneva freshwater lens.

rows and 30 columns with variable spacing, as shown in Figure 7.2. This mesh is coarser than those used in the 2-D cross-sectional analyses, to make the 3-D computation more efficient. The domain is divided into 7,714 elements by a total of 9,000 nodes. The mesh was carefully designed to avoid inaccurate numerical solutions with unacceptable oscillations or excessive numerical dispersion.

To test the performance of the DSTRAM code and the selected mesh, a simulation was performed in a 2-D cross-sectional mode, and compared with a 3-D simulation of the entire domain, with all cross-sections having identical material properties and boundary data to that of the 2-D simulation. The material zones and their thickness are depicted in Figure 7.3, and are representative of the cross-section A-A′ passing through Geneva (the mid-section of the domain). The boundary conditions used for these simulations are also depicted in Figure 7.3. The 2-D cross-sectional simulation gives identical results to all the planes of the 3-D simulation, thus verifying the code performance. The concentration profile through the cross-section is shown in Figure 7.4. This profile shows a lens similar to the 2-D scenarios of Chapter 5, verifying that the new conceptual model (with reduced length near the Econlockhatchee River) does not deviate significantly from the earlier development. The larger Ocala thicknesses of this simulation is considered more representative of the mid-section A-A′ than those used in Chapter 5, which are extrapolated from Figures 4 and 5 of Barraclough (1962). This is corroborated by the estimates of Phelps and Rohrer (1987) which incorporates data

X =

0.00	1000.00	2000.00	3000.00	4500.00	6000.00	8000.00	10000.00
12000.00	14000.00	16000.00	18000.00	20000.00	22500.00	25000.00	27500.00
30000.00	32500.00	35000.00	37250.00	39250.00	41250.00	44000.00	46000.00
48000.00	49500.00	51000.00	52000.00	53970.00	55440.00		

406 elements/slice
450 nodes/slice

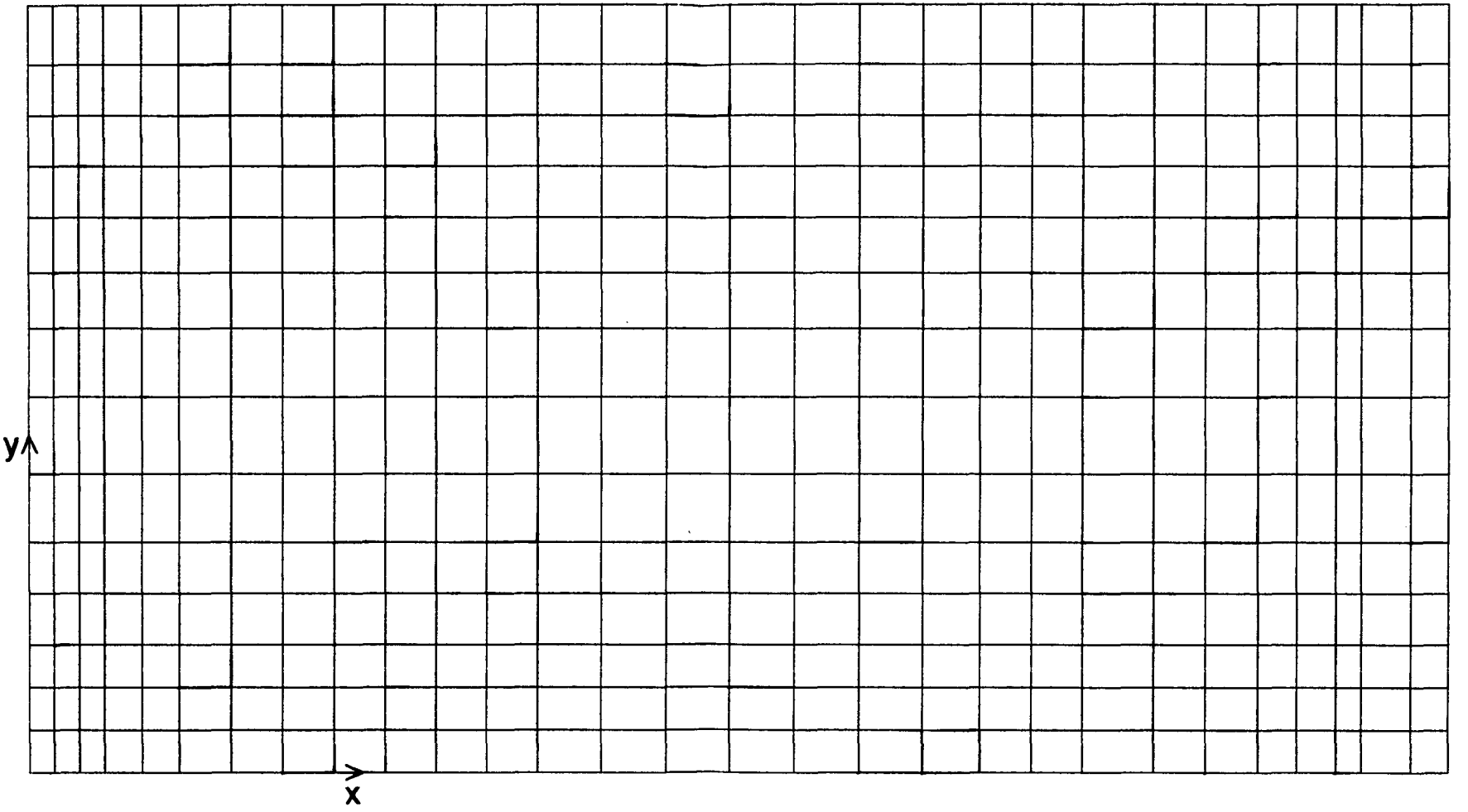

Y =

0.00	25.00	50.00	75.00	105.00	135.00	175.00	220.00
260.00	292.50	325.00	355.00	385.00	415.00	450.00	

Figure 7.2. Discretization of a cross-sectional slice for three-dimensional simulations.

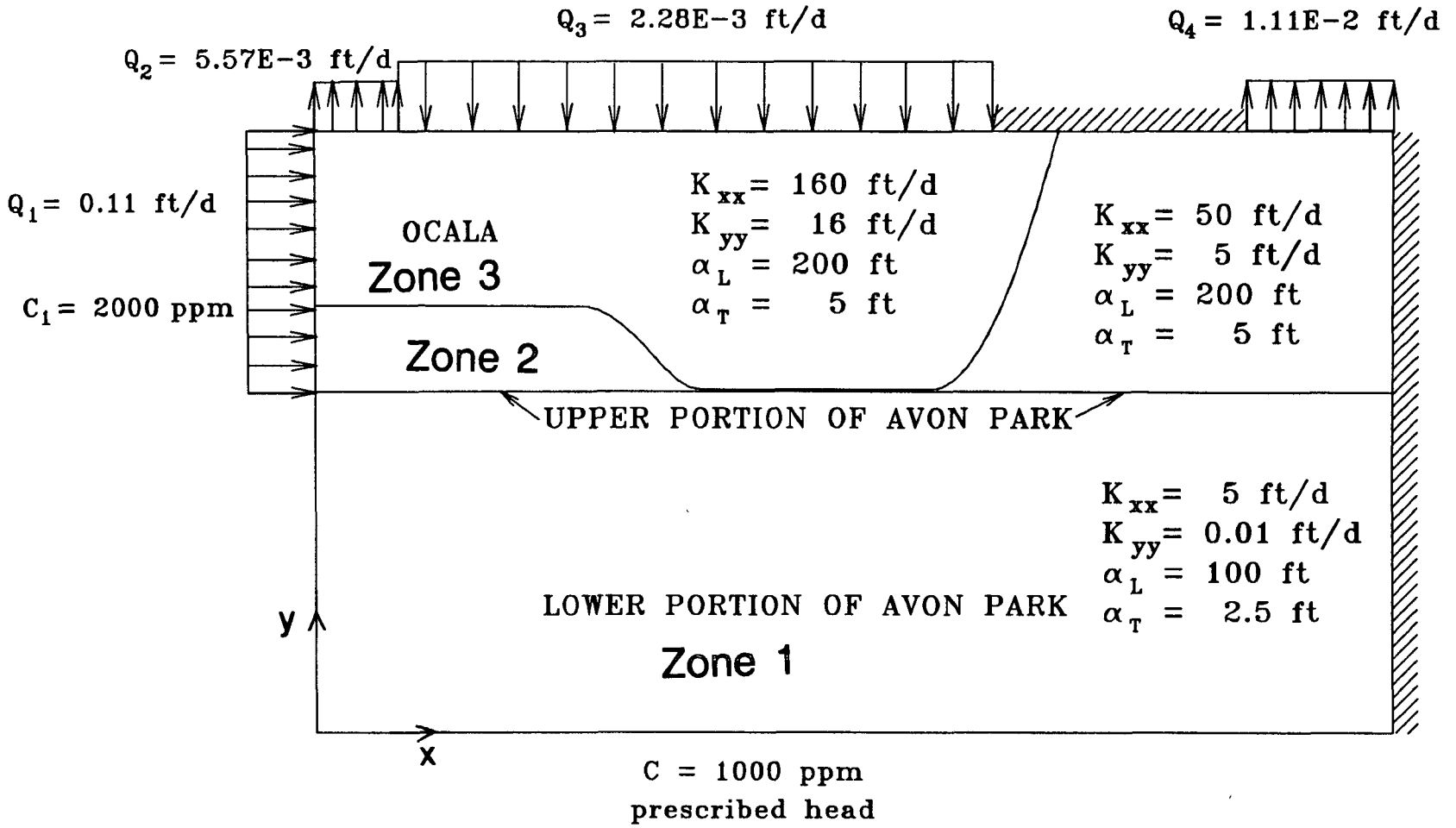

Figure 7.3. Vertical section of the simulation domain passing through Geneva (slice no. 10).

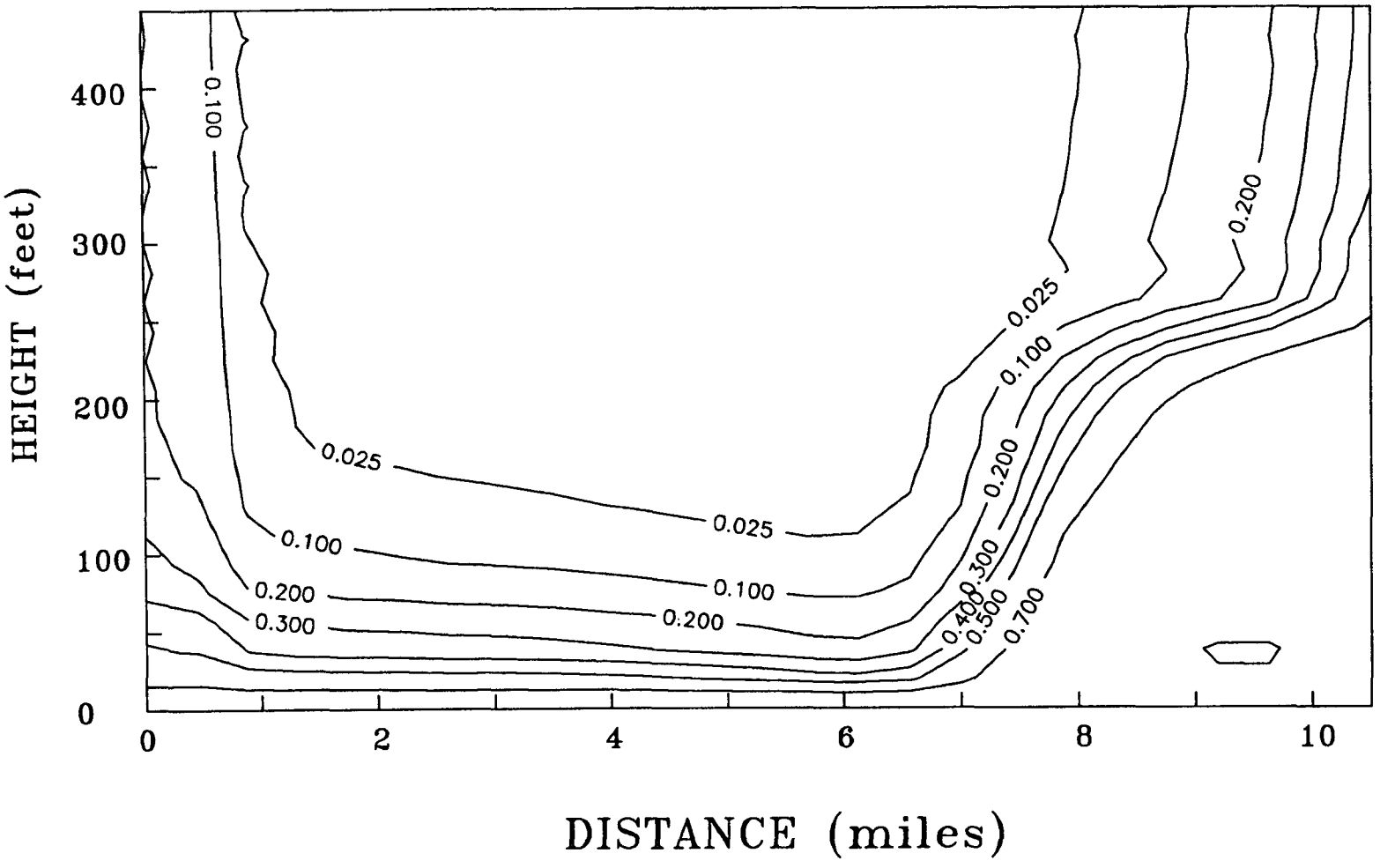

Figure 7.4. Relative concentration profile for a 2-D simulation or for each slice of the 3-D simulation with all slices being identically treated.

7-10

collected after 1962. The zone of no recharge along the top boundary reflects the areas of low recharge (and possibly seasonal discharge) as reported by Tibbals (1977) and confirmed by District personnel. The additional refinement of the conceptual model herein provides for a more reliable quantitative assessment of the Geneva lens system. The next simulation for testing the three-dimensional grid and model performance includes consideration of flow components in the transverse direction along the z-axis of the grid. This simulation was similar to the previous one except that there was no recharge supplied to slices 1-6, and 15-20 (Figure 7.1). A symmetric recharge zone is therefore provided in the central rectangular portion of the domain. Shown in Figure 7.5 is the areal distribution of chloride at the top of the upper Floridan.

Symmetry about the z-direction is reflected by the numerical solution, thus verifying the code performance. Furthermore, the concentration profiles obtained using the non-upstream weighted (Galerkin) scheme do not exhibit oscillations, thus verifying that the grid is sufficient. The concentration profile through the mid-plane A-A' (passing through Geneva) is plotted in Figure 7.6. The lens is significantly smaller in depth and extent for this case than for the previous case of strip-recharge where all slices were assigned uniform and identical recharge rates (see Figure 7.4). This is because total recharge is reduced, even through total discharges through the top surface remain the same. Furthermore, consideration of the third dimension leads to a significant

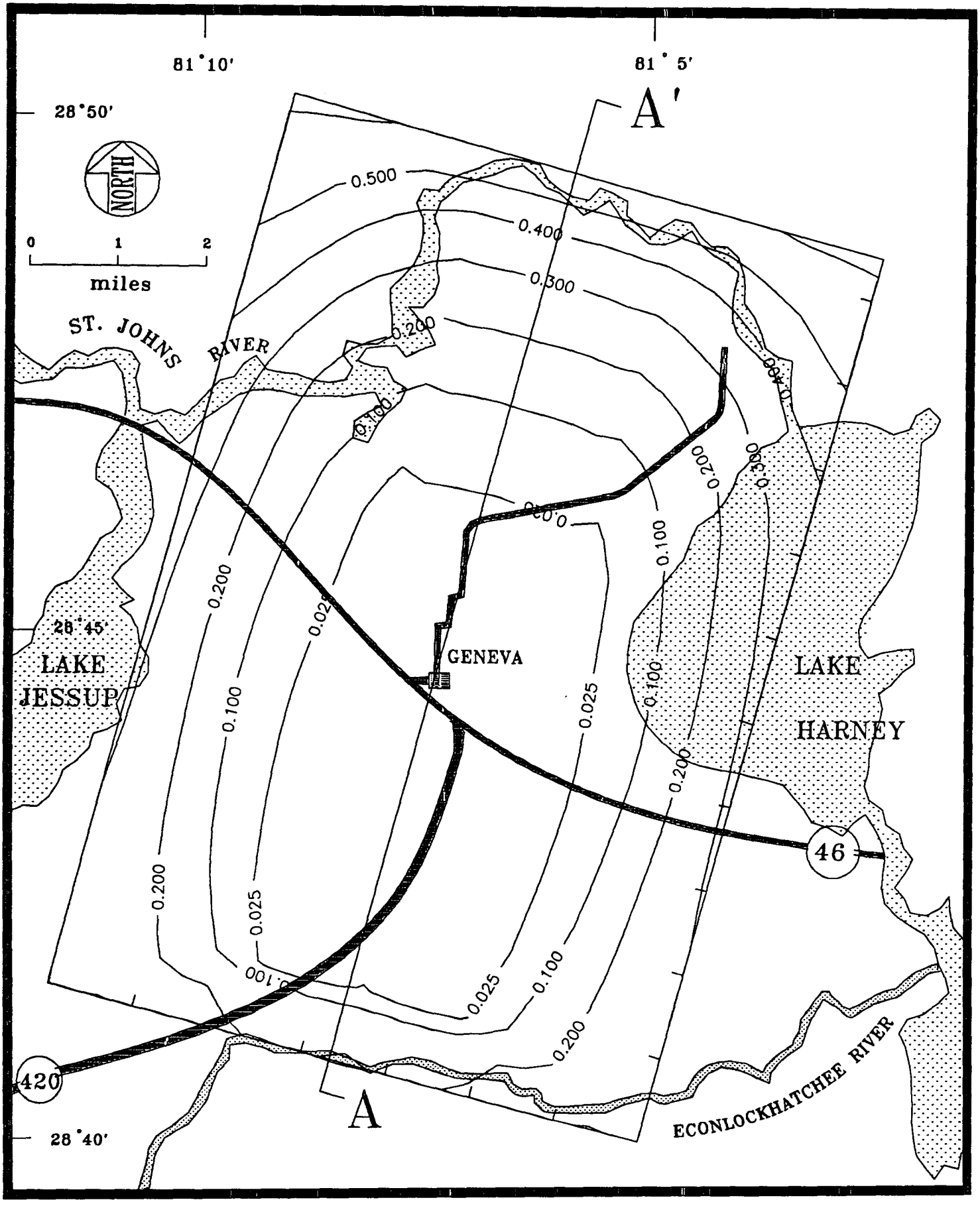

Figure 7.5. Areal distribution of chloride for symmetric rectangular recharge case.

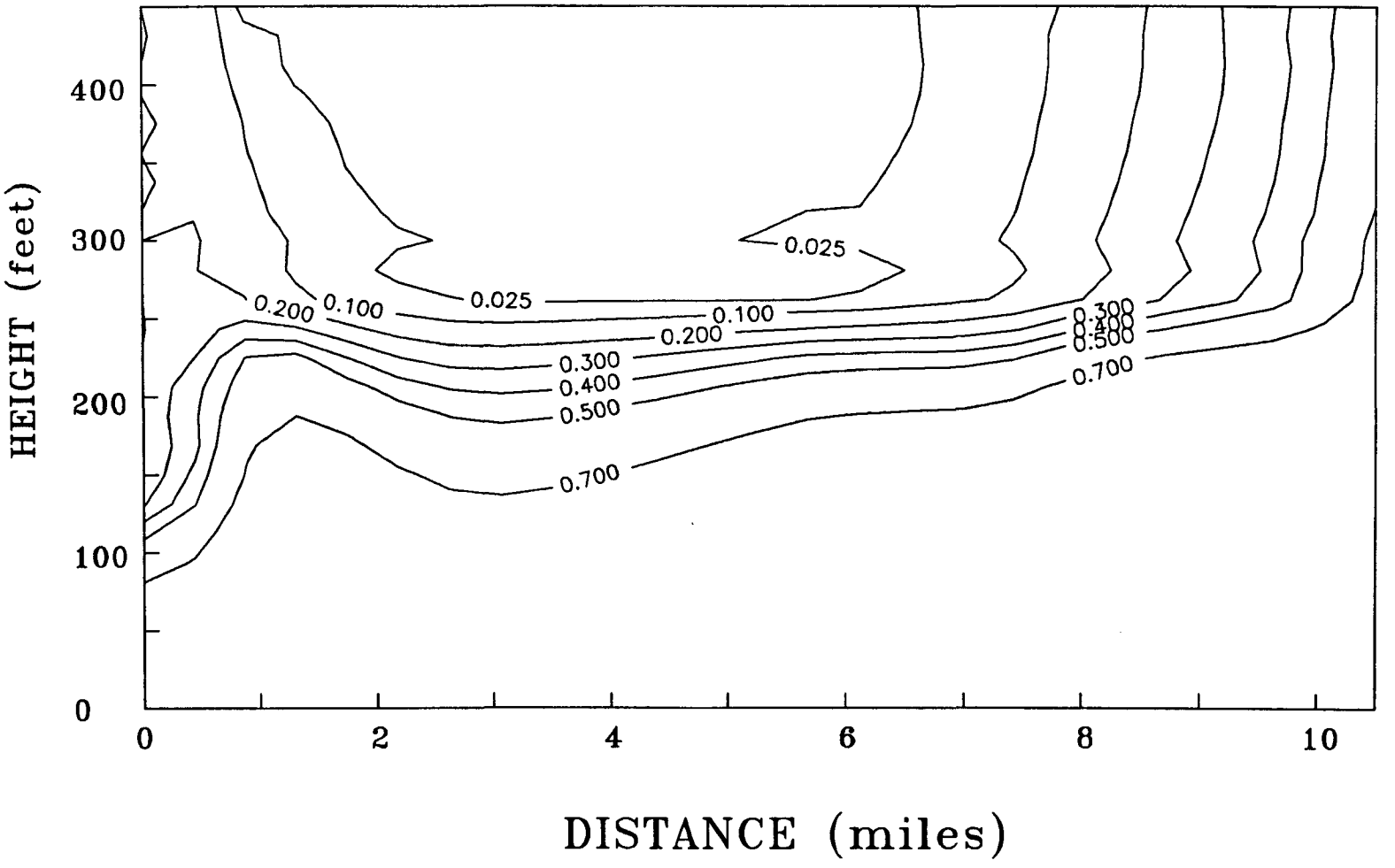

Figure 7.6. Relative concentration profile through A-A′ for the symmetric rectangular recharge case.

uplifting effect which was neglected in the 2-D simulations. This uplifting is caused by discharges that occur along the Lake Jessup and Lake Harney boundaries. The more realistic 3-D situation allows water flow in the transverse z-direction and hence less freshwater is available for developing the lens in the other two (x and y) directions. In view of these facts, it should also be noted that the calibrated 2-D model input data will therefore be insufficient to simulate the 3-D lens.

8. THREE-DIMENSIONAL STEADY STATE SIMULATIONS

8.1 GENERAL APPROACH

Steady-state three-dimensional (3-D) simulations of groundwater flow and chloride transport were performed for the selected region of the upper Floridan aquifer system. The main objectives of the steady-state analyses were to enhance our overall understanding of the Geneva lens system, and to identify the roles of key parameters controlling flow patterns, chloride distributions, and the configuration and extent of the freshwater lens. Additionally, the optimal steady-state 3-D solution obtained from model calibration provides a rational starting point (or initial condition) for subsequent transient 3-D simulations.

The steady-state 3-D simulation study was conducted in three stages. In the first stage, the grid and the code are verified, as discussed in section 7.3. Next, a series of model calibration runs was performed during the second stage of the steady-state simulations. Optimal values of material parameters and boundary conditions were determined for the system under study. Model results were compared with observed chloride concentration data for 1982 given by Phelps & Rohrer (1987), and by Tibbals (1977). In the third stage, sensitivity runs were made by varying the values of key parameters from those used in the model calibration.

The steady-state model calibration described in this chapter provides a sound basis for determining if the three-dimensional conceptualization gives results consistent with field observations.

Furthermore it is highly useful for gaining a preliminary understanding of the three-dimensional system under study, and identifying crucial data gaps. The significance of the overall response of the modeled system to data uncertainty can be determined via a sensitivity analysis. A carefully designed sensitivity analysis helps enhance our understanding of the system, and provides an indication of the level of confidence that can be placed on the simulation results. A refinement of conceptualization of the system is needed if the sensitivity analysis produces results contrary to physical behavior, even though calibrated results match field data.

8.2 MODEL CALIBRATION

The steady-state 3-D model for the Geneva lens system can be calibrated once the 3-D grid is designed and verified. The mesh described in section 7.3 is used throughout all simulations. The calibration process begins from the set of parameter values used to verify the grid. The methodology of calibration adopted is to change the parameter values one at a time, to those representing field conditions starting from the grid verification simulation shown in Figures 7.5 and 7.6. Effects of individual processes and key parameters on the lens system can therefore be determined. This step by step approach is most effective for calibrating complex systems. This calibration process is summarized in Table 8.1.

TABLE 8.1 SUMMARY OF CALIBRATION PROCESS

CALIBRATION RUN	PARAMETERS	FIGURE	REMARKS
0	Grid calibration conditions of Chapter 7. Material properties of 2-D simulations (Fig. 5.8).	7.6	Grid behaves properly. Symmetric recharge application leads to symmetric head and chloride distributions. The transport numerical solution (i.e. concentration) is oscillation-free.
1	Supply areal recharge/discharge in zones, according to estimated field conditions of Fig 8.1	8.2 8.3	Lens shape redistributed from previous simulation. Lens size is small in depth and in areal extent especially near the St. Johns River boundary.
2	Values of areal discharge halved from RUN1 (in order to observe its effect on lens size).	8.4 8.5	Lens size dramatically increased in all directions. Surface discharge constrains the lens by uplifting underlying brackish water.
3	Lateral conductivities of upper two formations halved Remaining parameters identical to RUN1. (in order to observe this effect on flow of recharge water).	8.6 8.7	Areal chloride distribution not affected significantly. Depth of freshwater increased considerably. Lateral movement of freshwater is large enough to push freshwater to the same areal extents. However, more recharge water is allowed to flow vertically, to increase lens depth.
4	Vertical conductivity of lowermost formation increased from 0.01 to 0.03 ft/d. Remaining parameters identical to RUN3 (in order to observe this effect on underlying brackish water movement)	8.8 8.9	Chloride distribution pattern does not change significantly.
5	Material zone thicknesses changed in all planes (Ocala thickness decreases). Remaining parameters identical to RUN4. (To observe sensitivity of lens to material distribution. This will determine the detail required in parameter input).	8.10 8.11	No large effects on chloride patterns. Material zone thickness is difficult to measure in detail, at the site. A detailed source of this parameter (Barraclough, 1966) has been shown by District logs (unpublished) to be inaccurate. Other sources (Phelps & Rohrer, 1987, District's unpublished data) are not as extensive. Fortunately, effects are not large.
6	Material zones varied throughout domain to best match field estimates. Remaining parameters identical to RUN5 (to zoom in on the actual field situation).	8.12 8.13	Chloride patterns between those developed in RUN4 and RUN5. The material thickness data are selected from Phelps and Rohrer (1987), and District logs (unpublished), where available. Barraclough's (1966) estimates are used in other locations. More detailed data is not necessary since chloride patterns are relatively insensitive to these thicknesses.
7	Discharge pattern re-distributed. Unit discharge = 0.0015 ft/d for all zones other than those along Econlockhatchee River. Remaining parameters identical to RUN6.	8.14 8.15	Lens re-distributes areally. Previous simulations restricted discharges with the assumption that all flow would be parallel to the elemental slices. Hence the net discharge in a slice was set equal to the net recharge into that slice, neglecting flow across slices.
8	Recharge/discharge values redistributed as shown in Fig. 8.16. (To get final calibrated lens).	8.17 8.18	Lens matches with field data. Recharge values are within field estimated range. Discharge values in the field are unknown. Logical calibration of this parameter invokes net discharge values to be equal to net influx into the simulation domain.

For the first calibration run, all vertical slices that combine to form the 3-D grid are assigned identical material properties. Recharge through the top of the Floridan system was prescribed in accordance with actual estimates of recharge and its distribution at the site, as provided by Tibbals (1977). The total discharge through the top of each cross-sectional plane is calculated to be equal to the sum of influx to that plane from the lateral boundary at the Econlockhatchee River and infiltration through the top.

The recharge/discharge zones have been mapped in Figure 8.1, with the low recharge areas receiving 4.56×10^{-4} ft/d (2 inch/yr), and the zones of higher recharge receiving 2.28×10^{-3} ft/d (10 inch/yr) of freshwater. Longitudinal dispersivities (α_L) for zones 1, 2, and 3 (see Figure 7.3) are 100, 200 and 200 ft respectively, and transverse dispersivities (α_L) are 2.5, 5 and 5 for the three zones respectively. The vertical conductivity of zone 1 is 0.01 ft/d. All other parameters are identical to the 2-D simulation parameters shown in Figure 5.8. This simulation will be referred to as RUN1. The areal distribution of chloride at the top of the upper Floridan is shown in Figure 8.2, and the concentration profile for cross-section 10 passing through the center of the domain (A-A′ of Figure 7.1) is shown in Figure 8.3. The resulting lens is seen to be small and shallow. Based on data from well site #36 of Phelps and Rohrer (1987), the maximum thickness in the center of the lens should be between 250 and 300 ft, and based on

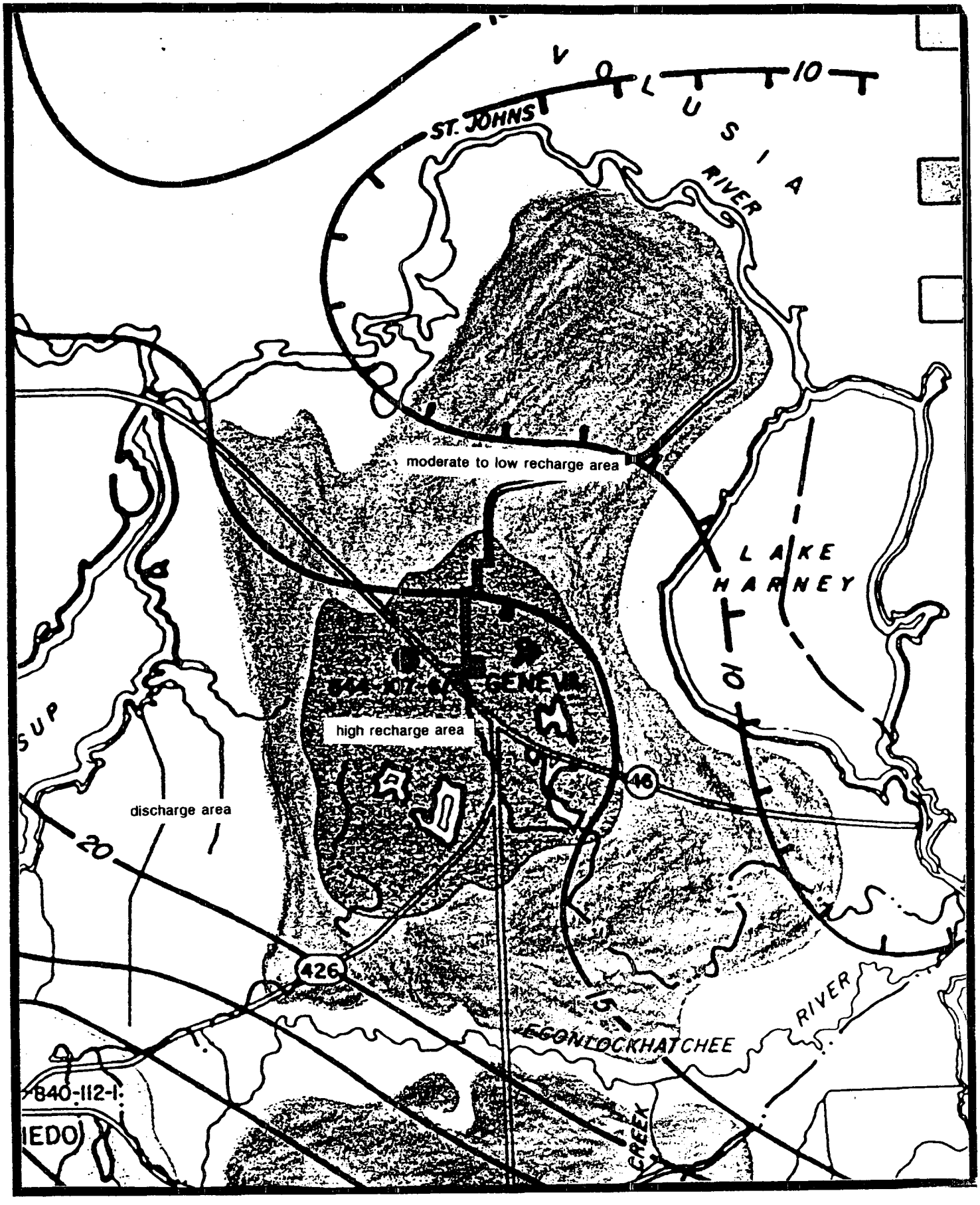

Figure 8.1. Recharge/discharge zones in the Geneva area (after Tibbals, 1977).

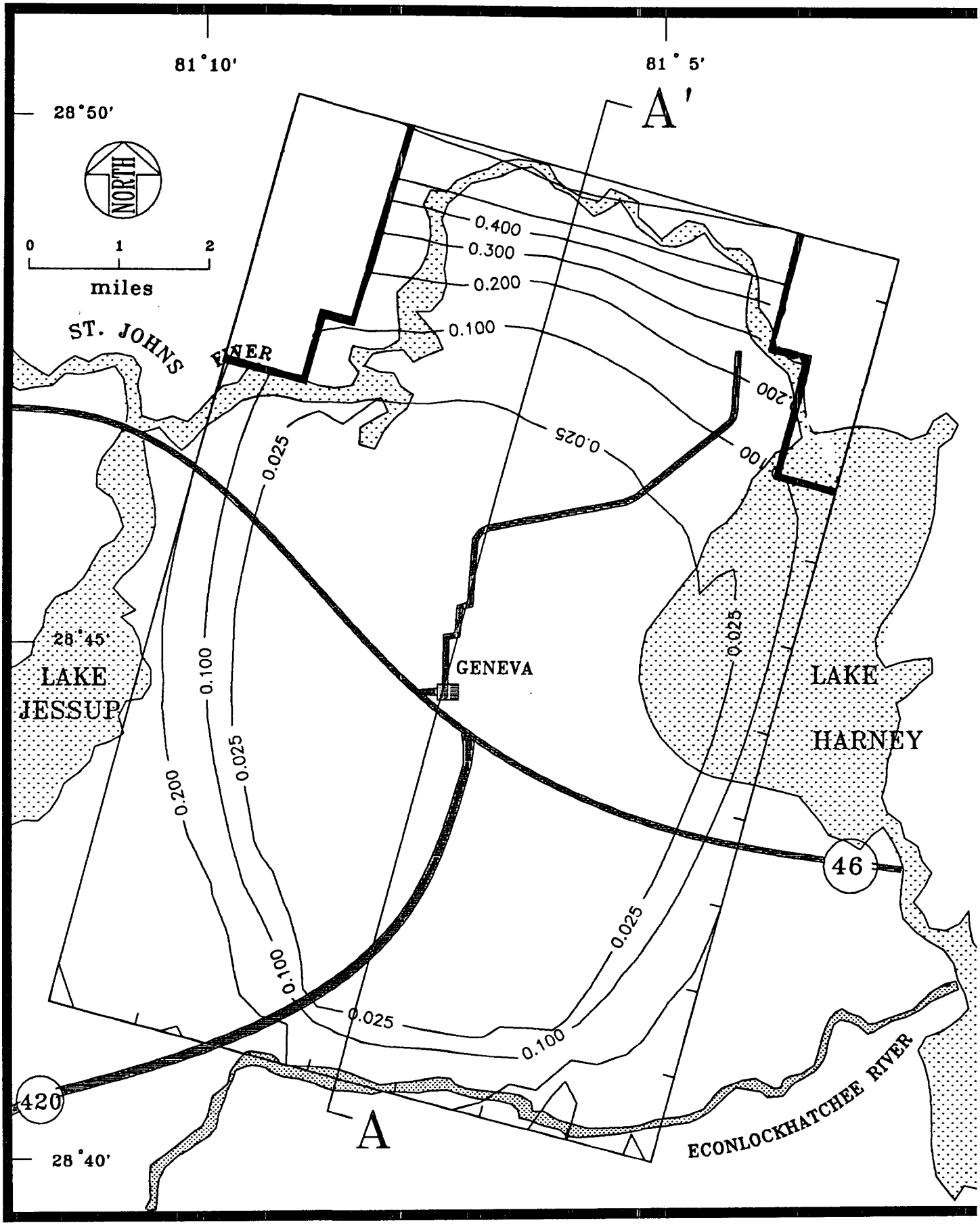

Figure 8.2. Areal distribution of chloride for calibration RUN1.

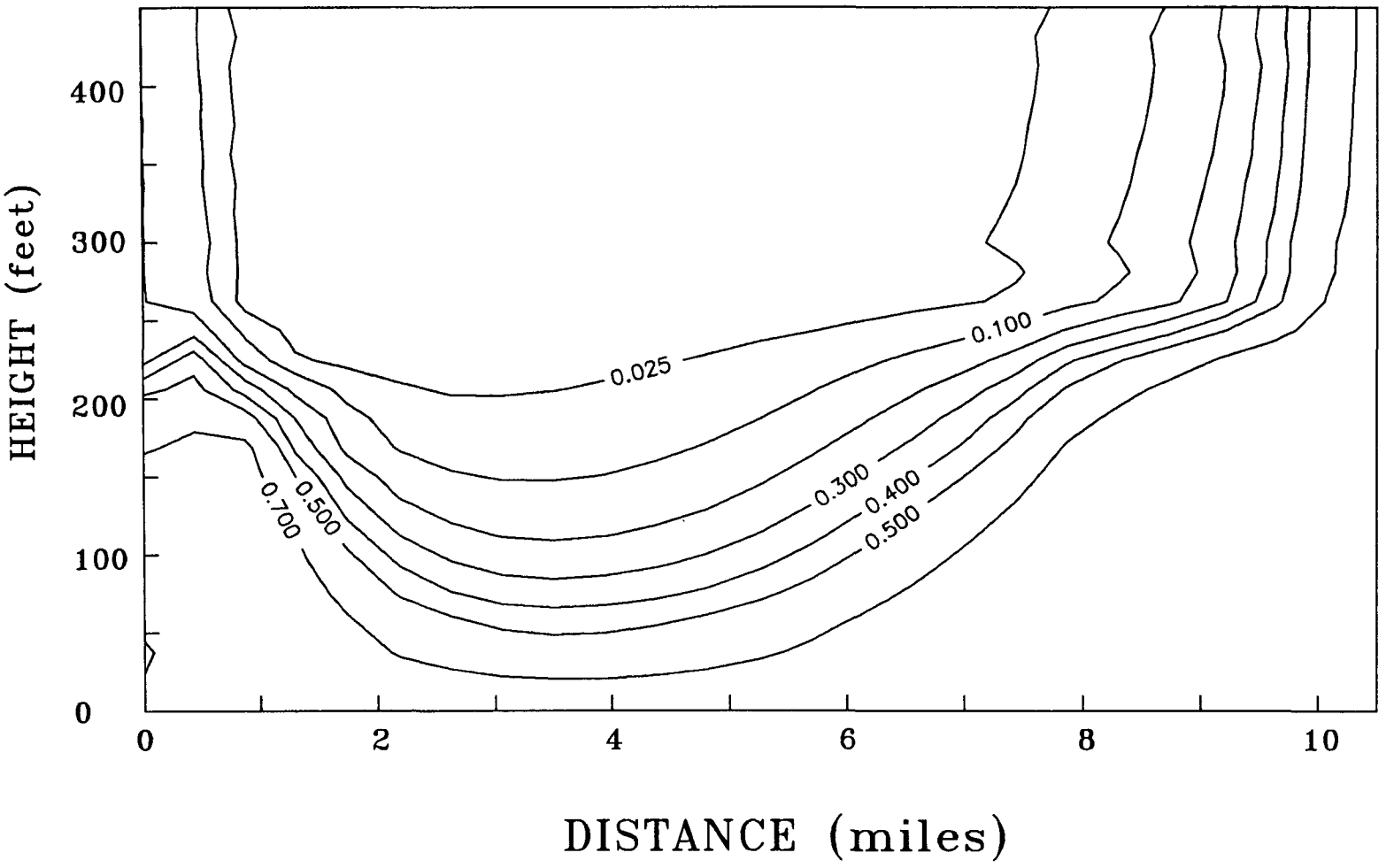

Figure 8.3. Relative concentration profile through A-A′ for calibration RUN1.

data from well #S-0087 (near site 58 of Figure 3.2) the maximum thickness in the downgradient area should be 170 to 180 ft.

All discharges were halved for the next calibration run (RUN2). Other parameters remain the same as in RUN1. The areal distribution of chloride for this case is shown in Figure 8.4 and the concentration profile of cross-section A-A' is shown in Figure 8.5. The lens is seen to be larger and deeper for this case. Reducing discharge from the surface tends to increase lens size vertically and laterally. Large discharges would create an upconing effect on brackish water from the deeper regions of the aquifer, thus reducing lens size.

The next calibration run (RUN3) is again identical to RUN1, except that the lateral hydraulic conductivities (K_{zz}) of the Ocala and of the upper portion of the Avon Park, are halved and equal to 80 ft/d and 25 ft/d, respectively. Concentration profiles at the surface of the upper Floridan aquifer and of cross-section A-A' are shown in Figures 8.6 and 8.7, respectively. The areal distribution of chloride at the surface was not affected significantly for this case. The depth of the lens is however, greatly increased. Reducing the two horizontal conductivities, K_{xx} and K_{zz}, of the upper two formations limits lateral movement of the recharge water thus pushing it downwards and increasing the thickness of the freshwater lens.

RUN4 is identical to RUN3 except that the vertical conductivity of the lower Avon Park formation (K_{yy} of zone 1) was increased from 0.01 ft/d to 0.03 ft/d. The areal chloride

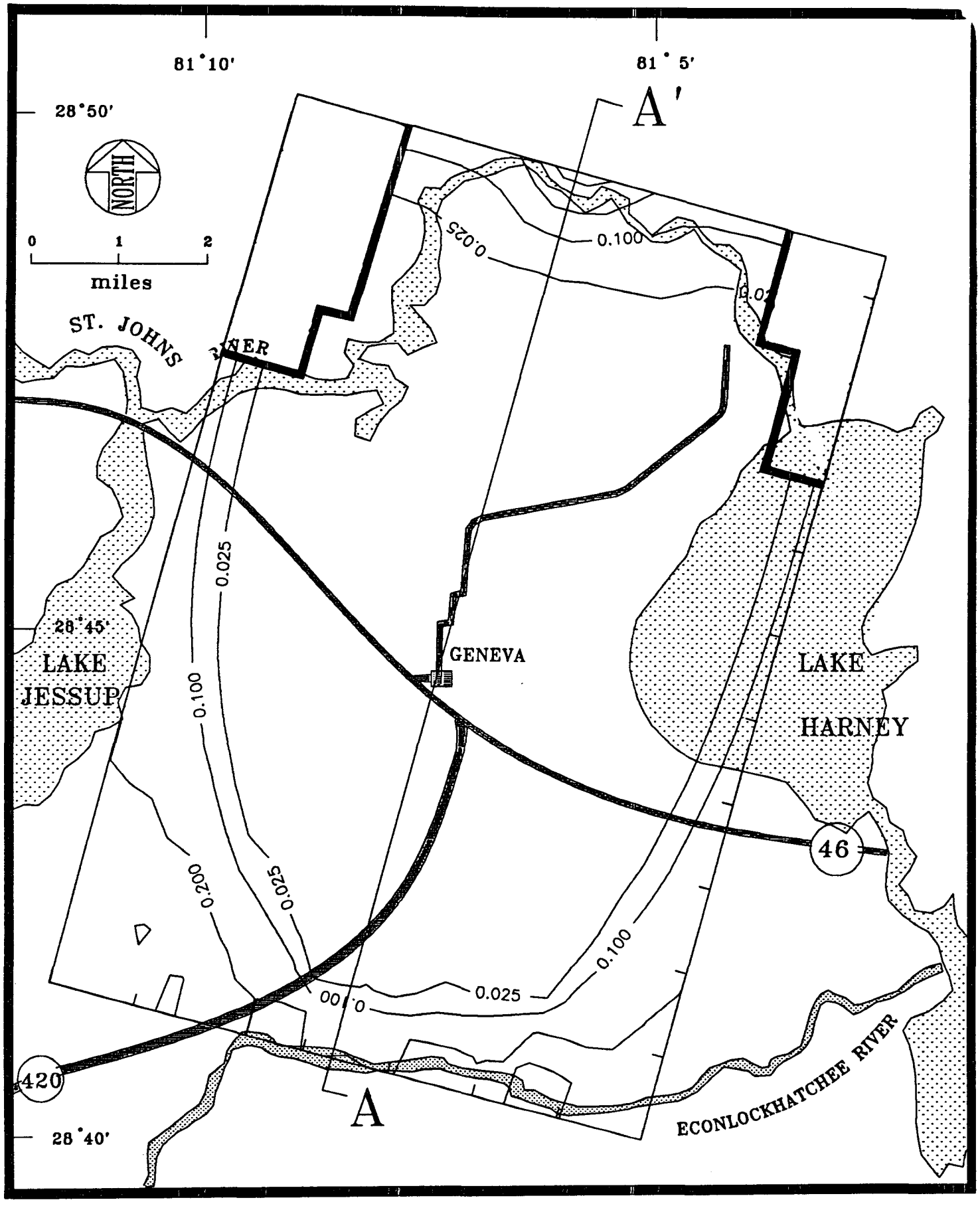

Figure 8.4. Areal distribution of chloride for calibration RUN2.

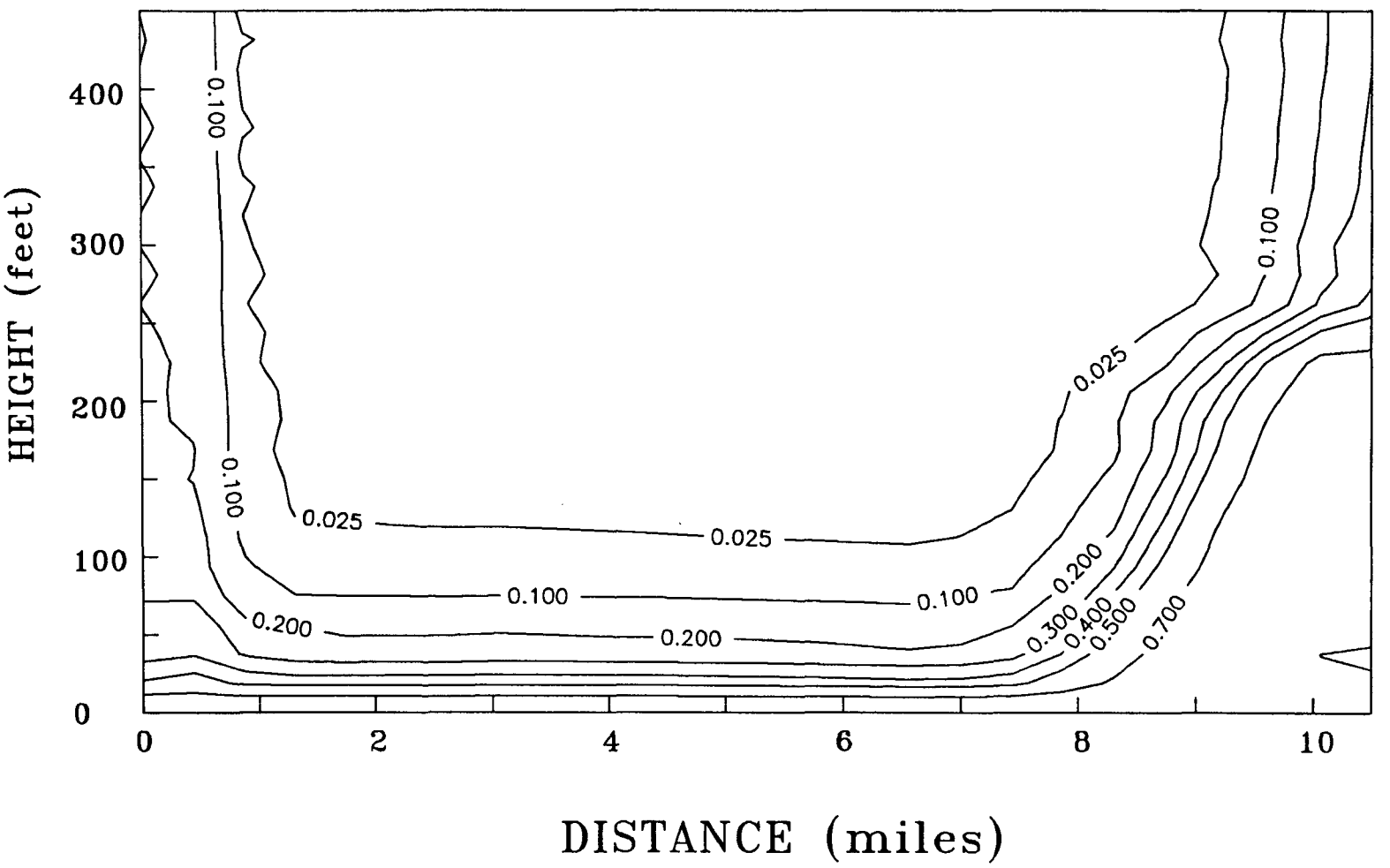

Figure 8.5. Relative concentration profile through A-A' for calibration RUN2.

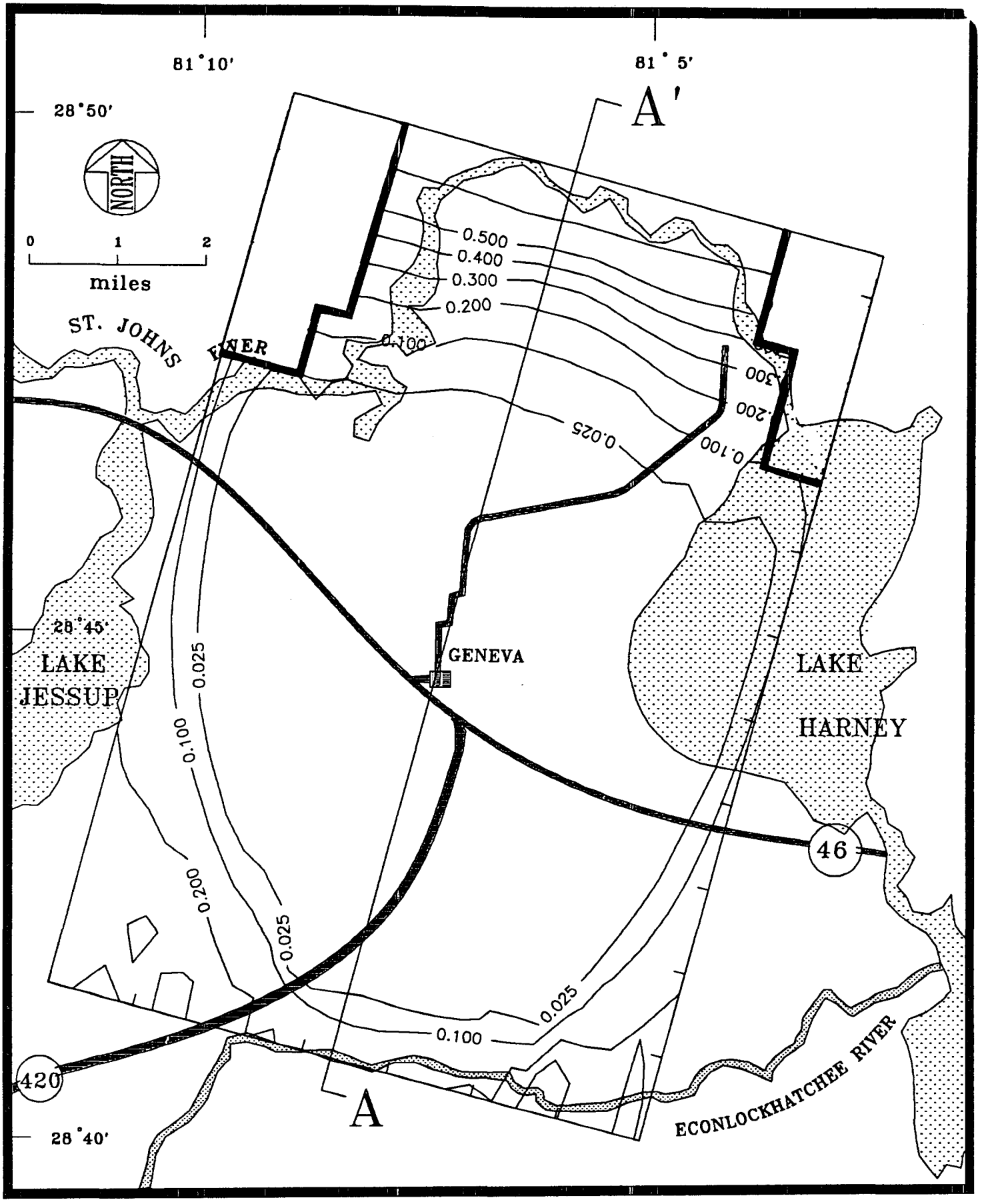

Figure 8.6. Areal distribution of chloride for calibration RUN3.

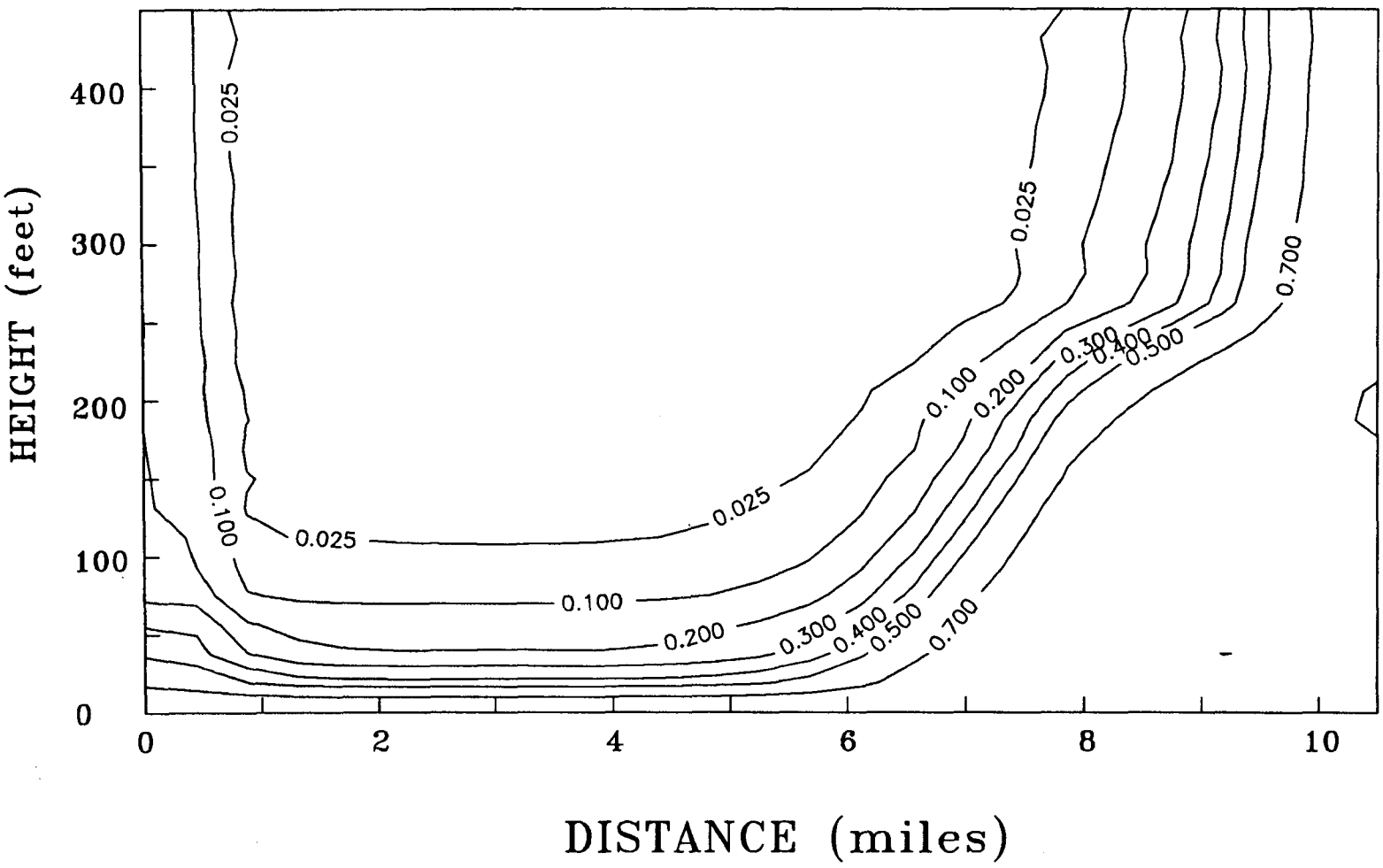

Figure 8.7. Relative concentration profile through A-A′ for calibration RUN3.

distribution at the top of the upper Floridan, and the vertical profile through section A-A′ are shown in Figures 8.8 and 8.9 respectively. This higher vertical conductivity was expected to reduce the lens size by allowing larger amount of flow of brackish water from the bottom. However, the average lens depth is not significantly different from that of RUN3, showing that the effect of recharge on the thickness of the lens is more dominant for the selected set of parameter values. Earlier test simulations showed K_{yy} in zone 1 to be a more sensitive parameter, when lateral conductivities of the Ocala and Avon Park were 160 ft/d and 50 ft/d, respectively.

The next simulation (RUN5) was performed to observe the effect of changing the thickness of the Ocala formation on lens behavior. Material zones in all cross-sections were changed to resemble those of the first cross-sectional plane shown in Appendix A. All other parameters are identical to those of RUN4. Figures 8.10 and 8.11 show the areal chloride distribution at the top of the upper Floridan, and the vertical variation of chloride concentration in the mid-plane A-A′, respectively. Vertically, the lens is somewhat smaller, near the Econlockhatchee River end, than for RUN4. Areally, the lens is slightly diminished from that of RUN4. The effect of different Ocala thicknesses is however, not pronounced, and hence a rough representation of the Ocala thickness as obtained from the scarce data available should be adequate to represent the Geneva lens system.

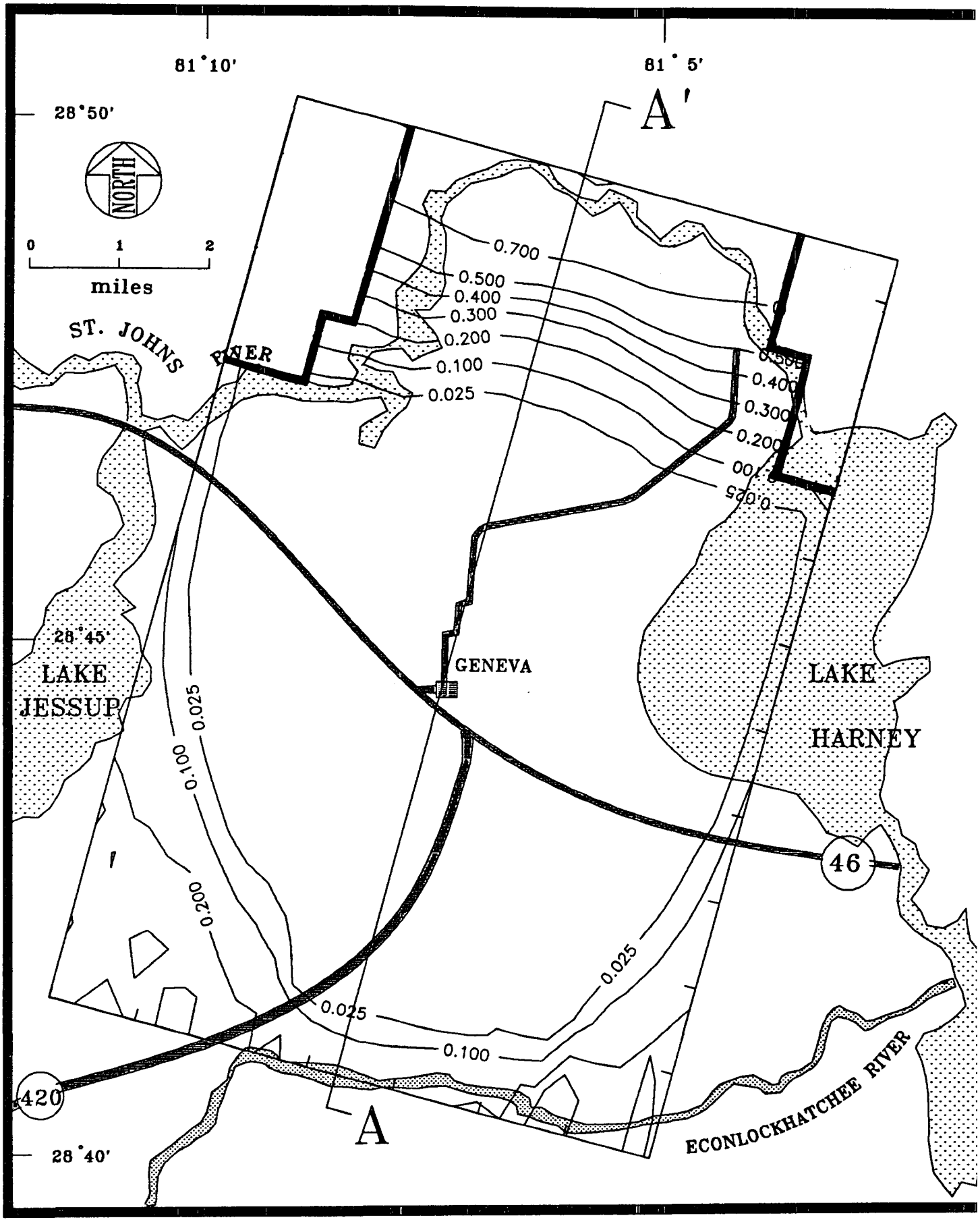

Figure 8.8. Areal distribution of chloride for calibration RUN4.

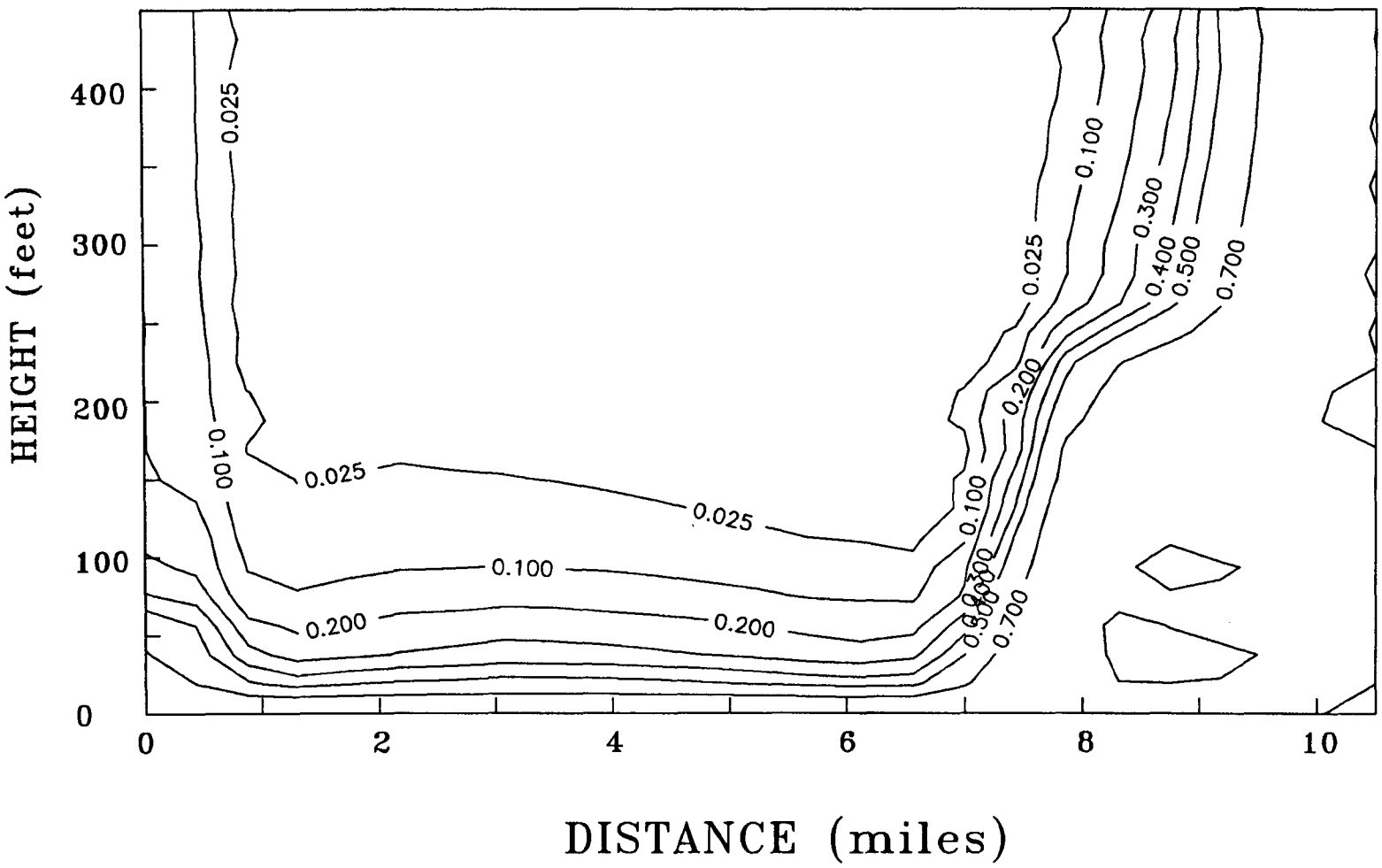

Figure 8.9. Relative concentration profile through A-A' for calibration RUN4.

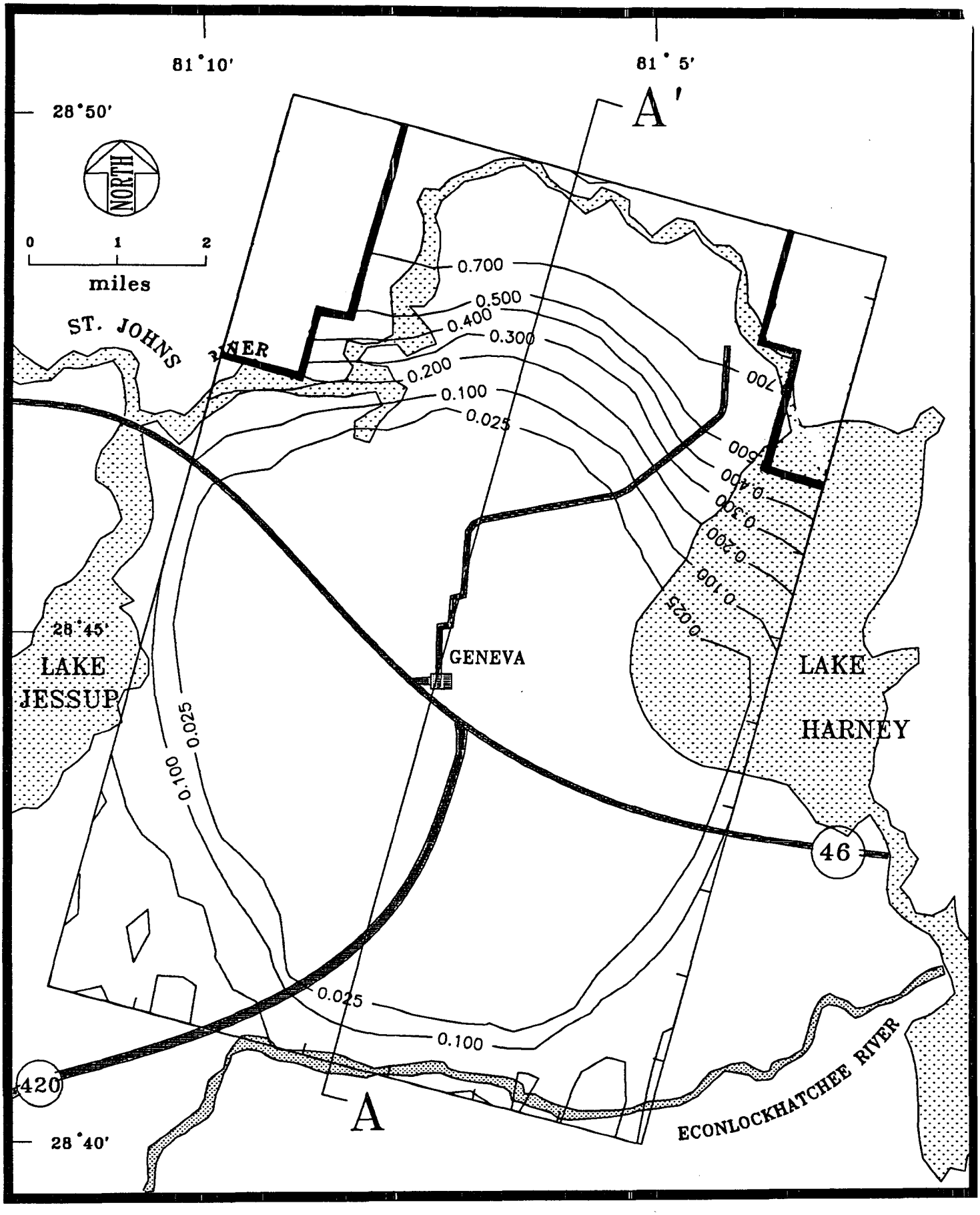

Figure 8.10. Areal distribution of chloride for calibration RUN5.

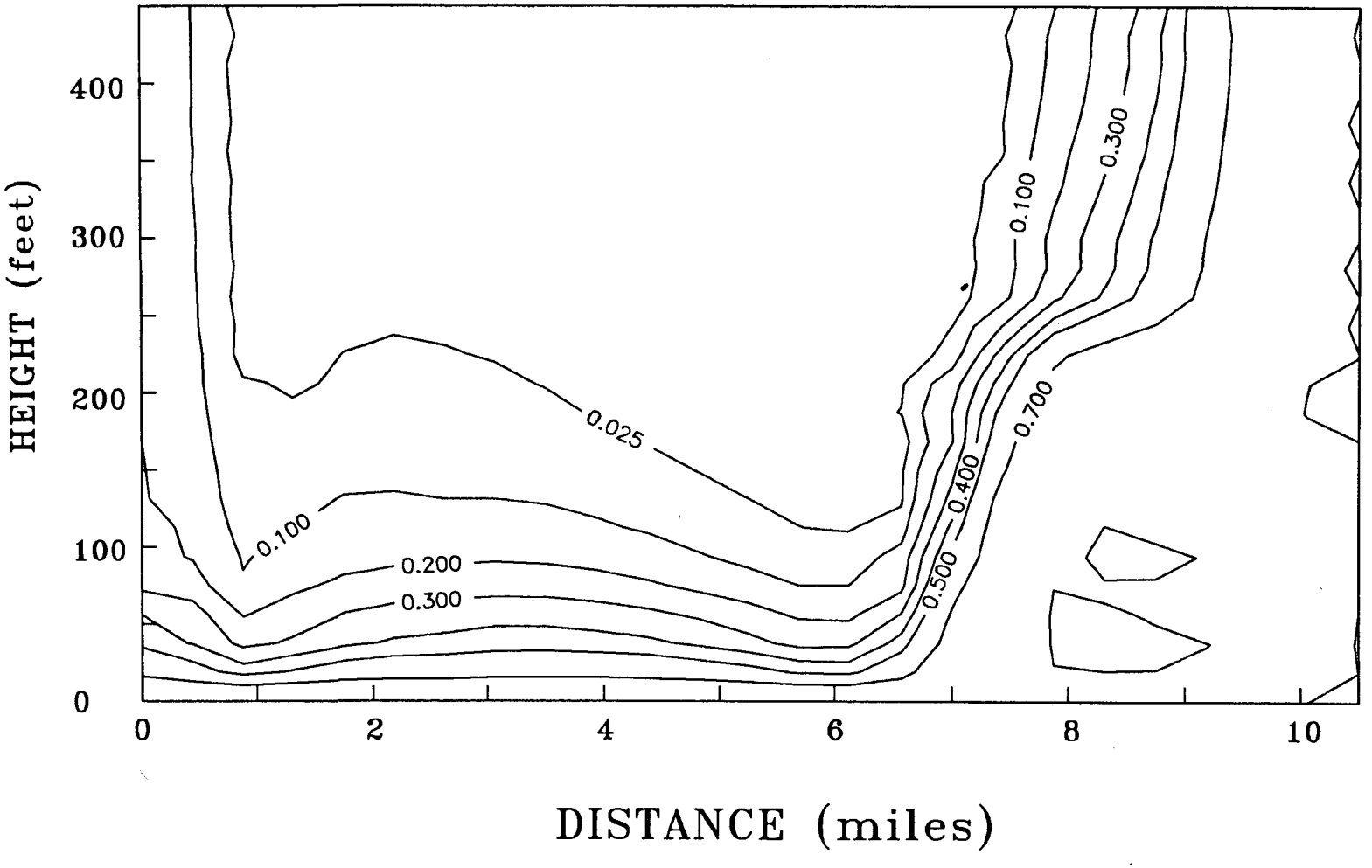

Figure 8.11. Relative concentration profile through A-A′ for calibration RUN5.

RUN6 was performed with all parameter and recharge/discharge values identical to RUN5. The material zones within each cross-section are however varying in thickness in an attempt to represent the stratigraphy of the Upper Floridan within the simulation domain. The available information on formation thicknesses, though sketchy, seems sufficient, since the lens is not overly sensitive to material stratigraphy, as seen in RUN4 and RUN5. The areal solute distribution at the top of the Upper Floridan and the vertical chloride distribution in the section A-A′ are shown in Figures 8.12 and 8.13, respectively. The lens pattern is seen to be between that of RUN4 and RUN5.

The calibration runs so far (RUN1-RUN6) applied a net discharge through the top of any cross-section such that it was equal to the net influx to that cross-section from the Econlockhatchee River boundary and the surficial recharge. The next simulation (RUN7) considers Econlockhatchee River side discharges to be the same as those used earlier. Discharge through the rest of the domain is re-distributed, however, such that the unit discharge is the same for all discharge zones. A discharge value of 1.5×10^{-3} ft/d is provided to all discharge zones not adjacent to the Econlockhatchee River boundary. The rest of the parameters are the same as those used in RUN6. The areal distribution of chloride at the top of the simulation domain and chloride concentration profile through the mid-section A-A′ are shown in Figures 8.14 and 8.15 respectively. Vertically the lens seems to conform well with field estimates. The shape of the lens

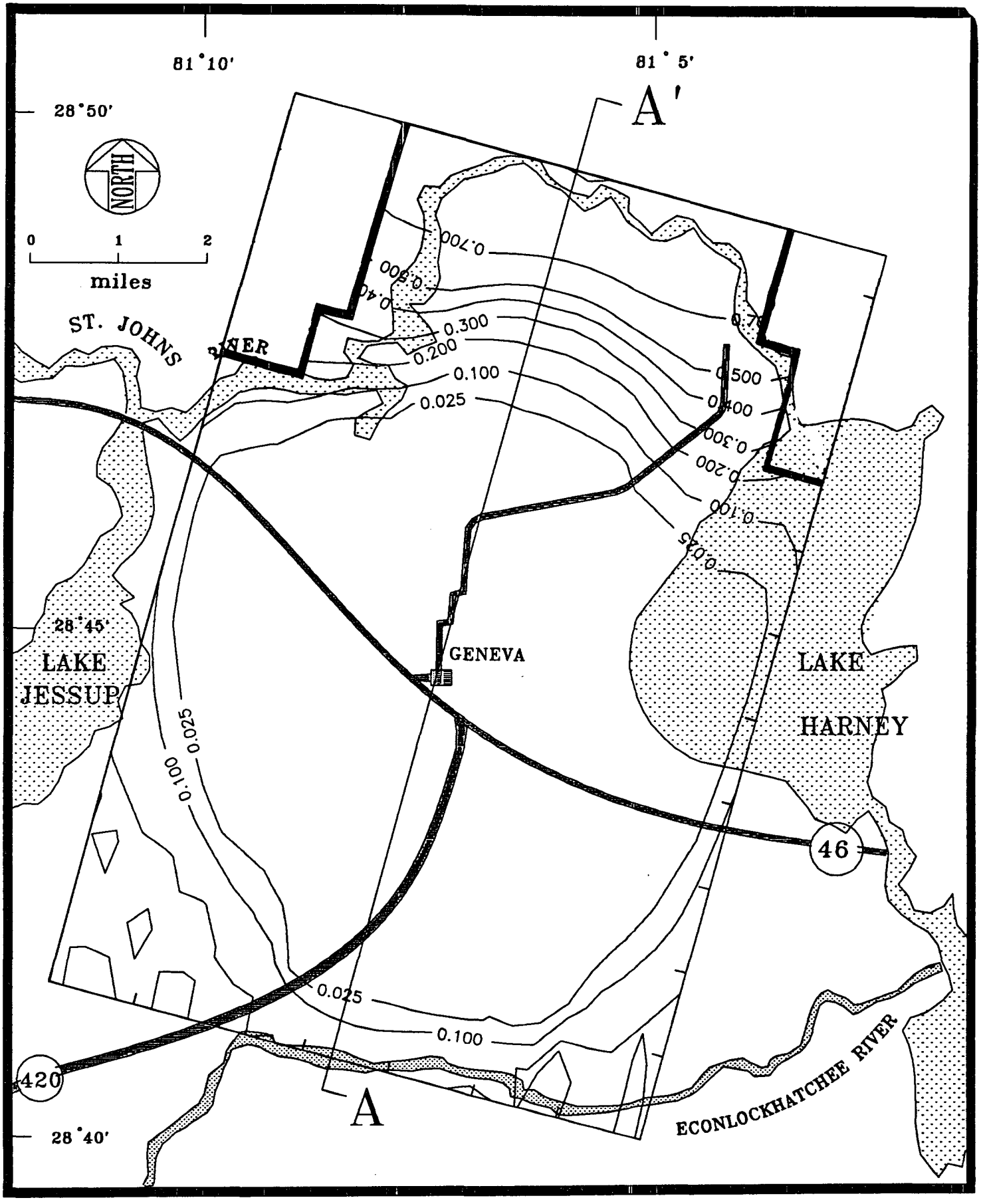

Figure 8.12. Areal distribution of chloride for calibration RUN6.

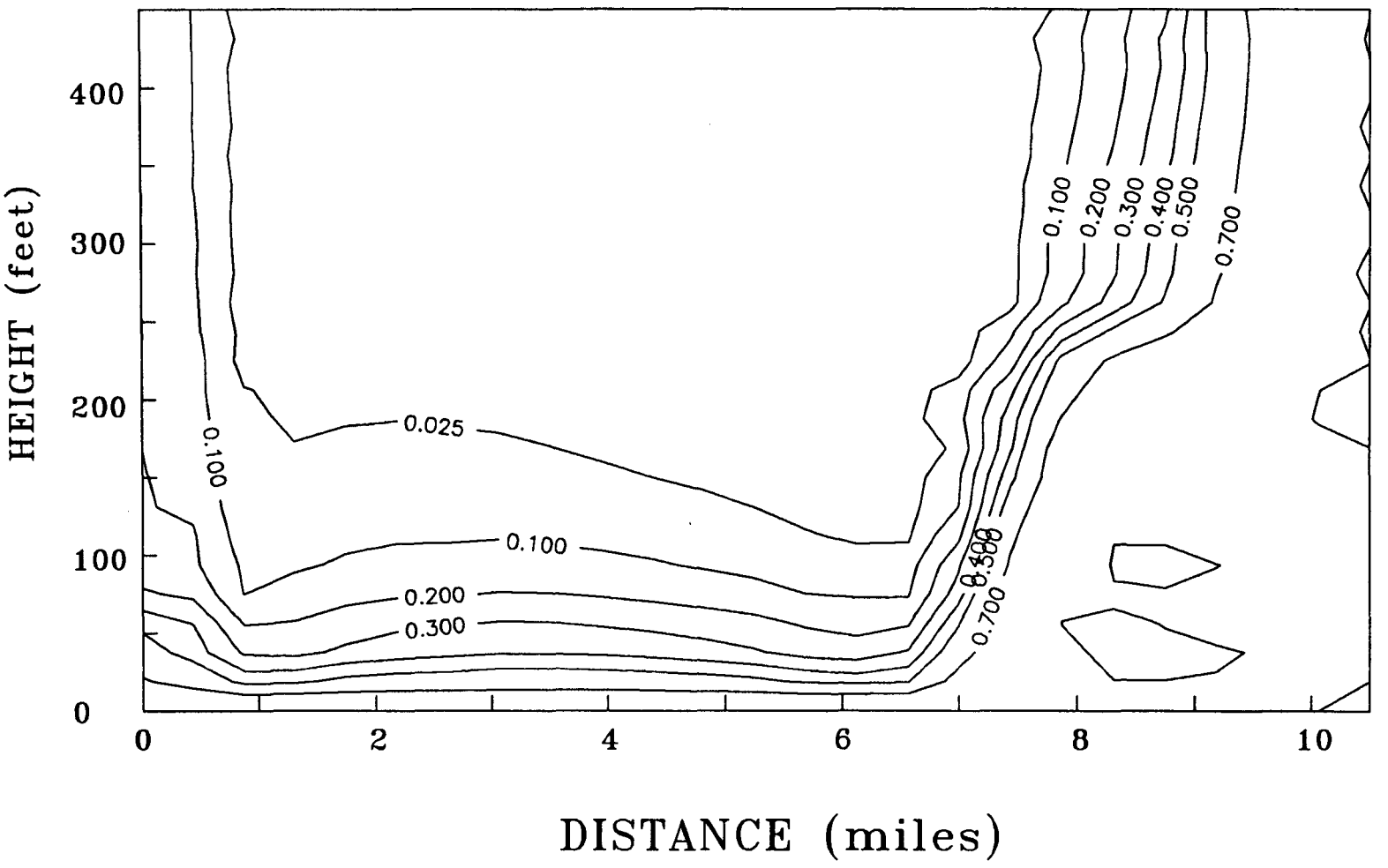

Figure 8.13. Relative concentration profile through A-A' for calibration RUN6.

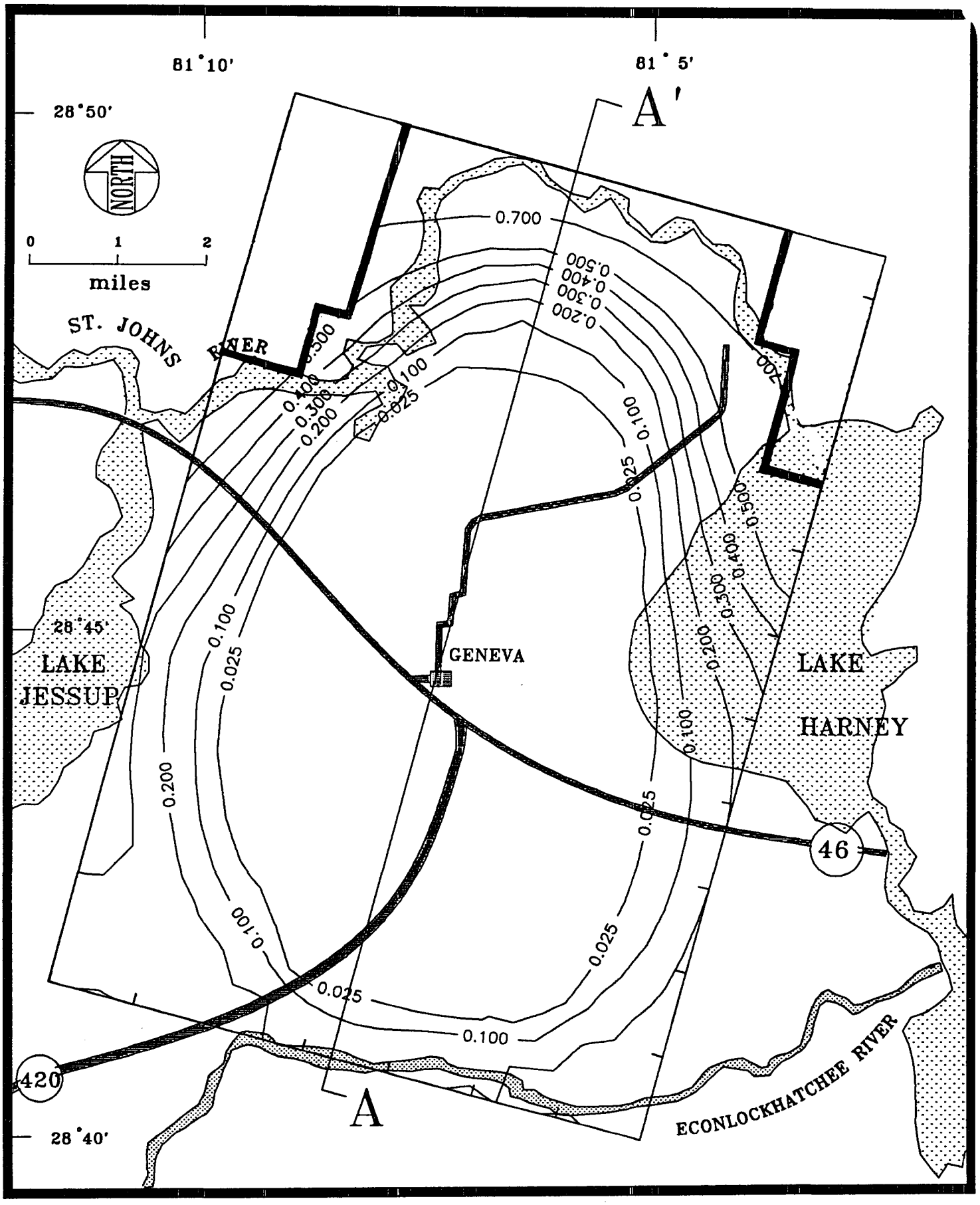

Figure 8.14. Areal distribution of chloride for calibration RUN7.

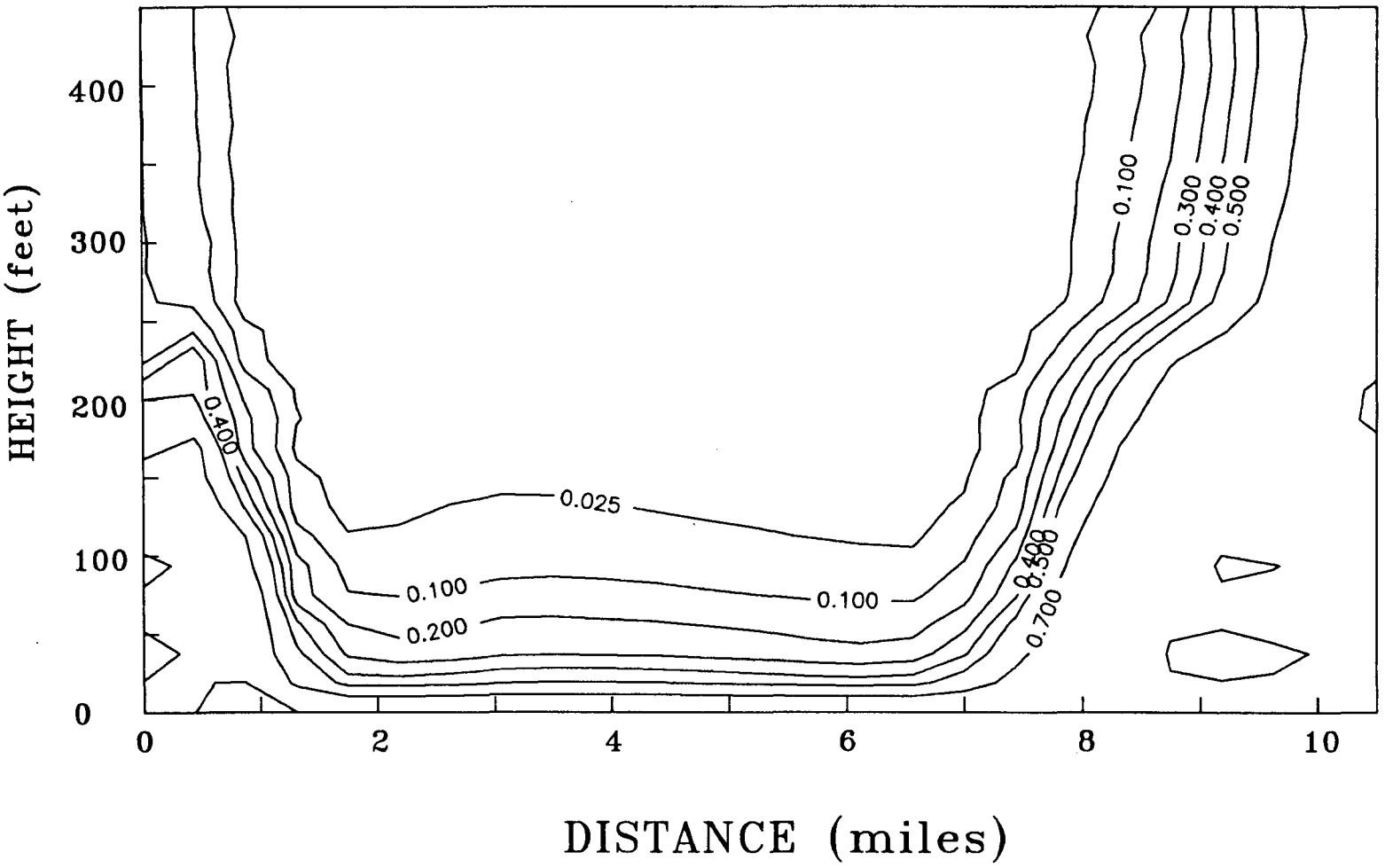

Figure 8.15. Relative concentration profile through A-A' for calibration RUN7.

also conforms areally with the estimated lens (Figures 16 and 17 of Phelps and Rohrer, 1987, Figures 11 of Tibbals, 1977). The lens however needs to be approximately 1.5 miles longer near the St. Johns river end of the domain.

RUN8 provides the final calibrated lens. Recharge/discharge rates and distributions have been adjusted for this simulation. The areal distribution of recharge and discharge for this calibrated run is depicted in Figure 8.16. Discharges near the Econlockhatchee River are equivalent to 20.9 cubic feet per day per unit foot in the z-direction. The quantity is equal to the amount of water entering the domain through the side boundary near the Econlockhatchee River. Discharge in the Lake Jessup side of the domain and near the St. Johns River equals 0.001 ft/d, and near the Lake Harney edge of the domain equals 0.0025 ft/d. Recharge is supplied to two zones; 0.00228 ft/d (10 inch/yr) in the zone of high recharge, and 0.0012 ft/d (5.25 inch/yr) in the zone of low to moderate recharge (Tibbals, Figure 3, 1977). The material properties and boundary conditions used for this calibrated steady-state lens are reported in Tables 8.2 and 8.3 respectively along with the rationale for their selection. Material zones for each elemental slice are depicted in Appendix A. The predicted areal distribution of chloride at the top of the simulation domain is depicted in Figure 8.17a along with the Phelps and Rohrer estimates of the 250 ppm isochlor for Oct. 1982. Figure 8.17b shows a perspective view of the simulated freshwater lens. Figure 8.18 shows Tibbals (1977) estimate of chloride distribution, which also

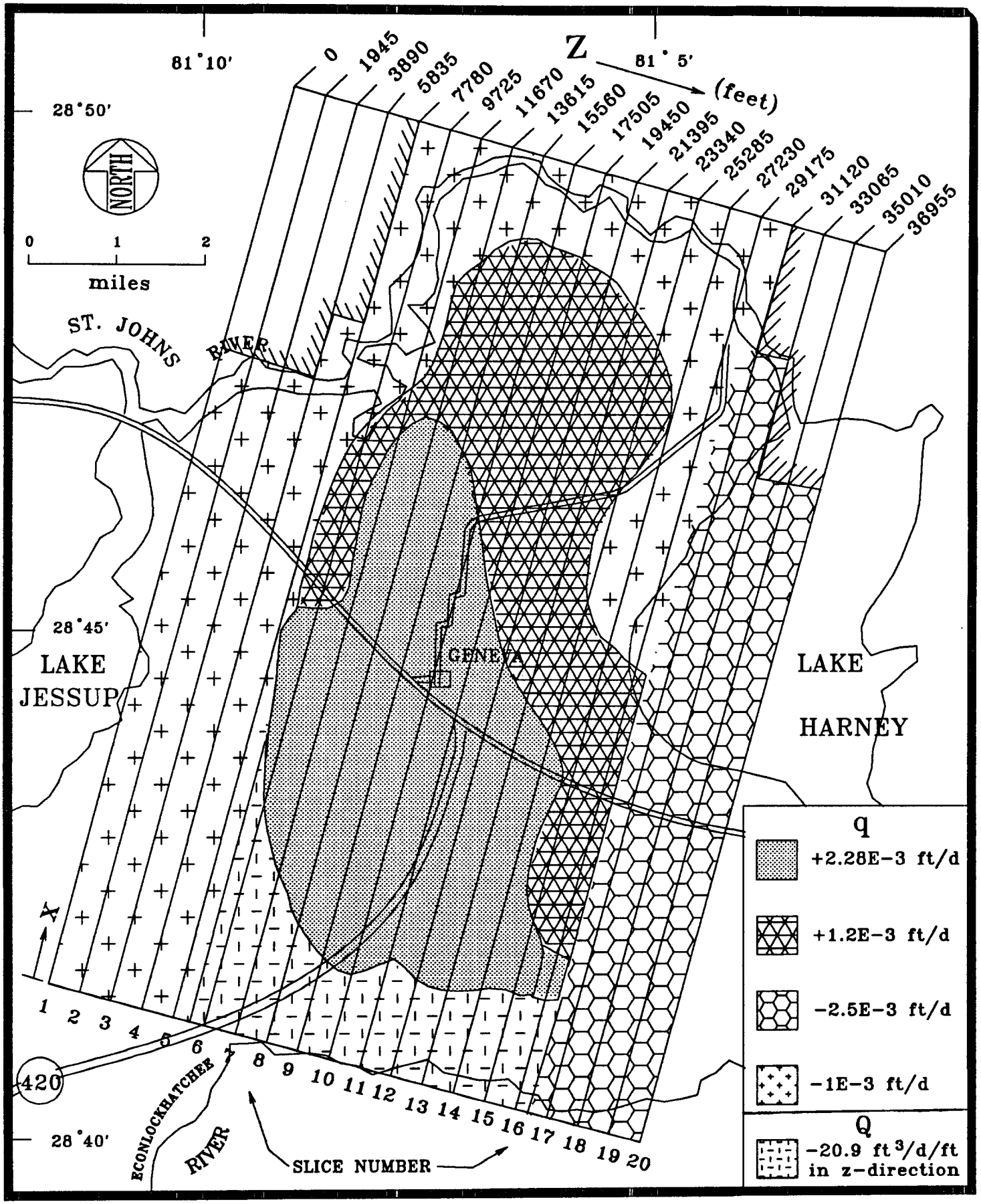

Figure 8.16. Areal distribution of recharge/discharge for the calibrated simulation of the Geneva freshwater lens.

TABLE 8.2 MATERIAL PARAMETERS FOR THE CALIBRATED THREE-DIMENSIONAL STEADY-STATE ANALYSIS.

MATERIAL	PARAMETER	VALUE	BASIS OR SOURCE FOR SELECTION (NOTE: EXACT VALUE FALLS WITHIN A REASONABLE RANGE)
Ocala	$K_{xx} = K_{zz}$ (ft/d)	80	Corroborates with Phelps and Rohrer (1987) estimates (within range). See effects of its variation in Table 8.1.
	K_{yy} (ft/d)	16	Skipp's modeling effort (unpublished). Within range of anisotropy values estimated by the District.
	α_L (ft)	200	Skipp's modeling effort (unpublished). See effect of its variation in Table 8.4.
	α_T (ft)	5	Anticipated value for the material and the size of the problem.
	areal extent and thickness	see Appendix A	Figures 4 and 5 of Barraclough (1962), and Phelps and Rohrer (1987). See effects of it's variation in Table 8.1.
Upper Avon Park	$K_{xx} = K_{yy}$ (ft/d)	25	Same basis as for K_{xx} of Ocala above.
	K_{yy} (ft/d)	5	Same basis as for K_{yy} of Ocala above.
	α_L (ft)	200	Same basis as for α_L of Ocala above.
	α_T (ft)	5	Same basis as for α_T of Ocala above.
	areal extent and thickness	see Appendix A	Skipp's modeling effort (unpublished).
Lower Avon Park	$K_{xx} = K_{yy}$ (ft/d)	5	Same basis as for K_{xx} of Ocala above.
	K_{yy} (ft/d)	0.03	Same basis as for K_{yy} of Ocala above.
	α_L (ft)	100	Same basis as for α_L of Ocala above.
	α_T (ft)	2.5	Same basis as for α_T of Ocala above.
	areal extent and thickness	see Appendix A	Skipp's modeling effort (unpublished).
Salt (chlorides)	water density	1 g/cc	Recorded value.
	max-solution density	1.013 g/cc	Recorded value for concentration of 10,000 ppm.
	Diffusion	0.001(ft^2/d)	Recorded value.

8-25

TABLE 8.3 BOUNDARY CONDITIONS FOR THE CALIBRATED THREE-DIMENSIONAL STEADY-STATE ANALYSIS.

BOUNDARY	PARAMETER	VALUE	RATIONALE FOR SELECTION
Bottom	head	See Fig 4.4a	Skipp's simulation (unpublished). Corroborates with reported values of Phelps & Rohrer (1987) for the average piezometric head. It is the best estimate possible with available data. See sensitivity to this parameter in Table 8.4. Note: Heads do not vary in the z-direction.
	conc.	10,000 ppm	Skipp's simulation (unpublished). Most wells show this value at depth of bottom boundary.
Top	recharges	See Fig 8.16	From Tibbals (1977) and Phelps and Rohrer (1987) for zones of recharge and average recharge rates.
	recharge conc.	0	Recharge water does not contain chlorides.
	discharges	See Fig 8.16	Discharge zones from Tibbals (1977) and Phelps and Rohrer (1987). Discharge rates calibrated. Roughly calculated to have as much total discharge as total water entering the system from Econlockhatchee River side, and recharge. See Table 8.4 for sensitivity to this parameter.
	discharge $\partial c/\partial x$	0	Natural condition for outflow boundary.
Lake Harney side and Lake Jessup side	flux	0	Boundary lies approximately parallel to ambient flow. (see pot. maps of Phelps and Rohrer, 1987).
	$\partial c/\partial x$	0	Natural condition for no-flow boundary.
St. Johns River side	flux	0	Hydraulic divide estimated here by District.
	$\partial c/\partial x$	0	Natural condition for no-flow boundary.
Econlockhatchee River side, upper 190 ft (in upper two zones)	flux	20.8 $ft^3/d/$ unit ft in z-direction	Calculated using Darcy's Law from the conductivity of this region and the ambient potential gradient as estimated by Phelps and Rohrer (1987).
	C	3,000 ppm	Phelps and Rohrer (1987) and Tibbals (1977) estimate for this location
Econlockhatchee River side lower 260 ft (in Lower Avon Park zone)	flux	0	Flux is negligible as compared to the flux in the upper 190 ft of this side boundary, as calculated by Darcy's law from horizontal conductivity and ambient potential gradient.
	$\partial c/\partial x$	0	Natural condition for no-flow boundary.

8-26

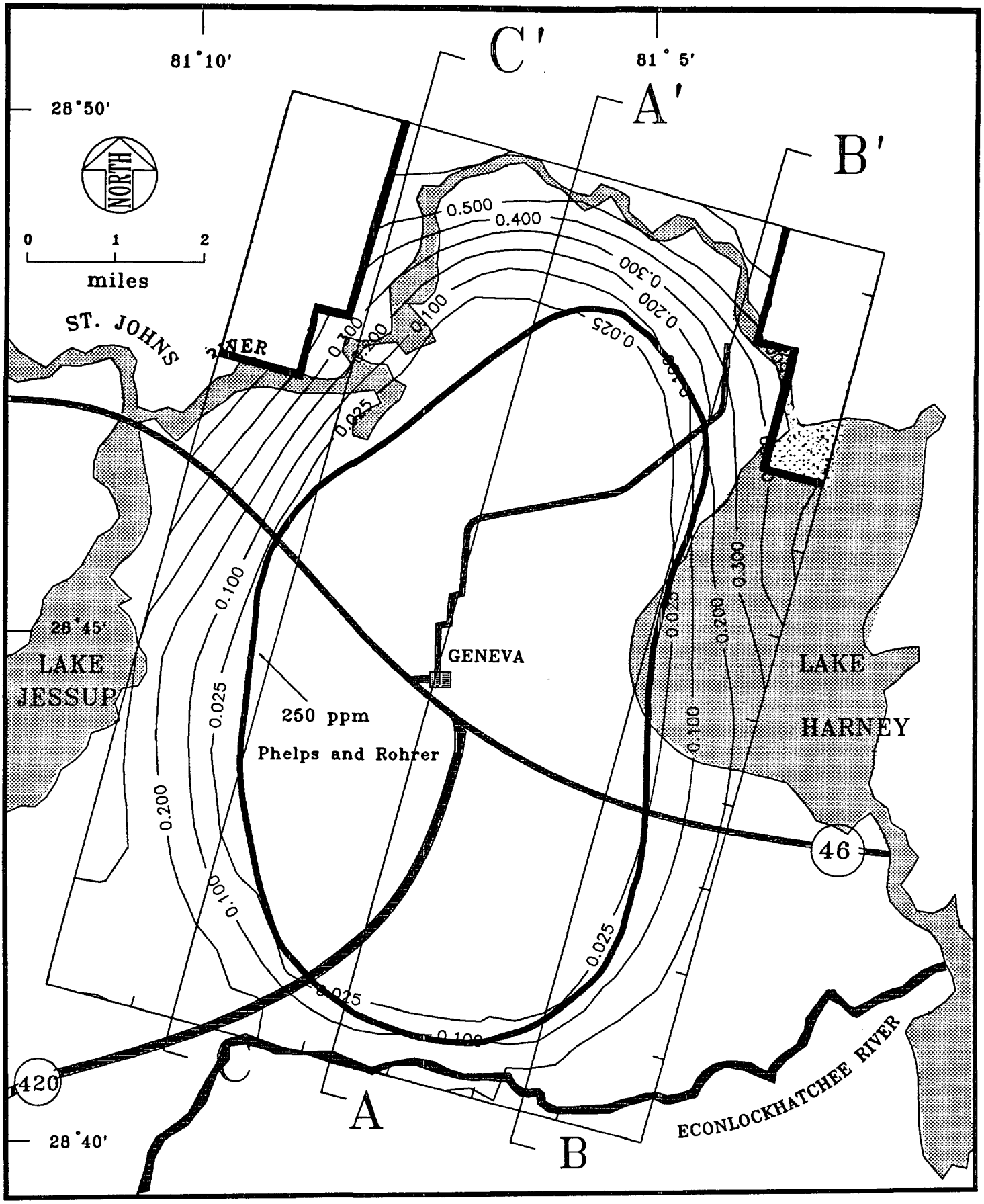

Figure 8.17a. Areal distribution of chloride for the steady-state simulation of the Geneva freshwater lens, compared to field data from Phelps and Rohrer (1987).

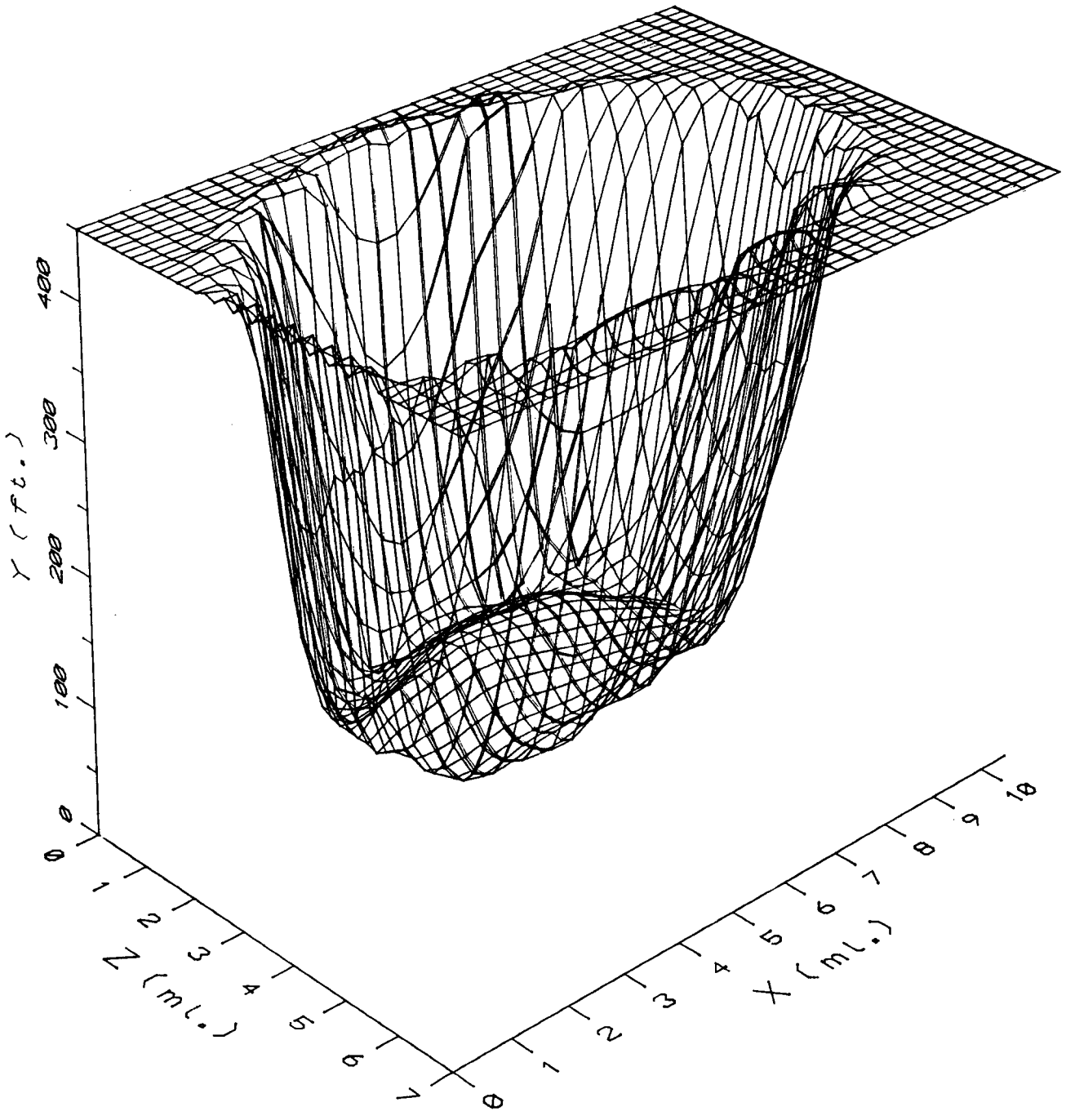

Figure 8.17b. Perspective view of the steady-state Geneva freshwater lens.

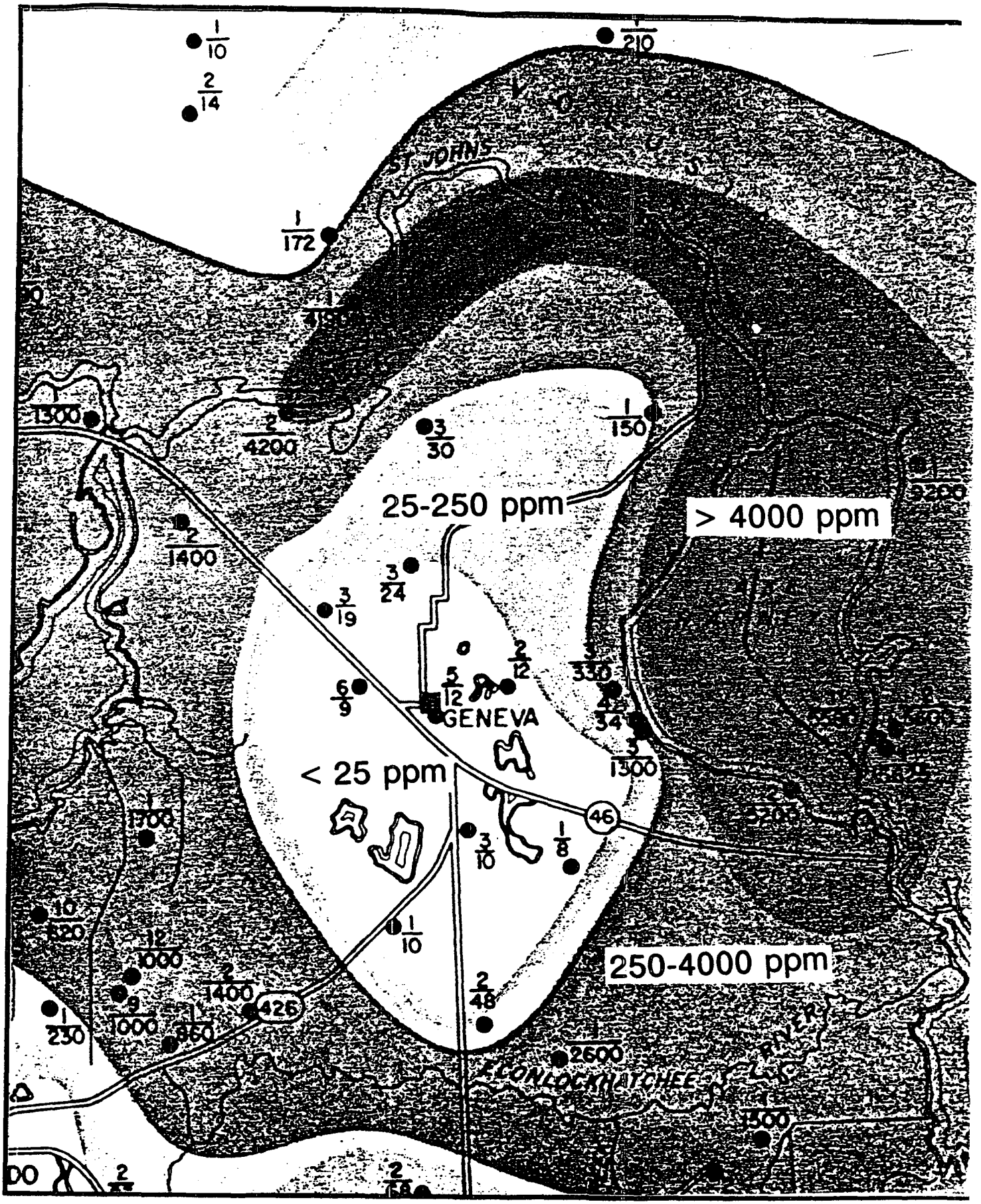

Figure 8.18. Field estimates of areal chloride distributions in the Geneva area (after Tibbals, 1977).

shows a good agreement with the model prediction. The vertical variation of concentration in cross-sections C-C′, A-A′, and B-B′ (slices 5, 10 and 16 of Figure 7.1, respectively) are depicted in Figures 8.19, 8.20, and 8.21, respectively. The chloride concentration versus depth profile for well S-0087 located near site 58 (see Figure 3.1) is shown in Figure 8.22. Measured and calculated chloride concentrations are in excellent agreement.

The true piezometric head distributions at 25 ft from the base of the domain, and along the top of the domain are depicted in Figures 8.23 and 8.24, respectively. Figures 8.25 and 8.26 show the true head distributions in sections A-A′ and B-B′ which lie in an x-y plane, and Figures 8.27 and 8.28 show the head distribution in sections D-D′ and E-E′, which lie in a z-y plane. These head patterns were obtained using the prescribed bottom head that varies in the x-direction according to Figure 4.4a. The prescribed bottom-head values were kept uniform in the z-direction. As depicted in Figure 8.24, the mounding of the head is pronounced in the top layer where recharge effects have the greatest impact. Significant variations in the true heads are noticed along the vertical direction and hence a direct comparison of the heads distribution in any layer with the reported field potentiometric map is not feasible. This is because the potentiometric surface map based on field data is composed of head data collected from wells with different open hole intervals and depths. Furthermore the use of average steady-state recharge rates instead of time varying fluxes affects the head distribution which is not

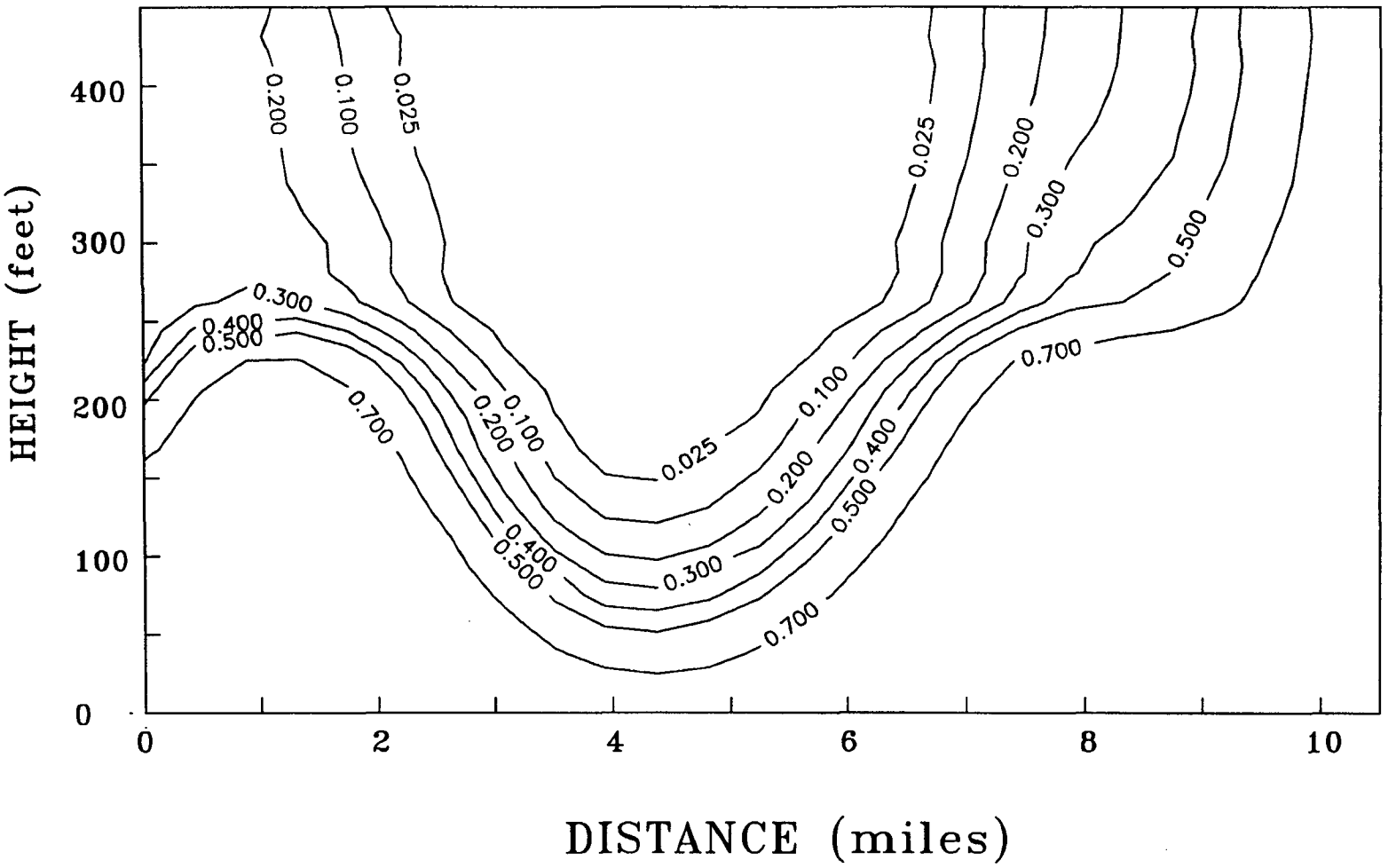

Figure 8.19. Relative concentration profile through C-C′ for a steady-state simulation of the Geneva freshwater lens.

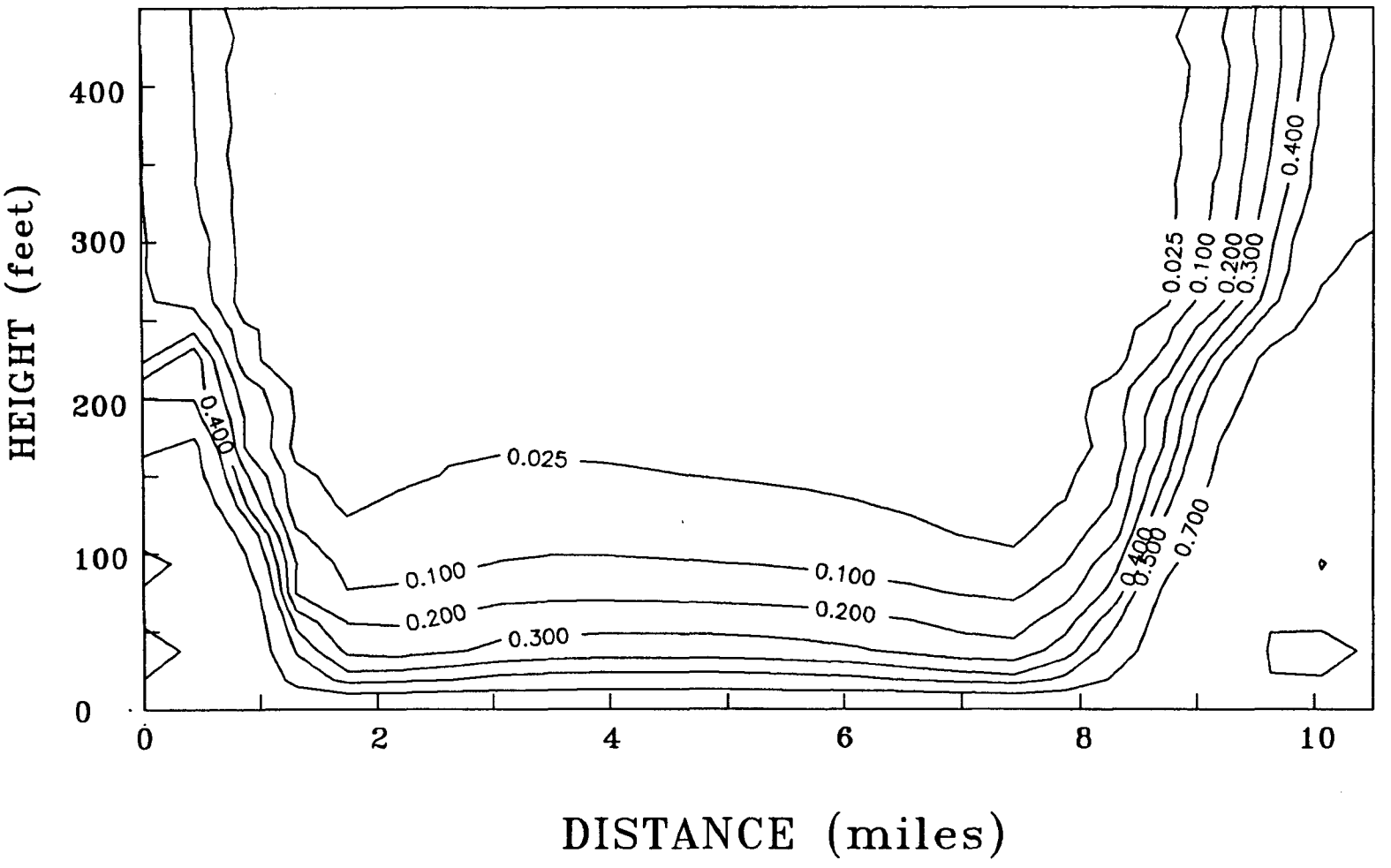

Figure 8.20. Relative concentration profile through A-A' for a steady-state simulation of the Geneva freshwater lens.

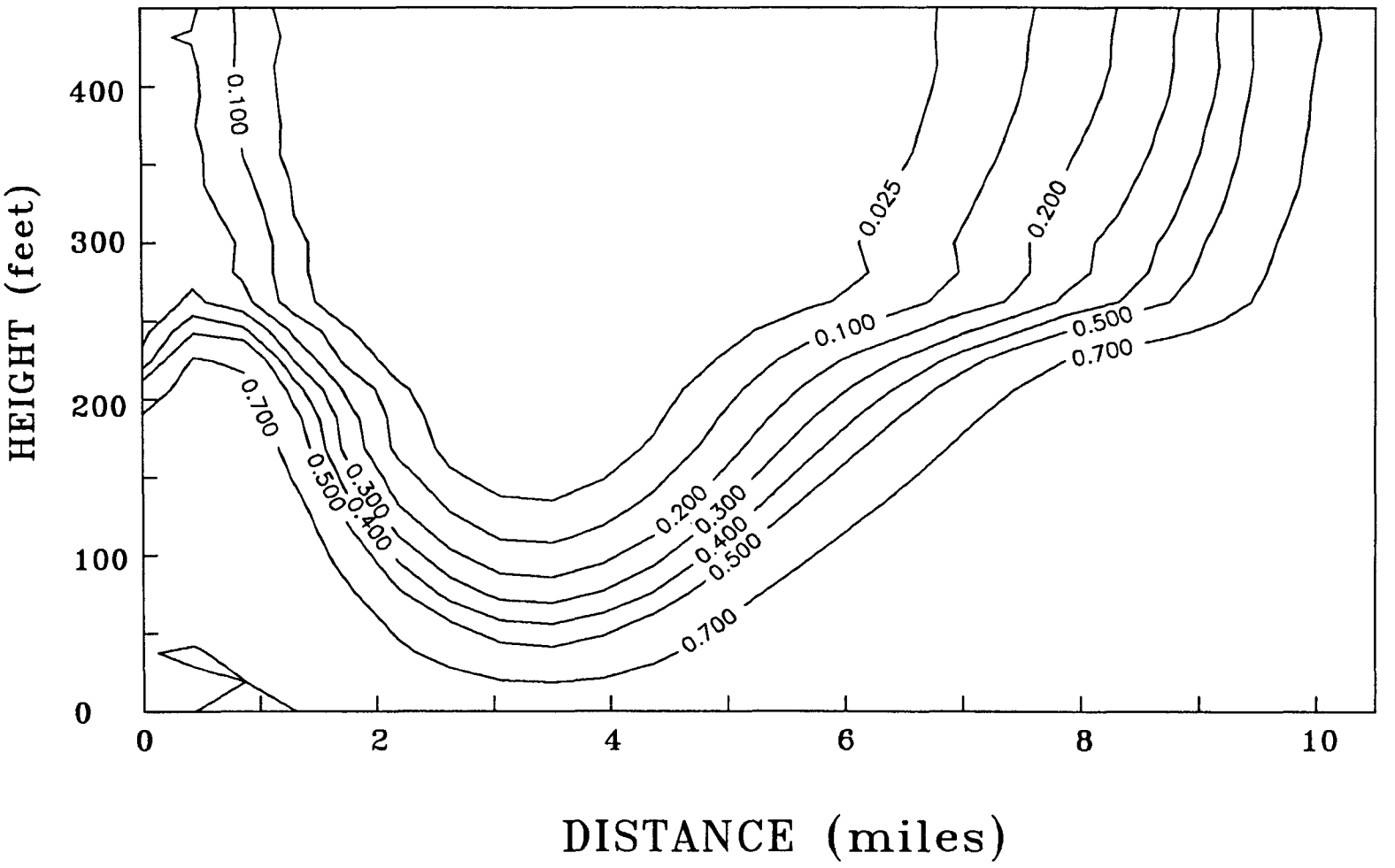

Figure 8.21. Relative concentration profile through B-B′ for steady-state simulation of the Geneva freshwater lens.

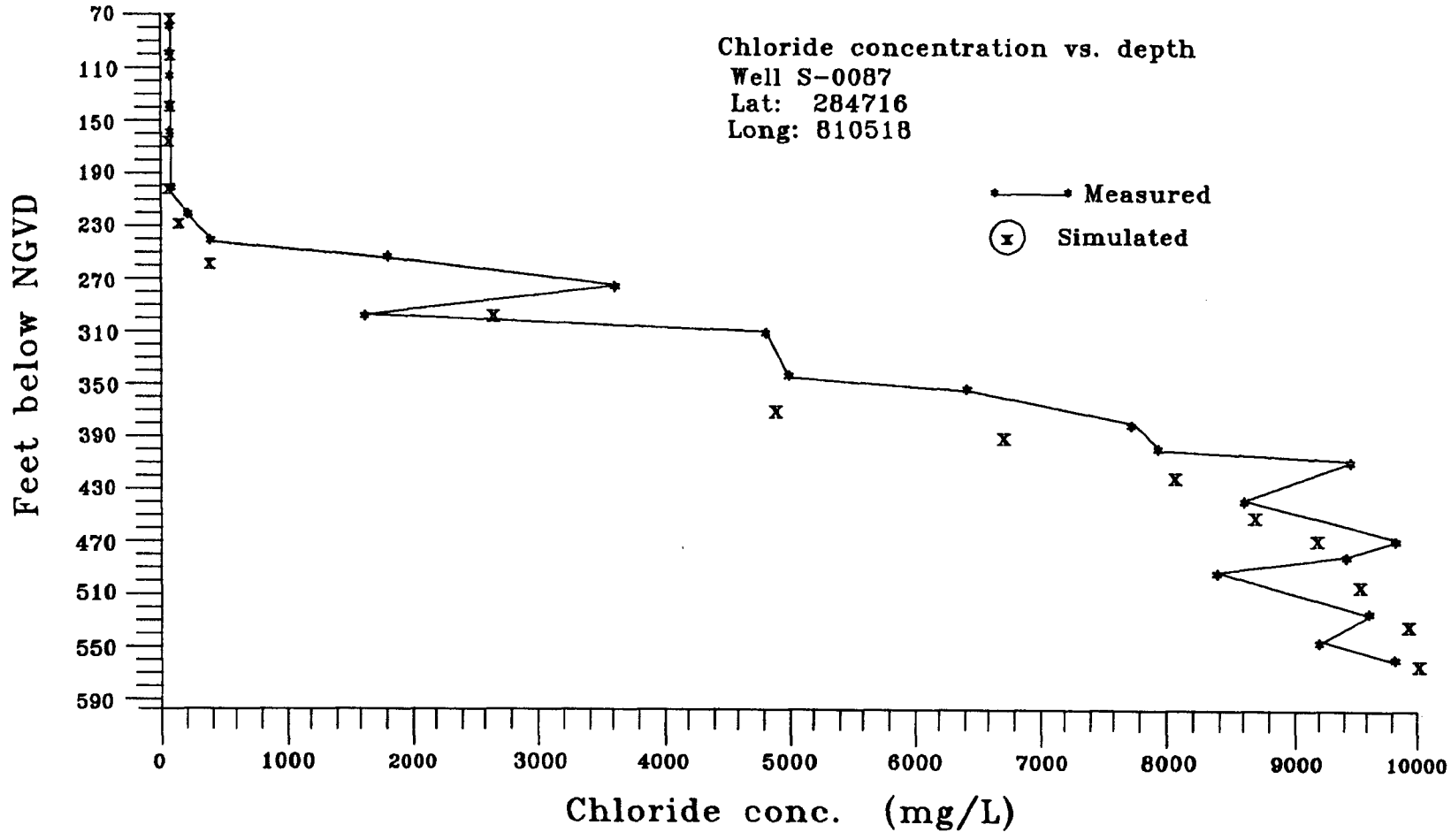

Figure 8.22. Measured and simulated chloride concentration variation with depth at well S-0087.

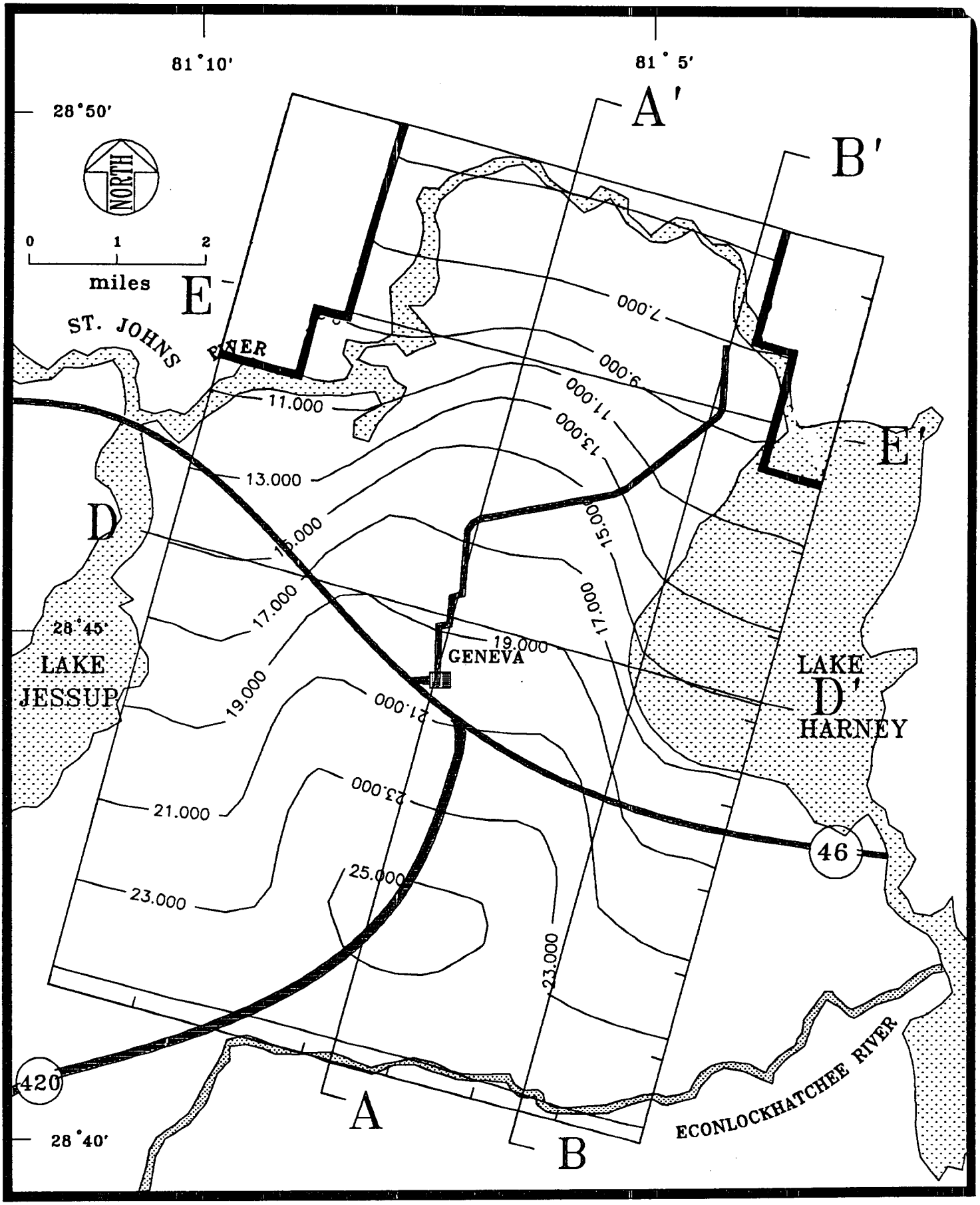

Figure 8.23. Areal distribution of true head at 25 ft above the bottom of the domain for the calibrated steady-state simulation of the Geneva freshwater lens.

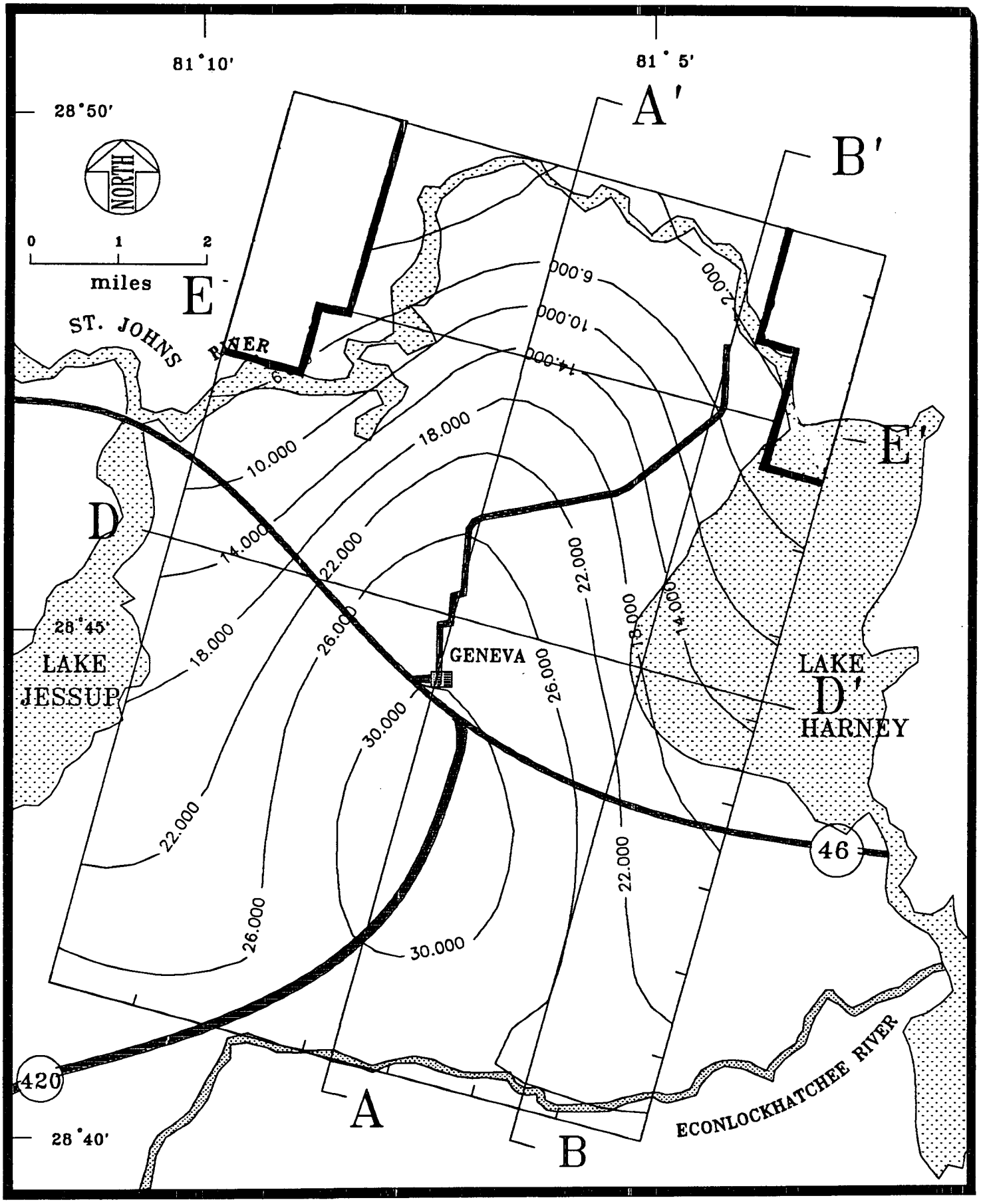

Figure 8.24. Areal distribution of true head at the top of the domain for the calibrated steady-state simulation of the Geneva freshwater lens.

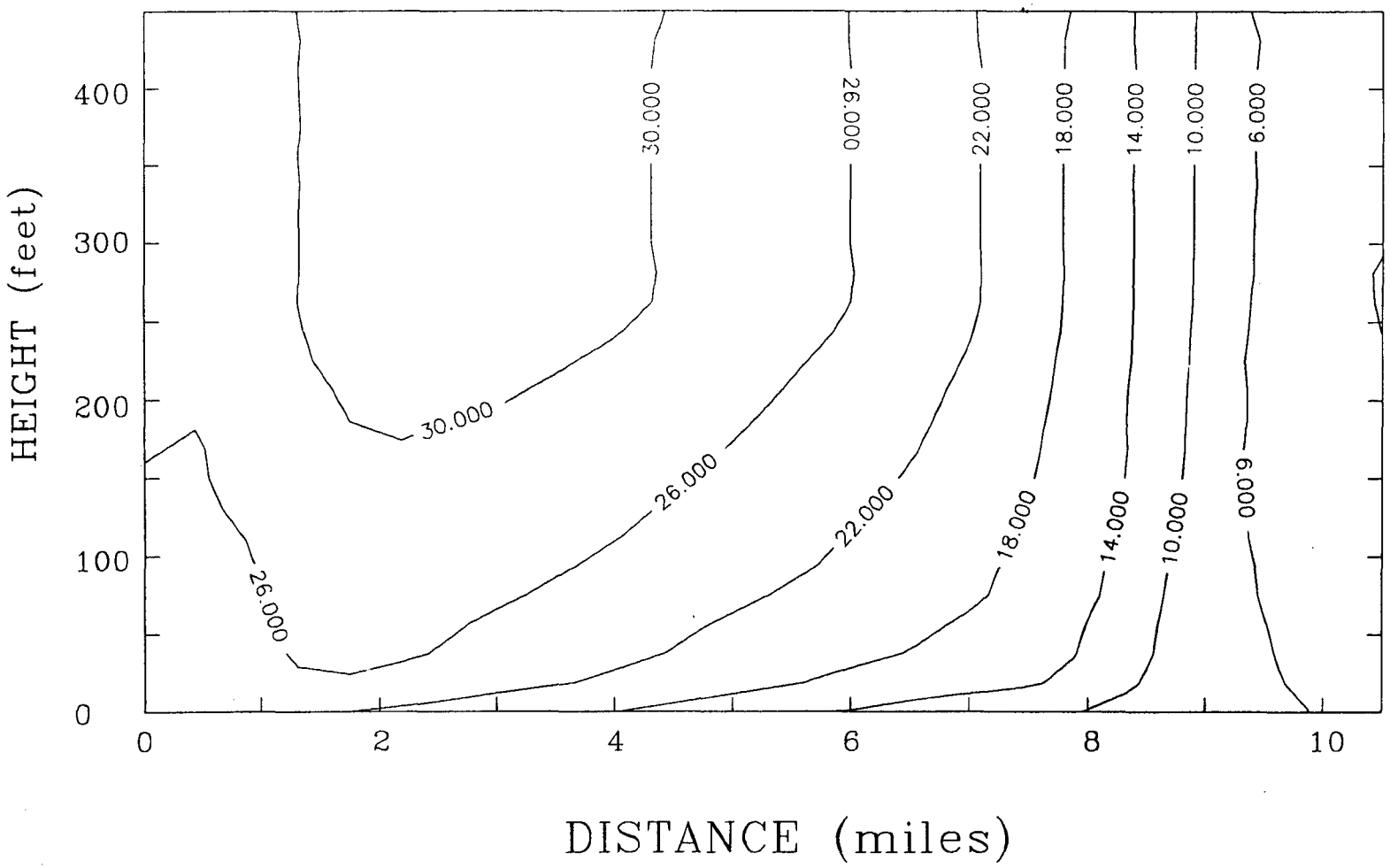

Figure 8.25. Cross-sectional distribution of true head through A-A′ for the calibrated steady-state simulation of the Geneva freshwater lens.

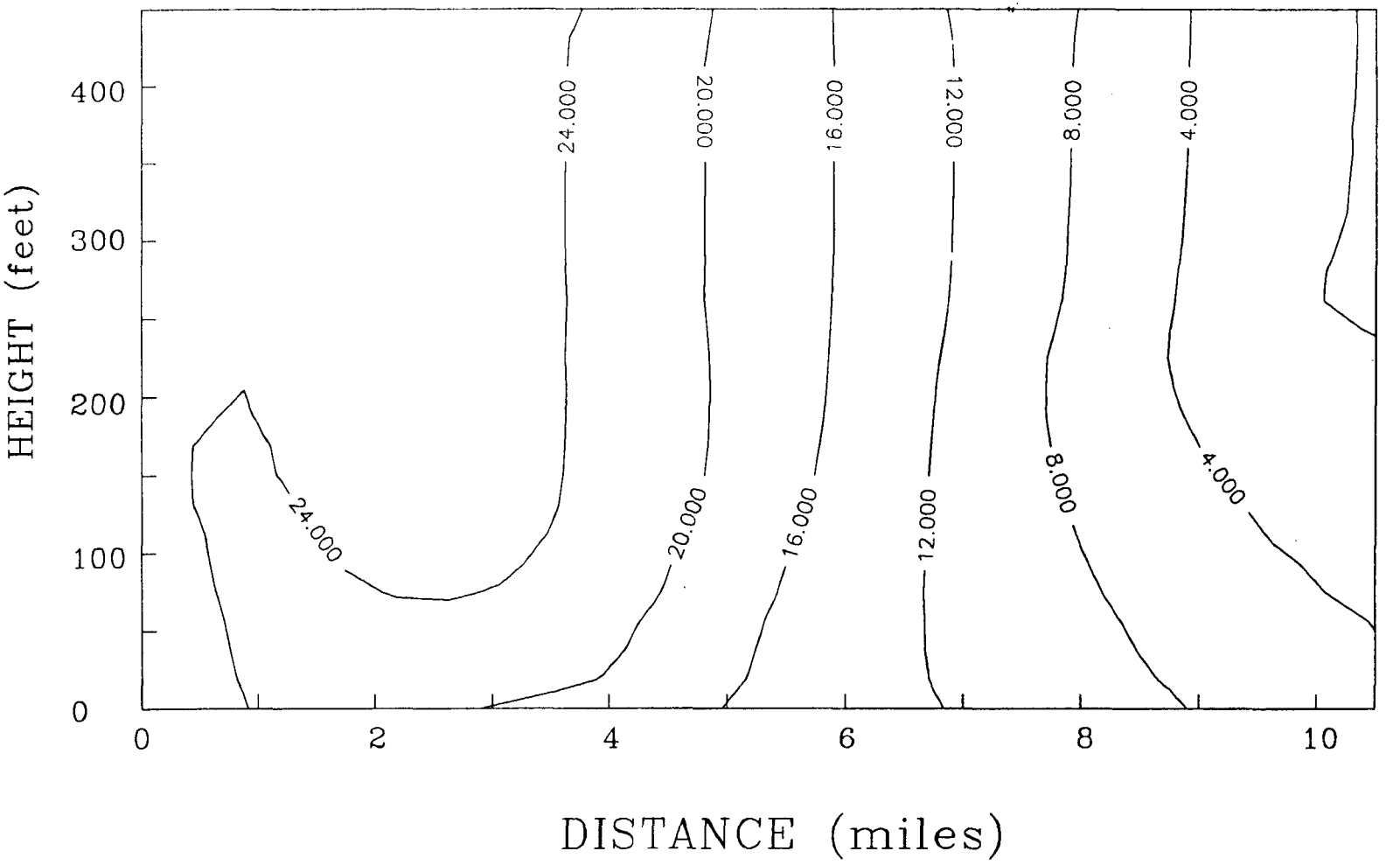

Figure 8.26. Cross-sectional distribution of true head through B-B′ for the calibrated steady-state simulation of the Geneva freshwater lens.

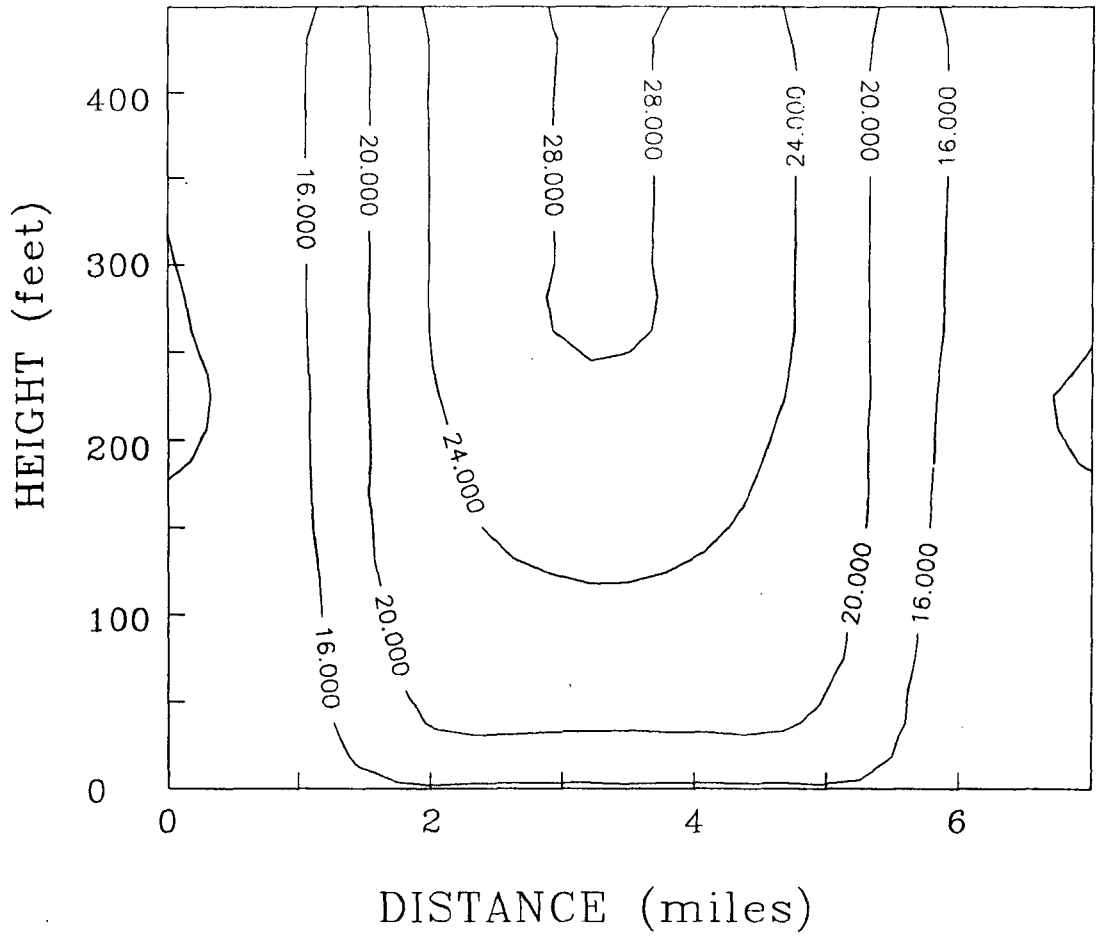

Figure 8.27. Cross-sectional distribution of true head through D-D' for the calibrated steady-state simulation of the Geneva freshwater lens.

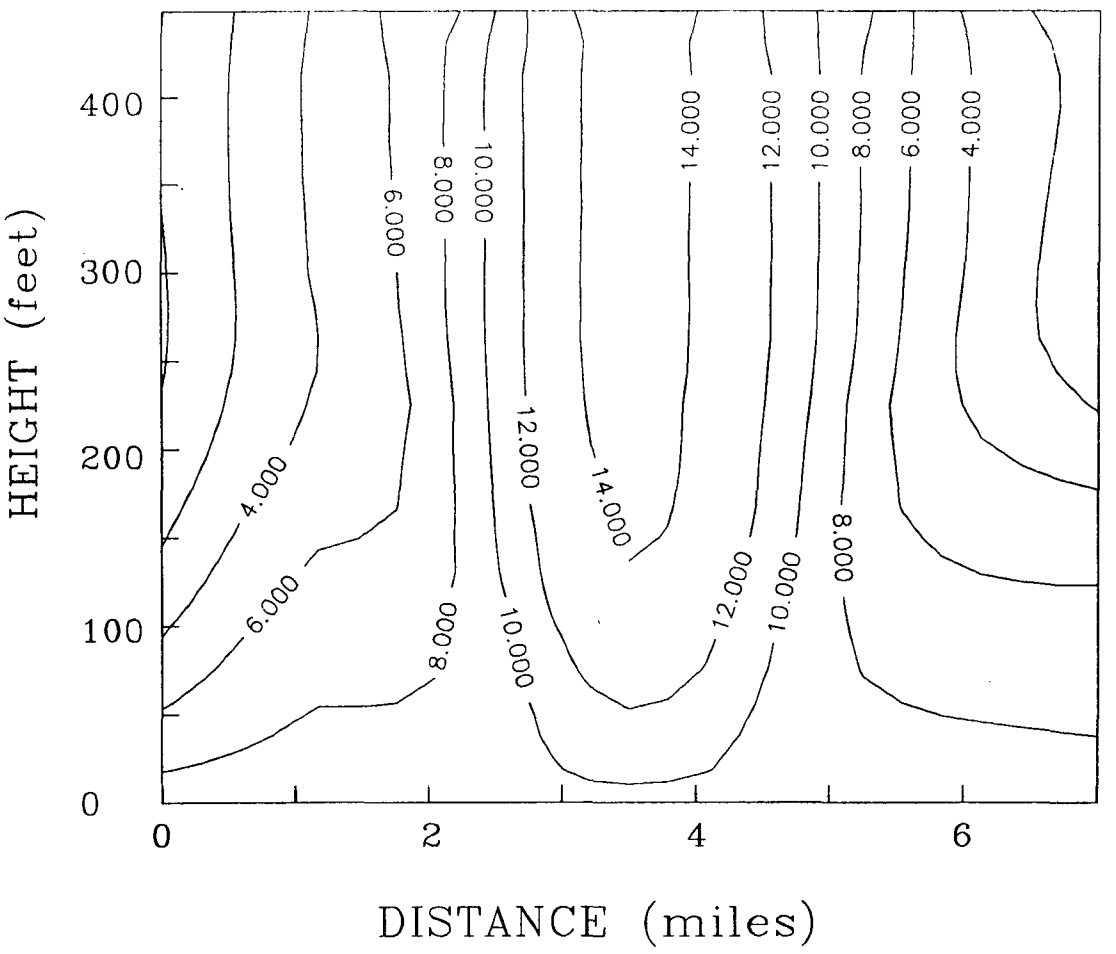

Figure 8.28. Cross-sectional distribution of true head through E-E′ for the calibrated steady-state simulation of the Geneva freshwater lens.

representative of the field values at the time of sampling. The head change in the upper part of the Floridan is recorded at about 5 ft for 1982 (Phelps and Rohrer, 1987). Recognizing these difficulties in matching we still elect to use information from the potentiometric map prescribing the bottom-head of the simulations. The reason is that the field map provides a general ambient flow condition for the entire regional system, and the bottom boundary lies in the domain of the regional ambient flow. Additionally, the absolute values of heads prescribed at the bottom do not affect the salt transport analysis (Table 5.3 case 12), and the horizontal gradient of the prescribed heads affects the freshwater lens only slightly (Table 5.3, case 13). However, these gradients are not known at the bottom of the domain since head at this depth is recorded at only one well location (well #S-0200 near site 58, Figure 3.2). Again it is true that the potentiometric map information may not give an accurate representation of the bottom-head condition for the same reason. A sensitivity analysis will be needed to determine the confidence that can be placed in the prediction of the chloride patterns generated by the model, with a rather uncertain bottom-head boundary condition.

The true head distribution may not accurately reflect the flow patterns in a density-dependent system, since buoyancy effects play a significant role in flow and transport. In view of this, the velocity patterns determined by the model are depicted in Figures 8.29 and 8.30 for the bottom and top layers, respectively, and in Figures 8.31 and 8.32 for the vertical cross-sections in the x-y

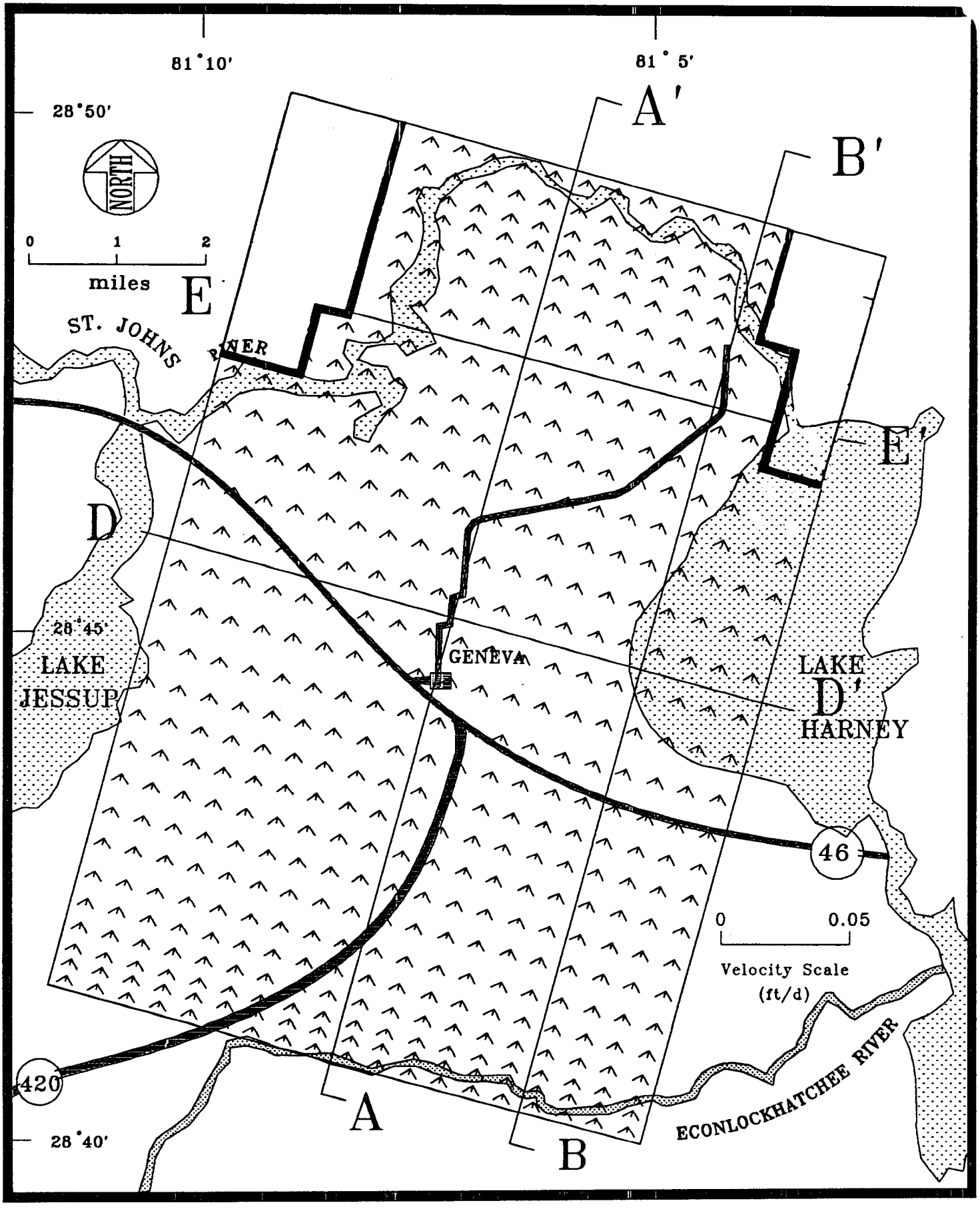

Figure 8.29. Areal plot of velocity field in the bottom layer of elements for the calibrated steady-state simulation of the Geneva freshwater lens.

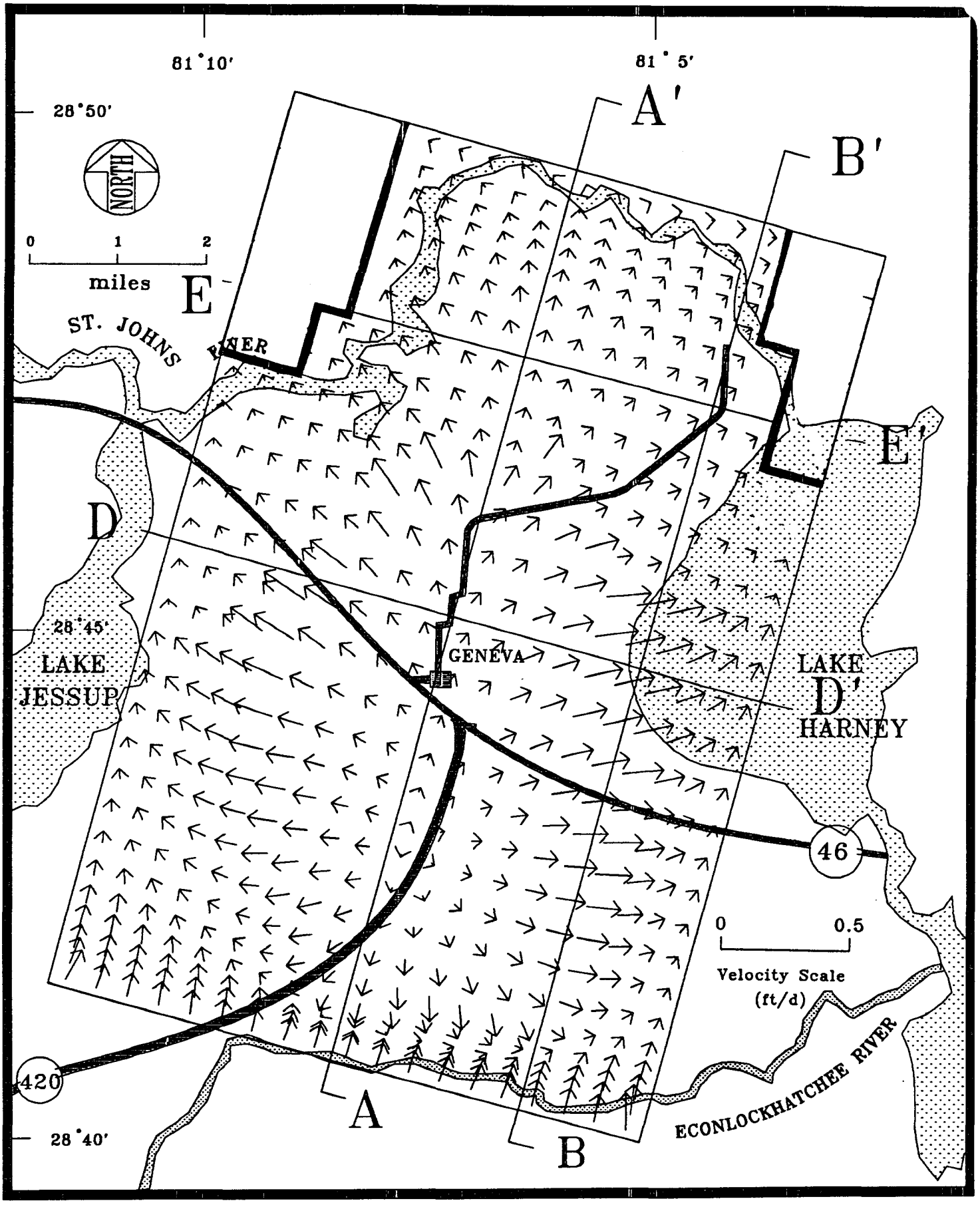

Figure 8.30. Areal plot of velocity field in the top layer of elements for the calibrated steady-state simulation of the Geneva freshwater lens.

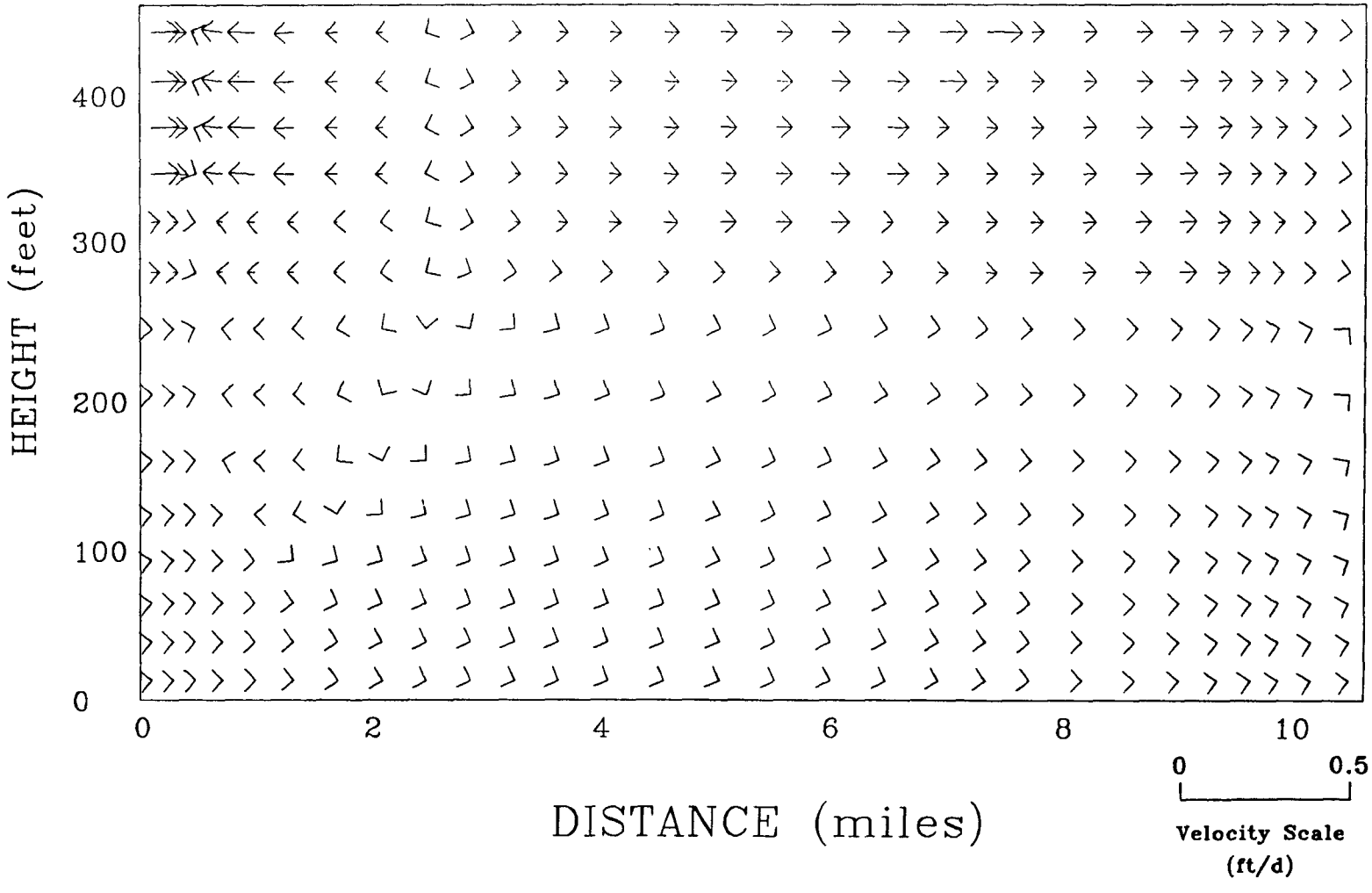

Figure 8.31. Cross-sectional plot of velocity field through A-A' for the calibrated steady-state simulation of the Geneva freshwater lens.

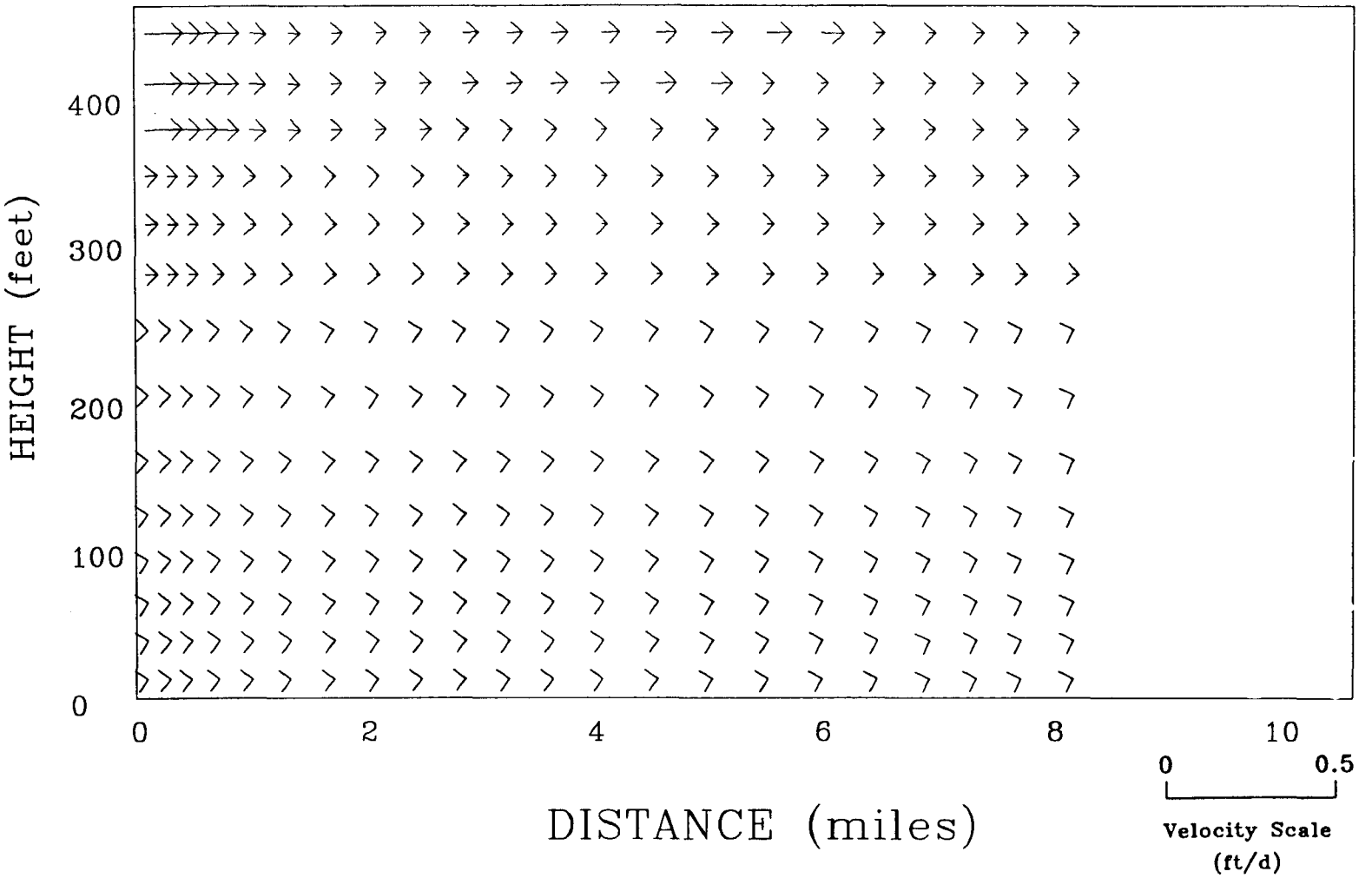

Figure 8.32. Cross-sectional plot of velocity field through B-B' for the calibrated steady-state simulation of the Geneva freshwater lens.

planes adjacent to sections A-A′, and B-B′, respectively. Figures 8.33 and 8.34 show the velocity patterns for the vertical sections adjacent to D-D′ and E-E′, respectively, in the z-y planes. The velocity vectors shown in these figures represent the components of the velocity in the plane of the figure and should be assessed accordingly (For instance, the areal plots cannot depict vertical components of velocity, and the cross-sectional plots cannot depict velocity components normal to the section). In general, it may be deduced that the recharge water flows downwards and outward from the recharge zone. Circulation patterns are noticed in the cross-sectional plots. Flow is oriented downwards in the central portions of the sections, and upwards towards the edges. The upward flow causes chlorides to be transported to the surface from the brackish water at the bottom of the domain.

8.3 SENSITIVITY ANALYSIS

A sensitivity analysis was performed as the final stage of the steady-state simulations. The calibrated lens depicted in Figures 8.16-8.21 is considered to be the base case. Material parameters and boundary conditions were individually varied to observe the effects of uncertainties in their values. A summary of key elements of the sensitivity analysis is provided in Table 8.4.

The first sensitivity simulation considers the effects of the bottom-head boundary prescription for the lens system. This is the least known condition of all available field data. Head at the bottom of the domain is known only at one location (well #S-020,

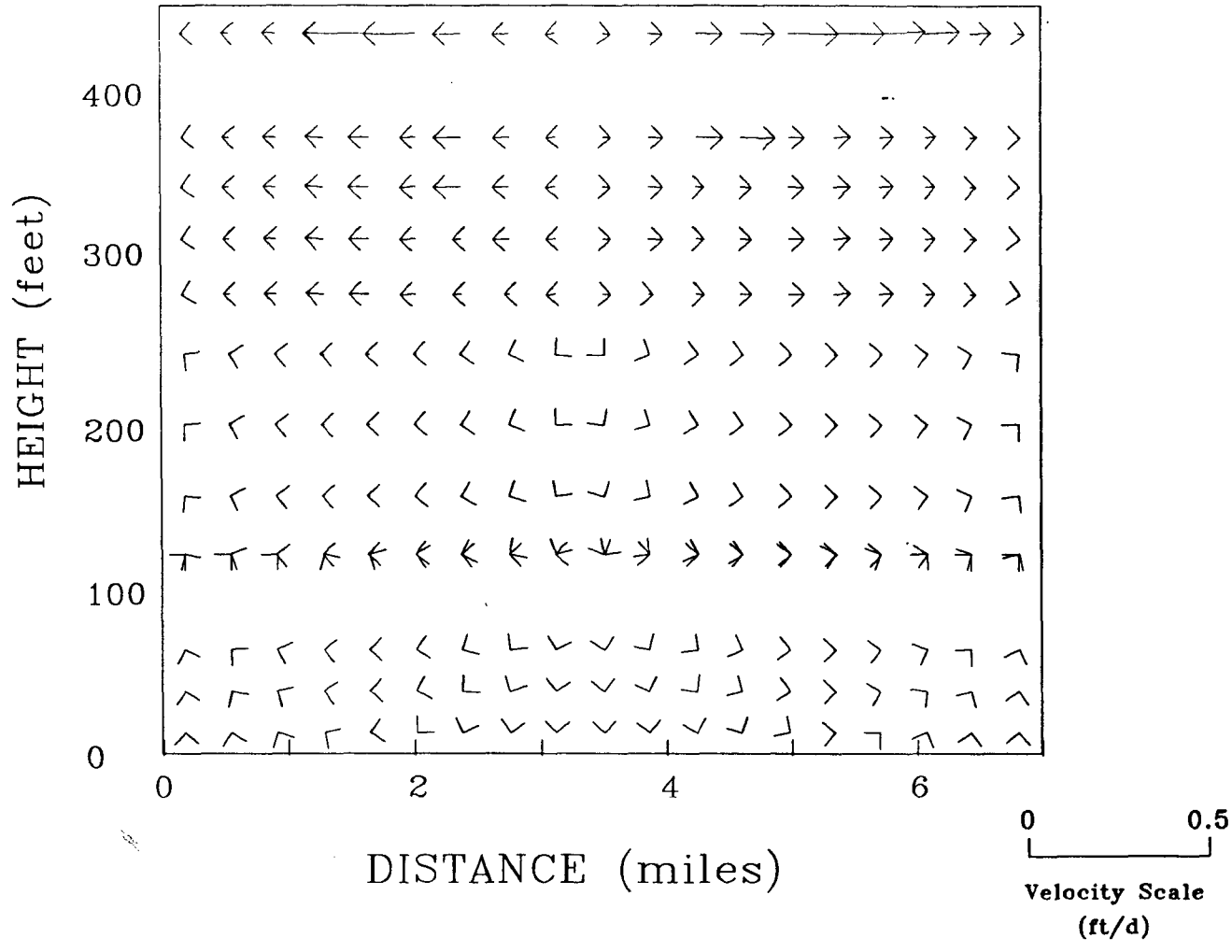

Figure 8.33. Cross-sectional plot of velocity field through D-D' for the calibrated steady-state simulation of the Geneva freshwater lens.

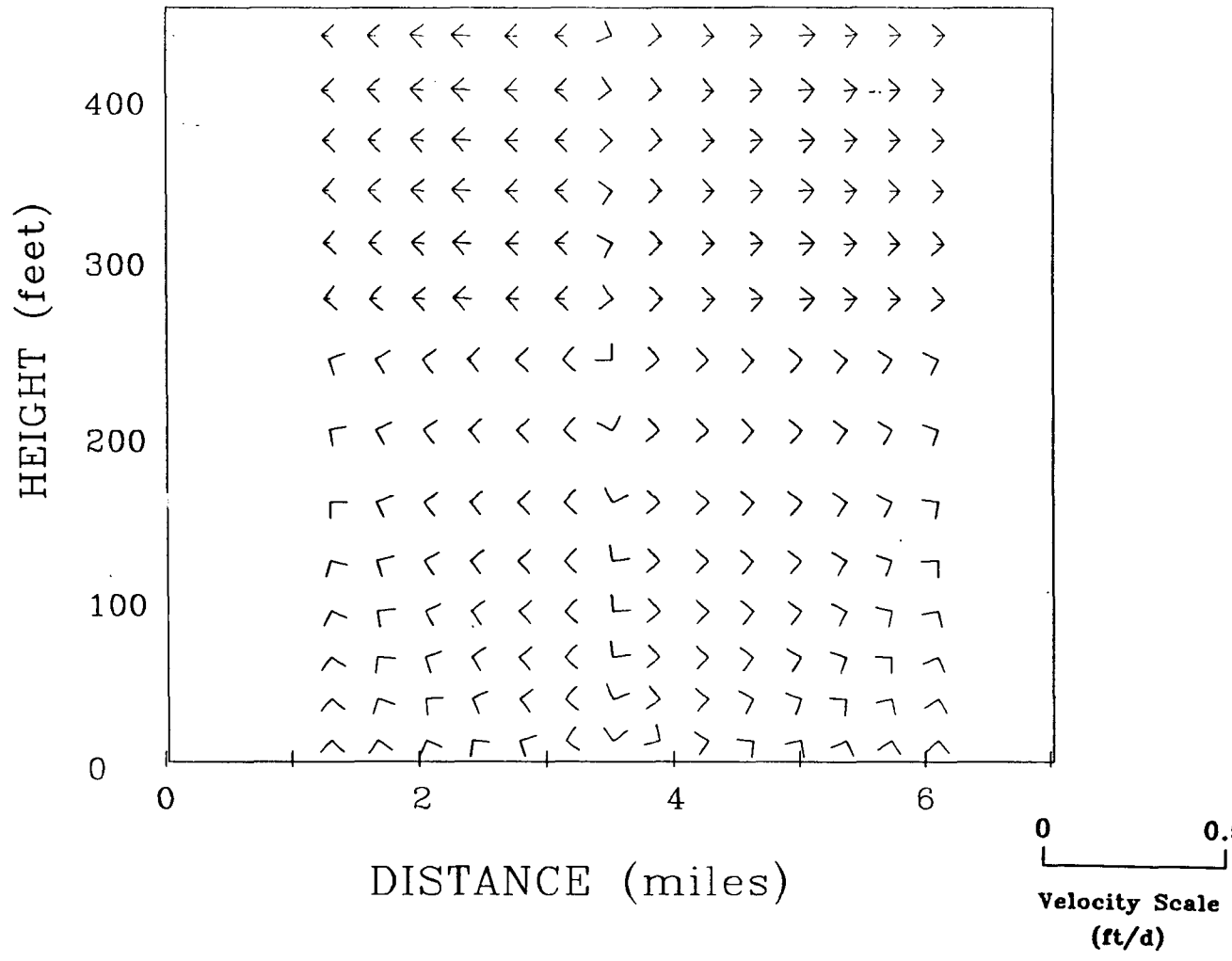

Figure 8.34. Cross-sectional plot of velocity field through E-E′ for the calibrated steady-state simulation of the Geneva freshwater lens.

TABLE 8.4 SUMMARY OF KEY ELEMENTS OF THE 3-D SENSITIVITY ANALYSIS.

CASE	KEY FACTOR	FIGURE	OBSERVED EFFECTS
0 (Base Case)	Calibration run. See Tables 8.2 and 8.3 for material parameters and boundary conditions	8.17 - 8.34	Lens shape and size corroborates estimates of Phelps and Rohrer (1987). Vertical chloride distribution agrees well with measured data at S-0087.
1	Base head prescription changed to that of Fig 8.35	8.36 - 8.40	Chloride distribution insensitive to this change near the surface. Larger horizontal velocities supplied at bottom (by larger potential gradients) causes greater dispersion here. True head distribution affected significantly. Head patterns near the top are similar to those of Case 0 and hence flows near the surface and the resulting freshwater lens are similar.
2	Longitudinal dispersivities of all formations halved	8.41, 8.42	Little effect on areal chloride distribution near the top. Lens depth increases vertically by approximately 75 ft.
3	Horizontal and vertical conductivities of Upper Avon Park formation doubled	8.43, 8.44	Zone within 250-ppm concentration of chlorides almost unchanged at top surface. Depth of lens increases by approximately 30 ft.
4	All discharges halved	8.45, 8.46	Effect near Econlockhatchee River negligible. Large effect near St. Johns river and Lake Jessup and Lake Harney side boundaries. Lens size increases in these areas. Chloride profiles are more dispersed vertically, especially near the Econlockhatchee River side.
5	Zero recharge provided to low recharge areas	8.47, 8.48	Maximum depth of lens increased by approximately 30 ft. Lens size decreases near St. Johns River side by approximately 1½ mi.

8-49

near site 58, Figure 3.2). Furthermore, the head pattern changes considerably between seasons, and hence a sensitivity analysis of the freshwater lens to this parameter is important. It has been shown in the two-dimensional simulations that the bottom-head boundary acts as a head datum, and that head distribution patterns are unaltered if all boundary head values are translated by the same amount. Reducing bottom boundary heads by 10 ft would therefore reduce heads throughout the domain by 10 ft. The bottom boundary head distribution along the x-axis for this simulation is shown in Figure 8.35. The horizontal gradients of the prescribed head are much larger than those shown in Figure 4.4a. A zero head gradient is assumed in the z-direction and hence all cross-sectional planes receive the same bottom-head boundary condition as depicted in Figure 8.35. The resulting areal distribution of chloride at the top of the simulation domain is shown in Figure 8.36, and the cross-sectional profile through section A-A′ is shown in Figure 8.37. Note that the areal chloride distribution on the top of the upper Floridan computed for this case is not substantially different from that of the calibrated case shown in Figure 8.17. However, the thickness of the lens in reduced by approximately 50 ft. Chloride distribution is disturbed near the bottom boundary due to the considerable increase in the horizontal gradients of the prescribed bottom head. Larger head gradients result in larger velocities and hence dispersion (which is proportional to velocity) is more pronounced. The same effect is noticed in the 2-D simulations (see Figures 8.17 and 8.20).

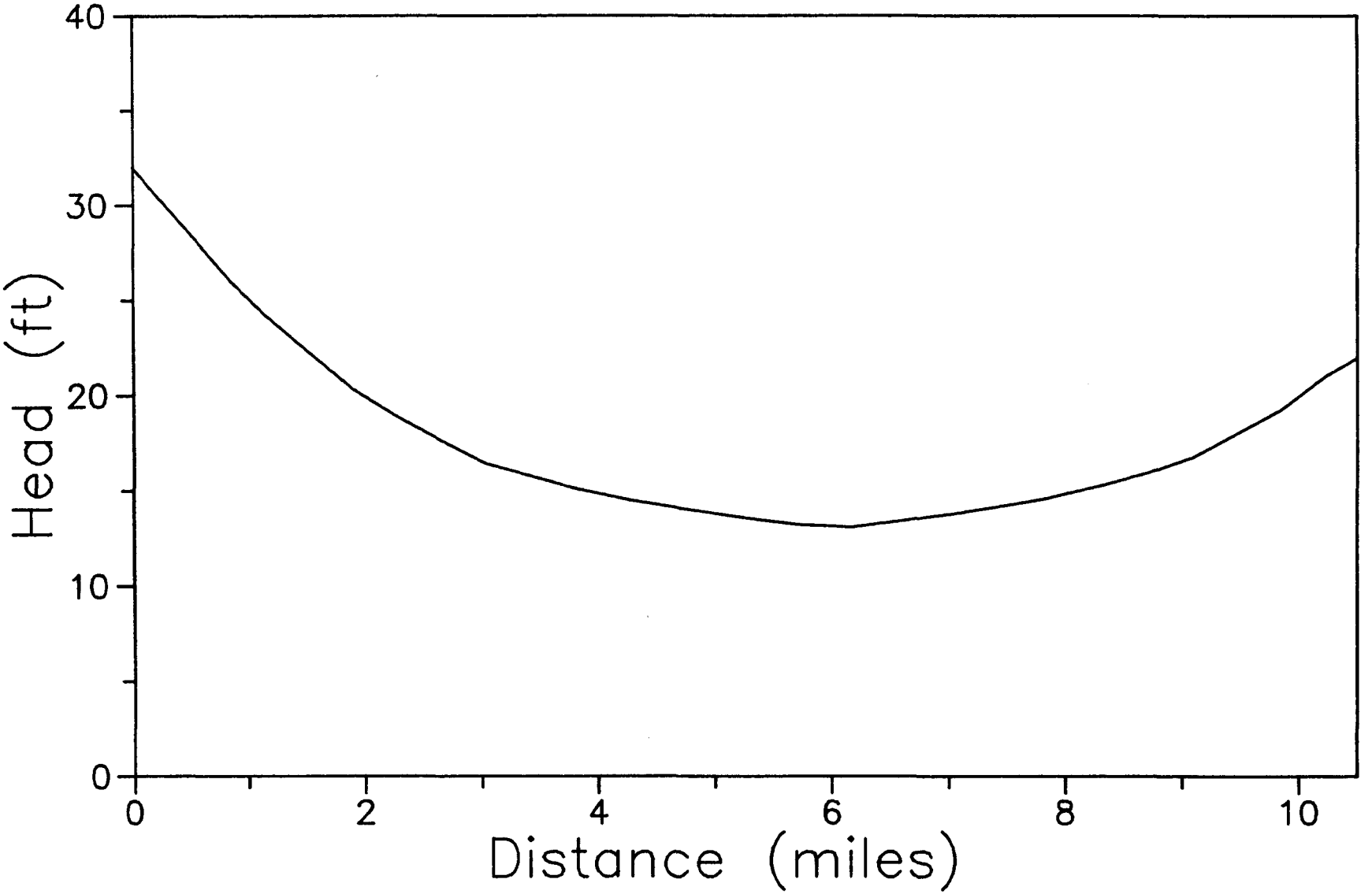

Figure 8.35. Equivalent freshwater hydraulic head prescribed at the base of the upper Floridan aquifer for the sensitivity run #1 [case 1, Table 8.4].

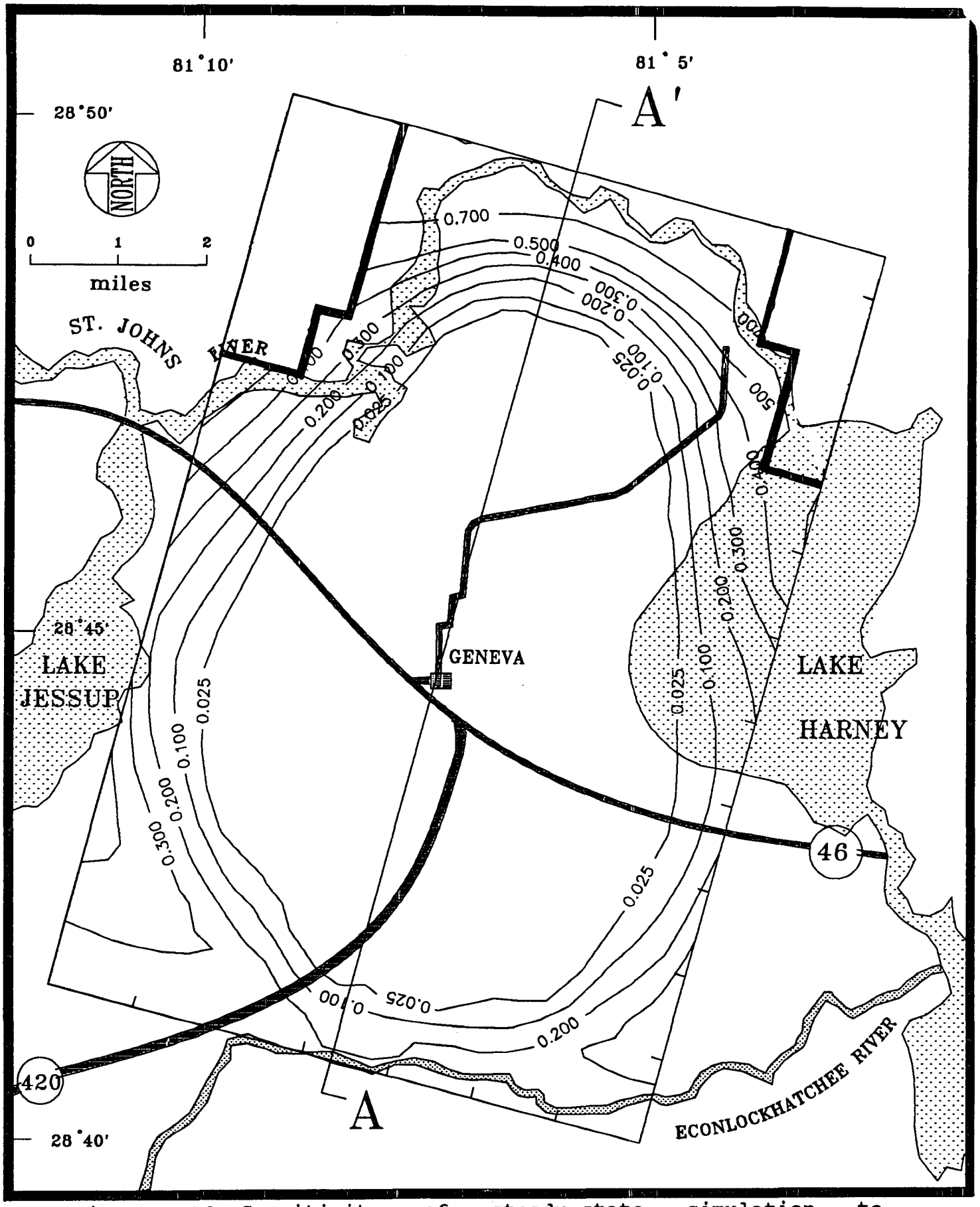

Figure 8.36. Sensitivity of steady-state simulation to prescribed bottom head. Shown in the Figure is the areal distribution of relative concentration of chloride at the top of the domain [case 1, Table 8.4].

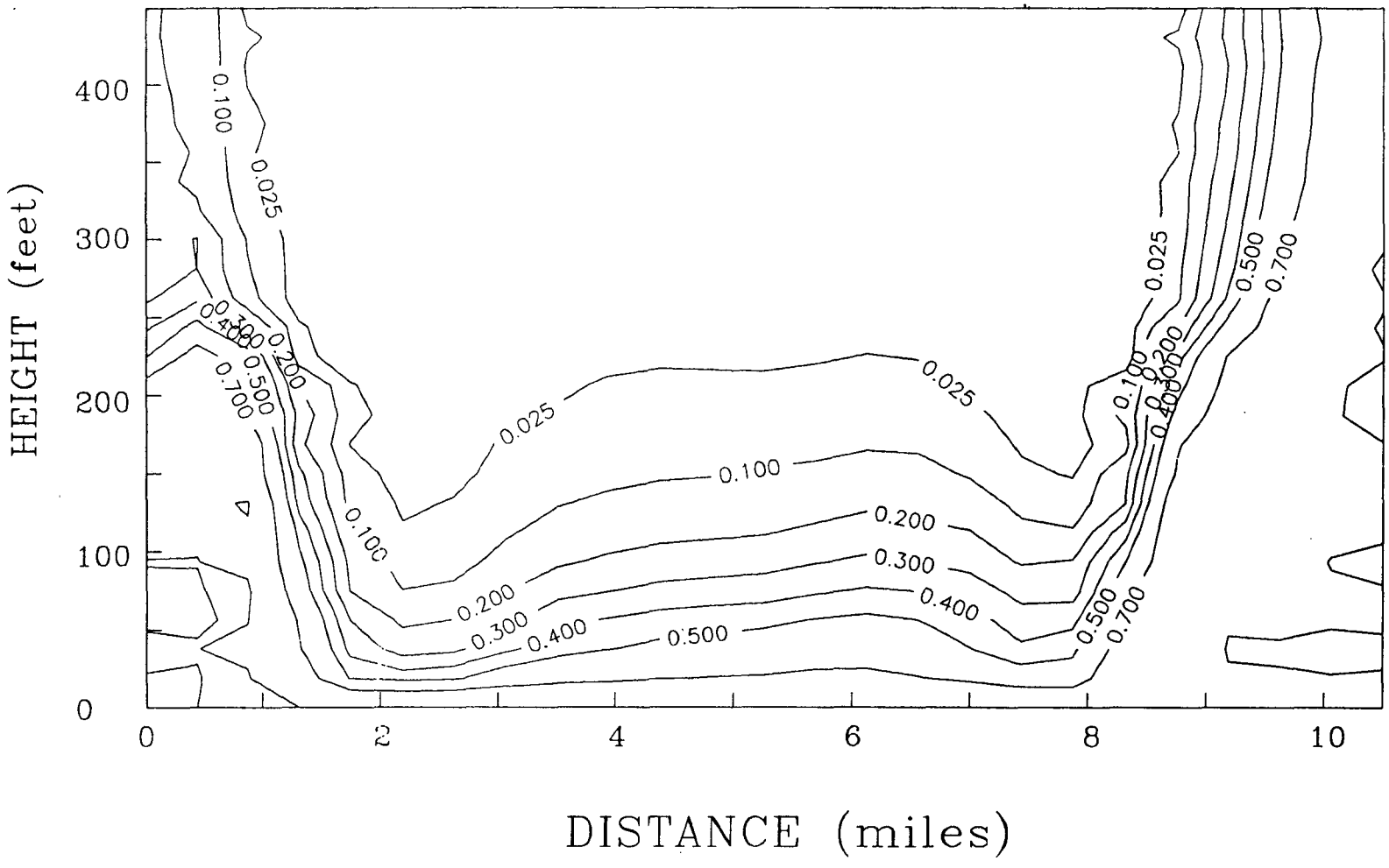

Figure 8.37. Sensitivity of steady-state simulation to prescribed bottom head. Shown in the Figure is the relative concentration of chloride through section A-A' [case 1, Table 8.4].

However, if all the prescribed bottom head values are changed by the same amount, so that the horizontal gradients are kept the same, the lens remains identical, because the entire datum is shifted. The true head distributions in a horizontal plane 25 ft above the base of the domain, and on the top of the domain are shown in Figures 8.38 and 8.39, respectively, for this first sensitivity case. Additionally, the vertical distribution of the simulated true head is shown in Figure 8.40 for section A-A'. As can be seen by examining this Figure and Figures 8.38 and 8.39, the computed true head pattern varies significantly from top to bottom of the flow domain. Furthermore, the head patterns have changed considerably from those of the calibration run shown in Figures 8.23-8.28. The patterns in the uppermost layer are, however, similar for the two cases, and hence the recharge water flows in a similar fashion for both cases, creating a lens in the upper part of the domain, that is insensitive to flow patterns occurring in the brackish water at the bottom. The head values computed for this case lie within the range of the field-measured average head values. A direct comparison of field head values with computed head values, however, cannot be justified since the field-measured average heads depend on the depth of sampling, the sampling (open hole) interval and the time of sampling. Furthermore, the effect of spatial variation of surface recharge and discharge on the head distribution is most pronounced in the upper regions of the flow domain. The true spatial variations of

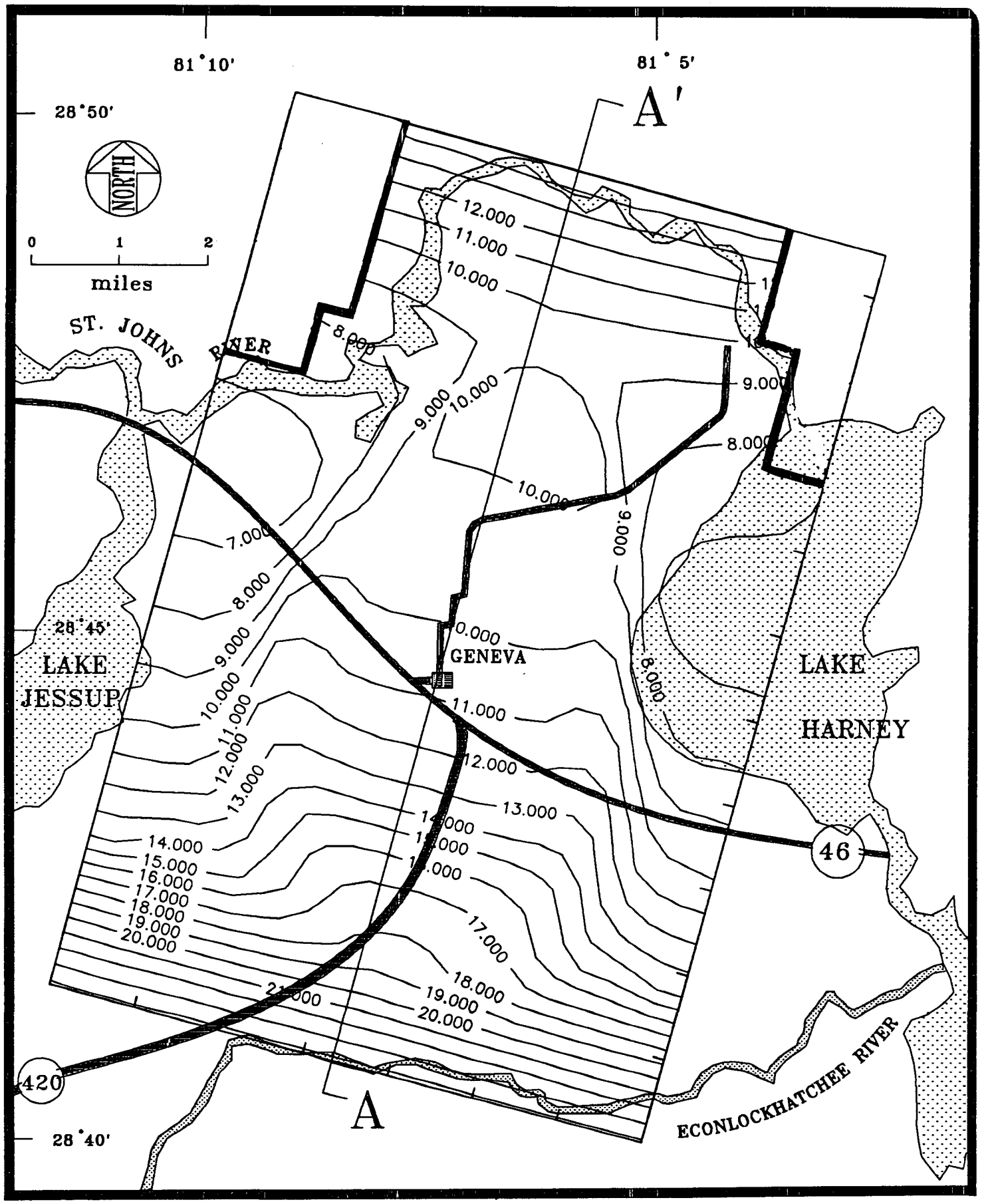

Figure 8.38. Sensitivity of steady-state simulation to prescribed bottom head. Shown in the Figure is the areal distribution of true head at 25 ft above bottom of domain [case 1, Table 8.4].

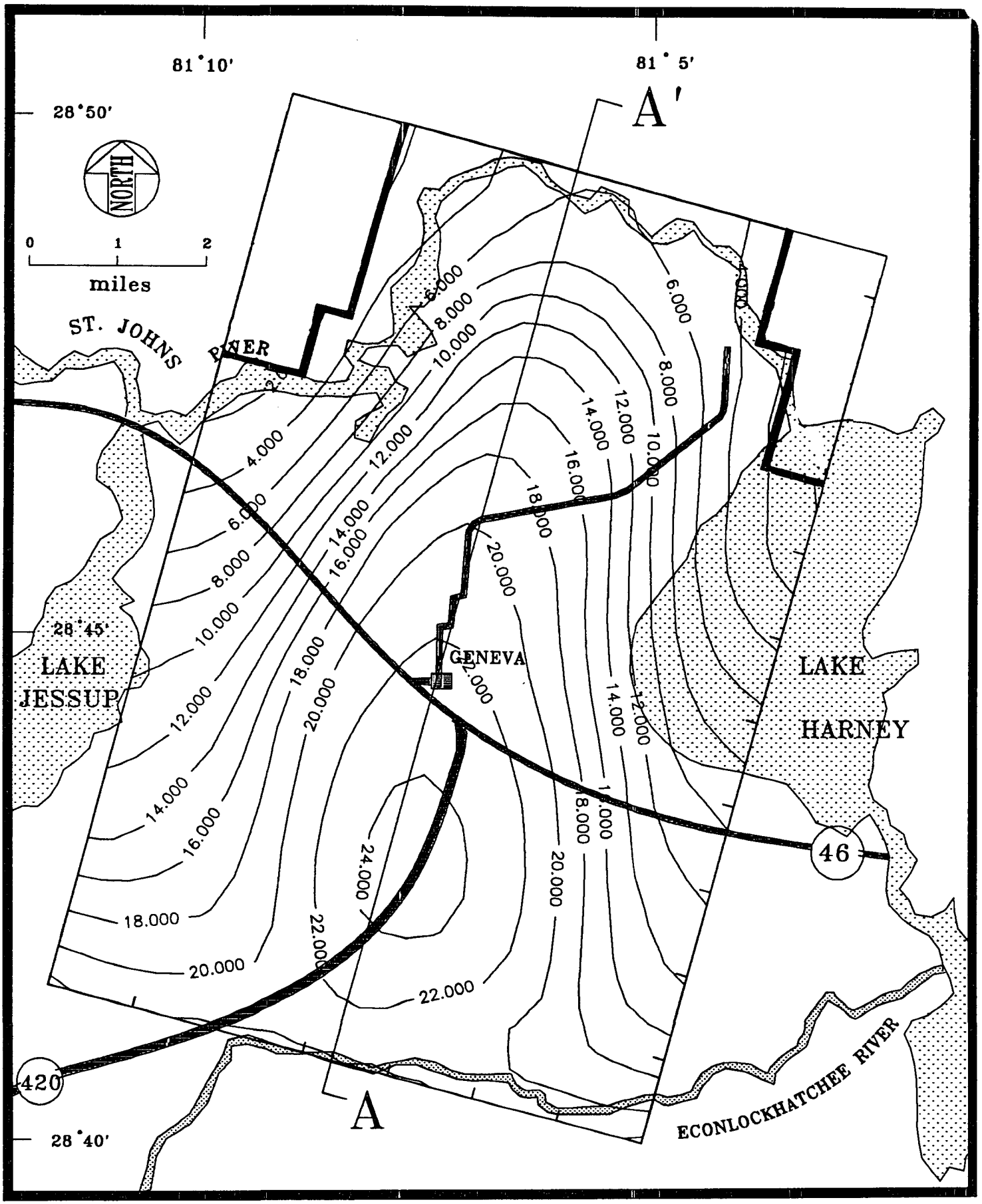

Figure 8.39. Sensitivity of steady-state simulation to prescribed bottom head. Shown in the Figure is the distribution of true head at the top of the domain [case 1, Table 8.4].

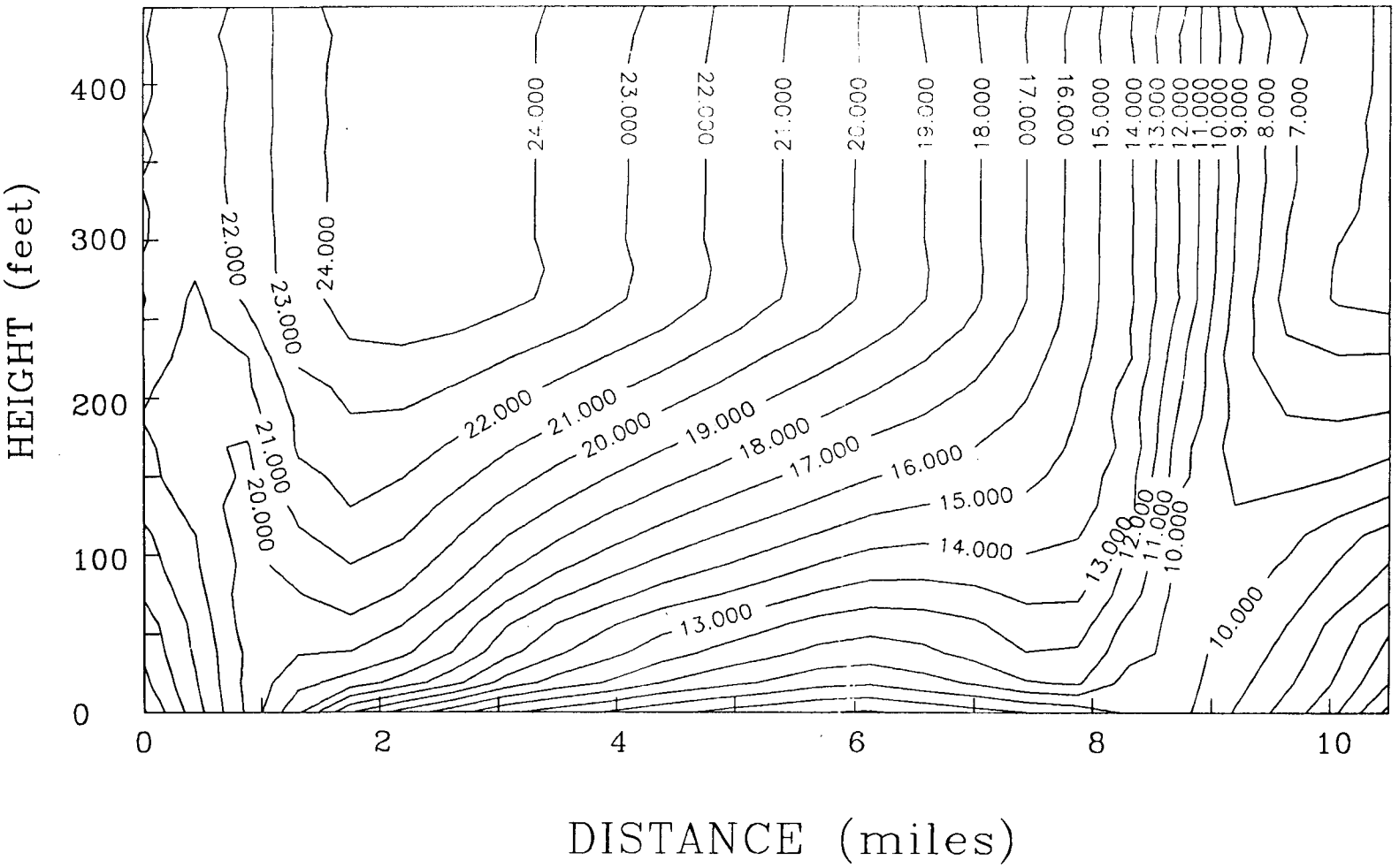

Figure 8.40. Sensitivity of steady-state simulation to prescribed bottom head. Shown in the figure is the cross-sectional distribution of true head for section A-A' [case 1, Table 8.4].

recharge/discharge have been averaged, and allocated to five zones for this modeling study (Figure 8.16).

The next sensitivity simulation involved the case where the longitudinal dispersivity values for the three material zones were reduced by one half of their original values. The grid used over the simulation domain is sufficient for the reduced dispersivity values, and the DSTRAM code converged smoothly without necessitating the use of upstream weighting. The predicted chloride distribution on the top of the upper Floridan and the vertical chloride distribution in section A-A′ are shown in Figures 8.41 and 8.42, respectively. The effect of changing longitudinal dispersivity on the areal pattern of chloride is negligible. Vertically, however, the lens depth increases substantially with decrease in the longitudinal dispersivity values.

The next sensitivity run involves doubling the horizontal and vertical conductivity values for the upper Avon Park formation. Figures 8.43 and 8.44 show the areal chloride pattern at the top of the lens, and vertical chloride distribution in section A-A′, respectively. The overall size of the freshwater lens (within the 250-ppm isochlor) has not changed significantly for this simulation, although the concentration pattern is more dispersed areally for this sensitivity case than for the calibrated base case. Vertically, the lens is about 30 ft deeper than for the base case. This is probably due to larger vertical flow of recharge water in the upper regions, caused by the larger vertical conductivity value of the upper Avon Park formation.

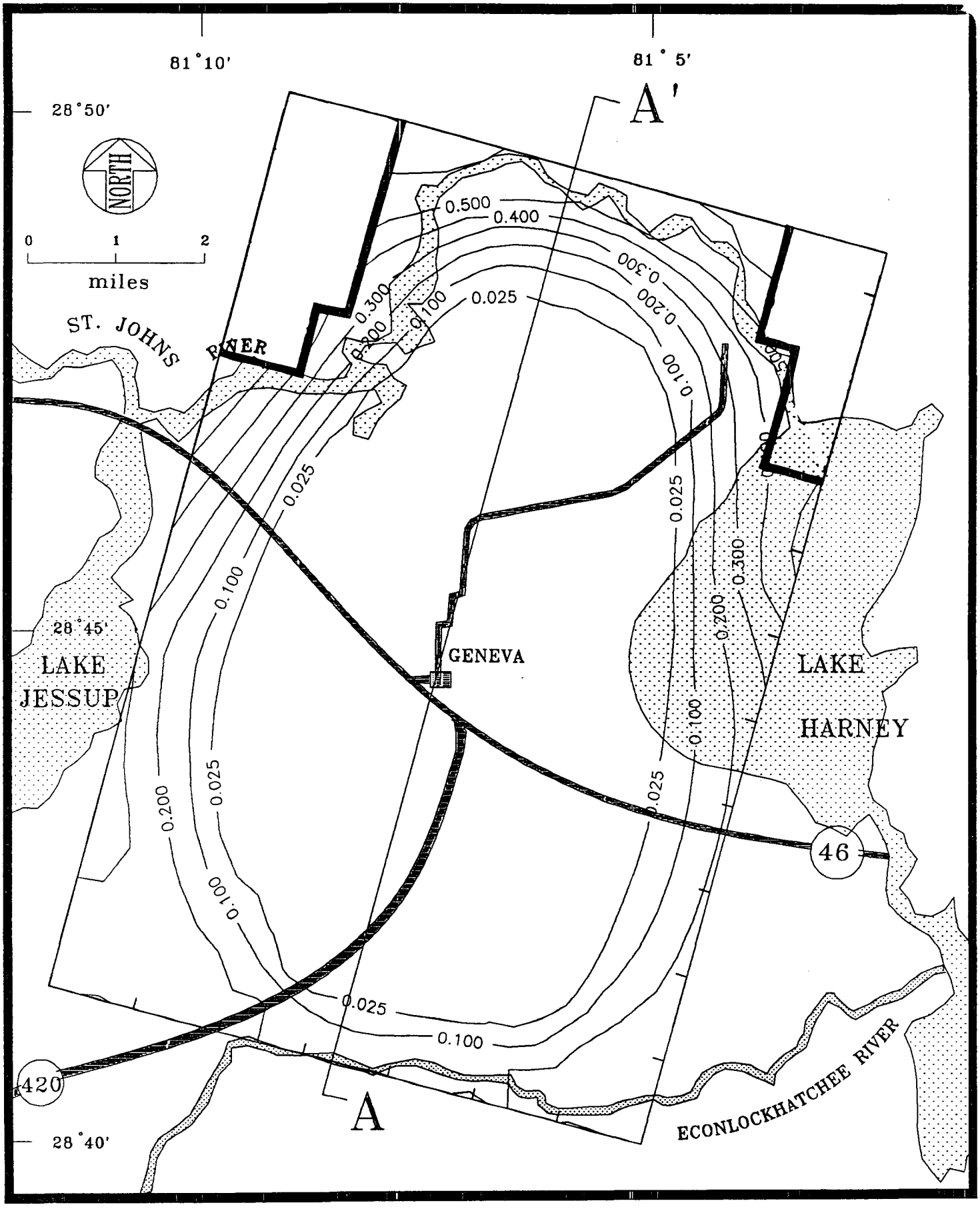

Figure 8.41. Sensitivity of areal distribution of chloride to longitudinal dispersivity (α_L reduced by one-half); [case 2, Table 8.4].

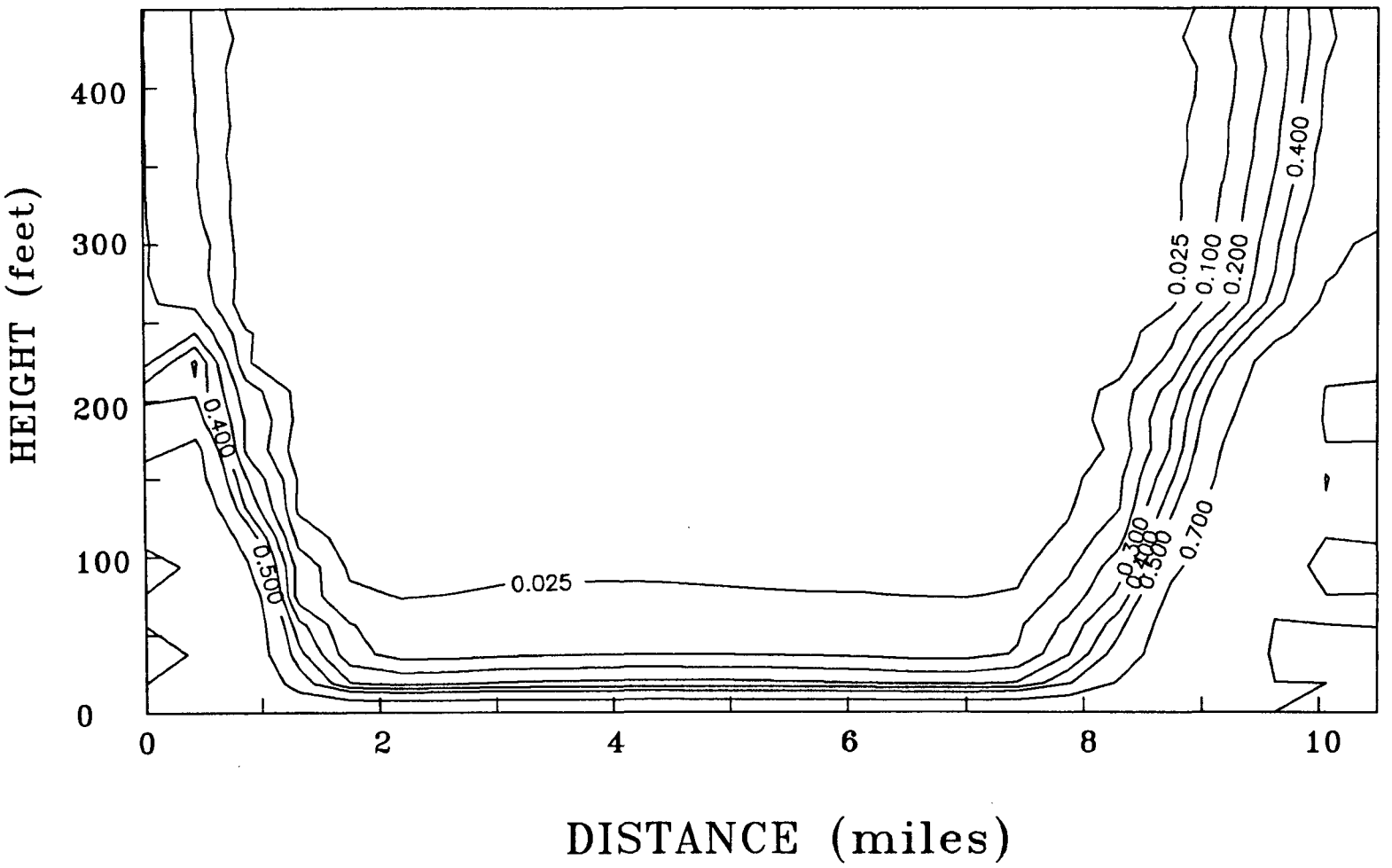

Figure 8.42. Sensitivity chloride distribution to longitudinal dispersivity (α_L value reduced by one-half); shown on the Figure is relative concentration of chloride through A-A' [case 2, Table 8.4].

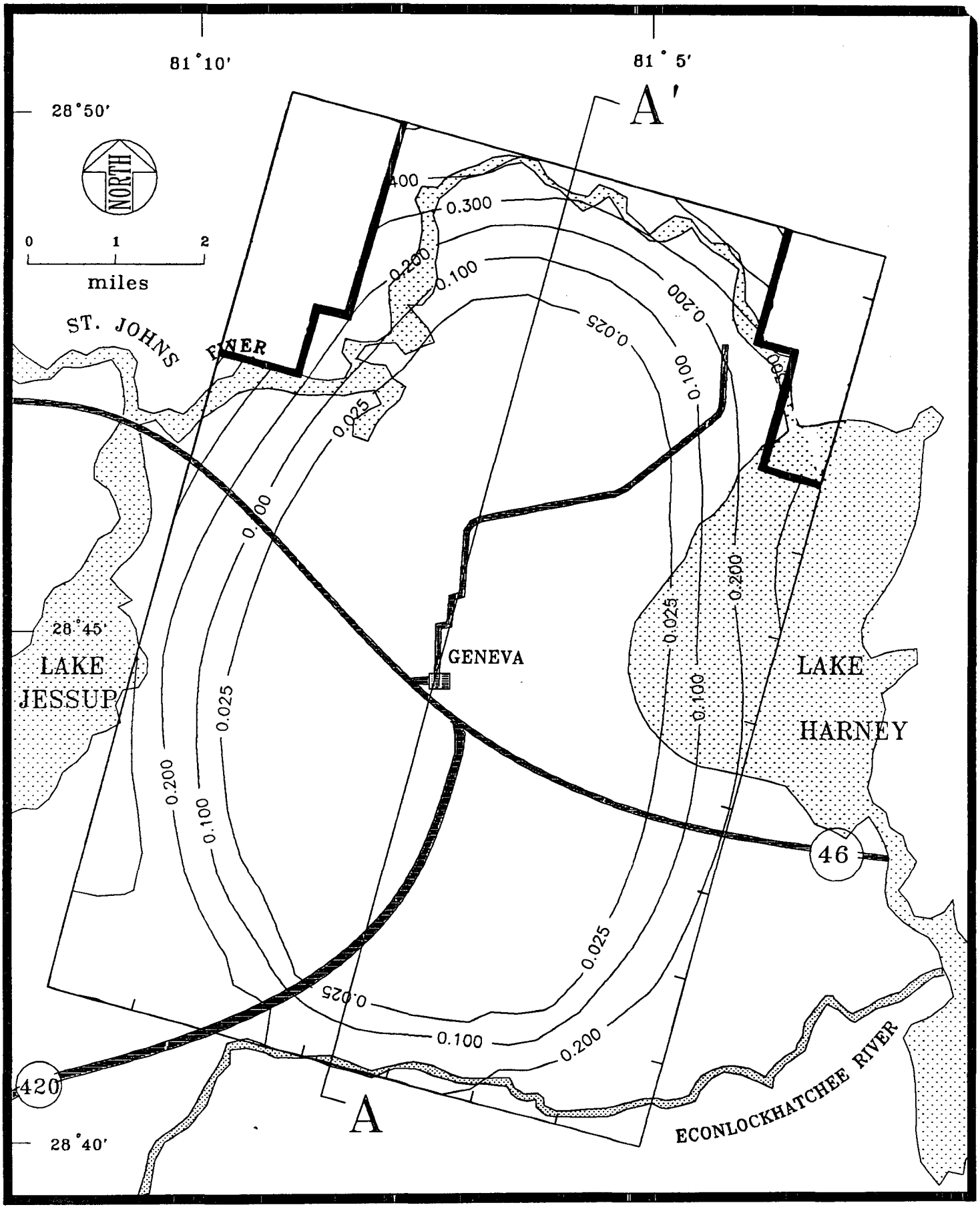

Figure 8.43. Sensitivity of areal distribution of chloride to doubling hydraulic conductivity of upper Avon Park formation [case 3, Table 8.4].

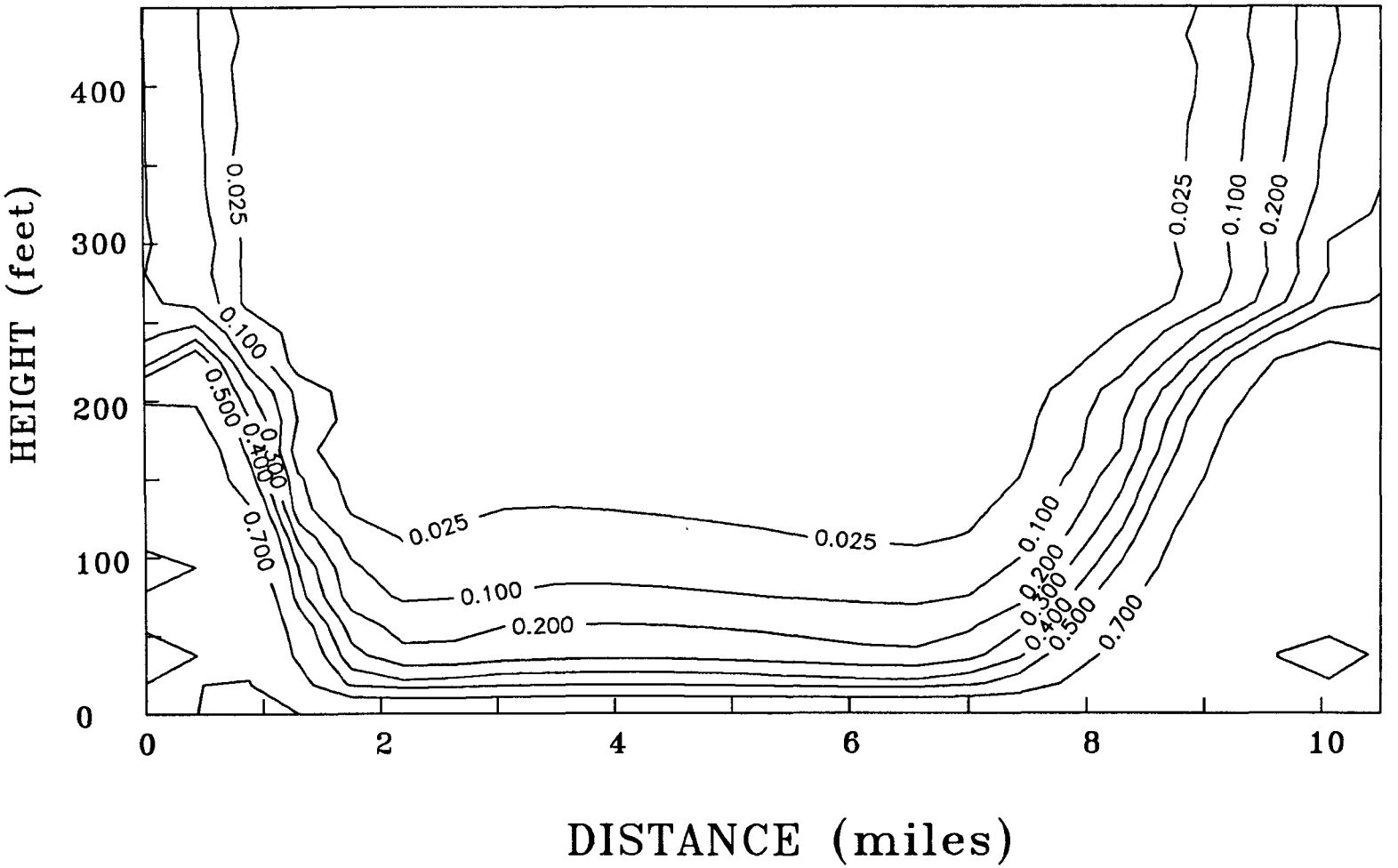

Figure 8.44. Sensitivity of chloride distribution to doubling hydraulic conductivity of upper Avon Park formation. Shown in the Figure is relative concentration of chloride through A-A' [case 3, Table 8.4].

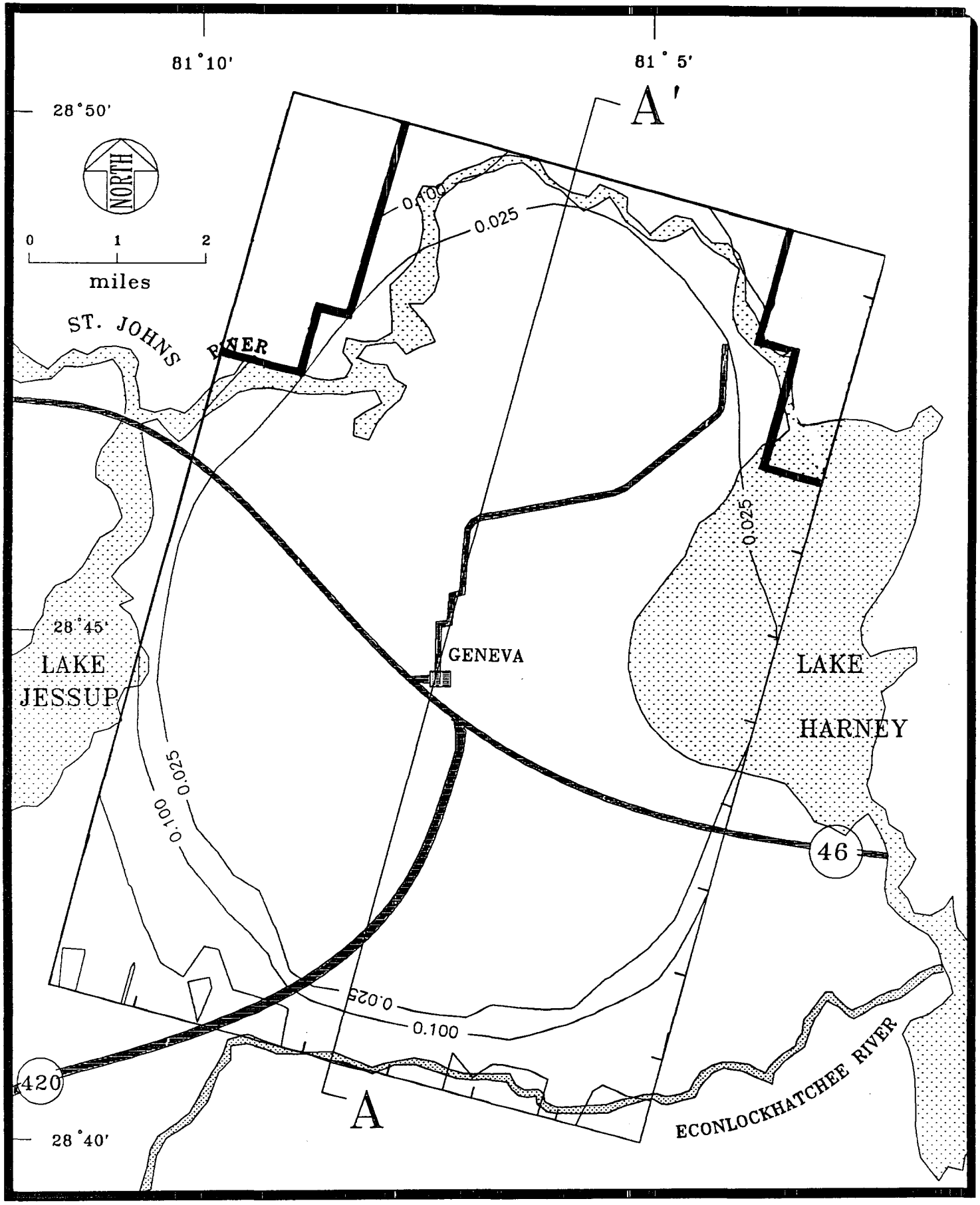

Figure 8.45. Sensitivity of areal distribution of chloride to reduced discharges (by factor of two) through the top surface [case 4, Table 8.4].

The next sensitivity run involves reduction of all discharges through the top surface by a factor of two. The areal distribution of chloride at the top of the upper Floridan is shown in Figure 8.45. The effect of reducing discharge near the Econlockhatchee River is not very significant on the lens size in that region. However, the lens is much larger between Lake Jessup and Lake Harney, and near the St. Johns River. Vertical chloride distribution are shown in Figure 8.46 for section A-A'. Upconing of chloride near the Econlockhatchee River boundary is less than for the steady-state calibrated lens. The 250-ppm isochlor is, however, at a shallower depth.

The next sensitivity analysis treats the low recharge areas of Figure 8.16 as no-flux zones. The areal distribution of chloride at the top of the upper Floridan, and the vertical profile of chloride in section A-A' are shown in Figures 8.47 and 8.48, respectively. The width of the lens decreases by about a mile and a half from the St. Johns River edge of the domain for this case. Vertically, the lens is approximately 30 ft deeper than the calibrated base case. Reducing the net recharge reduces the water flux and hence the dispersion near the bottom of the domain.

Two important factors seem to control the depth of the freshwater lens. First, the vertical component of flow in the upper regions should be sufficient for the recharge water to penetrate the lower Avon Park, and increase the lens thickness. Next, the flow components in the lower regions of the domain determine the dispersion of chlorides. Smaller flow components

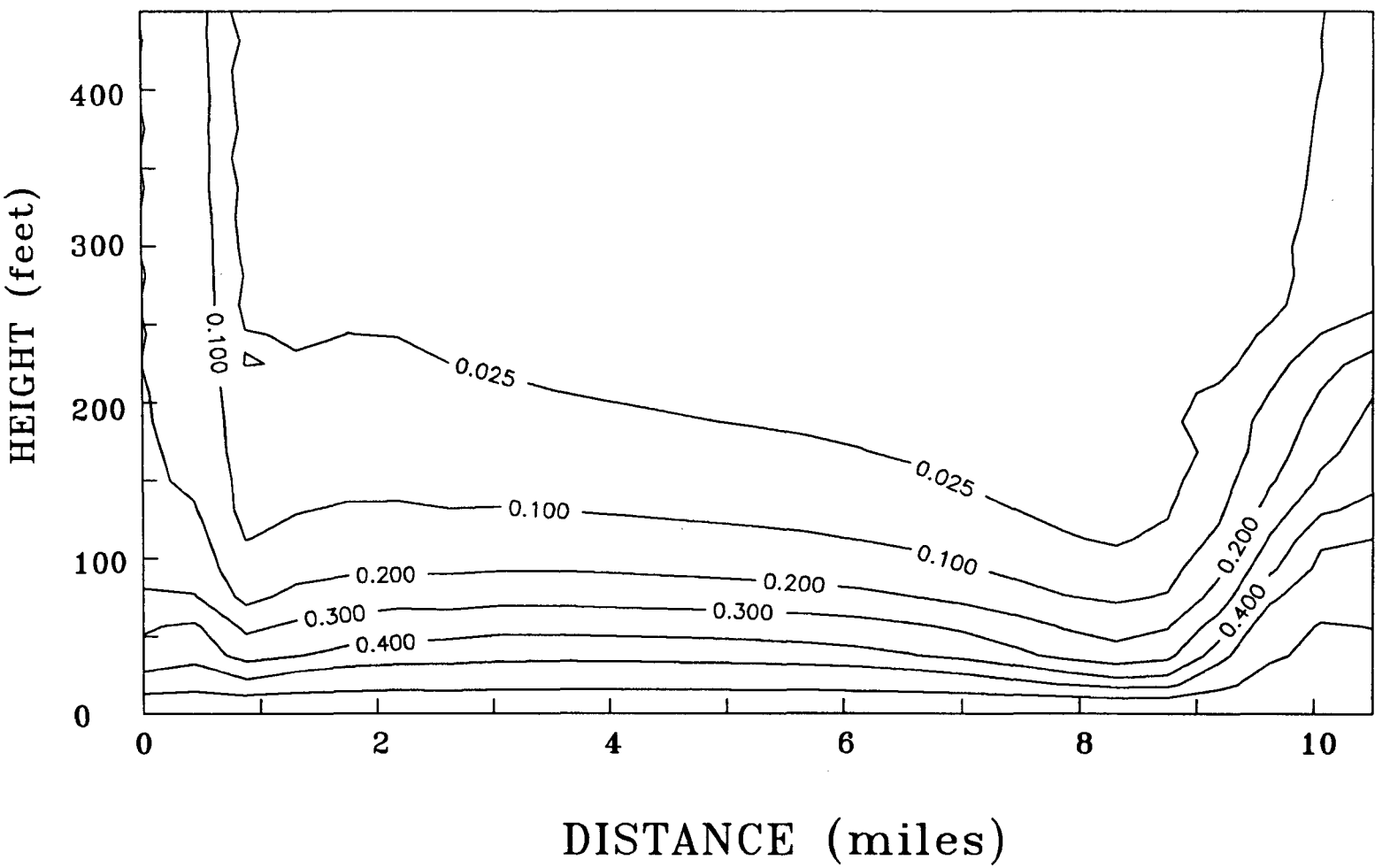

Figure 8.46. Sensitivity of chloride distribution to reduced discharges (by factor of two) through the top surface. Shown in the Figure is relative concentration of chloride through A-A' [case 4, Table 8.4].

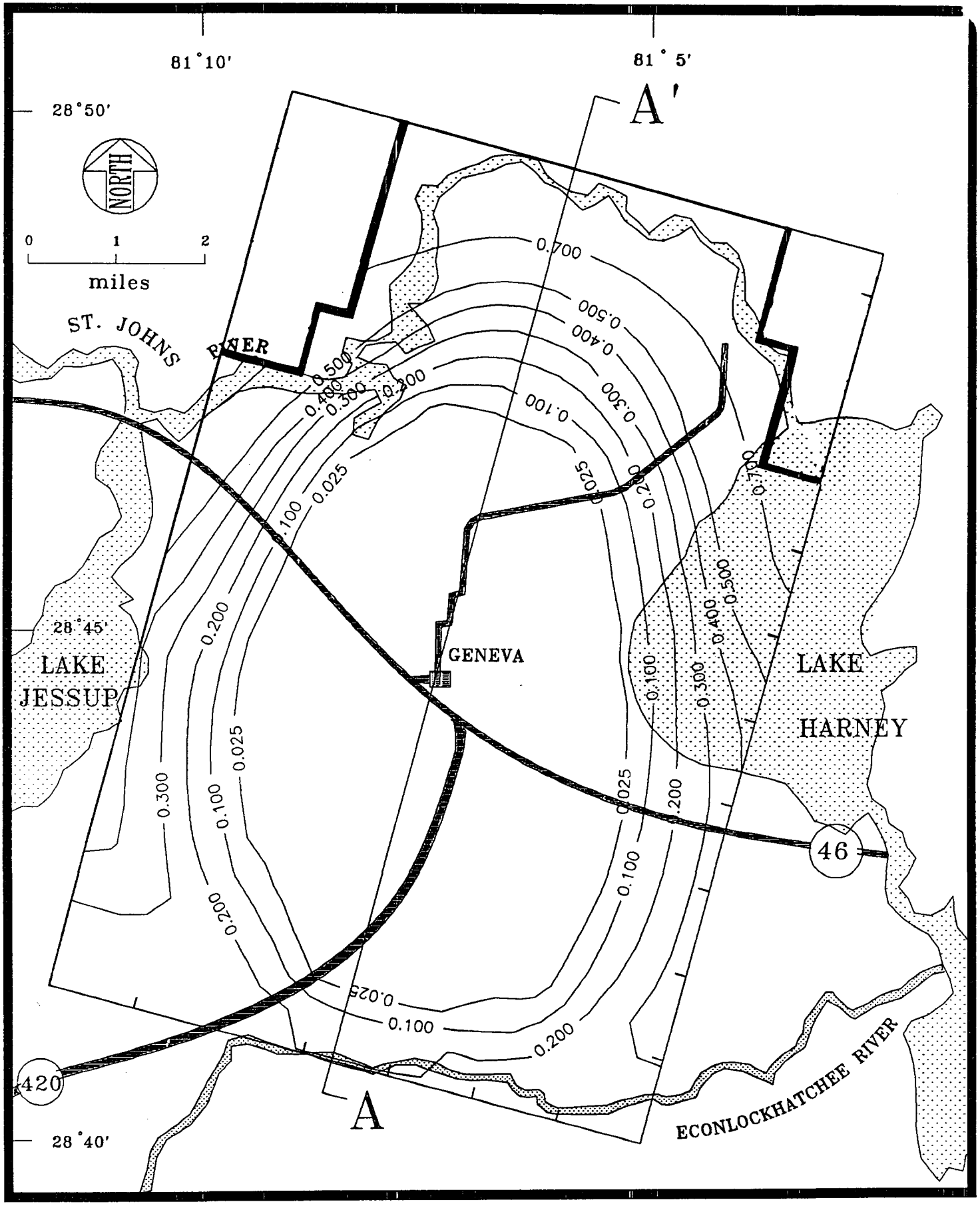

Figure 8.47. Sensitivity of areal distribution of chloride to reduced recharge through the top surface [case 5, Table 8.4].

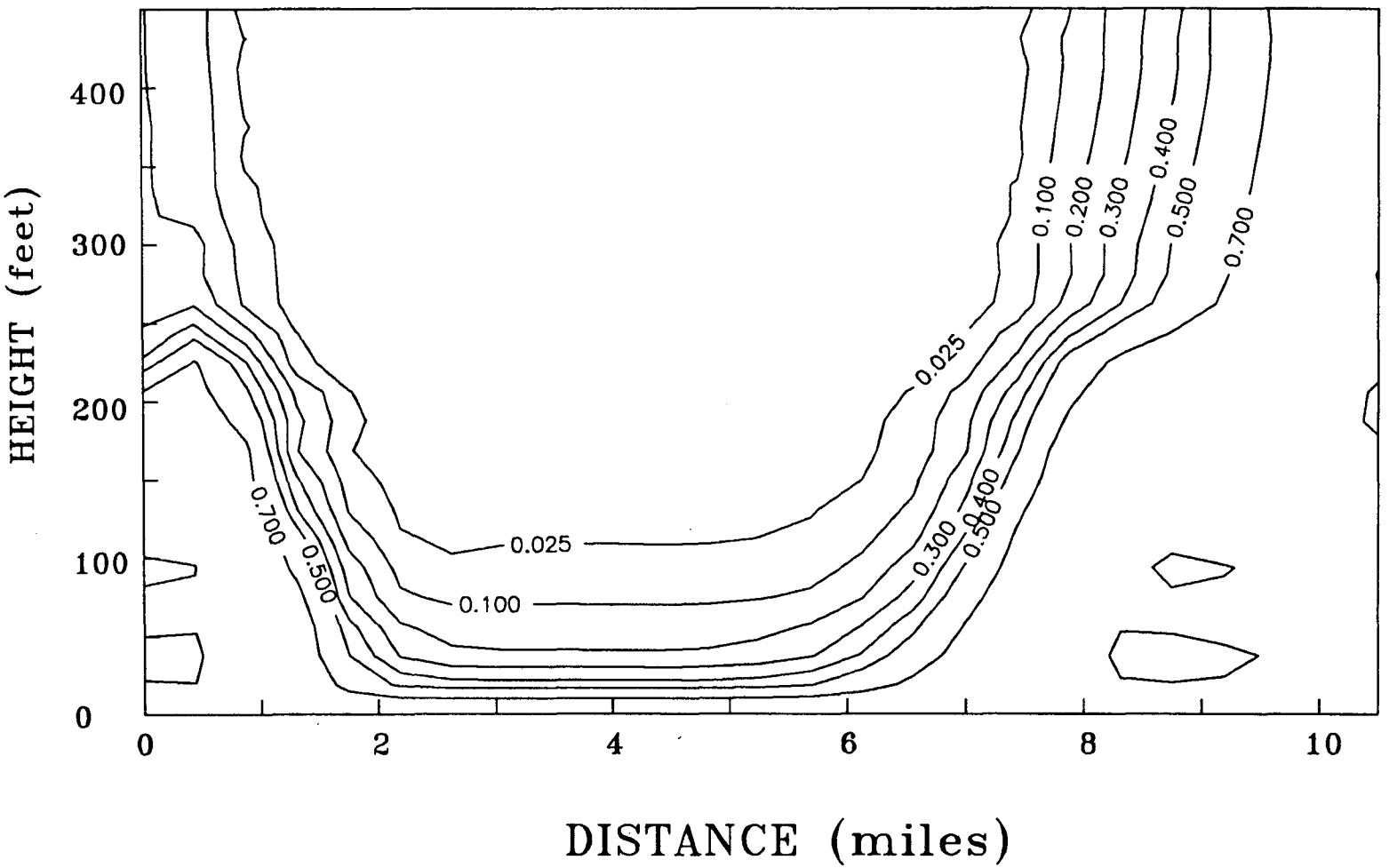

Figure 8.48. Sensitivity of chloride distribution to reduced recharge through the top surface. Shown in the Figure is relative concentration of chloride through A-A′ [case 5, Table 8.4].

near the bottom will provide for a thicker freshwater lens since dispersion is proportional to the flow velocity.

8.4 SUMMARY AND CONCLUSIONS OF THREE-DIMENSIONAL STEADY-STATE SIMULATIONS

Three-dimensional steady-state simulations of the Geneva freshwater lens system have been performed over the areal domain shown in Figure 4.2. The domain is oriented such that its edges are approximately parallel to the ambient groundwater flow. The top of the simulation domain is marked by the surface of the upper Floridan aquifer and the bottom lies 450 ft below, in a zone of brackish water. The upper Floridan is hydraulically connected to the surficial aquifer through a confining unit, and recharge/ discharge values are directly prescribed at the top of the domain to describe vertical flow components occurring at this surface. Necessary modeling data for the region were assimilated from various sources summarized in Table 3.1.

A three-dimensional grid was first calibrated as described in Chapter 7. Calibration of the freshwater lens system followed, as summarized in Table 8.1. Parameter values obtained from the two-dimensional cross-sectional modeling approach produced a much smaller freshwater lens due to the three-dimensional nature of the problem as explained at the end of Chapter 7. The calibrated steady-state, three-dimensional lens depicts field conditions fairly accurately. Chloride distributions predicted by the model match field estimates, and agree well with field data from monitoring wells. Material properties and boundary conditions used

to obtain the steady-state calibrated model are reported in Tables 8.2 and 8.3. Appendix A shows the material zones in various sections of the domain.

The sensitivity of the system to various unknowns or uncertainties in the field was also studied and is summarized in Table 8.4. Areal chloride distribution at the upper surface of the aquifer was insensitive to a different head profile prescribed at the bottom. This is because the lens "floats" on the top, where the recharge/discharge effects dominate its shape, as can be seen from the head patterns near the top, which are similar those of the calibrated case. Head patterns (and hence the flow pattern) near the bottom of the domain, however, were significantly different due to the larger gradients of the prescribed bottom head, which increase dispersion of chloride in this region. Improved data on the bottom head is needed to obtain an accurate prediction of flow in the lower part of the system. Accurate field information on vertical variations in the head and spatial and temporal variations of recharge and discharge are also required to properly calibrate the flow component of the model. The lens, however, is only slightly affected by the uncertainty in the bottom head values. As was shown in the 2-D sensitivity simulations (case 12, Figures 5.22-5.24), the lens and flow patterns are unaffected by the magnitude of the prescribed bottom head, as long as its gradients remain the same. The calibrated lens of Figures 8.16-8.20 was therefore developed by using the bottom-head gradients based on information supplied by Phelps and Rohrer (1987).

Decreasing longitudinal dispersivities increase the lens thickness, as does increasing the hydraulic conductivities of the upper Avon Park formation. Decreasing discharges increases the areal extent of the lens near the St. Johns River, as well as near the Lake Jessup and Lake Harney boundaries. Decreasing discharge does not, however, significantly affect the lens near the Econlockhatchee River boundary. Reducing recharge to the value used in the low recharge zones decreases the areal extent of the lens.

The calibration exercise also provides some insight into the lens behavior (Table 8.1). Decreasing the lateral conductivities of the upper two formations (Ocala and upper Avon Park) increases the lens depth, but does not have a significant impact on the areal configuration of the lens. Varying the thickness of the Ocala formation has only a slight impact on the lens system, within the probable range of thicknesses of the Ocala in the study region.

The most critical data gaps in the system appear to be the rates of discharges in the discharge areas, because they have the largest impact on the lens. Additional data on vertical chloride distribution and vertical head profiles would also be useful.

9. THREE-DIMENSIONAL TRANSIENT SIMULATIONS

9.1 OBJECTIVES

The principal objective of this study is to develop a numerical model that can be used by the SJRWMD personnel to evaluate potential water quantity and quality impacts due to current and future withdrawals of freshwater from the Geneva lens, or due to potential future changes in recharge/discharge conditions. This will assist the District in developing and implementing water management policies for the area. This section of the report describes transient simulations of various withdrawal scenarios that have been performed with the calibrated model described in Section 8. Lens responses to withdrawal rates of 0.5 Mgal/d and 2.5 Mgal/d from different locations within the lens are examined. A condition of dispersed pumping over a large area was also applied to the "Suburban Estates" region to assess the resultant response of the lens. The persistence of the lens to a sustained no-recharge condition was also studied. All transient simulations performed are summarized in Table 9.1.

9.2 DESCRIPTION OF SIMULATION SCENARIOS AND RESULTS

The initial condition for the transient analyses is the steady-state lens developed in Chapter 8 (see Figure 8.19 - 8.21). At the beginning of a simulation period (t=0), a steady impulse is applied to the system (i.e., a constant pumping stress, or a no-recharge condition is imposed on the lens). All other boundaries

TABLE 9.1 SUMMARY OF TRANSIENT SIMULATIONS.

SIMULATION NUMBER	SIMULATION CASE	FIGURE	REMARKS
1	Recharge to top is zero	9.1 - 9.6	Lens collapses totally by 150 years. Head profiles change very rapidly, and almost reach equilibrium within days.
2	Pumping 2.5 Mgal/d from lens center	9.7 - 9.11	Lens shrinks areally. Upconing of brackish water from bottom occurs. Depth of pumping does not affect chloride patterns. Wells not contaminated by brackish water by 150 years.
3	Pumping 2.5 Mgal/d from Lake Harney edge of lens	9.17 - 9.23	Lateral intrusion of salt water occurs from Lake Harney edge within 25 years. Wells contaminated very quickly. Depth of pumping does not significantly affect chloride patterns.
4	Pumping 0.5 Mgal/d from Lake Harney edge of lens	9.24 - 9.28	Lateral intrusion of about half a mile occurs from Lake Harney edge within 25 years. Small change in chloride patterns after 25 years. Well placement has significant effects on breakthrough patterns for wells. Depth of pumping does not significantly affect final chloride patterns.
5	Pumping 0.5 Mgal/d from shallow wells at Lake Harney edge of lens. Well placement is different from simulation 4	9.31 - 9.32	Chloride patterns similar to those of simulation 4. However, shallow wells remain uncontaminated throughout simulation period.
6	Distributed pumping in shallow zone throughout lens. (Net withdrawal = 4.2 Mgal/d).	9.33 - 9.39	Lens reduces areally by approximately ½ mile from all directions. Lens depth decreases by 50 ft after 150 years of simulation. Shallow wells not contaminated.

are unchanged from the steady-state conditions imposed on the calibrated lens (Table 8.3). The material parameters used in all transient simulations are assumed to be those used for developing the calibrated steady-state lens (Table 8.2). The storage-coefficient estimated for the system is 0.002 (Phelps and Rohrer, 1987) and this value is used for all formations. The lens response is computed and displayed for each scenario, for up to 150 years.

The first transient simulation examines the persistence of the lens with zero recharge conditions. Figures 9.1a and 9.1b show the areal chloride distribution and a vertical mid-section chloride distribution, respectively, at 25 years of simulation. As can be seen, the areal extent of the lens is diminished greatly. Most of the saltwater encroachment is from the Econlockhatchee River side of the domain, where the 250-ppm isochlor has intruded more than two miles into the original (initial) steady-state lens. The depth of the lens at section A-A′ reduces to less than 250 ft. Figures 9.2a and 9.2b show the areal chloride relative concentration contours at the top of the upper Floridan and in the vertical chloride distribution for the section passing through the mid-plane A-A′, respectively, at 50 years. The lens has shrunk laterally another two miles from the Econlockhatchee River edge of the domain, and thins to a little over 200 ft vertically. By 100 years, the lens has contracted even further, as shown in the areal and vertical mid-section concentration distributions of Figures 9.3a and 9.3b. By 150 years, the lens is almost completely collapsed. A comparison of the 3-D results with those situations

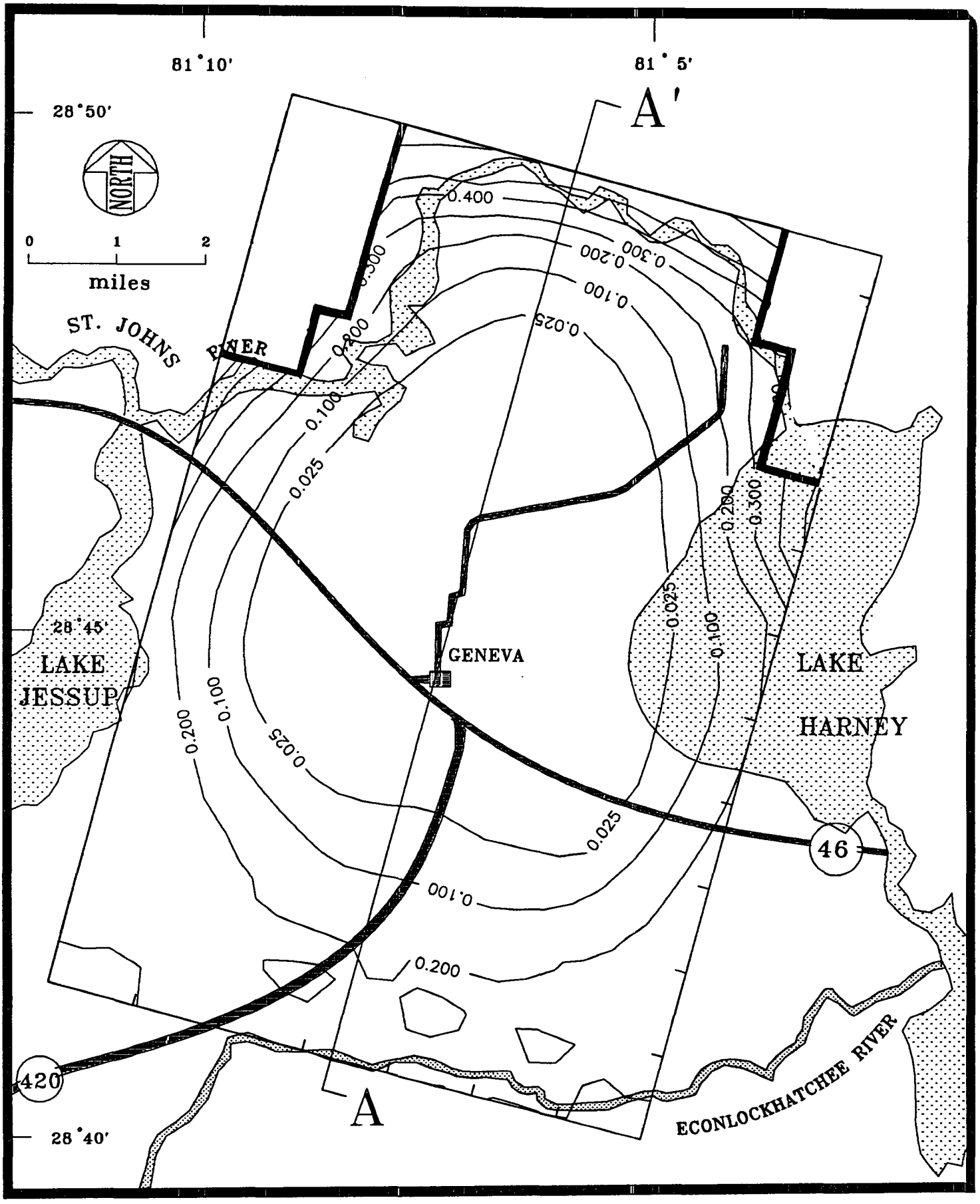

Figure 9.1a. Areal distribution of chloride after 25 years of no recharge. [case 1, Table 9.1]

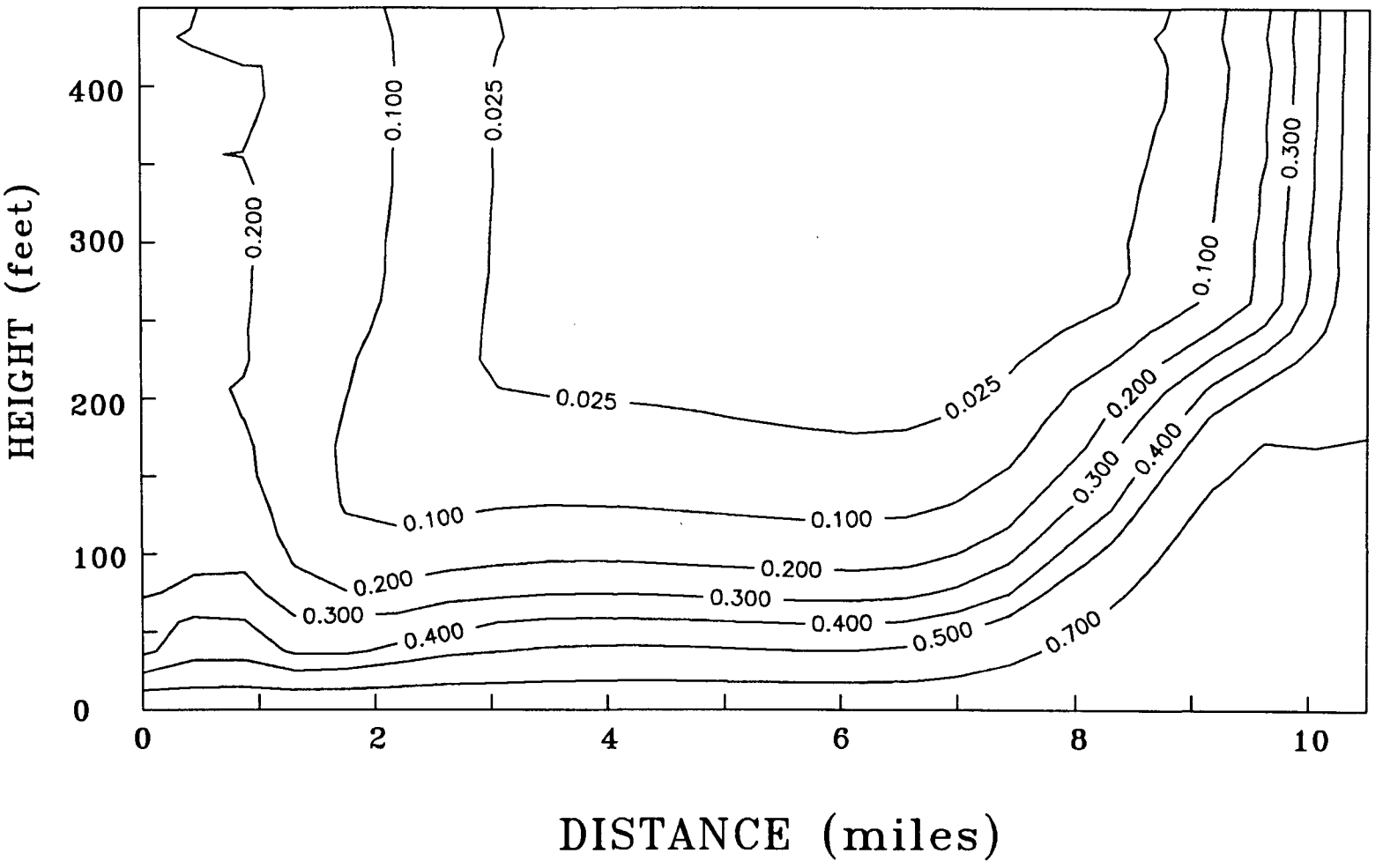

Figure 9.1b. Relative concentration of chloride through A-A′ after 25 years of no recharge. [case 1, Table 9.1]

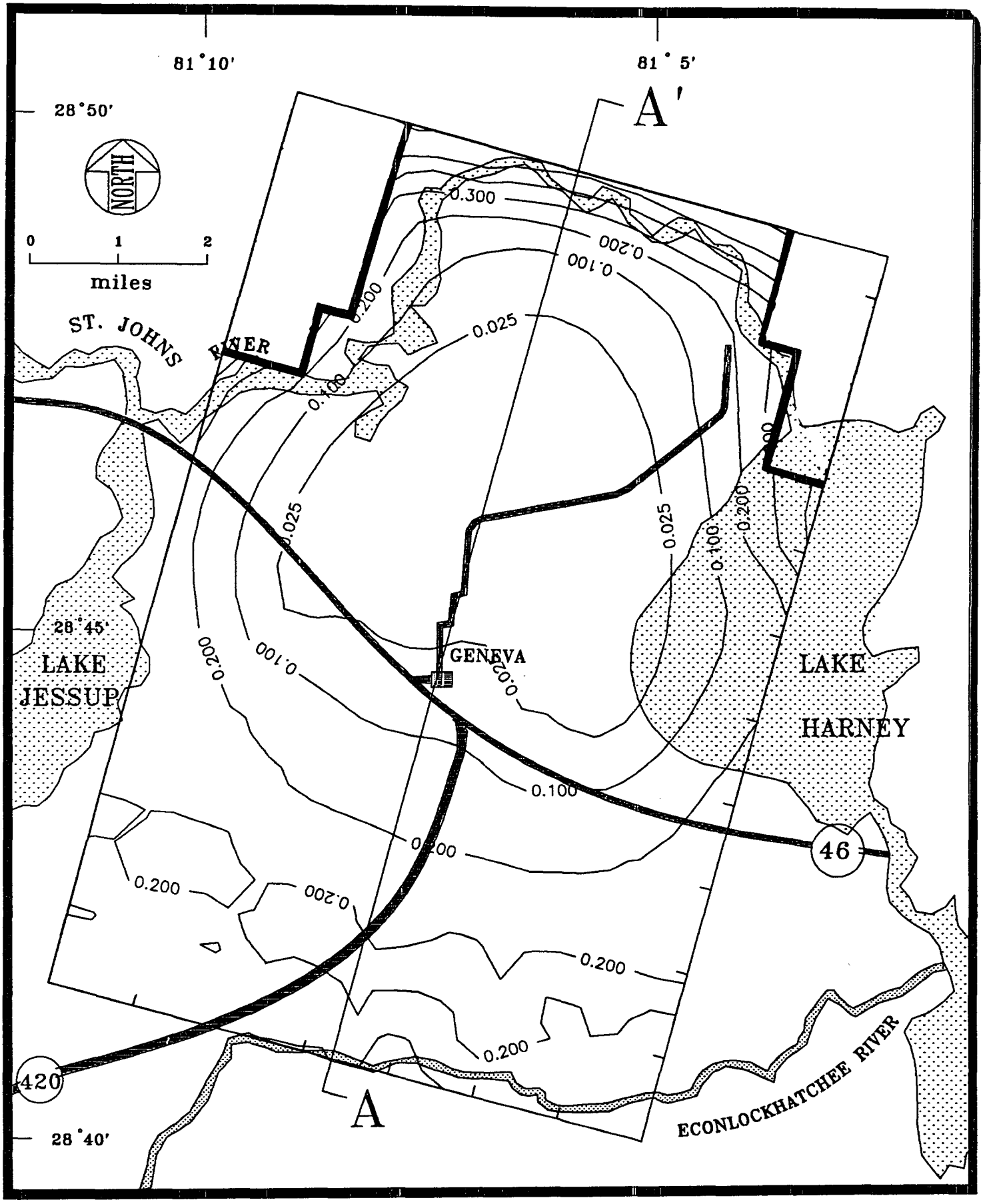

Figure 9.2a. Areal distribution of chloride after 50 years of no recharge. [case 1, Table 9.1]

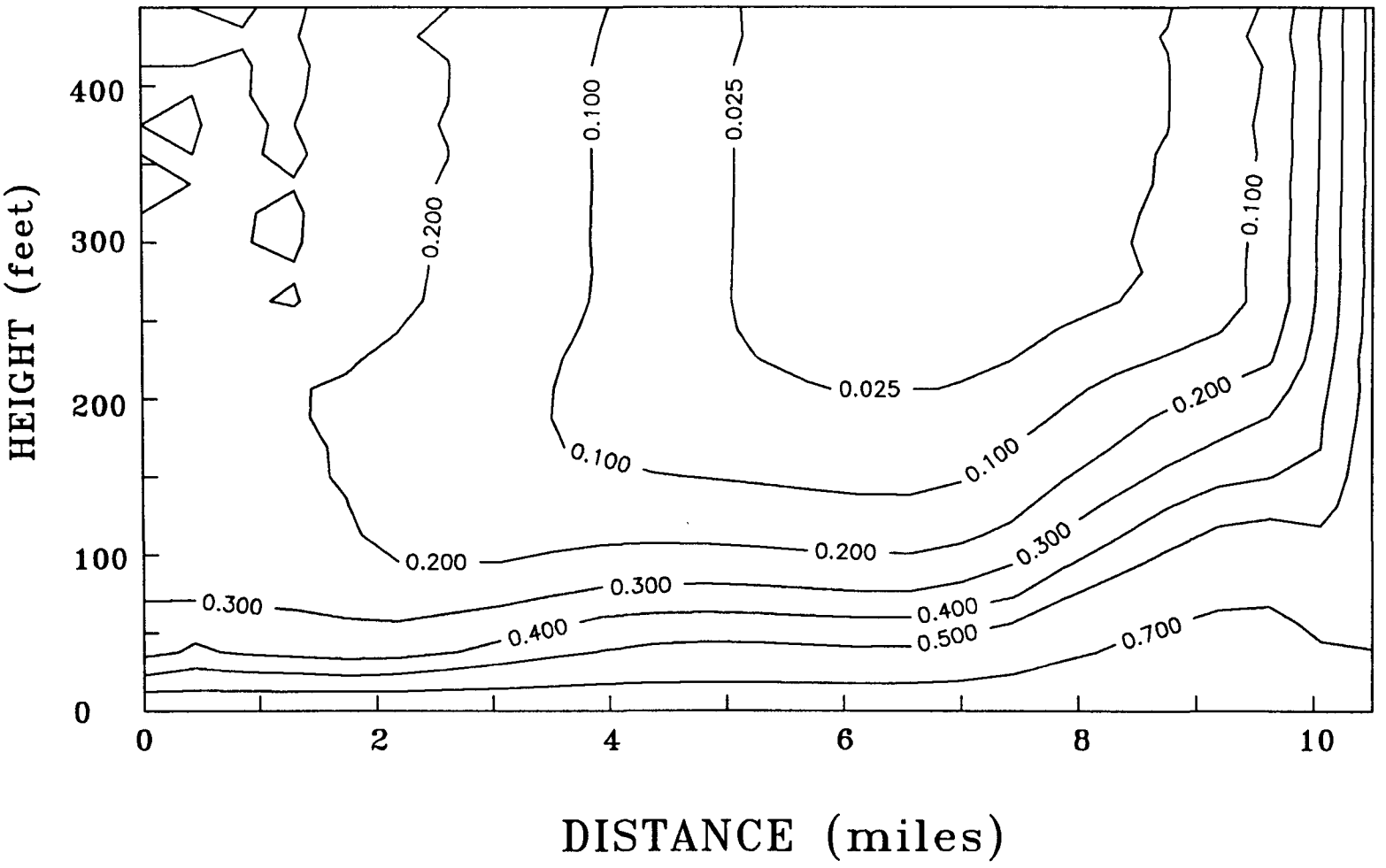

Figure 9.2b. Relative concentration of chloride through A-A′ after 50 years of no recharge. [case 1, Table 9.1]

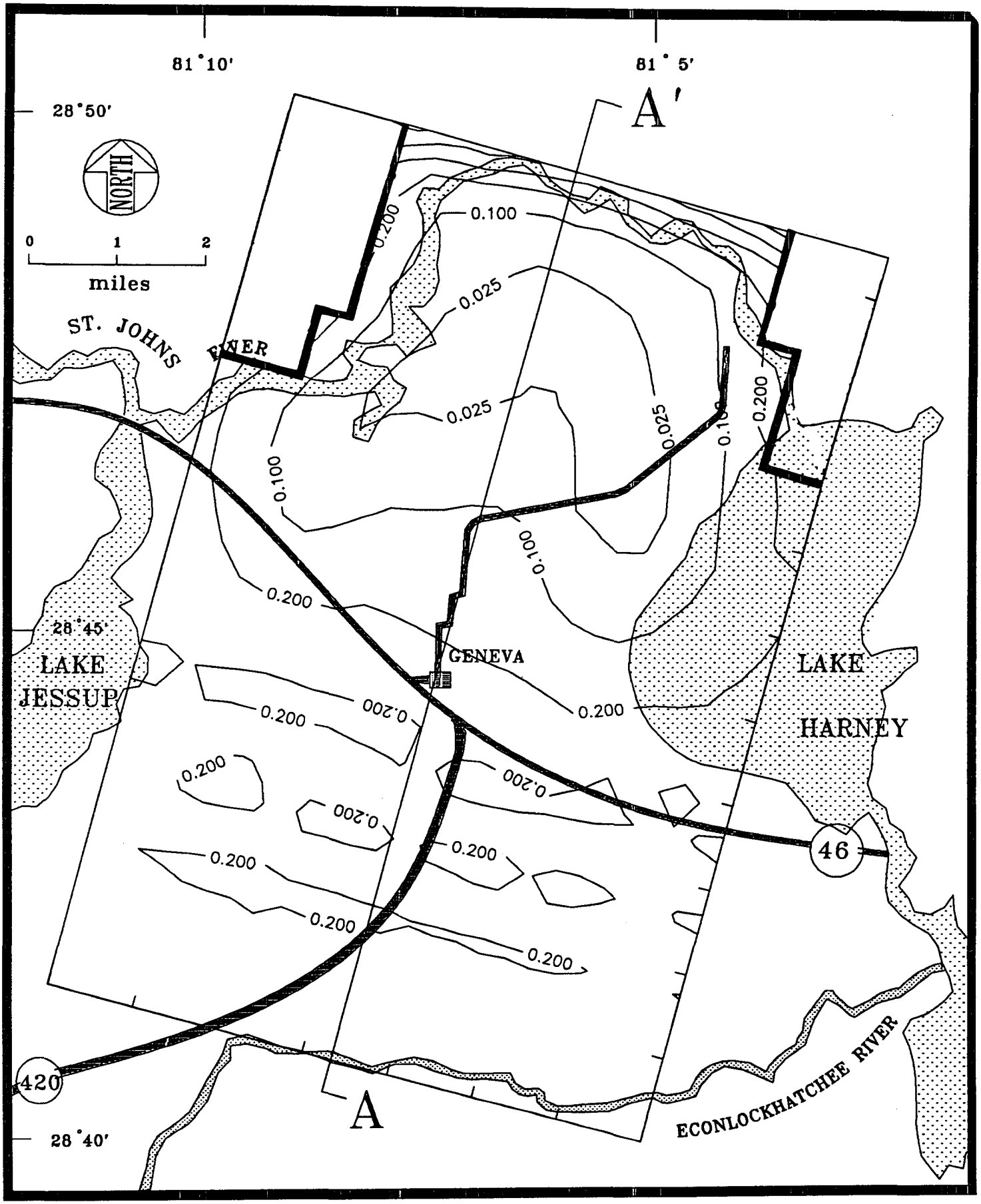

Figure 9.3a. Areal distribution of chloride after 100 years of no recharge. [case 1, Table 9.1]

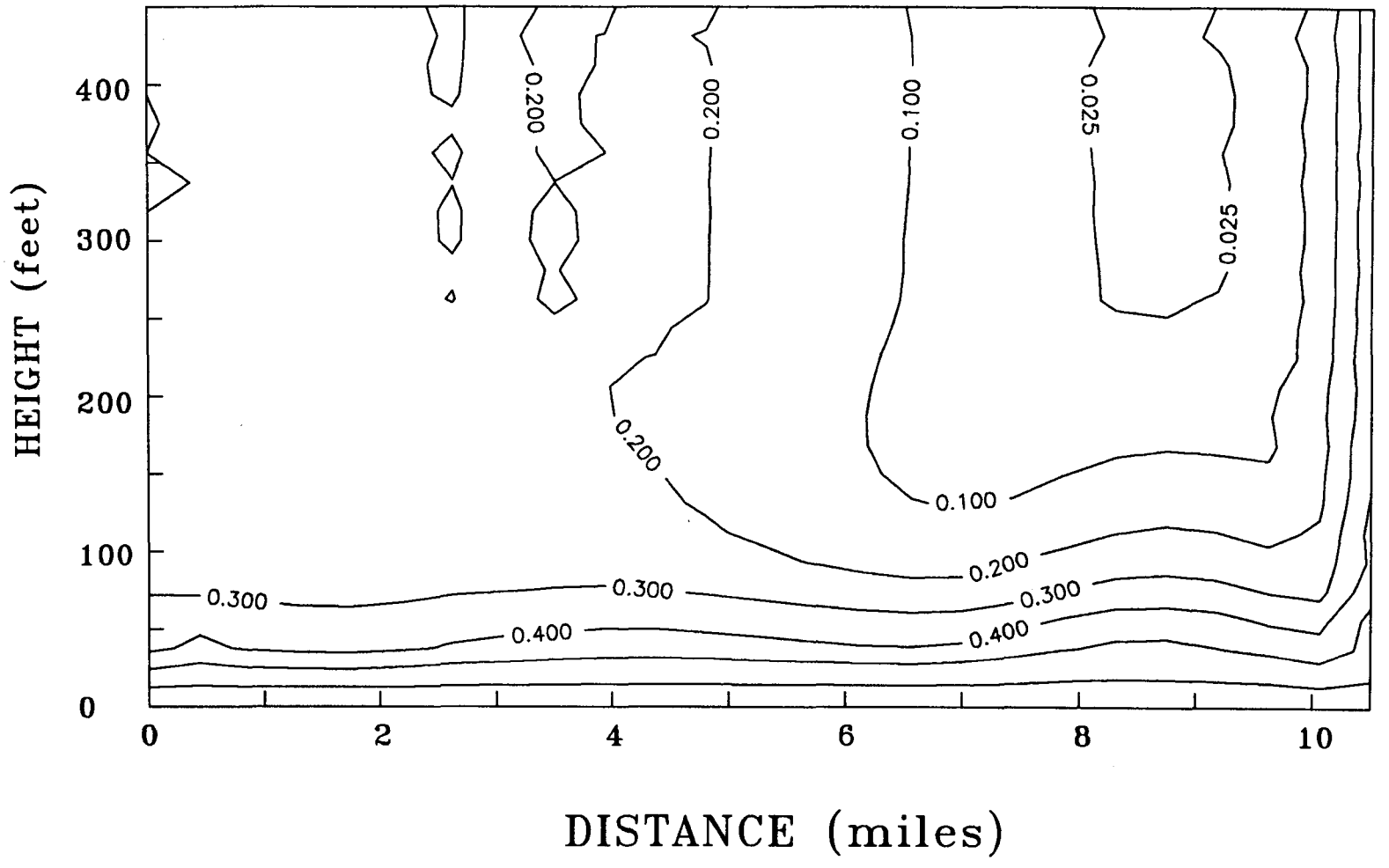

Figure 9.3b. Relative concentration of chloride through A-A′ after 100 years of no recharge. [case 1, Table 9.1]

of no-recharge modeled in a 2-D cross-sectional mode (Figure 6.7) indicate an apparent discrepancy in the persistency of the lens. This is due to the two-dimensional assumption that neglects effects of discharges and intrusion from the transverse horizontal direction. The different discharges for the two scenarios also contribute to the differences.

The simulated true head distributions in a plane 25 ft above the bottom of the domain, and at the top of the domain are shown in Figures 9.4 and 9.5, respectively, for a 7-day simulation time value, and Figure 9.6 shows variations of head in section A-A'. Comparing these with the initial steady-state heads of Figures 8.23, 8.24 and 8.25, it can be seen that the heads have changed substantially. However, the concentration profile is virtually unchanged over the 7-day time value. As noted earlier, the time scale for groundwater flow is several orders of magnitude smaller than the time scale for chloride transport. Thus, heads can fluctuate rapidly, without significantly affecting chloride concentrations. A temporally averaged head distribution can therefore be used in the transport modeling. However, such a head distribution cannot be directly compared to the reported field values, since these are dependent on the recharge/discharge rates at the time of measurement. The temporal fluctuations of the head field can be significant, as seen above, but are obscured in the averaging process.

The next transient simulation examines the lens response to pumping 2.5 Mgal/d from deep wells at the center of the lens. The

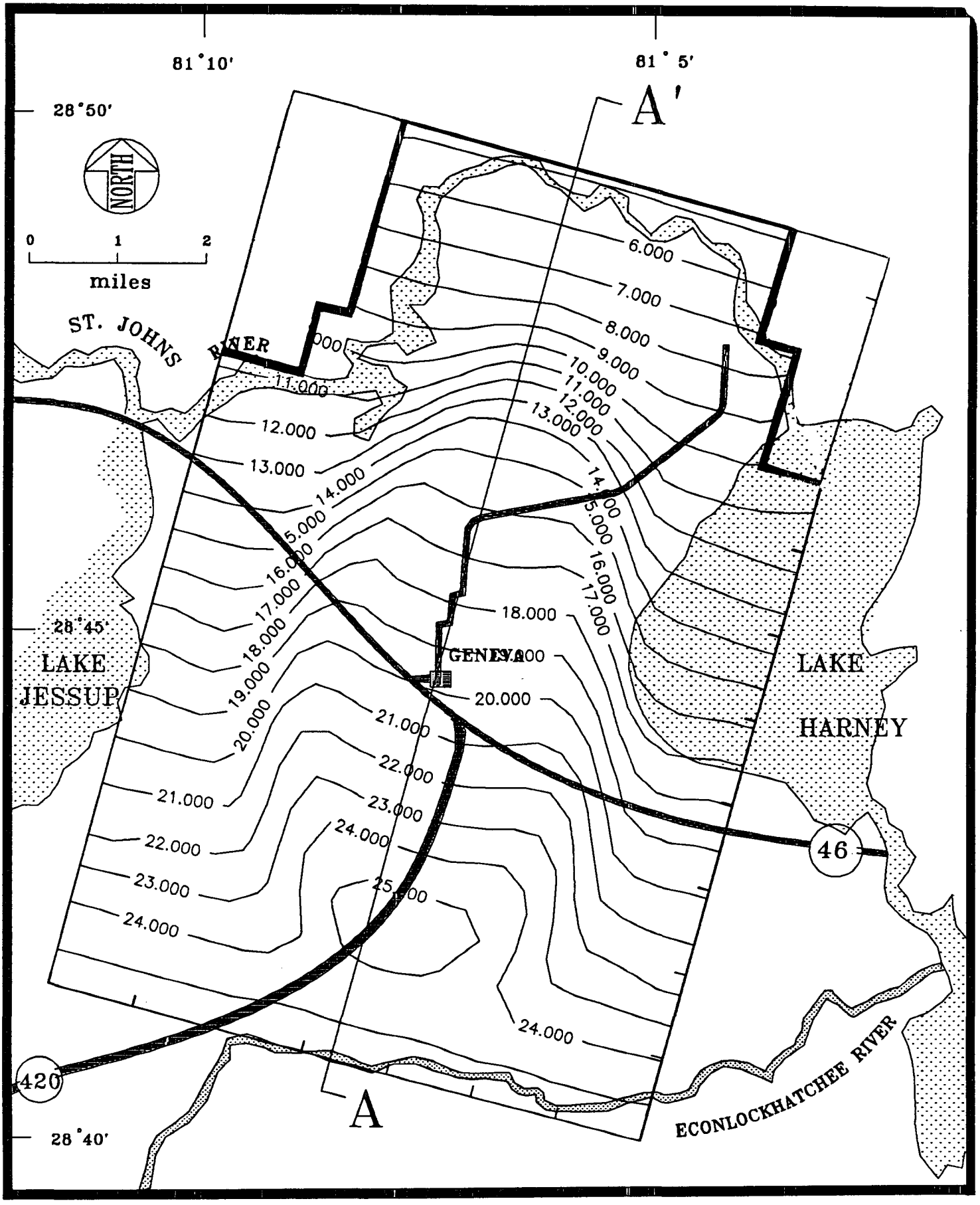

Figure 9.4. Areal profile of true head at 25 ft above the bottom of the domain after a week of no recharge [case 1, Table 9.1].

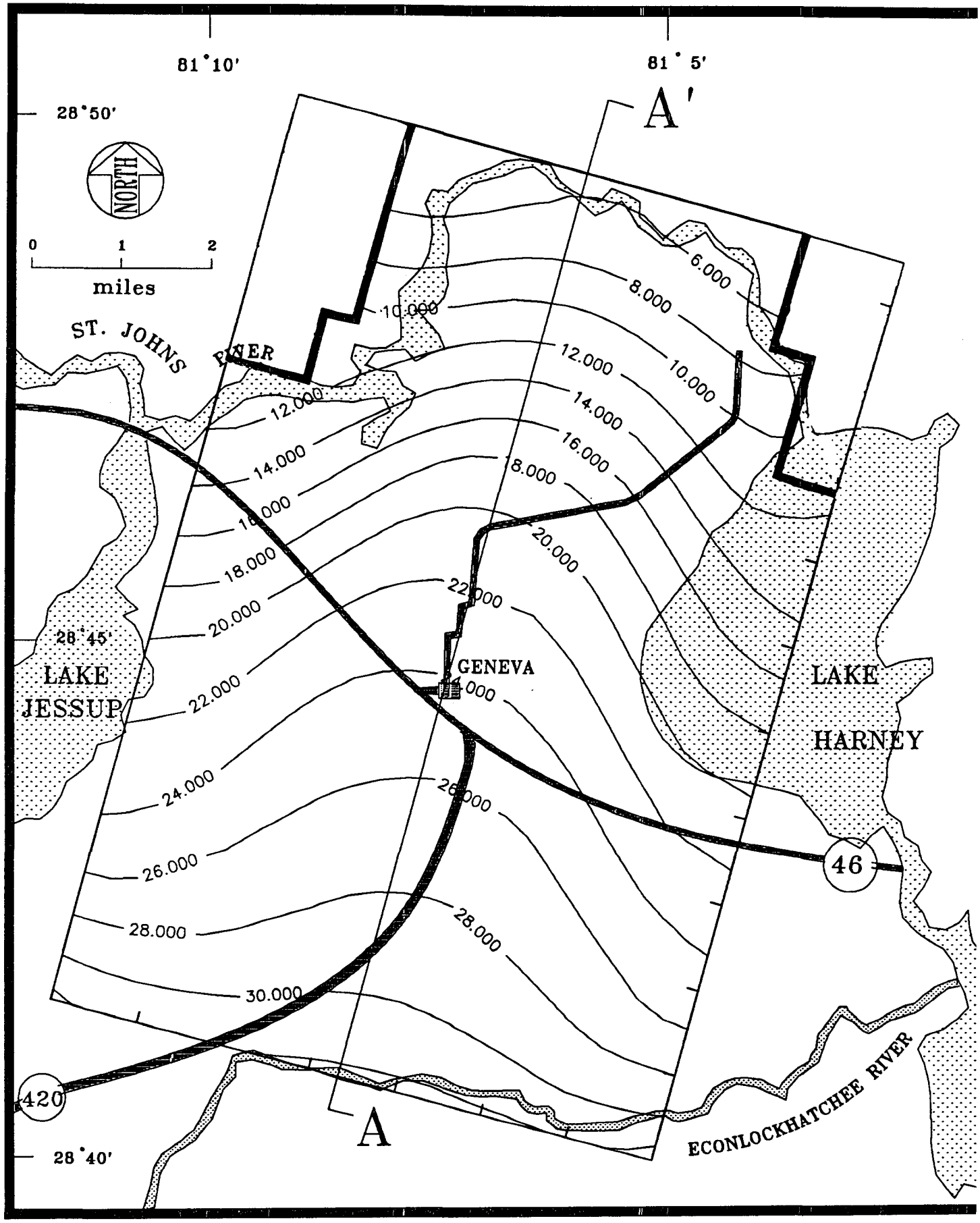

Figure 9.5. Areal distribution of true head at the top of the domain [case 1, Table 9.1].

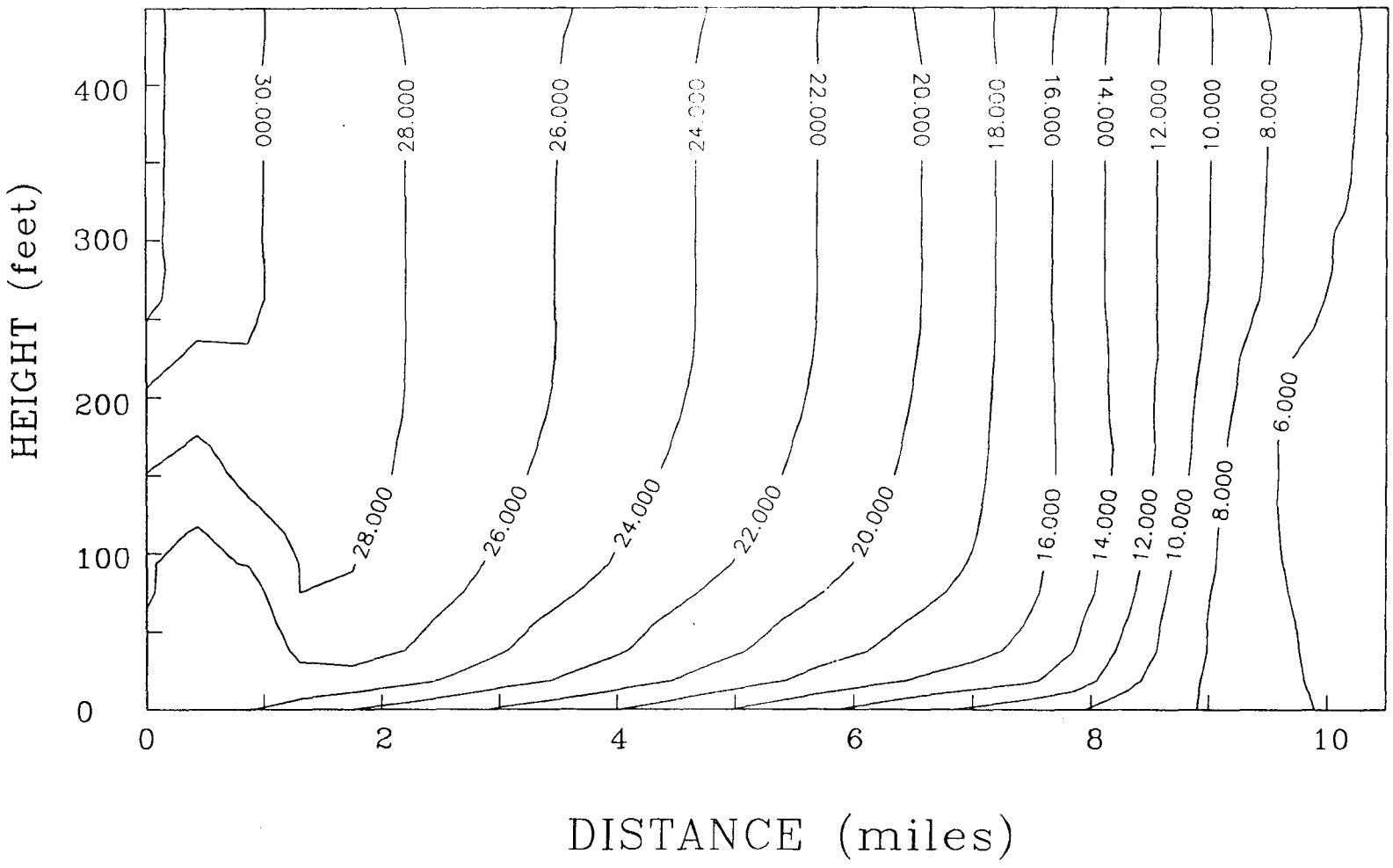

Figure 9.6. Cross-sectional distribution of true head after 7 days of no recharge [case 1, Table 9.1].

well field consists of 4 wells located at x = 5.53 mi, 5.89 mi, and z = 3.41 mi and 3.79 mi, on the x - z coordinate system shown in Figure 7.1. All wells are screened from 80 ft to 210 ft in depth from the top of the upper Floridan. Figure 9.7a shows the areal distribution of chloride at the top of the upper Floridan at 150 years of simulation, and Figure 9.7b shows the perspective view of the freshwater lens. Longitudinally (along the x-direction), the lens shrinks by less than 1/4 mi, near the St Johns River side of the domain. Laterally, the lens shrinks evenly from both the Lake Harney and Lake Jessup sides by approximately 3/4 mi. Figures 9.8, 9.9 and 9.10 show the vertical chloride profile through section a-a' (see Figure 9.7) at 150 years, 50 years, and 25 years respectively. Upconing is considerable at 25 years, and a steady-state condition is almost reached by 50 years. The 250 ppm chloride isochlor has not however reached any of the wells. The breakthrough curves for chloride at the bottom of the wells is shown in Figure 9.11. Well 1, located at x = 5.53 mi, z = 3.41 mi shows the lowest salt concentrations. Well 2, at x = 5.89 mi, z = 3.41 mi shows concentrations of up to 80-ppm at the bottom. Well 3, located at x = 5.53 mi, z = 3.79 mi reaches chloride concentrations of 30 ppm, and Well 4 at x = 5.89 mi, z = 3.79 mi shows the largest chloride concentration, reaching a value of 210 ppm at the bottom by 150 years, by which time the steady-state condition has been reached.

The next transient simulation considers a well field at the same location with a total withdrawal rate of 2.5 Mgal/d. The

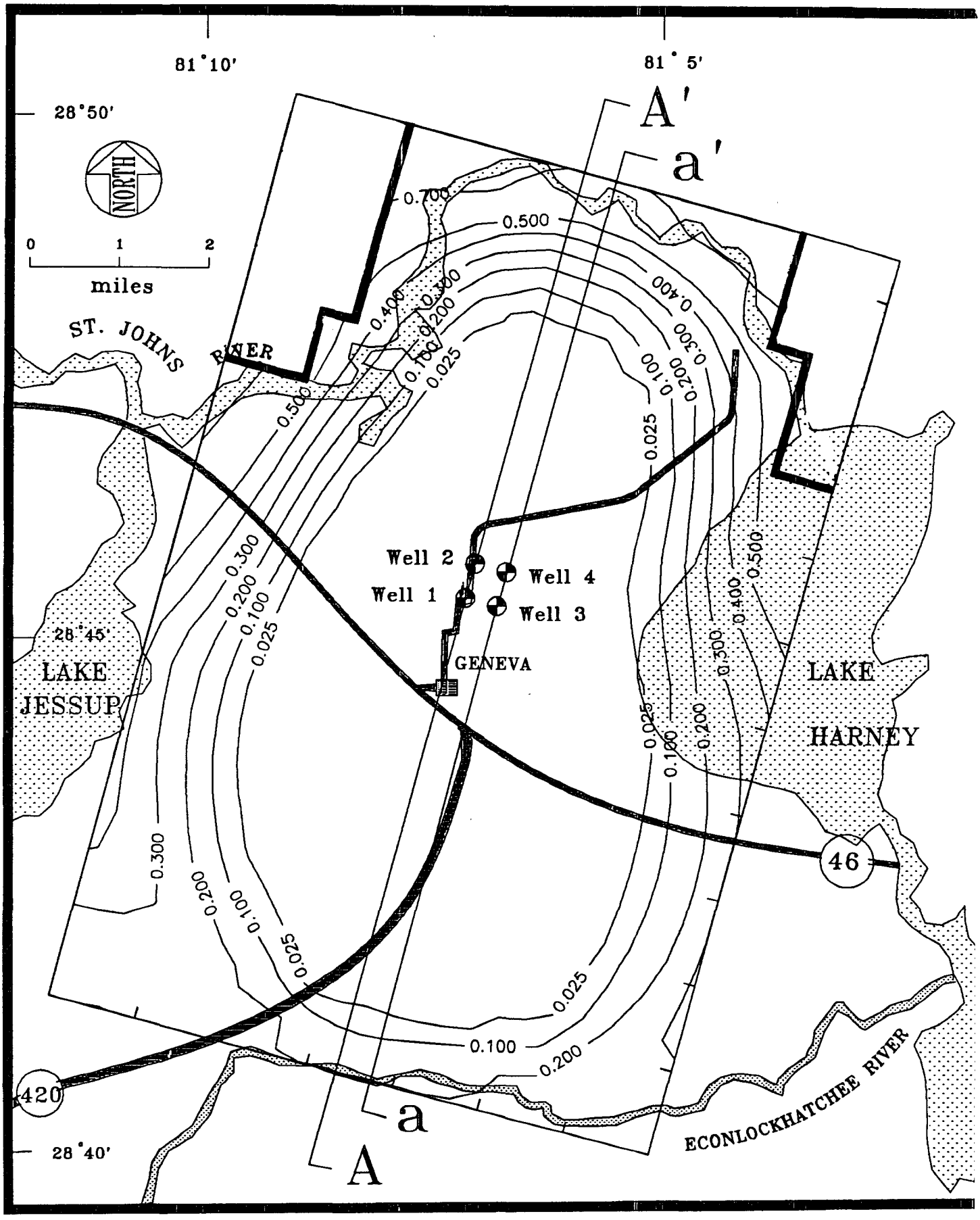

Figure 9.7a. Areal distribution of chloride after 150 years of pumping 2.5 Mgal/d from deep wells at the center of the lens [case 2, Table 9.1].

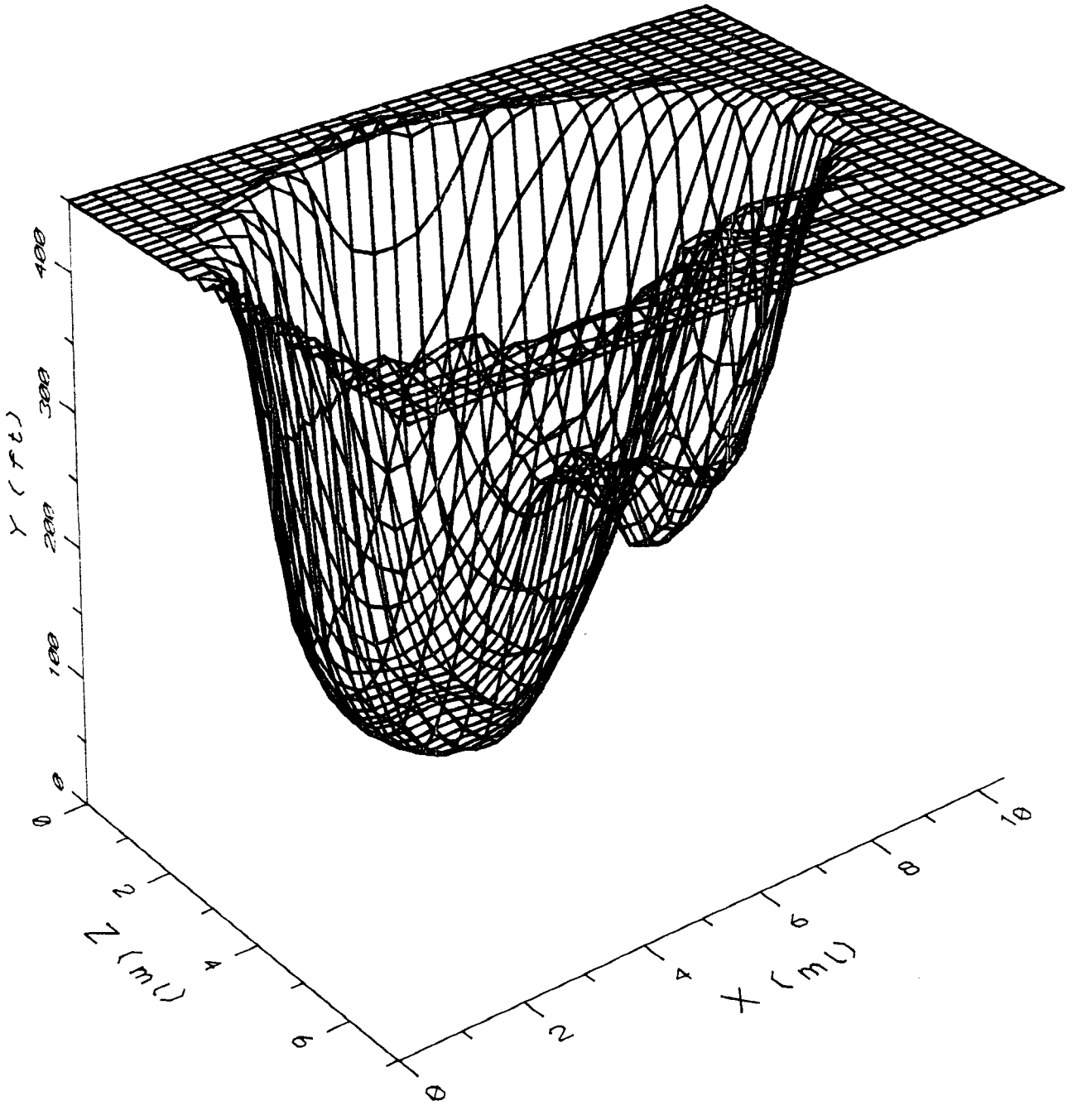

Figure 9.7b. Perspective view of freshwater lens after 150 years of pumping 2.5 Mgal/d from deep wells at the center of the lens [case 2, Table 9.1].

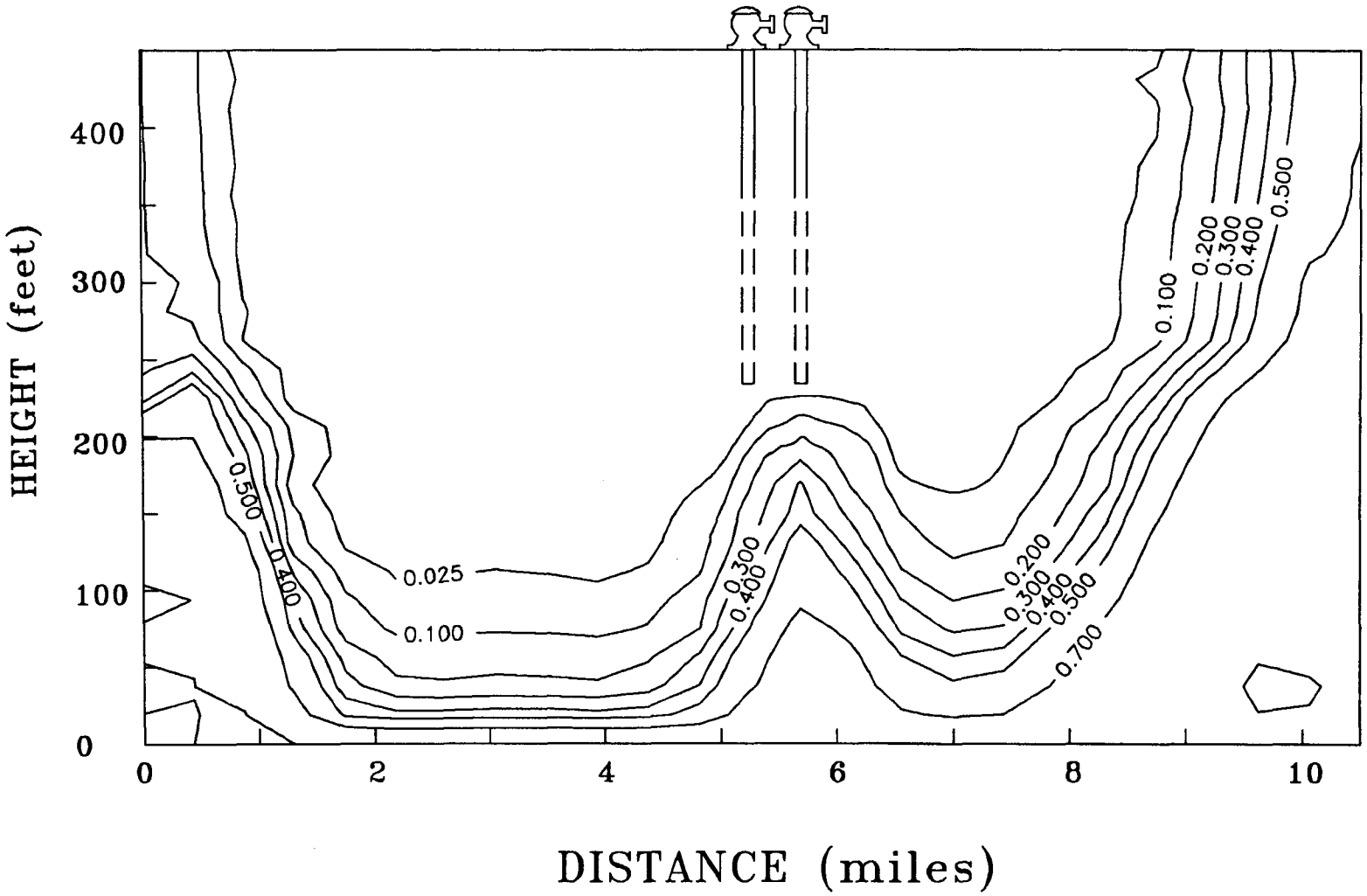

Figure 9.8. Relative concentration of chloride through A-A′ after 150 years of pumping 2.5 Mgal/d from deep wells at the center of the lens [case 2, Table 9.1].

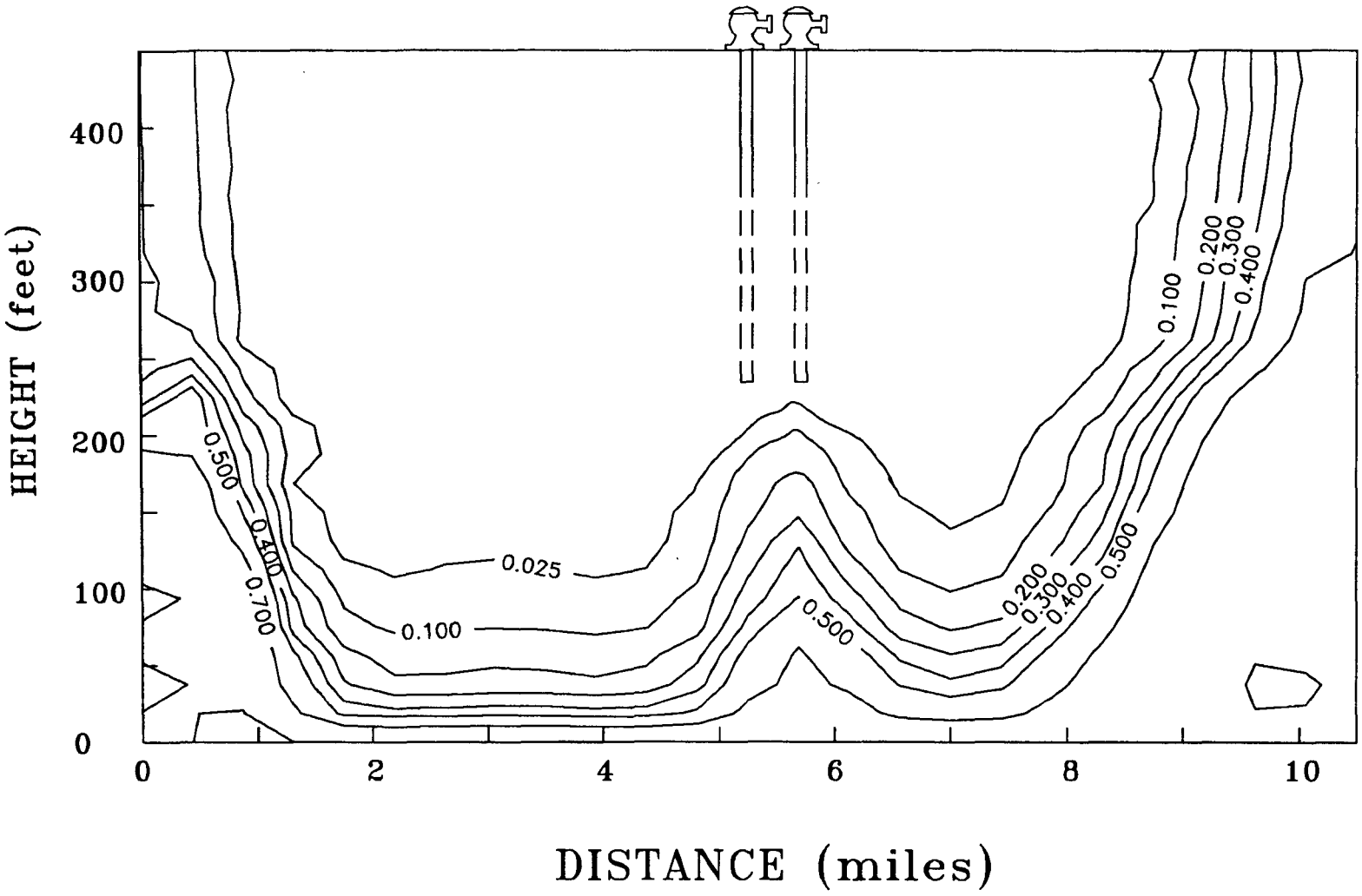

Figure 9.9. Relative concentration of chloride through A-A′ after 50 years of pumping 2.5 Mgal/d from deep wells at the center of the lens [case 2, Table 9.1].

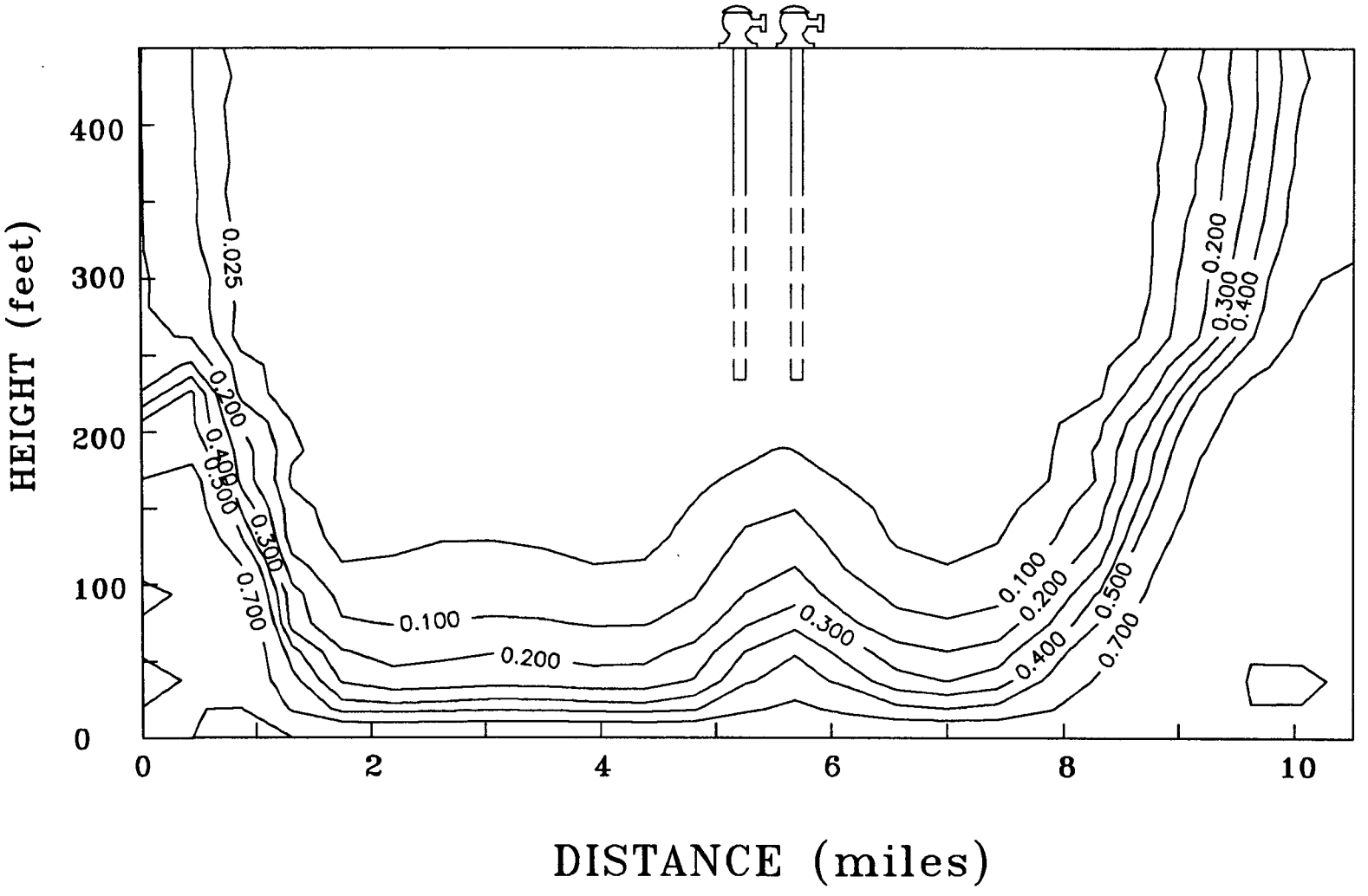

Figure 9.10. Relative concentration of chloride through A-A' after 25 years of pumping 2.5 Mgal/d from deep wells at the center of the lens [case 2, Table 9.1].

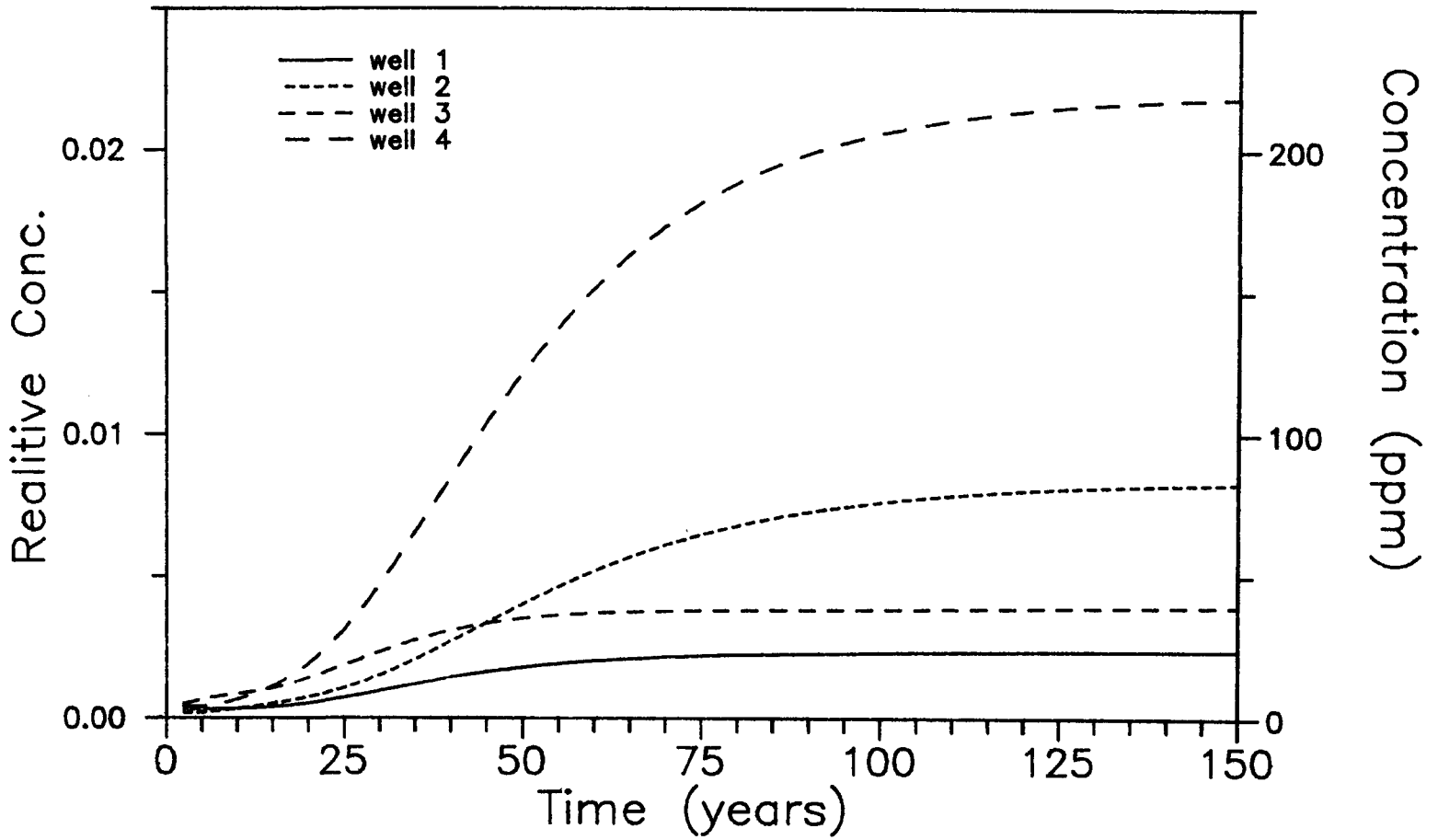

Figure 9.11. Breakthrough curves at the bottom of pumping wells, for a total withdrawal of 2.5 Mgal/d from deep wells at the center of the lens [case 2, Table 9.1].

wells are, however shallow for this simulation, screened from 80 ft to 141 ft below the top of the upper Floridan aquifer. The movement of chloride was essentially the same as that of the previous simulation, where the wells pumped deeper, over a larger screen interval. The depth of pumping therefore seems to have a negligible effect on chloride distributions for this pumping case, as long as pumping is from the freshwater.

The next pumping scenario was a steady-state scenario with deep wells at the same location pumping a total rate of 0.5 Mgal/d. The steady-state chloride distribution in section A-A′ is shown in Figure 9.12. The lens was only slightly affected by this withdrawal. Upconing of chloride from the bottom did not occur. The final steady-state areal distributions on top of the upper Floridan, a perspective view of the freshwater lens, and the vertical profiles through the mid-section A-A′ for a pumping rate of 3.75 Mgal/d from the same well field are shown in Figures 9.13a, 9.13b and 9.14 respectively. Upconing and lateral intrusion of saltwater towards the wells is seen to occur. Shown in Figures 9.15 and 9.16 are the areal chloride distribution at the surface, and the vertical section through A-A′ respectively, for a steady-state pumping rate of 5 Mgal/d. Long term high pumping effects are seen to be detrimental to the lens.

The next set of pumping scenarios considers the effects of large-scale withdrawals from a hypothetical well field located just east of the existing Lake Harney Water Assoc. well field, near the fringe of the lens. This well field consists of 4 wells located at

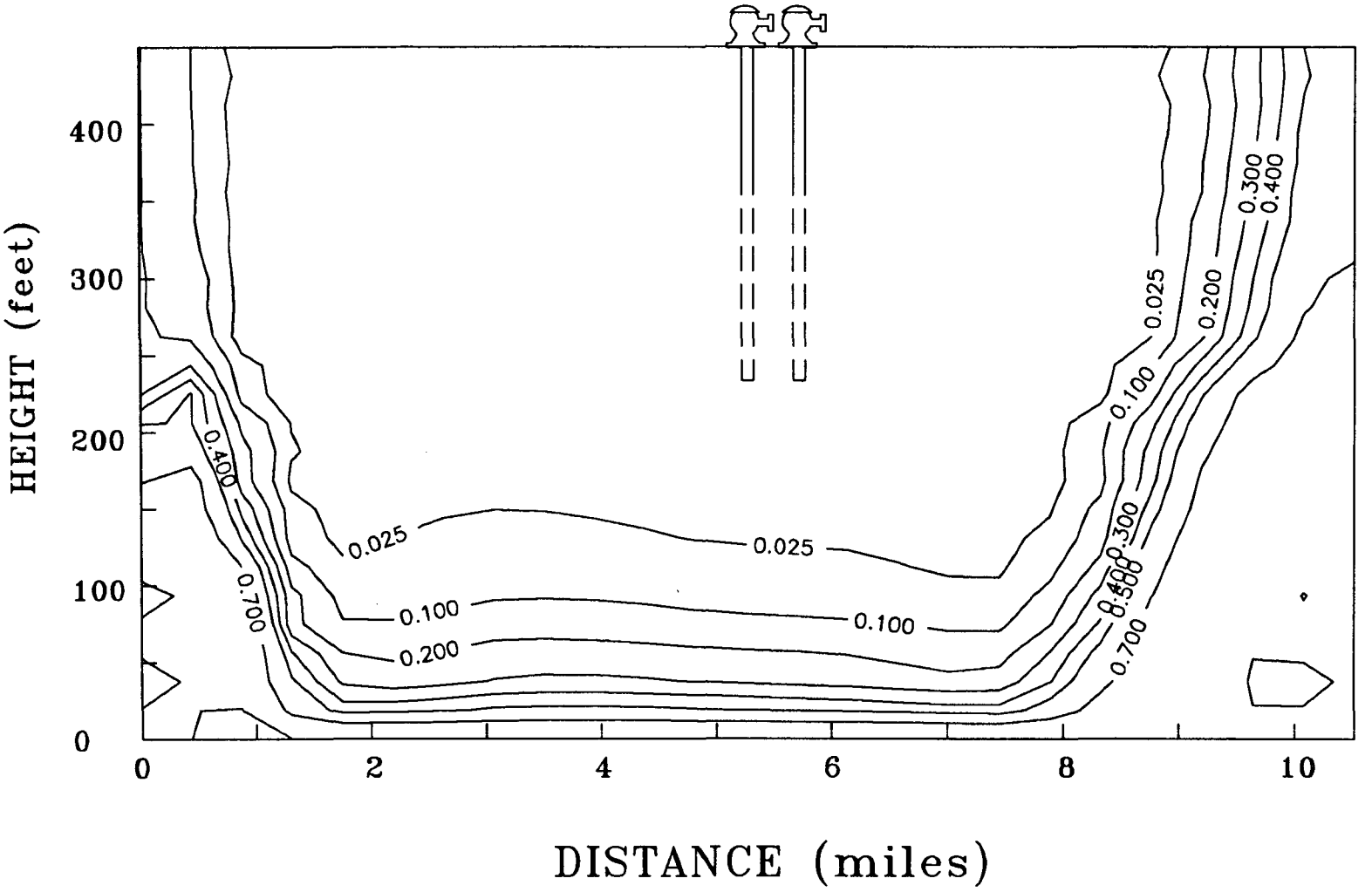

Figure 9.12. Relative concentration of chloride through A-A′ for a steady-state pumping of 0.5 Mgal/d from deep wells at the center of the lens.

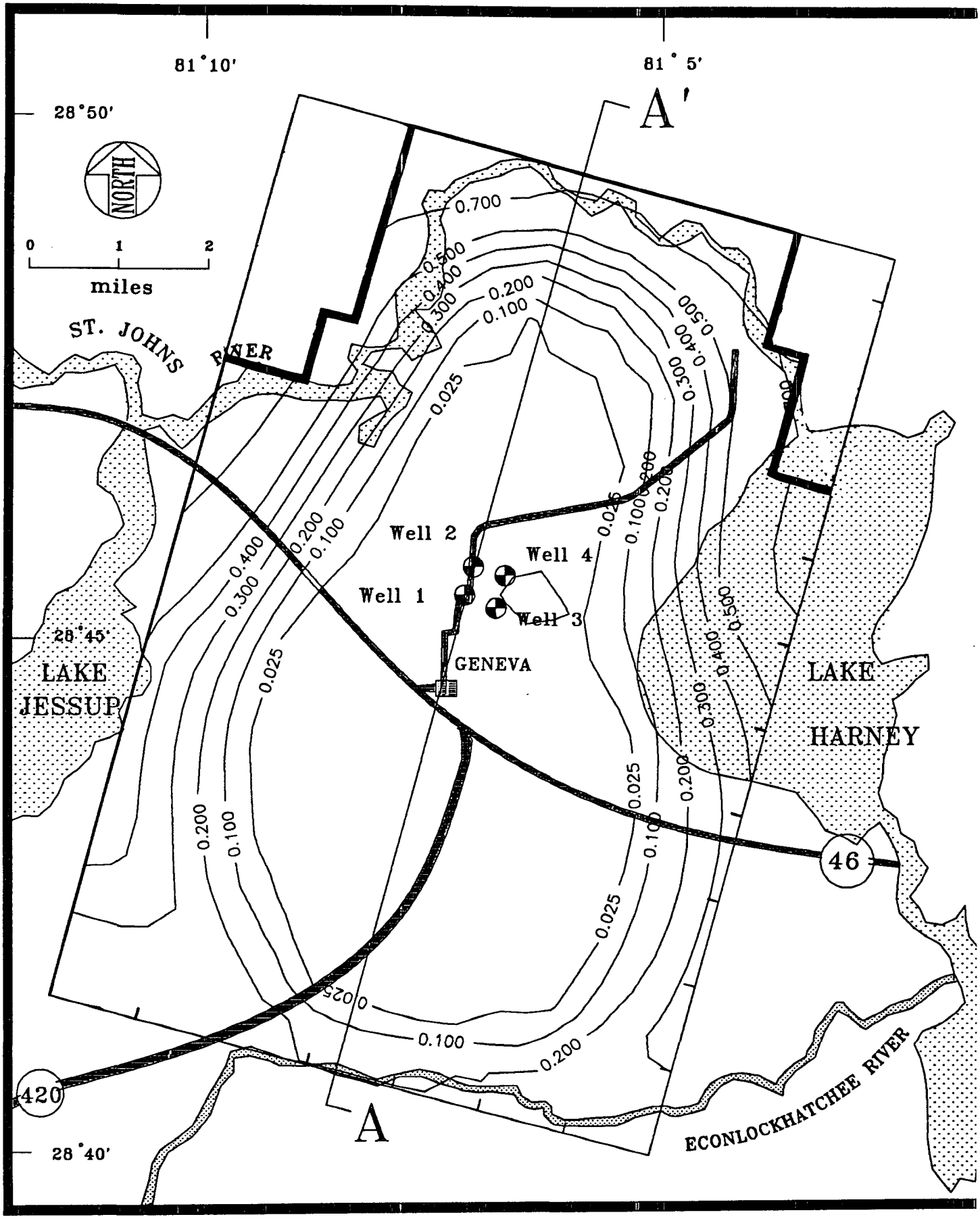

Figure 9.13a. Areal distribution of chloride for a steady-state pumping of 3.75 Mgal/d from deep wells at the center of the lens.

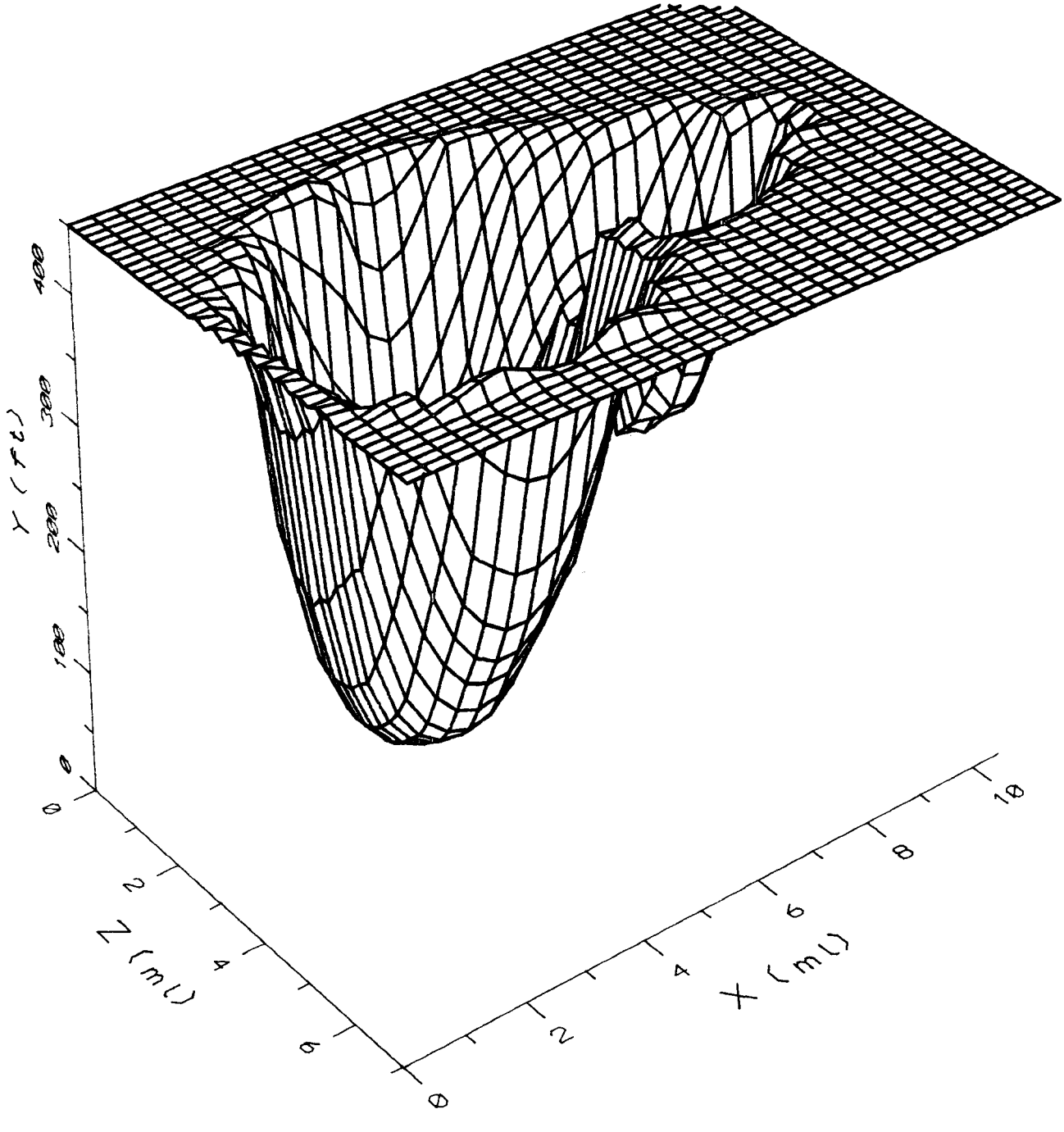

Figure 9.13b. Perspective view of freshwater lens for a steady-state pumping of 3.75 Mgal/d from deep wells near the center of the lens.

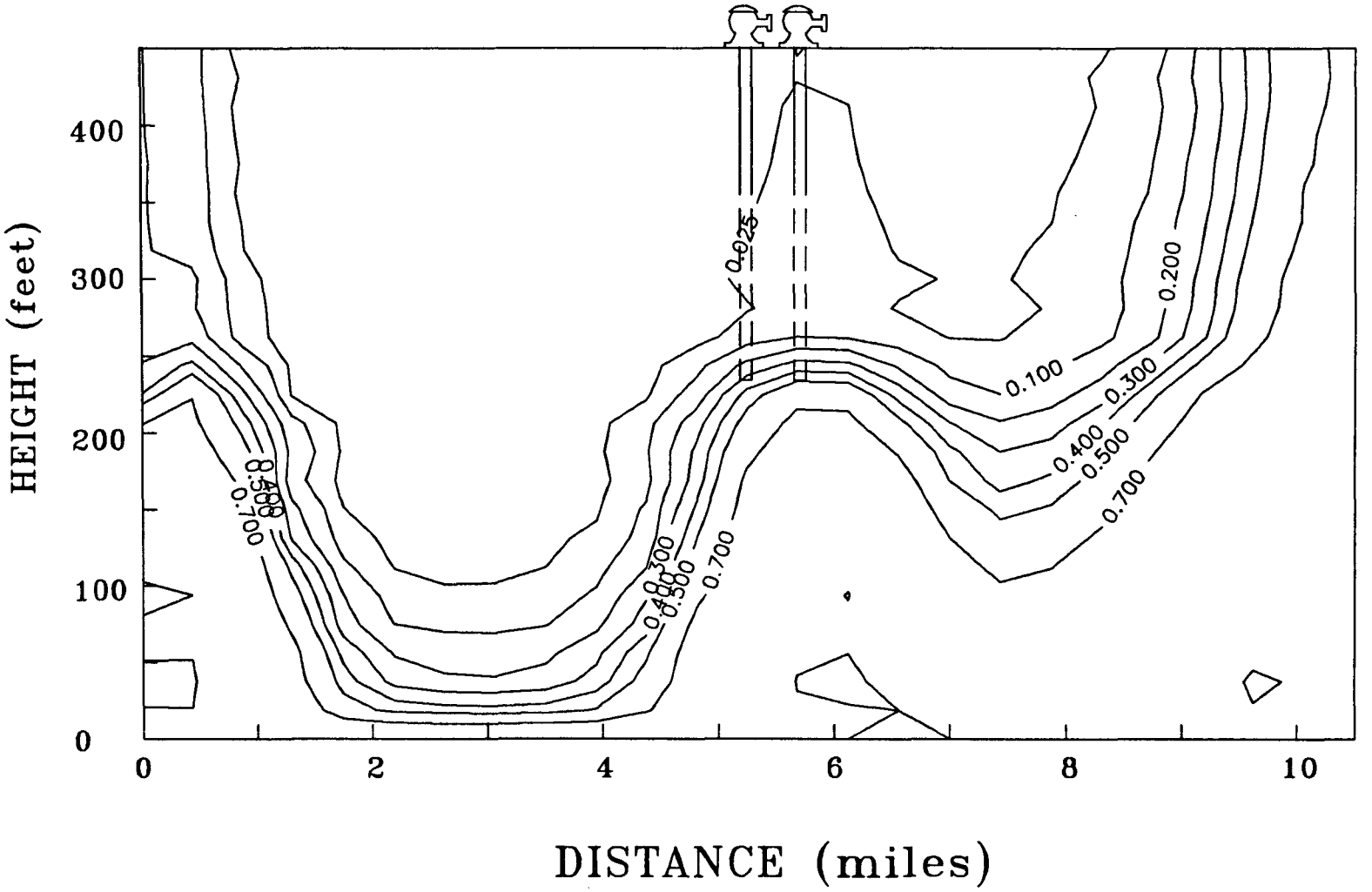

Figure 9.14. Relative concentration of chloride through A-A′ for a steady-state pumping of 3.75 Mgal/d from deep wells at the center of the lens.

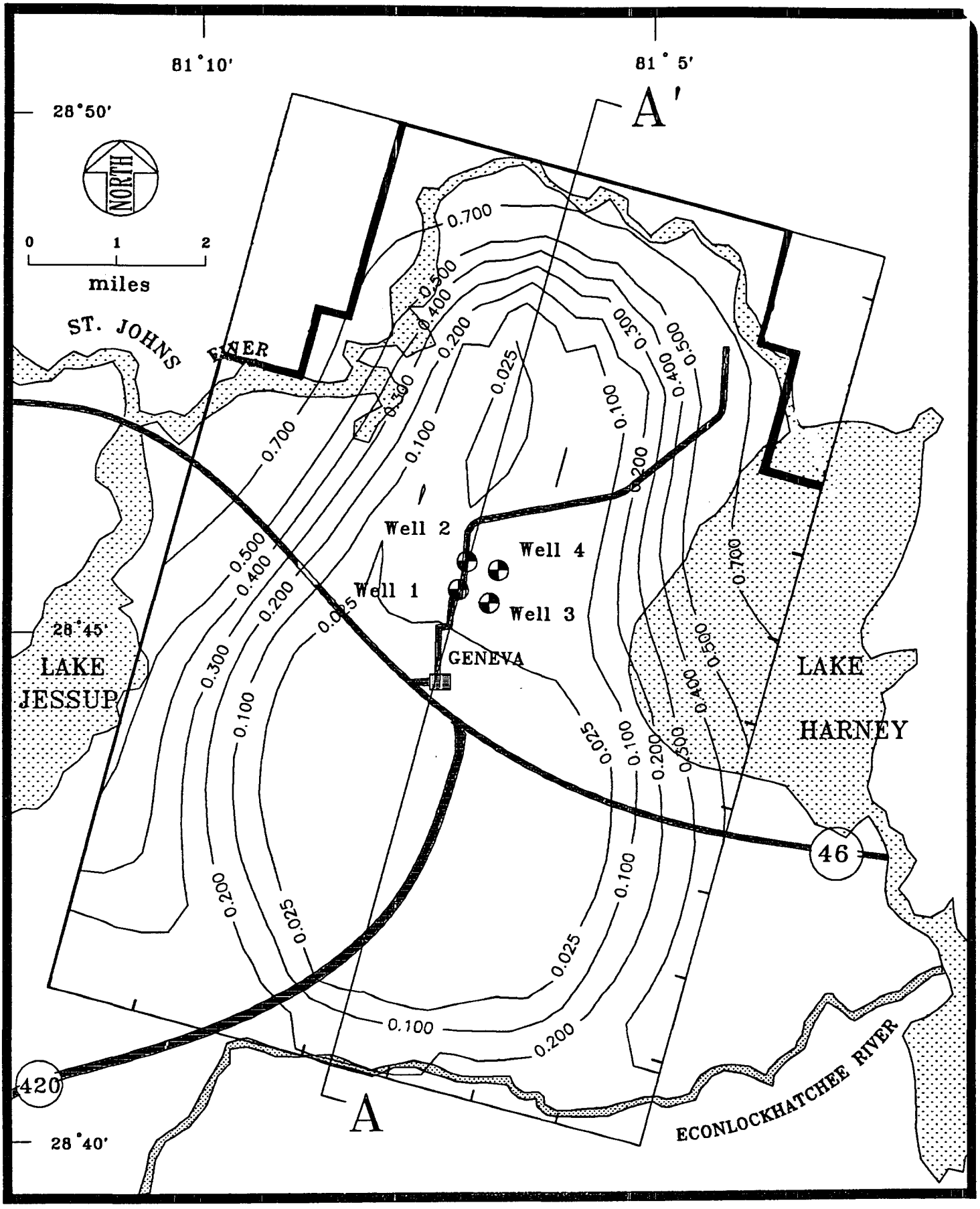

Figure 9.15. Areal distribution of chloride for a steady-state pumping of 5 Mgal/d from deep wells at the center of the lens.

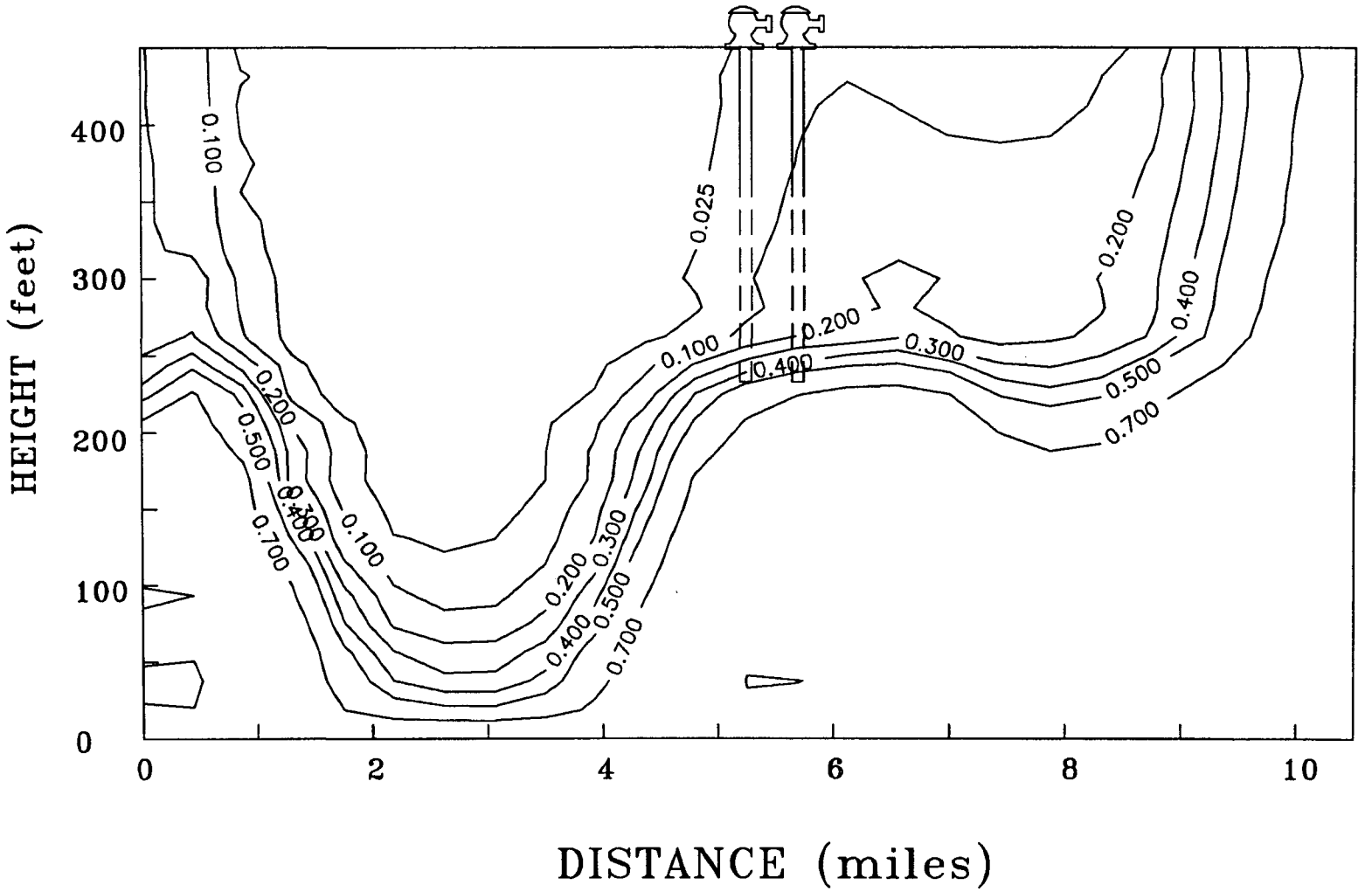

Figure 9.16. Relative concentration of chloride through A-A′ for a steady-state pumping of 5 Mgal/d from deep wells at the center of the lens.

x = 3.41 mi, and 3.79 mi, and z = 5.52, and 5.89 mi. Both deep and shallow pumping scenarios were considered. The first case studied considers a deep well screened from 80 ft to 210 ft below the top of the upper Floridan. A total pumping rate of 2.5 Mgal/d is applied at the well field. The areal distribution of chloride at 25, 50 and 150 years are shown in Figures 9.17, 9.18 and 9.19, respectively. Comparing these with the no pumping steady-state lens of Figure 8.17, it can be seen that pumping has led to a decrease in the lens size by approximately half a mile from the Lake Harney edge of the domain after 25 years. The areal change of lens size during the time period 25 to 150 years is small. Figures 9.20, 9.21 and 9.22 show the vertical chloride distributions for section B-B′ at 25, 50 and 150 years, respectively. Comparing these with the no-pumping steady-state chloride distributions of Figure 8.21 for that section, it may be noted that over the first 25 years of continuous pumping, the thickness of the lens has decreased substantially. This is due to lateral intrusion of chloride from the Lake Harney edge of the lens. From 25 years to 150 years, the depth of the lens decreases only slightly. Figure 9.23 shows breakthrough curves for the 4 wells. Chloride concentrations in wells 1 and 2 (located at z = 5.52 mi) have reached the 250 ppm level within 10 years of pumping. Wells 3 and 4 located at z = 5.89 mi are closer to the edge of the lens and become contaminated within one year. Steady-state for the system has been reached by 150 years. A steady-state simulation for pumping 2.5 Mgal/d at the same well field location, from shallow

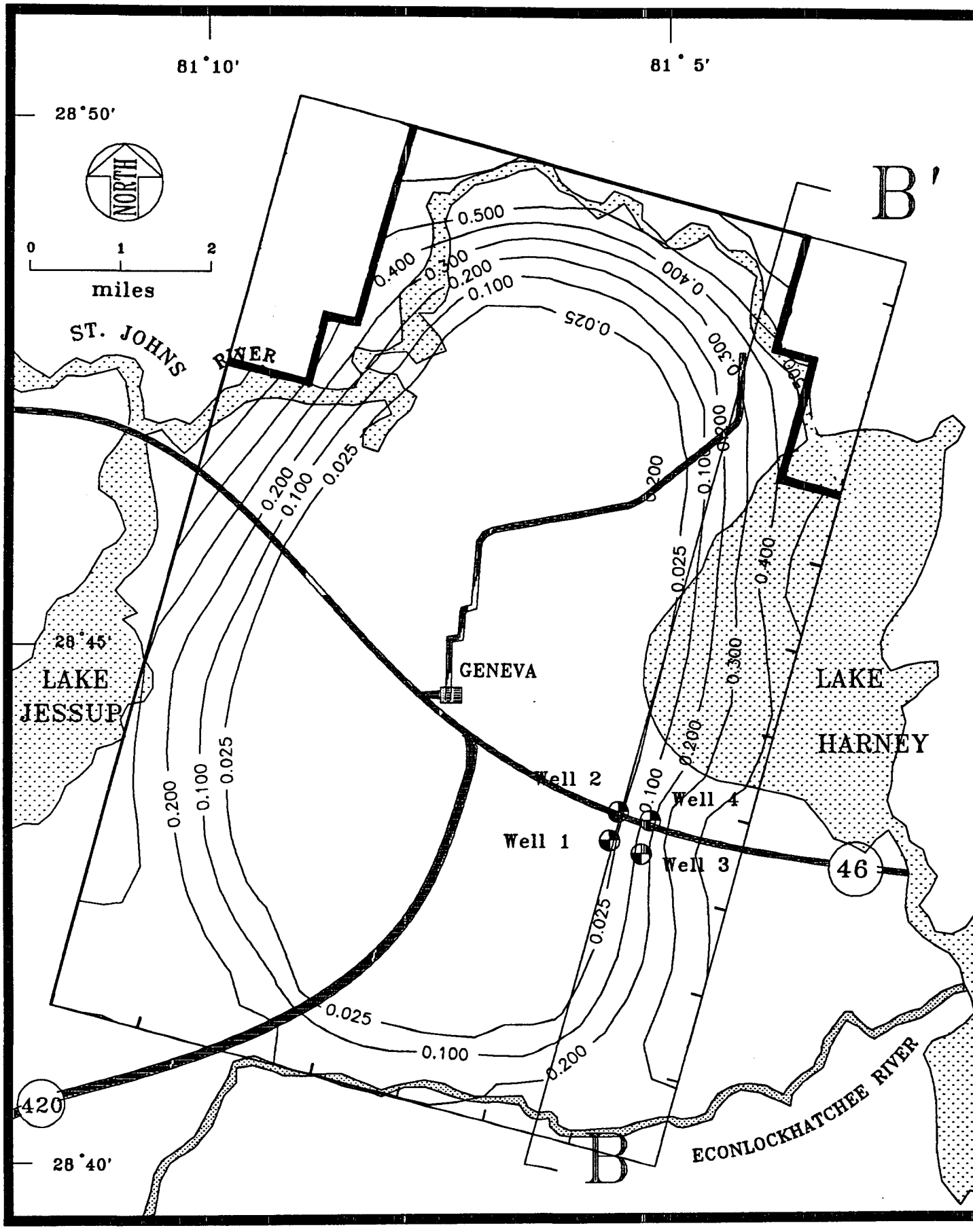

Figure 9.17. Areal distribution of chloride after 25 years of pumping 2.5 Mgal/d from deep wells at Lake Harney edge of the lens [case 3, Table 9.1].

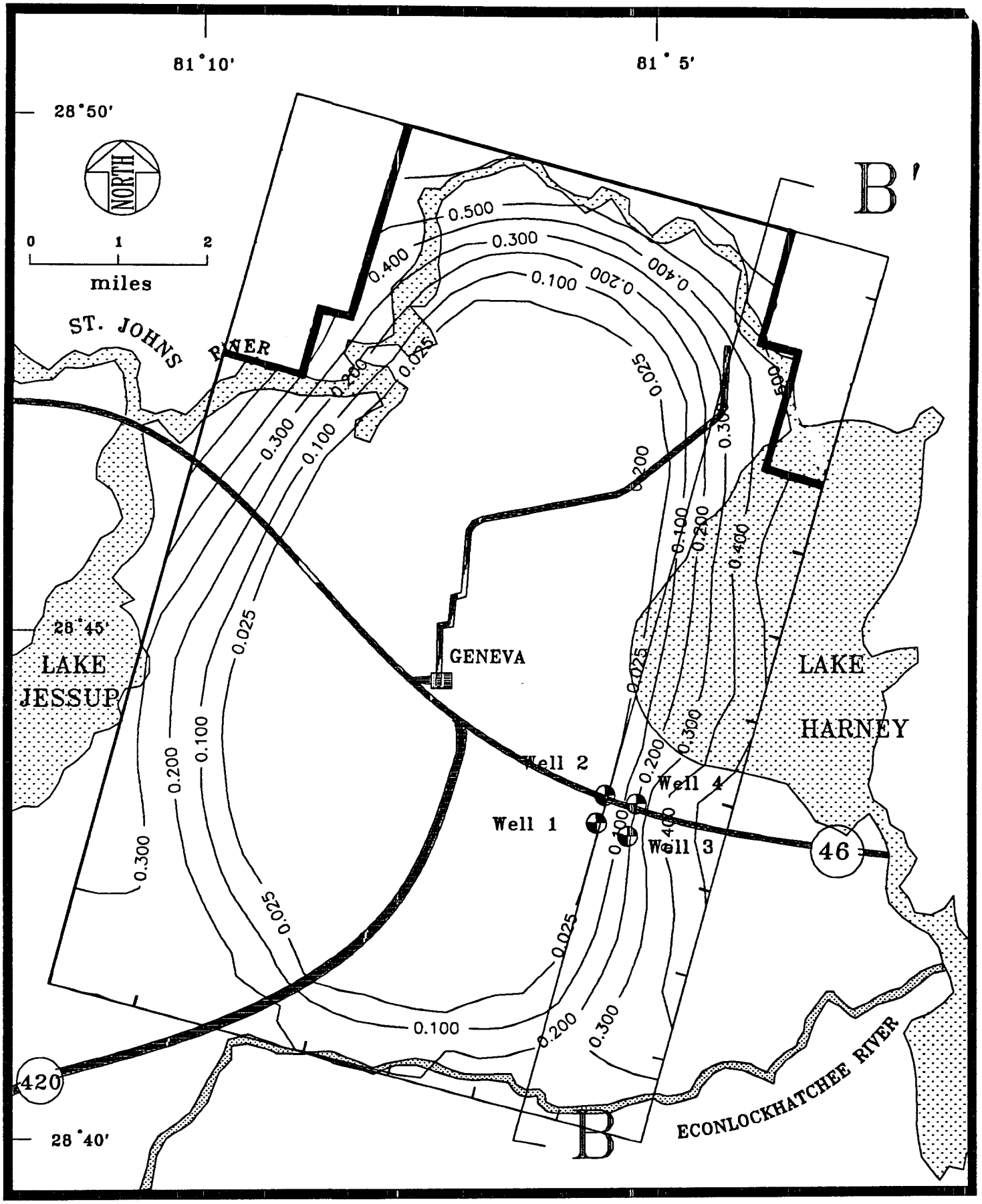

Figure 9.18. Areal distribution of chloride after 50 years of pumping 2.5 Mgal/d from deep wells at Lake Harney edge of the lens [case 3, Table 9.1].

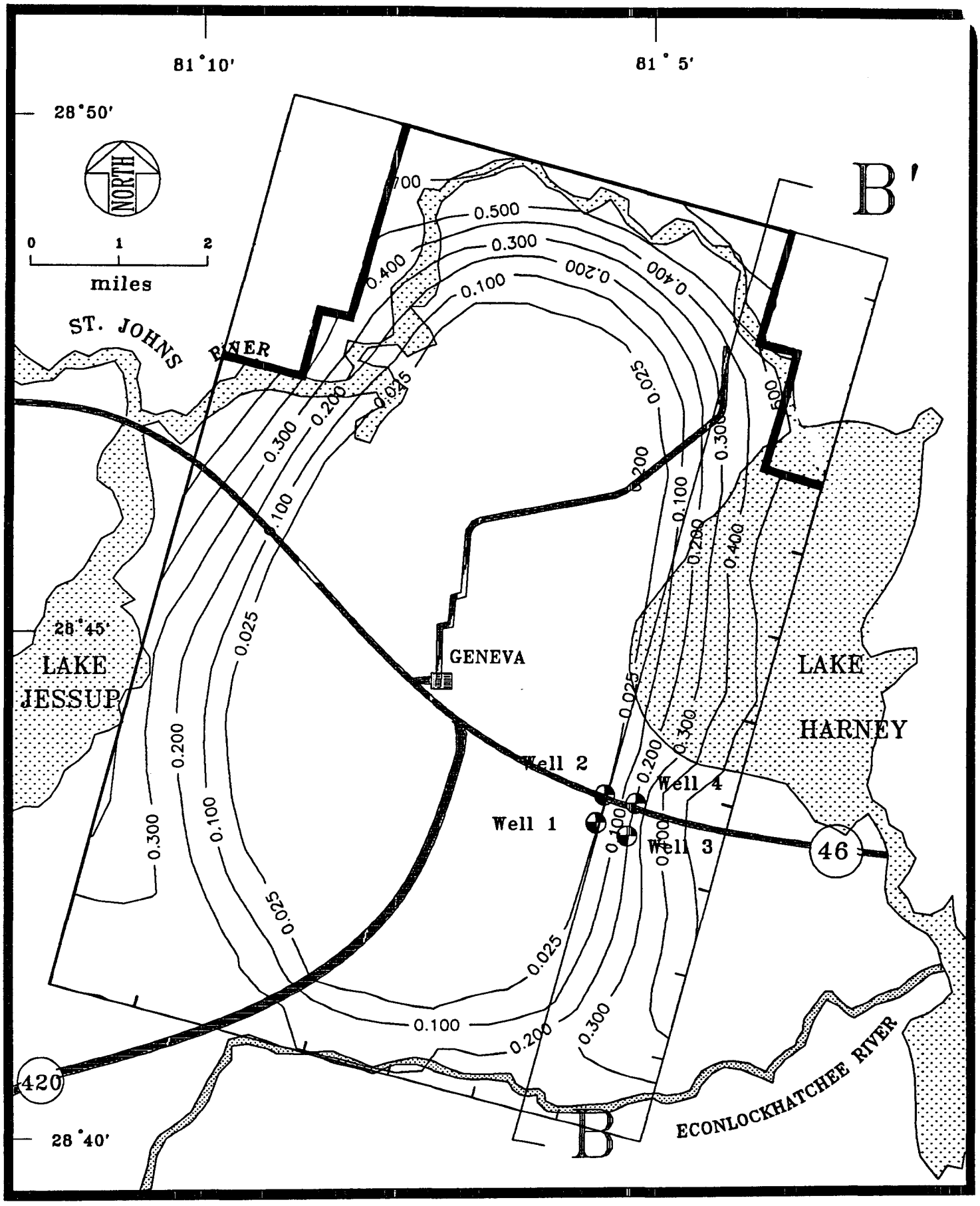

Figure 9.19. Areal distribution of chloride after 150 years of pumping 2.5 Mgal/d from deep wells at Lake Harney edge of the lens [case 3, Table 9.1].

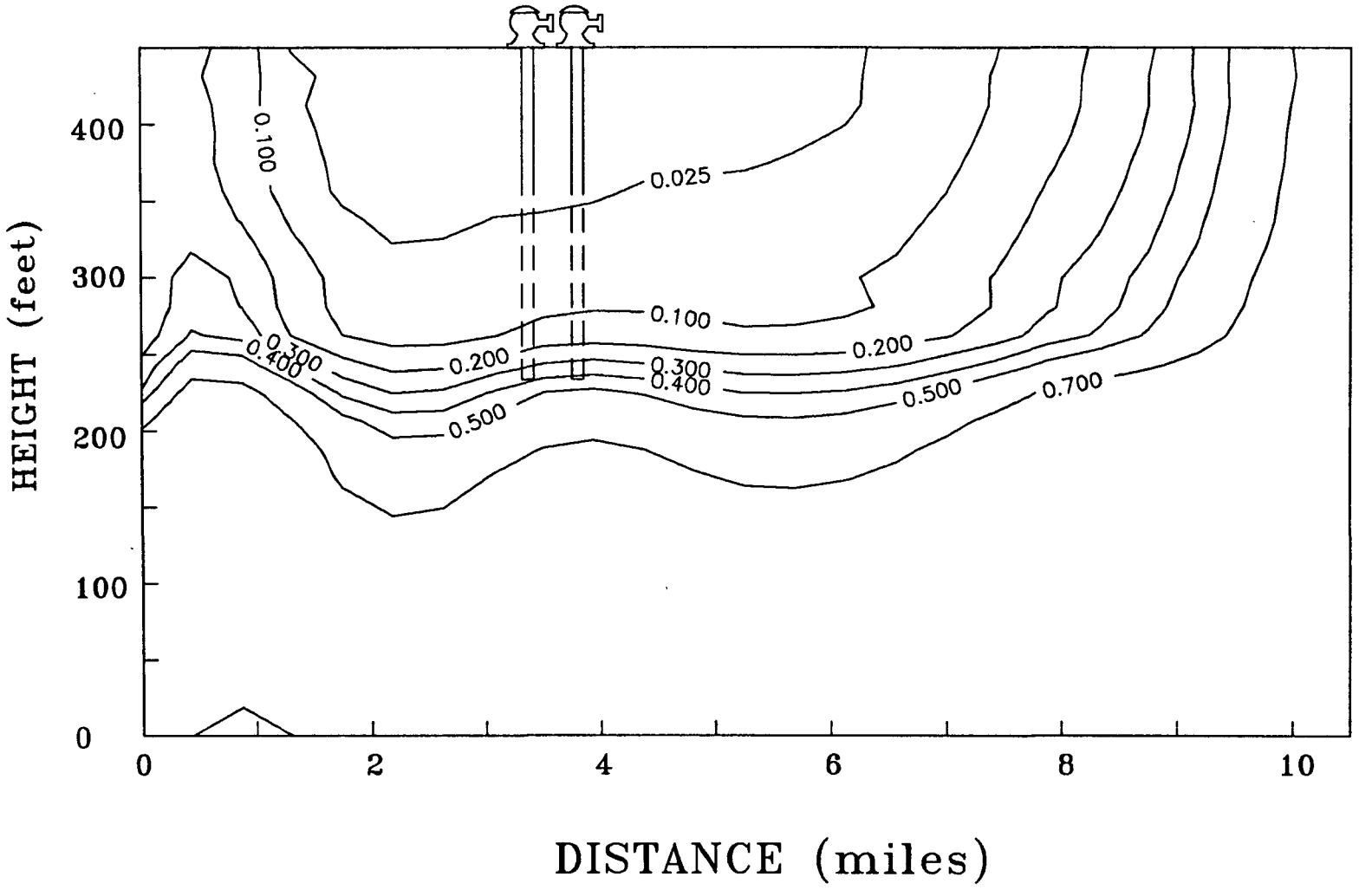

Figure 9.20. Relative concentration of chloride through B-B′ after 25 years of pumping 2.5 Mgal/d from deep wells at the Lake Harney edge of the lens [case 3, Table 9.1].

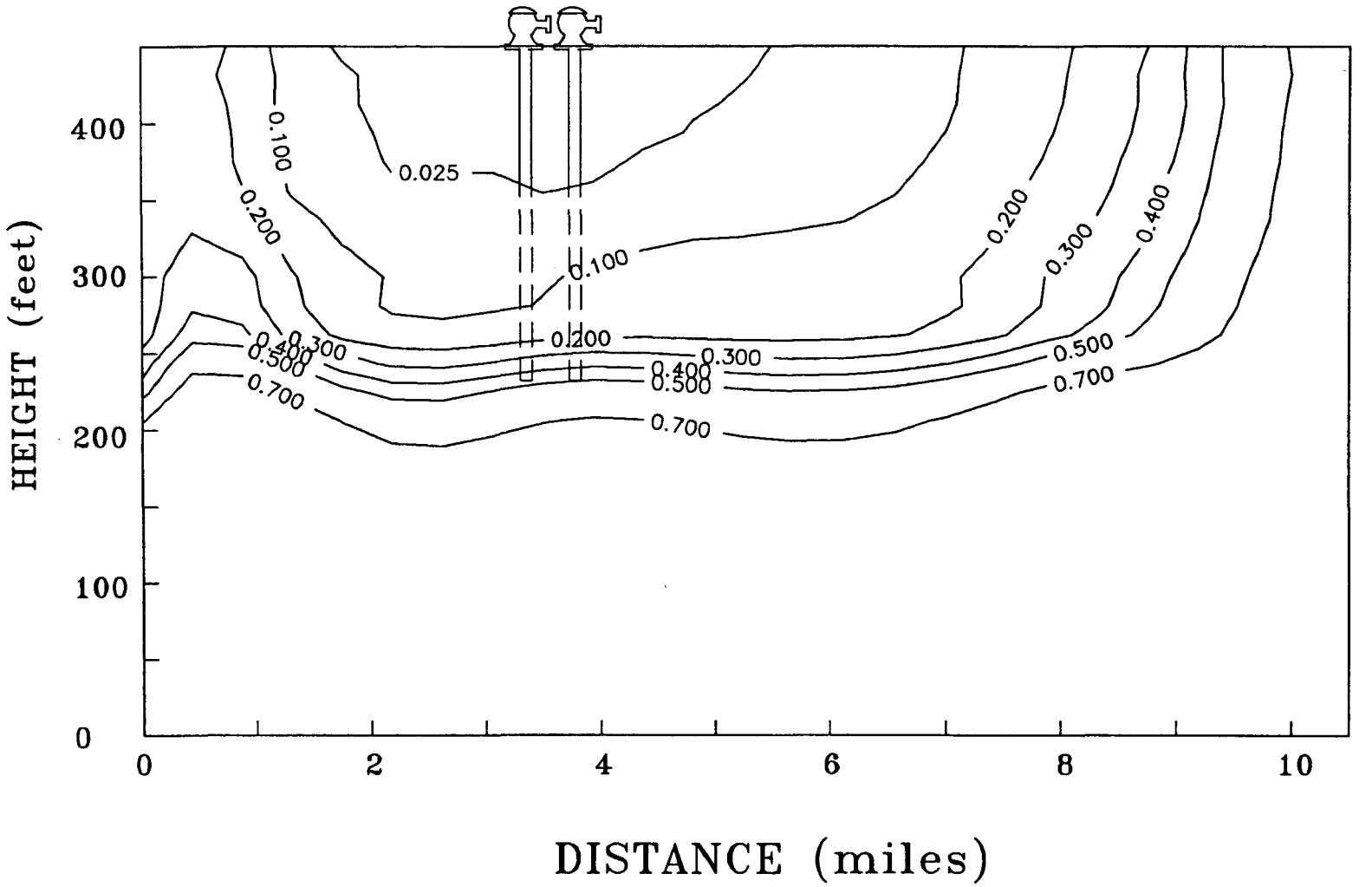

Figure 9.21. Relative concentration of chloride through B-B′ after 50 years of pumping 2.5 Mgal/d from deep wells at the Lake Harney edge of the lens [case 3, Table 9.1].

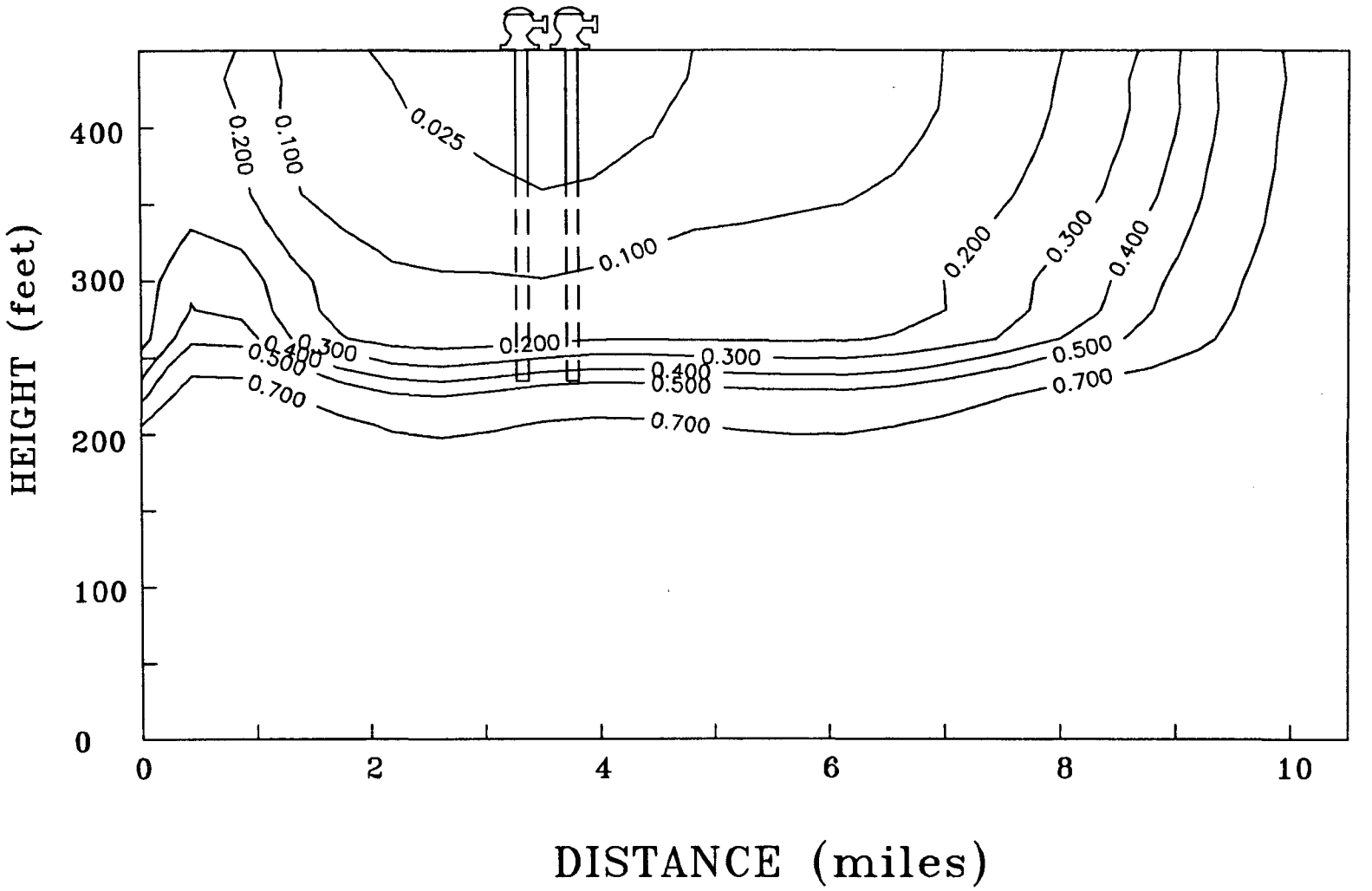

Figure 9.22. Relative concentration of chloride through B-B′ after 150 years of pumping 2.5 Mgal/d from deep wells at the Lake Harney edge of the lens [case 3, Table 9.1].

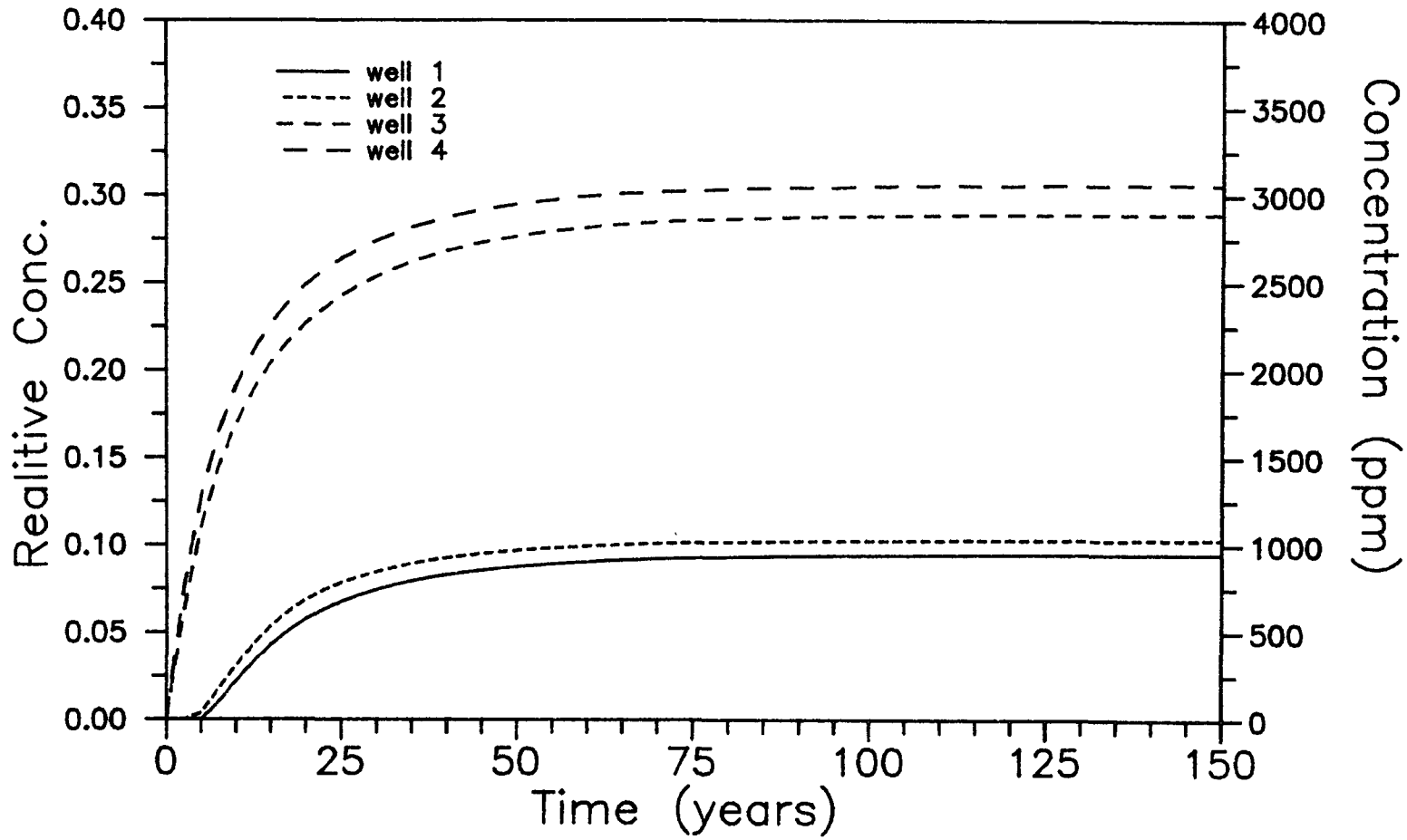

Figure 9.23. Breakthrough curves at bottom of pumping wells for a total withdrawal of 2.5 Mgal/d from deep wells at the Lake Harney edge of the lens [case 3, Table 9.1].

wells with an open hole interval from a depth of 80 ft to 141 ft below the top of the upper Floridan, produces an identical lens to the case of pumping from an open hole depth of 80 ft to 210 ft, with similar convergence characteristics. Depth of pumping therefore, seems to be an insignificant factor on the shape of the lens, for this case.

The next pumping scenario considers withdrawals of 0.5 Mgal/d from the well field at the Lake Harney edge of the lens. The wells are screened from 80 ft to 210 ft below the top of the upper Floridan aquifer. The areal distribution of chloride at the top of the upper Floridan, and the vertical chloride distribution through B-B′ are shown in Figures 9.24 and 9.25 respectively after 25 years of simulation, and Figures 9.26 and 9.27 after 150 years of simulation. The lens is seen to intrude laterally from the Lake Harney edge by about half a mile. This intrusion occurs within the first few years of simulation. Between 25 years and 150 years, the change of the lens profile (areally as well as vertically) is small. Figure 9.28 shows the breakthrough curves at the four wells. The average chloride concentration of the entire screened length of the well is depicted in this figure. Wells 1 and 2 remain uncontaminated throughout the simulation. Wells 3 and 4 get contaminated rapidly; the 250-ppm chloride intrusion occurs within 8 years. Pumping at a shallower depth does not affect the lens profile, as was seen from a steady-state analysis of the same scenario pumping from screened depths of 80 to 141 ft below the top of the upper Floridan. The areal and vertical chloride

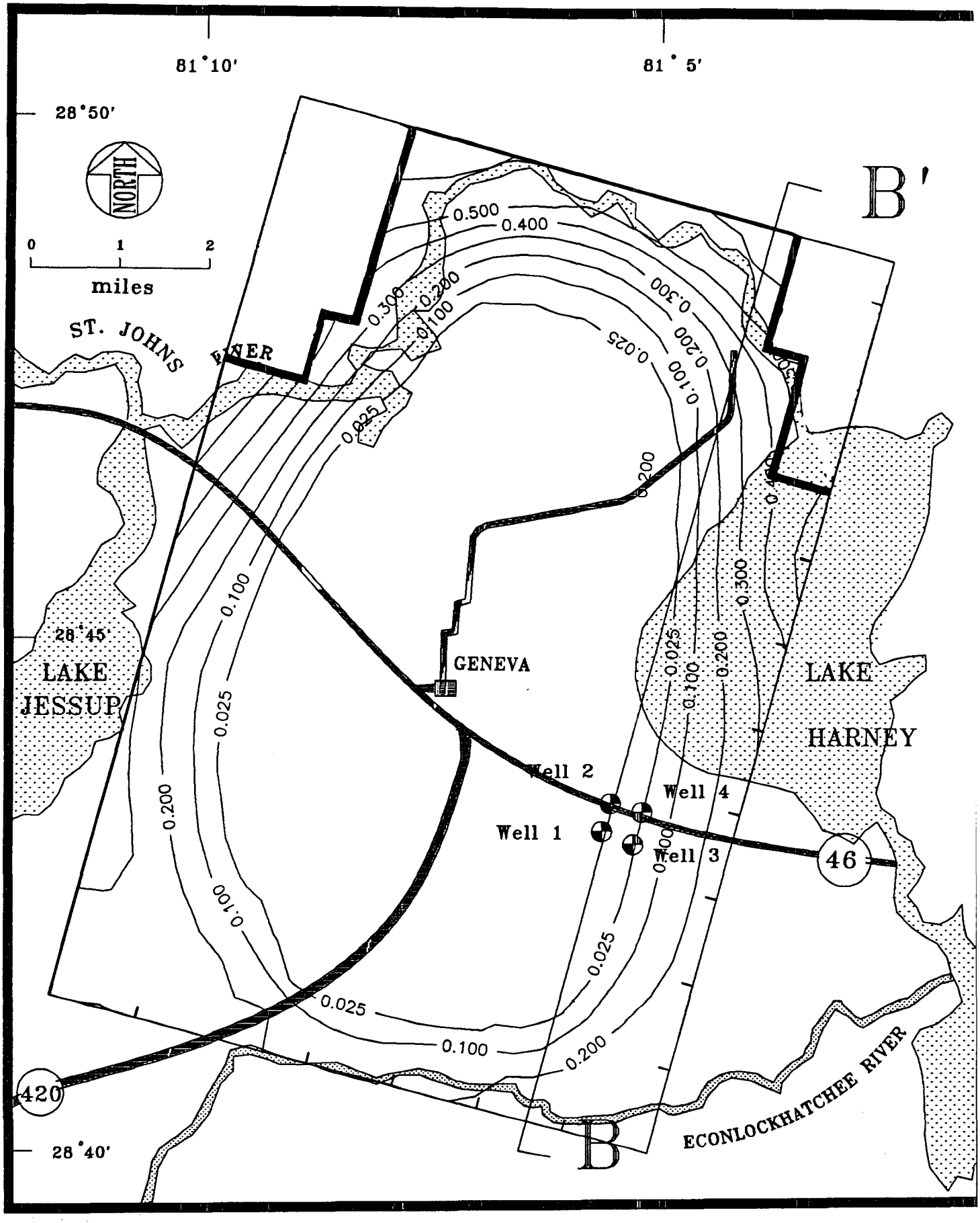

Figure 9.24. Areal distribution of chloride after 25 years of pumping 0.5 Mgal/d from deep wells at Lake Harney edge of the lens [case 4, Table 9.1].

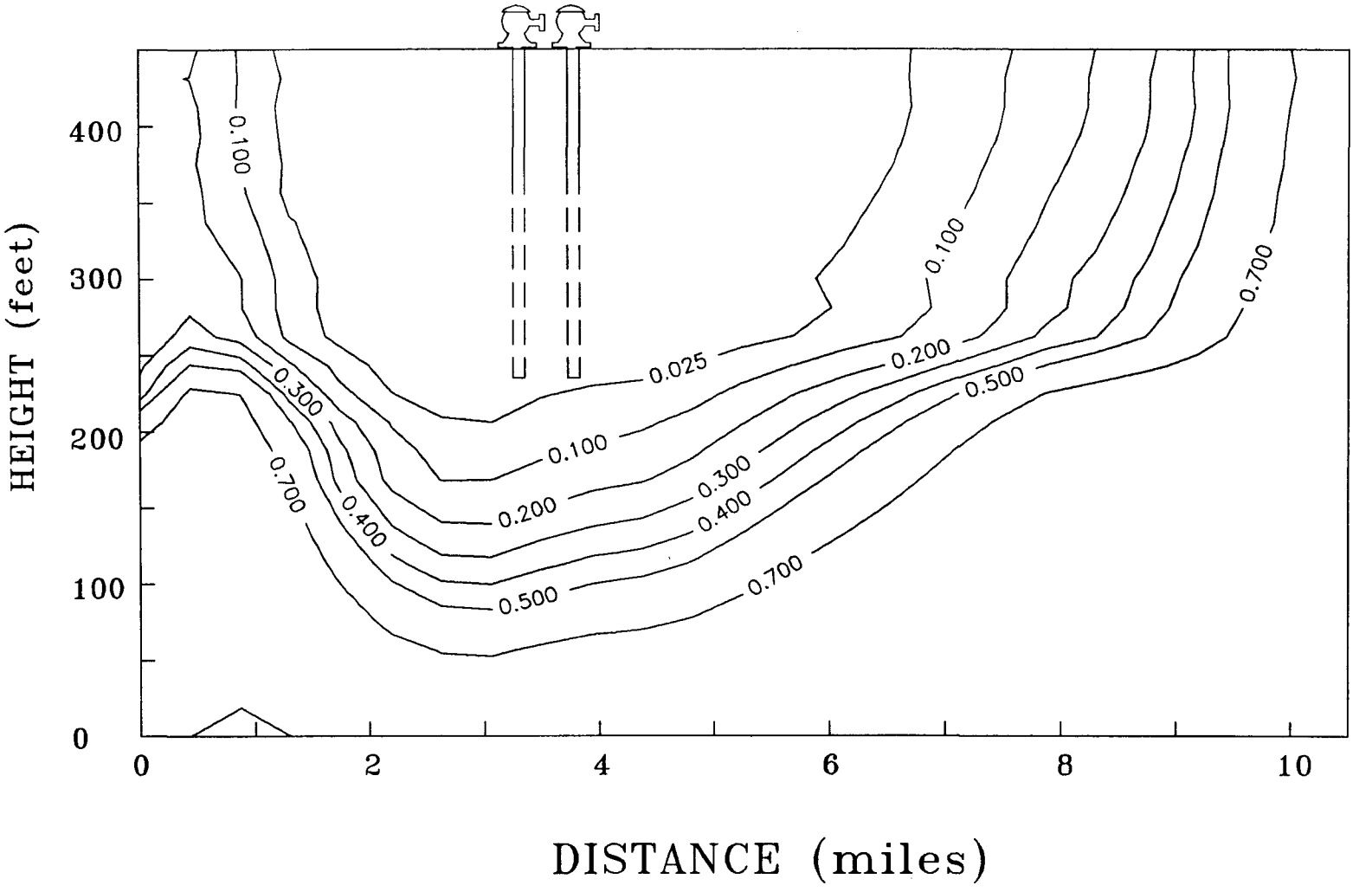

Figure 9.25. Relative concentration of chloride through B-B′ after 25 year of pumping 0.5 Mgal/d from deep wells at the Lake Harney edge of the lens [case 4, Table 9.1].

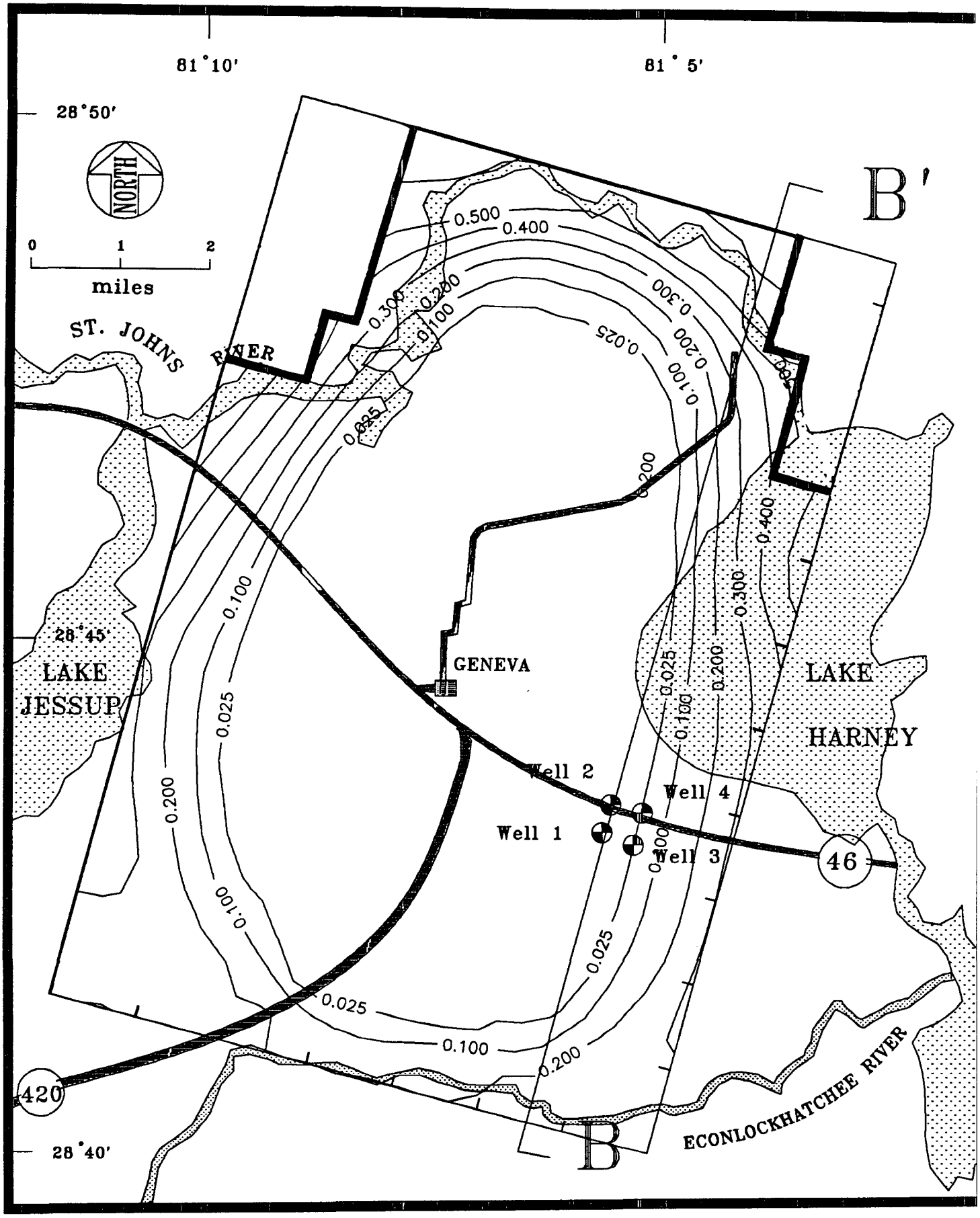

Figure 9.26. Areal distribution of chloride after 150 years of pumping 0.5 Mgal/d from deep wells at the Lake Harney edge of the lens [case 4, Table 9.1].

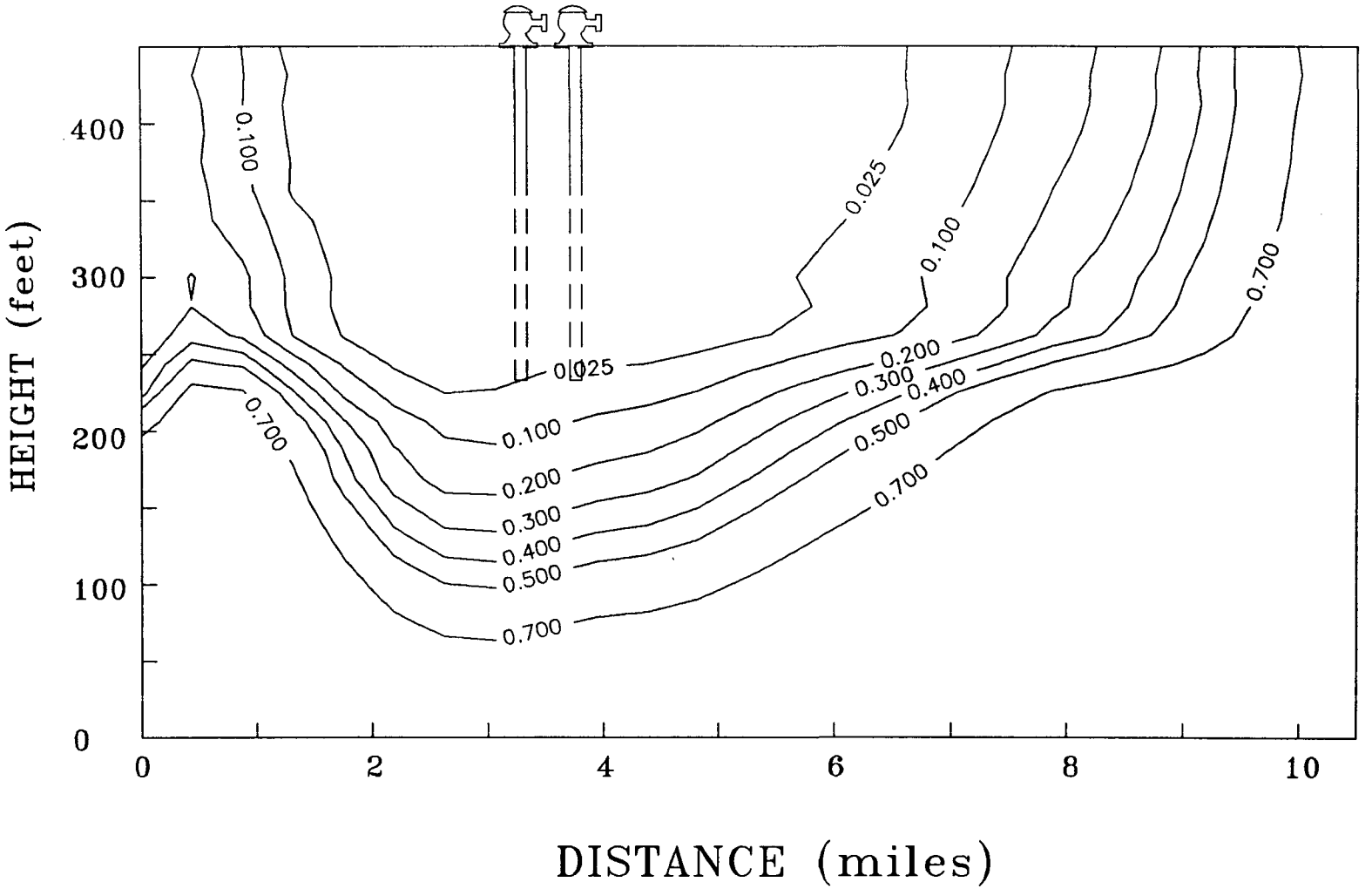

Figure 9.27. Relative concentration of chloride through B-B′ after 150 years of pumping 0.5 Mgal/d from deep wells at Lake Harney edge of lens [case 4, Table 9.1].

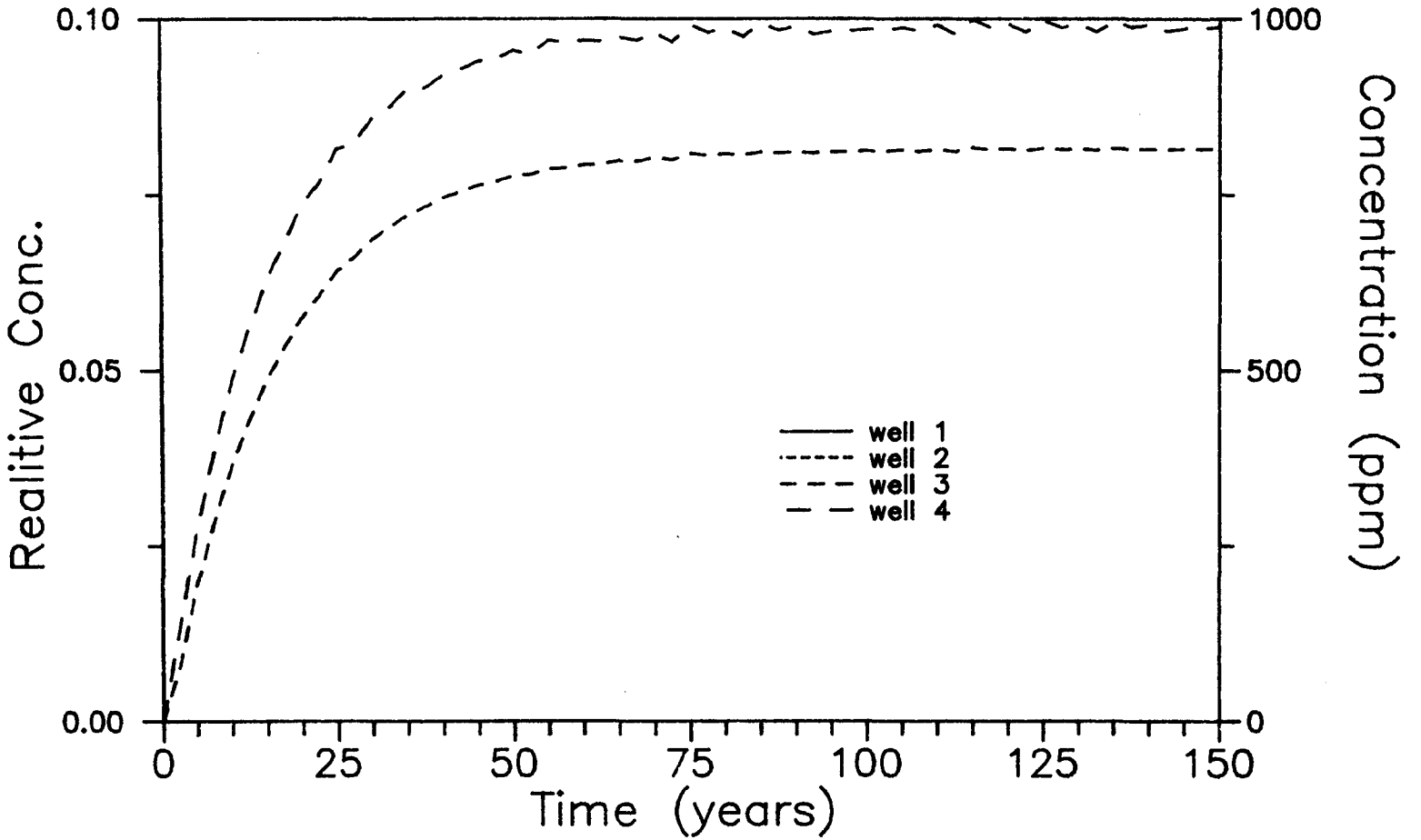

Figure 9.28. Breakthrough curve at the pumping wells for a total withdrawal rate of 0.5 Mgal/d from deep wells at the Lake Harney edge of the lens [case 4, Table 9.1].

distributions for this steady-state scenario are shown in Figures 9.29 and 9.30, respectively.

The next scenario considers pumping 0.5 Mgal/d from only two wells located near the Lake Harney edge of the domain. The wells are situated at x = 3.41 mi, and x = 3.79 mi, in the cross-sectional plane B-B′ (i.e., at z = 5.52 mi). The steady-state areal chloride distribution at the top of the upper Floridan aquifer is shown in Figure 9.31, and a vertical chloride distribution in section B-B′ is shown in Figure 9.32. The intrusion of the lens is similar to the case of four wells pumping 0.5 Mgal/d (see Figures 9.26 and 9.27). However, none of the wells are contaminated for this case.

The next pumping scenario was performed to estimate the effects of dispersed domestic well withdrawals on the lens. The area considered for "Suburban Estates" is pumped at 375 gal/d per acre, from depths of 17 ft to 50 ft below the top of the upper Floridan aquifer. "Suburban Estates" is a zoning classification requiring one household per acre. The total area of dispersed withdrawals is shown in Figure 9.33, and comprises approximately 15,000 acres. Approximately 11,000 acres (or 75%) of this area is composed of "Suburban Estates", the rest is zoned as conservation land. Withdrawals of 8.63×10^{-4} ft/d (375 gal/d/acre) are hence prescribed over this area. The total withdrawal from the lens is 4.2 Mgal/d. A transient analysis was performed for up to 150 years. The areal distributions of chloride at the top of the upper Floridan at 25 years, 50 years and 150 years are shown in Figures

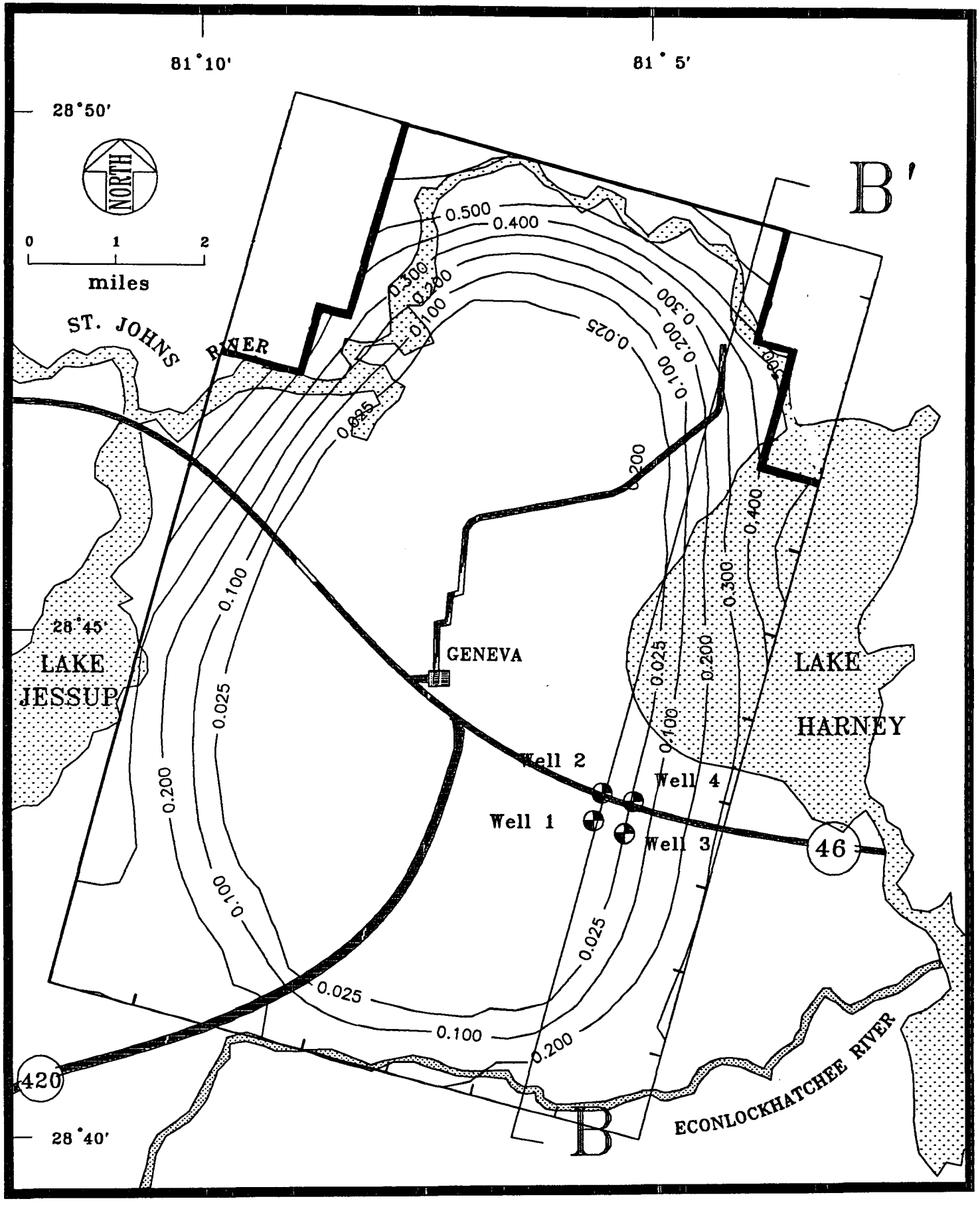

Figure 9.29. Areal distribution of chloride for steady-state withdrawals of 0.5 Mgal/d from shallow wells at the Lake Harney edge of the lens.

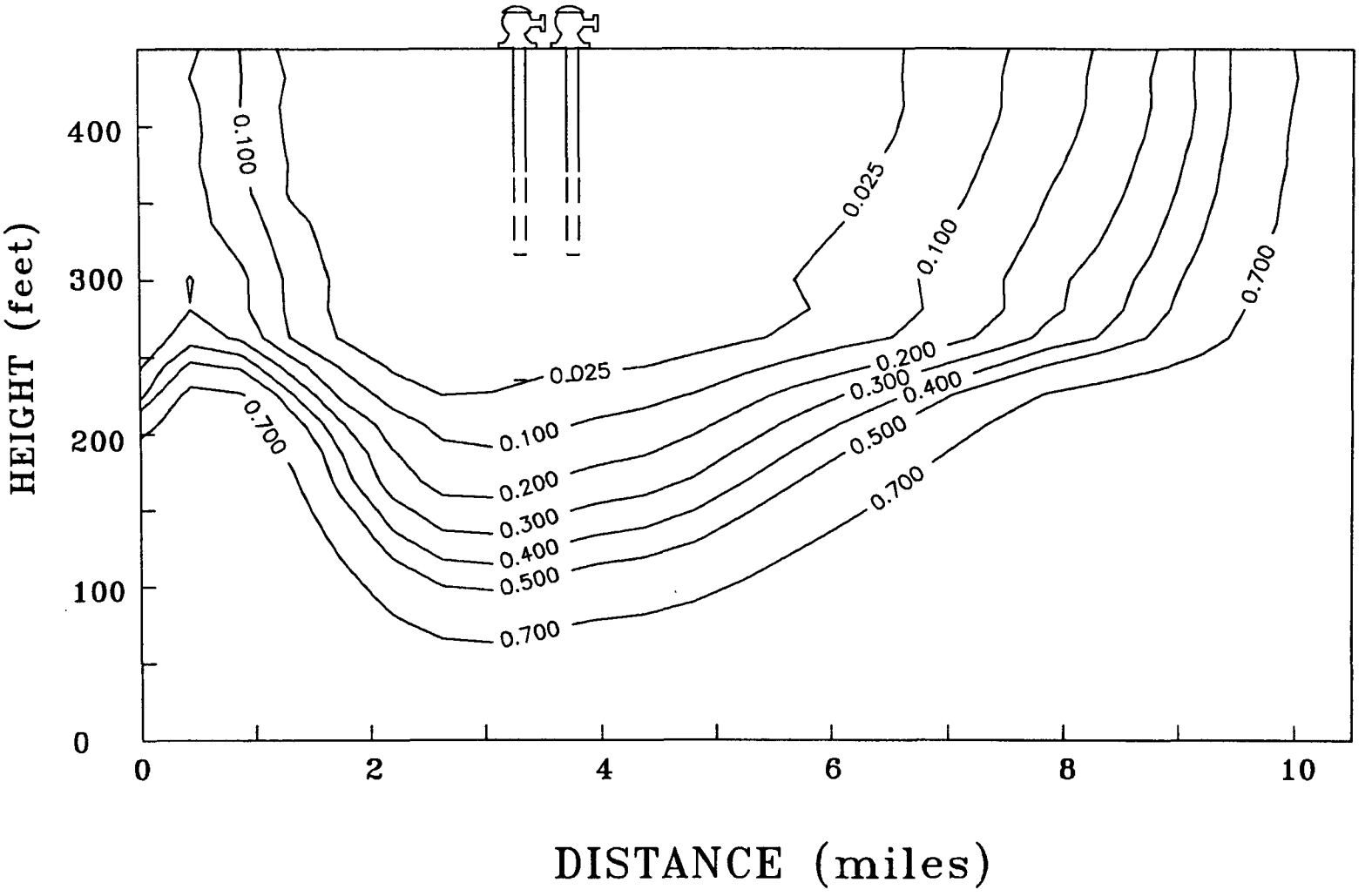

Figure 9.30. Relative concentration of chloride through B-B′ for steady-state withdrawals of 0.5 Mgal/d from shallow wells at the Lake Harney edge of the lens.

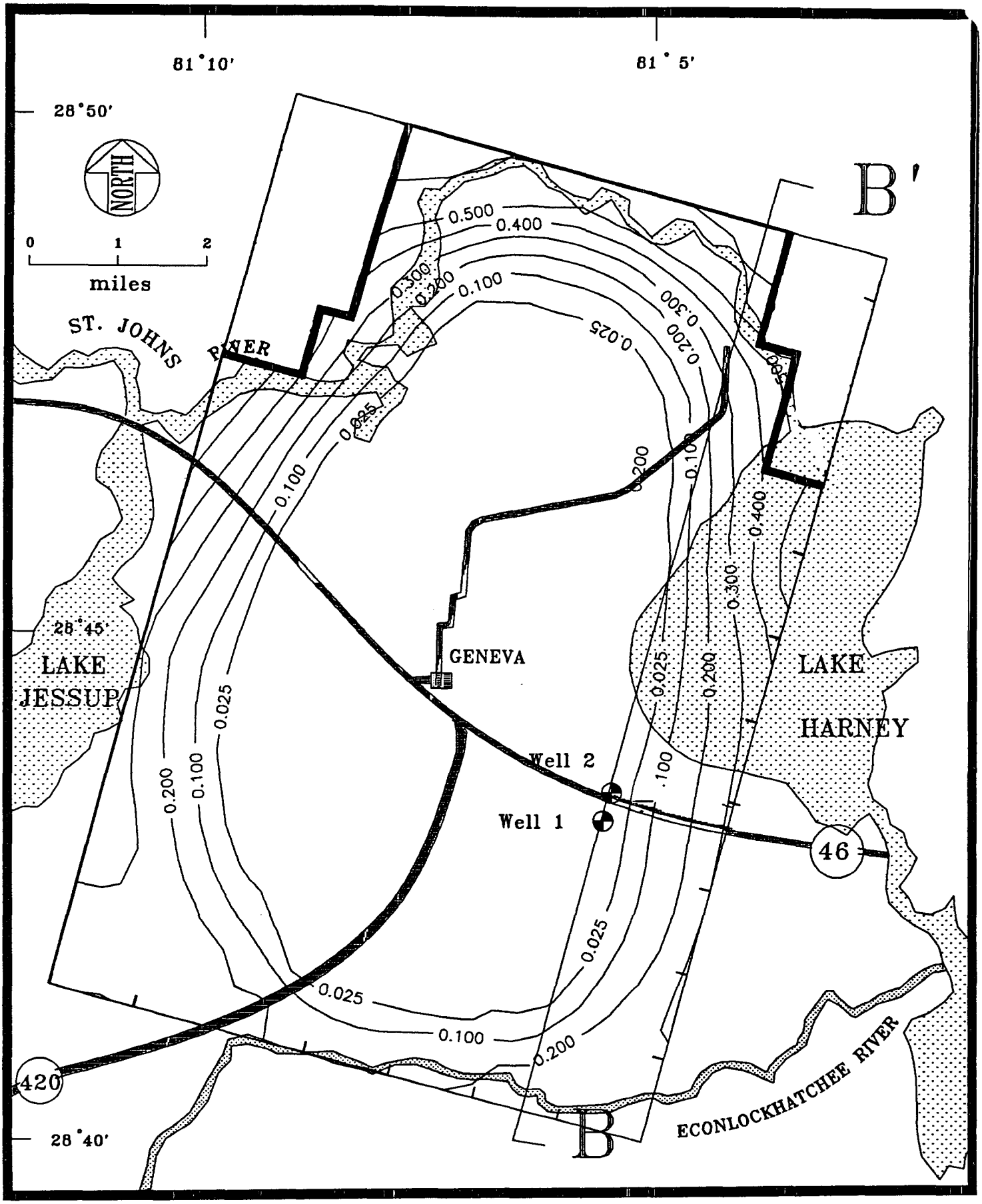

Figure 9.31. Areal distribution of chloride for steady-state withdrawals of 0.5 Mgal/d from two shallow wells at the Lake Harney edge of the lens [case 5, Table 9.1].

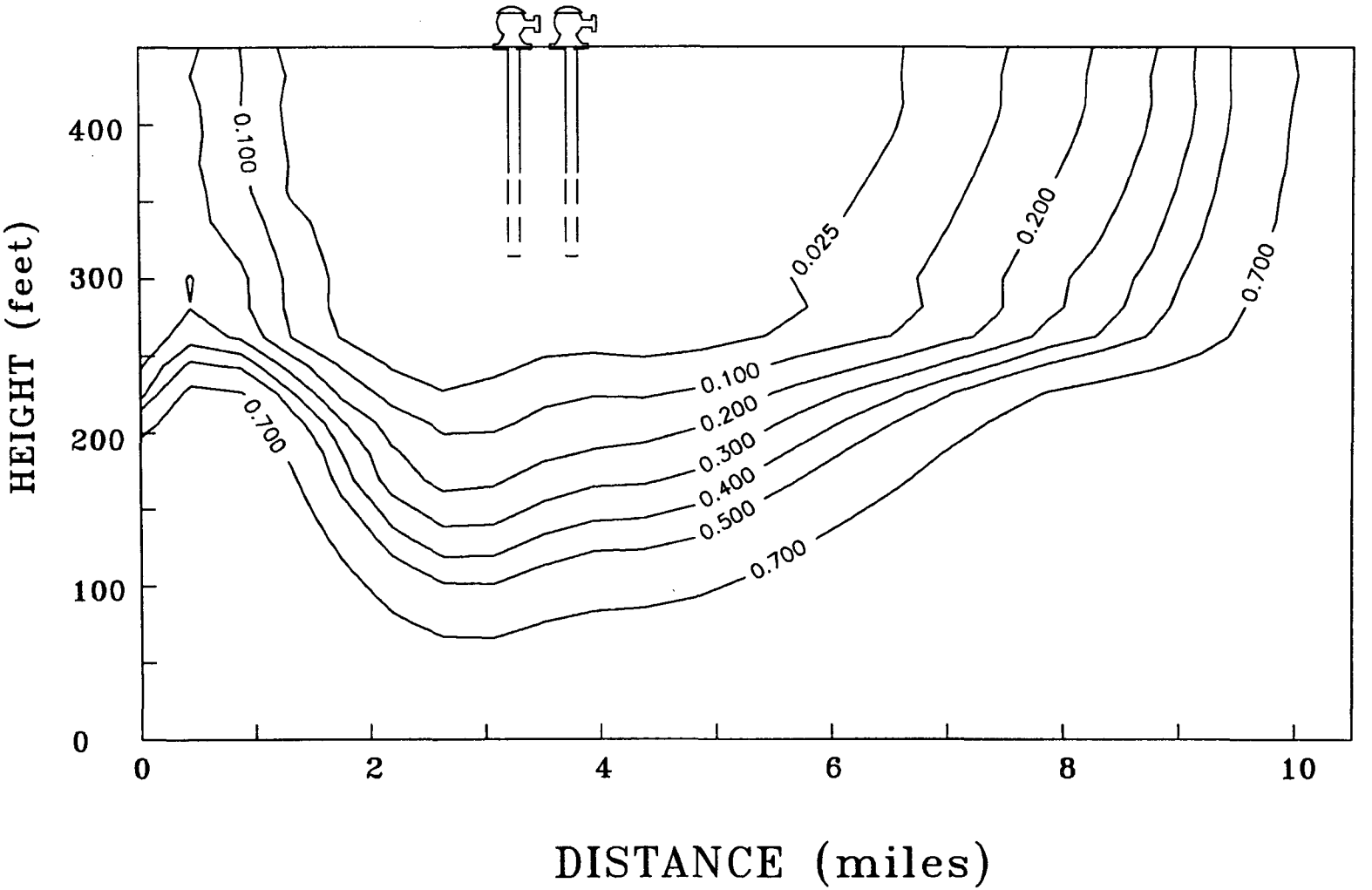

Figure 9.32. Relative concentration of chloride through B-B′ for steady-state withdrawals of 0.5 Mgal/d from two shallow wells at the Lake Harney edge of the lens [case 5, Table 4.1].

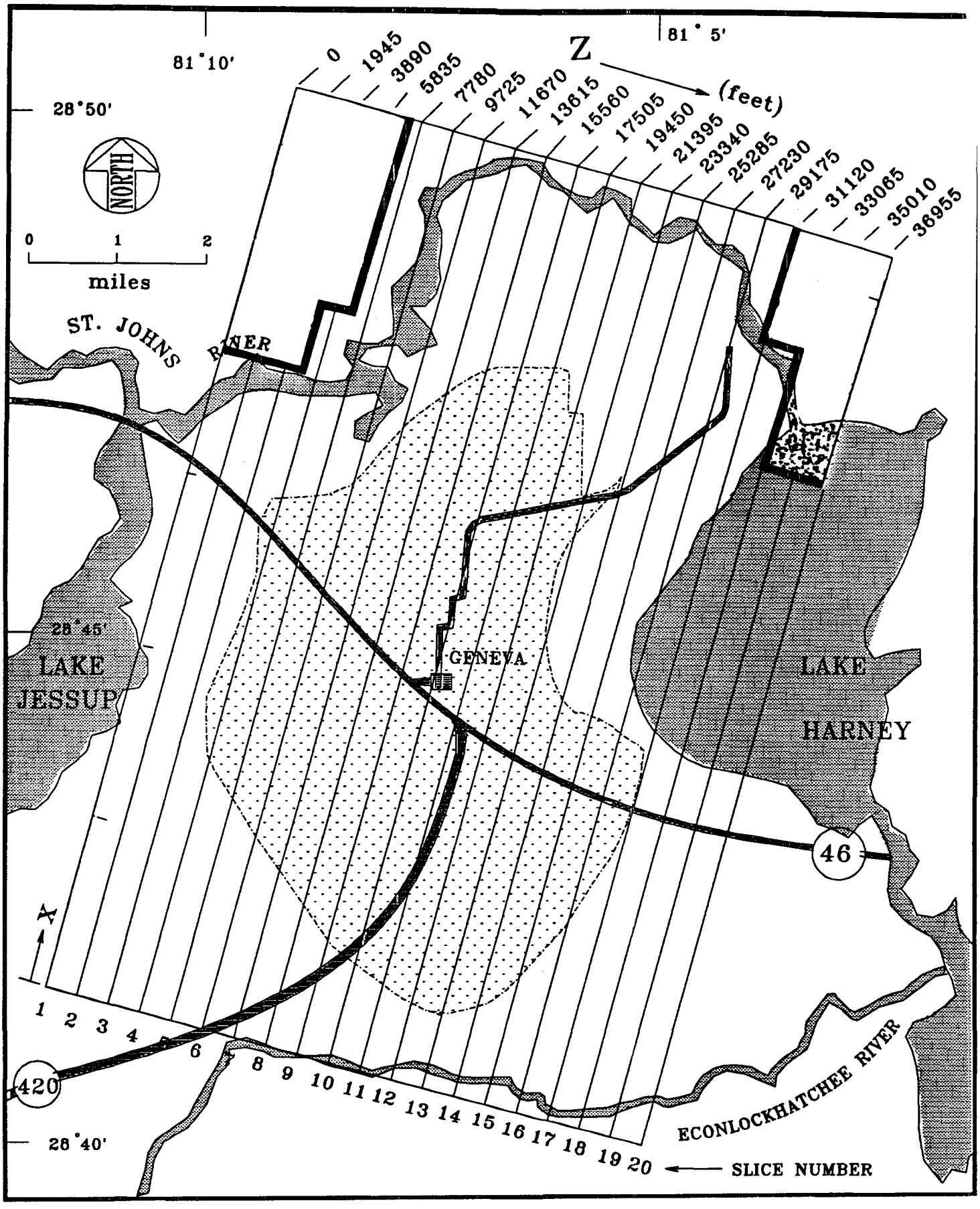

Figure 9.33. Region of dispersed domestic withdrawals from the Geneva lens.

9.34, 9.35 and 9.36, respectively. The relative concentration contours in the vertical plane A-A' are shown in Figures 9.37, 9.38 and 9.39 for 25 years, 50 years and 150 years, respectively. The areal reduction of the lens is steady from all directions. The thickness of the lens has reduced by approximately 50 ft over 150 years of simulation. However, upconing of brackish water from the base has not occurred. Distributed pumping is seen to be less detrimental to the Geneva lens, at higher pumping rates, than localized withdrawals.

9.3 SUMMARY AND CONCLUSIONS OF THREE-DIMENSIONAL TRANSIENT SIMULATIONS

Three-dimensional transient simulations of the Geneva freshwater lens system have been performed and are summarized in Table 9.1. The starting condition for the transient simulations was the calibrated lens developed in Figures 8.16-8.20. The chloride patterns responded slowly to shutting off the recharge. The lens could not sustain itself for more than 150 years when the freshwater recharge was cut off. Head patterns respond very rapidly to any hydraulic impulse on the system, and hence the calculated heads of the steady-state simulation cannot be directly compared with the measured field values. The significance of a comparison of measured head values and simulation results is limited due to the time-averaged recharge/discharge imposed on the model. Recharges and discharges of groundwater on the surface are also averaged by considering zones within which recharge/discharge values are uniform. High pumping from the center of the lens

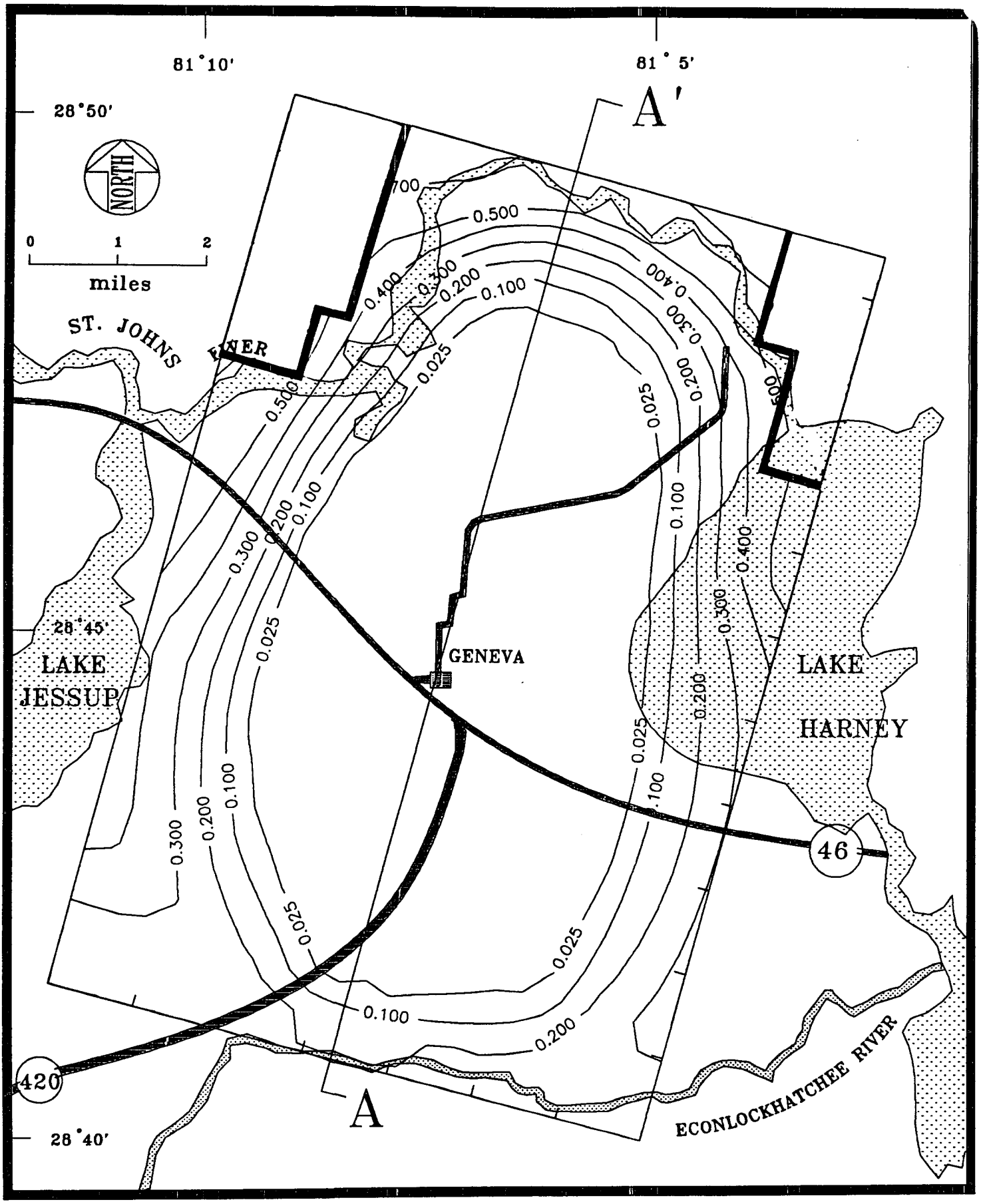

Figure 9.34. Areal distribution of chloride after 25 years of dispersed domestic withdrawals of 375 gal/d per acre of Suburban Estates [case 6, Table 9.1].

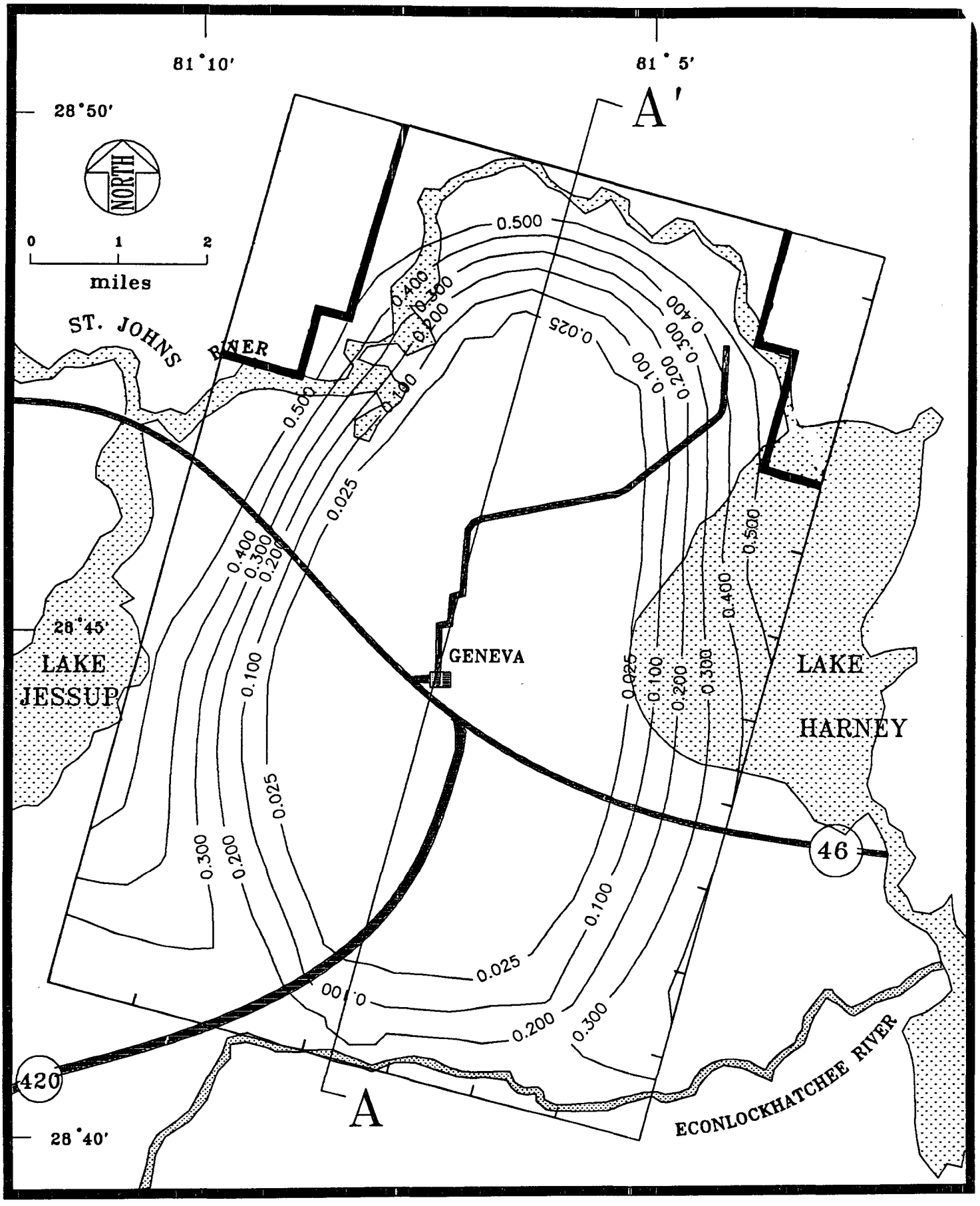

Figure 9.35. Areal distribution of chloride after 50 years of dispersed domestic withdrawals of 375 gal/d per acre of Suburban Estates [case 6, Table 9.1].

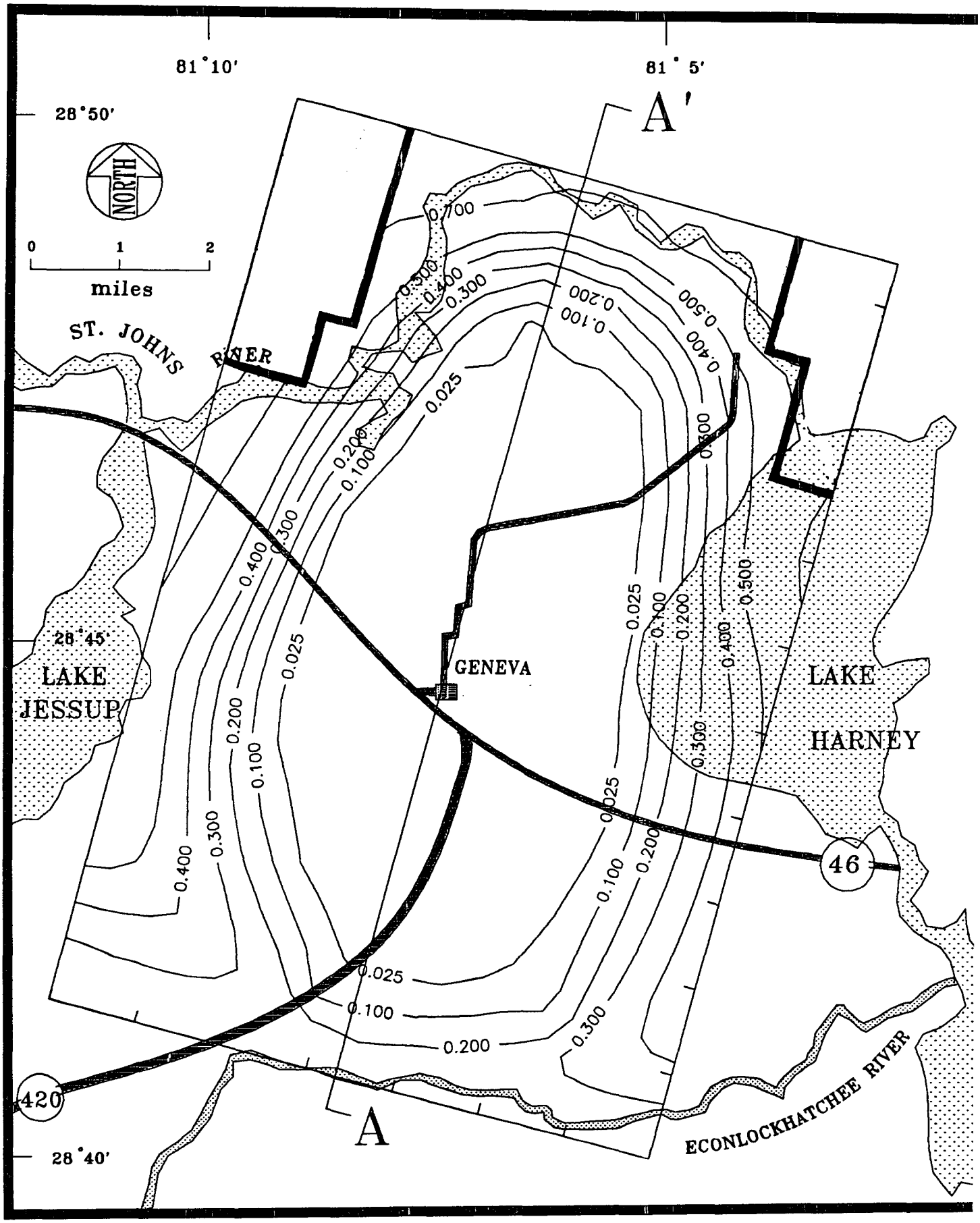

Figure 9.36. Areal distribution of chloride after 150 years of dispersed domestic withdrawals of 375 gal/d per acre of Suburban Estates [case 6, Table 9.1].

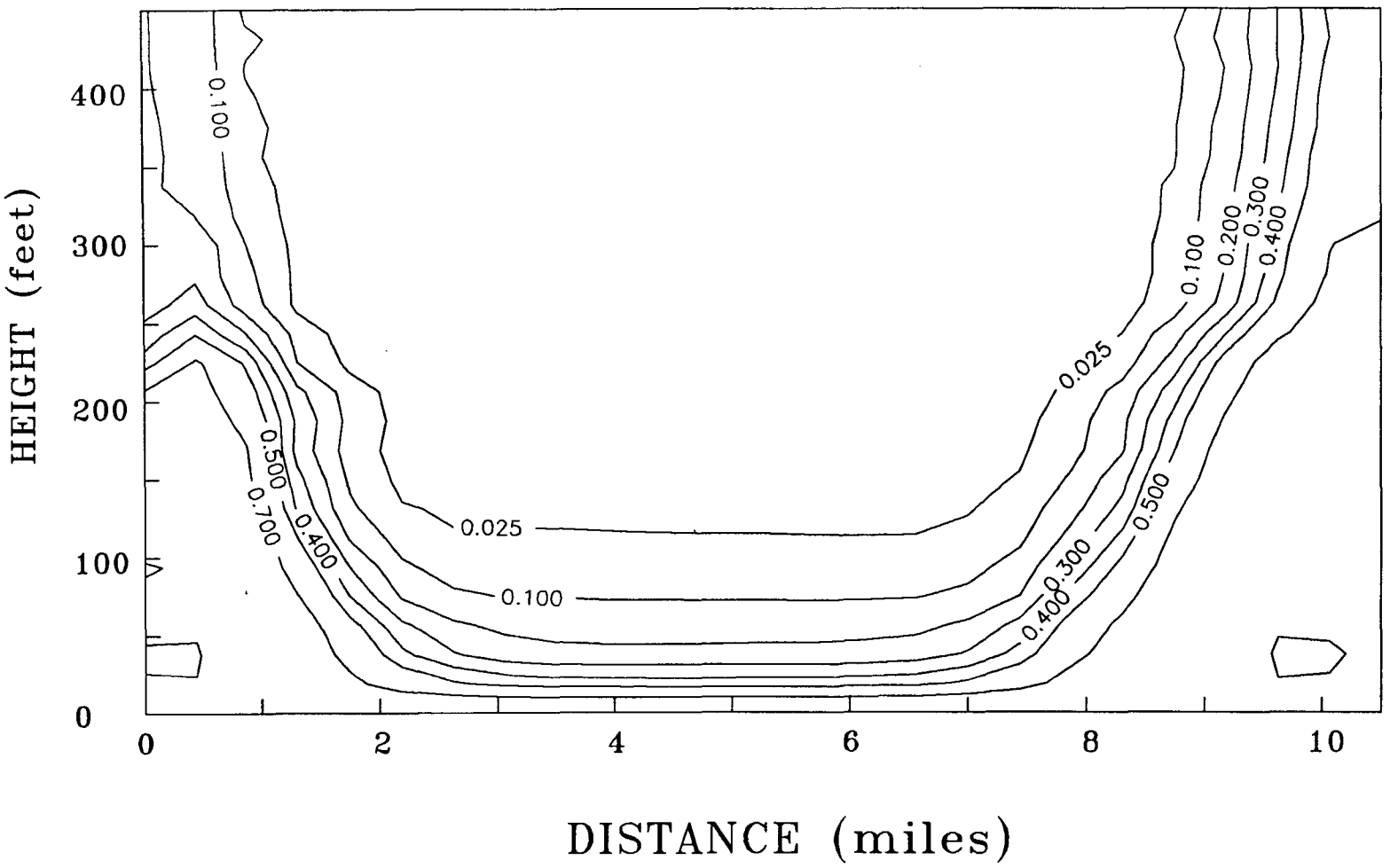

Figure 9.37. Relative concentration of chloride through A-A′ after 25 years of dispersed domestic withdrawals of 375 gal/d per acre of Suburban Estates [case 6, Table 9.1].

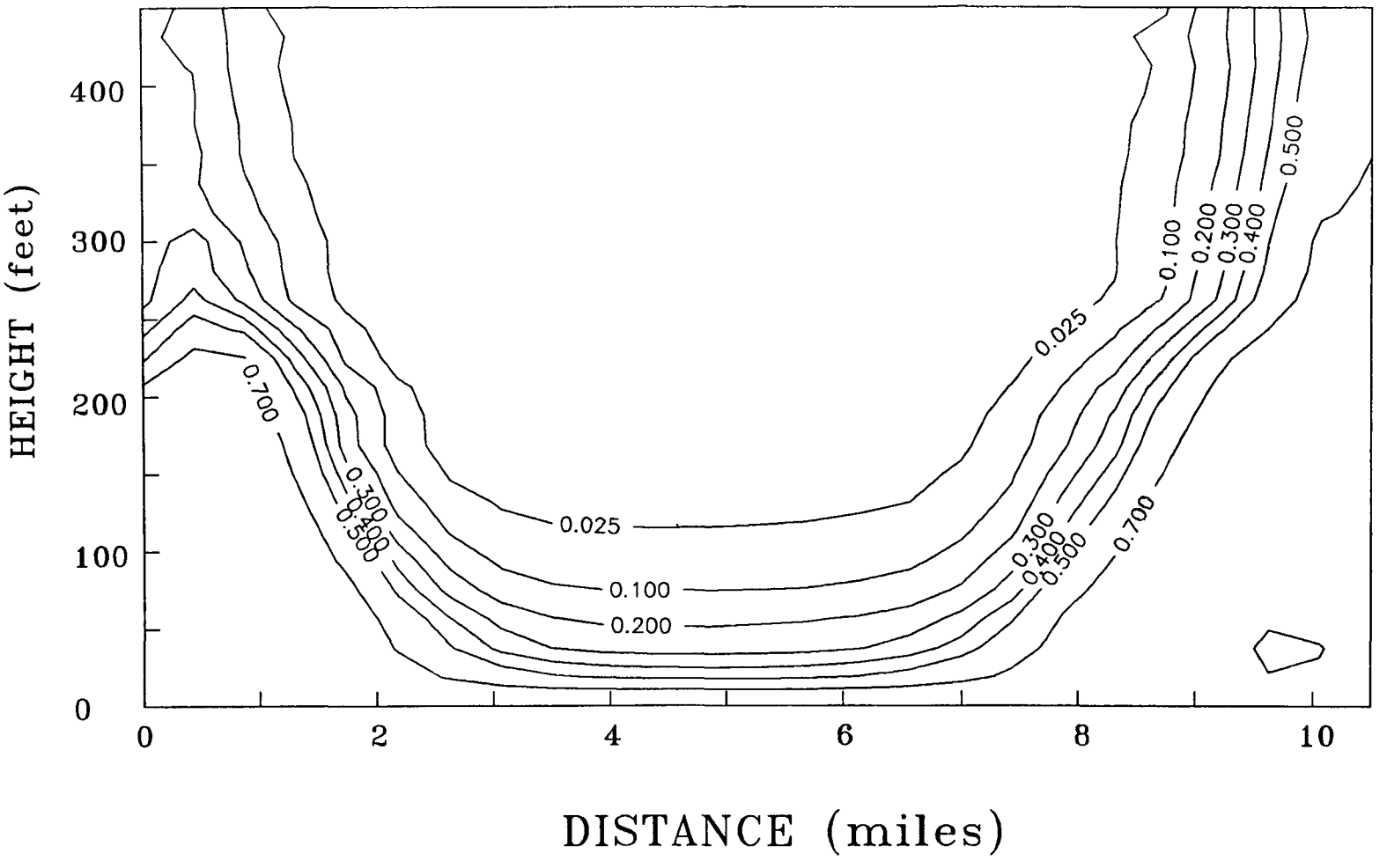

Figure 9.38. Relative concentration of chloride through A-A′ after 50 years of dispersed domestic withdrawals of 375 gal/d per acre of Suburban Estates [case 6, Table 9.1].

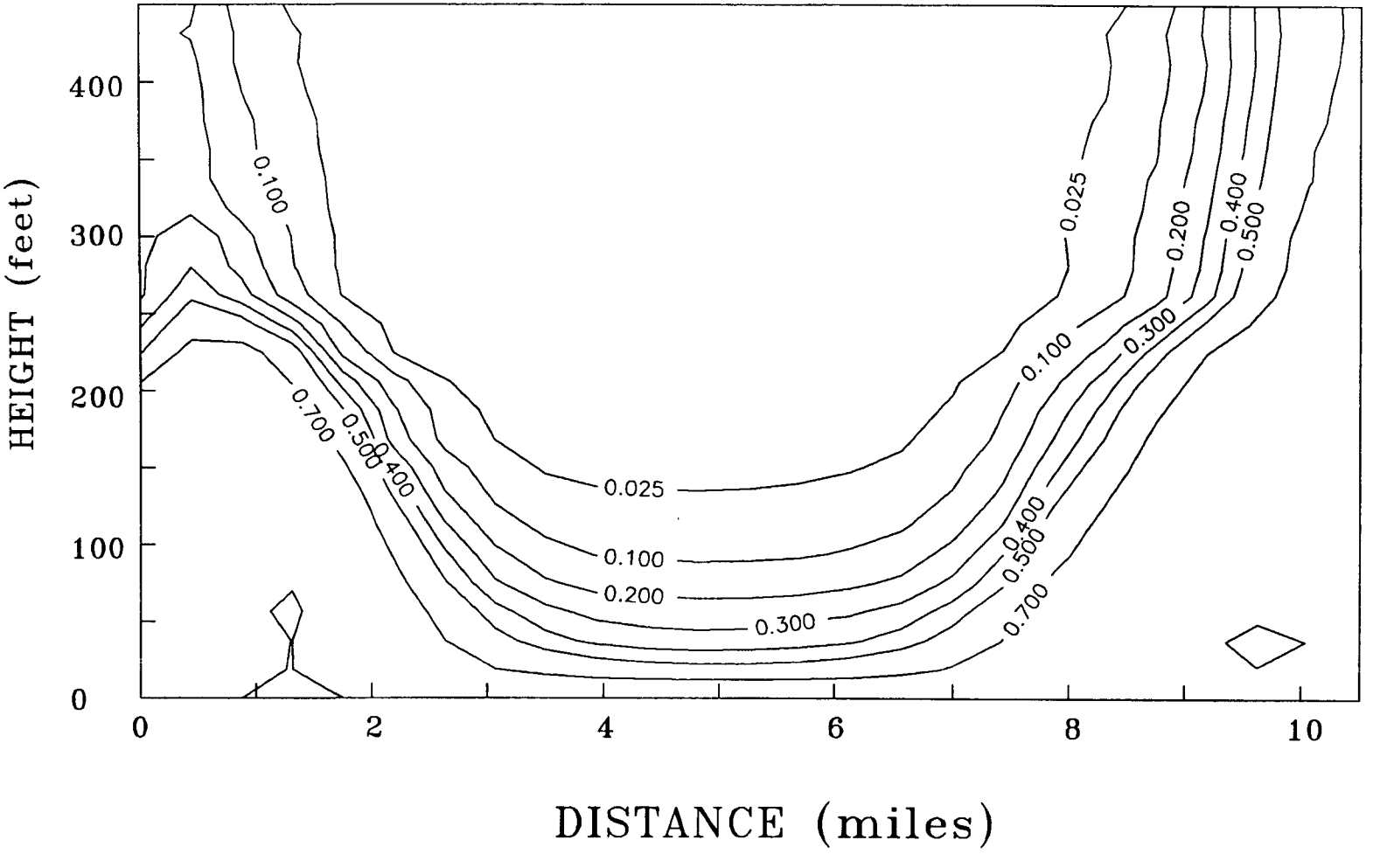

Figure 9.39. Relative concentration of chloride through A-A′ after 150 years of dispersed domestic withdrawals of 375 gal/d per acre of Suburban Estates [case 6, Table 9.1].

induces upconing of brackish water from the bottom. Lateral intrusion effects dominate when high withdrawals occur over the edge of the lens. Chloride patterns were not affected by depth of pumping for the various cases studied. Breakthrough of chloride would therefore occur earlier in deeper wells than shallow wells. Distributed withdrawals are more effective in managing the lens than localized withdrawals. Localized withdrawals of 3.75 Mgal/d lead to well contamination, irrespective of where the withdrawal center is located. Distributed withdrawals of 4.2 Mgal/d could, however, be sustained by the lens without contaminating the withdrawal sites. The lateral extent of the lens decreases by half a mile from all sides for this case, hence, pumping should be located at least half a mile into the domain of the current freshwater lens. Otherwise, long term effects of pumping may be detrimental to the peripheral wells. If the demand for water grows to large extents, a combination of withdrawal strategies would probably be the best solution.

10. CONCLUSIONS

10.1 GENERAL CONCLUSIONS

10.1.1 Two-dimensional cross-sectional simulations

The steady-state and transient two-dimensional simulations have led to the following conclusions:

1. The DSTRAM code is well suited for application to two-dimensional, density-dependent saltwater intrusion problems. For the same set of input conditions, DSTRAM yields the same results as its predecessor code, SWICHA.
2. The general width and thickness of the Geneva freshwater lens can be accurately simulated in two dimensions using realistic boundary conditions and material properties consistent with field measurements and best-judgement estimates.
3. Steady-state simulated chloride patterns match field data reasonably well; the maximum depth of freshwater in the lens, about 350 ft from land surface, and the lateral concentration gradient patterns agree well with limited field data.
4. Modeling results indicate that transverse dispersivities for the system are probably significantly smaller than earlier estimates.

Best-fit chloride distributions were obtained with transverse dispersivities in the range of 2.5 to 5 feet.

5. As would be expected, the size and shape of the lens are sensitive to amounts and distribution of recharge and discharge to the lens.
6. The lens is moderately sensitive to rates and distributions of discharge at the north end of the lens. Increasing upward discharge into the St. Johns River reduces the steady-state lens size. Increasing lateral discharge through the north boundary tends to increase the lens size. This is significant because there are uncertainties in discharge patterns along the northern portion of the lens.
7. The lens is sensitive to imposed chloride concentration boundary conditions. Increased chloride concentrations at the southern (upgradient) boundary tend to reduce lens size.
8. Recharge to the lens can be adequately accounted for in the model using two different approaches: directly specifying recharge inflow rates or incorporating head-dependent fluxes into the model using surficial aquifer

boundary conditions and leakance through the Miocene aquitard units overlying the Floridan aquifer. Leakance can be adjusted to achieve the desired estimated recharge rates.

9. Under low-pumping rate conditions the simulated lens is insensitive to changes in horizontal-to-vertical anisotropy ratios in hydraulic conductivity.

10. The lens is sensitive to the estimated thickness of the Ocala formation. If this highly permeable layer is 190 ft thick throughout the cross-section, the lens extends further into the St. Johns river edge of the domain, due to the recharge water traveling across the highly permeable Ocala.

11. Transient simulations demonstrate that if a well-designed finite element mesh is used, together with well-posed initial and boundary conditions, a relatively coarse mesh comprised of 1020 nodes can yield efficient and numerical solutions.

12. The lens is insensitive to temporal variations in recharge rate. Shutting off recharge totally over a 150 year period reduces the lateral extent of the lens by approximately 3½ miles. Owing to the slow transient response

of the lens to fluctuation in recharge an annually averaged recharge rate would be sufficient for modeling scenarios.

13. The transient response is insensitive to the specific storage of the aquifer materials. This is because the time scale for response of the flow field is orders of magnitude smaller than time scales for response of the chloride patterns. This behavior makes it more difficult to match calculated head values to field data since field data are collected at specific times, while the calculations proceed using an estimated averaged flux input.

14. The chloride distribution and flow field are undisturbed when the bottom head values are translated by a constant. This is because the bottom heads act as a datum for the flow equation calculations. Head patterns throughout the domain are also identical, with absolute values being translated by the same constant value as the prescribed values at the base.

15. Varying the horizontal head gradients prescribed at the base affects the head distribution and flow field. The freshwater lens, however, is only slightly affected since

the flow field near the top is dominated by the recharge/discharge conditions.

16. With the understanding that the two-dimensional, cross-section modeling approach treats groundwater withdrawal using a line strip sink, the following conclusions may be drawn. Lens shape and size are affected by groundwater withdrawal when the withdrawal rate is sufficiently large to create an upconing of brackish water. An upconing is noticed at a pumping rate of 50 ft^2/d. However, the well was not invaded by the 250-ppm isochlor within 150 years for this case. For a withdrawal rate of 75 ft^2/d from one pumping location, the upconing was significant, and the well was contaminated within 30 years.

17. Distributing the pumping load over a larger portion of the flow system can significantly affect chloride distribution and upconing.

18. Modeling results suggest that it may be better to distribute pumping over a significant area of the central portion of the lens than to have it concentrated at one small central location. The wider areal distribution reduces localized upconing effects.

19. Two-dimensional (2-D) cross-sectional modeling should not be used to make quantitative predictions of the actual lens behavior under field conditions. This is because major effects of three-dimensional flow and boundary conditions cannot be accounted for in the cross-sectional approach. However, the two-dimensional approach is highly useful for qualitative and semi-quantitative assessments of relative responses, for sensitivity analysis, for improving conceptual models, and for developing initial and boundary conditions for three-dimensional simulations.

10.1.2 Three-dimensional simulations

The steady-state and transient three-dimensional simulations have led to the following conclusions:

1. The DSTRAM model code is well suited for simulating the fully three-dimensional problem on a personal computer.
2. Two-dimensional cross-sectional simulations of the Geneva freshwater lens are incapable of modeling the lens system accurately. Transverse components of flow due to recharges and discharges are neglected in the 2-D modeling approach, and these components have

significant influences on the shape and size of the lens. Furthermore, well withdrawals cannot be properly studied using the cross-sectional model, since the two-dimensionality of the problem can only handle strip-withdrawal cases.

3. The general configuration and thickness of the Geneva freshwater lens can be accurately simulated in three dimensions using realistic boundary conditions and material properties consistent with field measurements and best-judgement estimates (Table 8.2 and 8.3). These calibrated conditions however, are substantially different from the 2-D estimates which neglect flow components in the third dimension.
4. Steady-state simulated chloride patterns, obtained from the three-dimensional model, match field data reasonably well; the maximum depth of freshwater in the lens, about 350 ft from land surface, and the lateral concentration gradient patterns agree well with limited field data.
5. A rectangular grid of variable spacing comprising of 9,000 nodes is sufficient for the fully three-dimensional simulations.

Grid-related problems were not encountered for any of the cases studied.

6. The lens was insensitive to the prescribed bottom heads. Simulated patterns of true head (i.e. actual piezometric head measured in the field) were significantly affected by changes in horizontal gradients of the prescribed head at the base of the flow domain. However, head patterns near the surface were not greatly affected, since recharges and discharges are the major controlling factors in that vicinity. The freshwater lens that develops, therefore, is not greatly affected in the upper portion of the system. The lens is shallower, however, if larger horizontal head gradients are prescribed at the bottom. This is due to larger dispersion caused by the greater horizontal velocities. If the horizontal gradients of the prescribed bottom-head are unchanged, the freshwater lens and flow patterns would remain unchanged, and would not depend on the absolute value of head prescribed at the bottom, as seen in Figures 5.22-5.24. It can therefore be concluded that the absolute value of the head at any location at the base of the domain is an insignificant

parameter; therefore it would be inappropriate to expend significant time, effort and money determining this value, provided the horizontal gradients of head along the base are known. These gradients were estimated from Phelps and Rohrer (1987) for the simulations described herein.

7. As would be expected, the size and shape of the lens are sensitive to amounts and distribution of recharge to the lens. The lens size reduced by 1.5 miles near the St. Johns River when recharge to the zones of "low to moderate recharge" was cut off.

8. The lens is moderately sensitive to rates and distributions of discharge at the north end of the lens. Decreasing upward discharge into the St. Johns River and the areas near Lake Jessup and Lake Harney increases the lens size in these zones considerably. Decreasing discharge near the Econlockhatchee River did not have as significant an impact as reducing discharges near the St. Johns River. The uncertainty in discharge patterns is hence less significant near the Econlockhatchee River than in the rest of the domain.

9. The simulated lens is not highly sensitive to large changes in hydraulic conductivity of the upper Avon Park formation. It is, however, more sensitive to the vertical conductivity of the lower Avon Park formation.

10. For a recharge rate of 10 in/yr, the size of the predicted three-dimensional lens is not highly sensitive to pumping withdrawal rates until the withdrawals approach 2.5 Mgal/d. Note that in the 2-D simulations, four times larger withdrawal rates were required to obtain a similar response.

11. The lens is relatively insensitive to temporal variations in recharge rate. Shutting off recharge totally, reduces the lens size by half over a 50 year period. By 150 years, the lens was diminished. Note again the misrepresentation of the 2-D simulation, wherein the lens size reduces by 3½ miles in 150 years.

12. Lens shape and size are affected by pumping rates when the pumping is sufficiently large to create an upconing of brackish water. An upconing is noticed at a pumping rate of 2.5 Mgal/d from the lens center. However, the well field was not contaminated by the 250-ppm

isochlor within 150 years for this case. For a pumping rate of 3.75 Mgal/d from the center of the lens, the upconing was significantly larger and the wells were contaminated.

13. Pumping from the Lake Harney edge of the lens induces lateral intrusion of chloride, which invade the wells. Upconing effects are hence not noticed. A withdrawal of 2.5 Mgal/d from the Lake Harney edge of the lens is detrimental to the quality of water being pumped. Withdrawal of freshwater from the Lake Harney edge of the lens is possible with pumping rates of 0.5 Mgal/d, with judicious selection of well location.

14. Well depth was insignificant on the shape and size of the lens or on the depth to which upconing occurs for any particular pumping rate. Shallower wells would therefore produce freshwater, while deeper wells with the same withdrawals may not.

15. Domestic pumping of 375 gal/d per acre of suburban estates uniformly affects lens size from all directions. Freshwater production for all domestic use is still possible from the Geneva lens. The net withdrawal from the

lens for the entire suburban estates region is 4.2 Mgal/d.

16. The areal distribution of pumping wells can significantly affect chloride distribution, upconing and lateral intrusion. Modeling can be used to optimize areal well placement and pumping rates to minimize water quality degradation from chloride invasion and upconing.

17. Modeling results suggest that it is beneficial to distribute pumping over a significant area of the central portion of the lens than to have it concentrated at one small central location. The wider areal distribution greatly reduces localized upconing effects. A net pumping of 4.2 Mgal/d over the "suburban estates" does not produce large degradation of the lens. However, concentrated pumping of 2.5 Mgal/d from a central location produces upconing effects.

18. The three-dimensional model developed in this project may be used by the District to test additional scenarios of interest for planning and managing water development in the Geneva area.

10.2 ADDITIONAL DATA NEEDS

All hydrologic and modeling studies have significant uncertainties associated with them; this one is no different. Uncertainties can result due to limited sampling of field data, large local variations of field data and limitations associated with modeling assumptions. The field hydrologic, geologic, and water quality conditions associated with the Geneva freshwater lens are relative well defined. However there remain some significant weaknesses in the data and in the definition of quantitative hydraulic and chemical conditions of the system.

Although it is possible to calibrate and verify two- and three-dimensional modeling results to a limited degree on the Geneva area freshwater lens, additional data would be useful to increase confidence and to decrease uncertainty in model results and predictions.

The most significant data limitations are in the following categories:

1. Three-dimensional chloride concentrations in the deeper portion of the lens. Very few data are available on the position or shape of the lens base and the vertical chloride concentration gradients.
2. Discharge rates and distributions in the northern portion of the lens (into the St. Johns River and its vicinity).

3. Three-dimensional distributions of hydraulic head, especially in the deeper portions of the lens and beneath it. This would help confirm that the horizontal head gradients supplied by Phelps and Rohrer (1987), act as the base of the domain (where they have been used in the current simulations). Very few data are apparent on vertical head profiles to depths of 500 feet or more in the Geneva area. Also, vertical head gradients in the vicinity of the St. Johns River would be useful in estimating discharge.

4. Accurate data on locations, depths and screened or open intervals of existing pumping wells are needed. Also desirable is information on locations of anticipated additional development wells, for further use of the model as a planning and development tool.

5. More definitive information on hydraulic conductivities of the aquifer units are needed in order to better calibrate the model.

6. Water level data for the surficial aquifer in the area is probably available, but would need to be compiled for input into a model which would directly account for changes in those

water levels and the resultant impacts on recharge to the upper Floridan aquifer. For this process to be incorporated directly, information on leakances of the confining Miocene units would also be required. Also desirable is the piezometric head data collected from deep wells that would enable a more accurate determination of the prescribed hydraulic head at the bottom of the modeled region. Such information is necessary for better calibration of the predicted head and flow pattern.

7. Data on anisotropy ratio of horizontal to vertical hydraulic conductivity of the upper Floridan aquifer would be desirable to assess the influence of that factor on chloride responses to increased pumping scenarios. Anisotropy has been shown to have no major effect on the non-pumping behavior of the lens but has not been assessed for high-pumping conditions.

11. REFERENCES

Andersen, P.F., Mercer, J.W., and White, H.O., Jr., 1988. Numerical modeling of salt-water intrusion at Hallandale, Florida, Ground Water, vol. 26, no. 5, pp. 619-630.

Barraclough, J.T., 1962. Ground-water resources of Seminole County, Florida, Florida Geological Survey Report of Investigations no. 27, 91 pp and 10 sheets.

Cederstorm, D.J., Boswell, E.H., and Tarver, G.R., 1979. Summary appraisals of the nation's ground-water resources-South Atlantic-Gulf Region, U.S. Geological Survey Professional paper 813-0, 35 pp.

Chen, C.S., 1965. Regional lithostratigraphic analysis of Paleocene and Eocene rocks of Florida: Florida Bureau of Geology Bulletin 45, 105 pp.

Duguid, J.O., and Reeves, M., 1977. A comparison of mass transport using average and transient rainfall boundary conditions, Proc. of 1st Int. Conf. on Finite Elements in Water Resources, Princeton University, July 1976, pp. 2.25-2.36.

Huyakorn, P.S., Andersen, P.F., Mercer, J.W., and White, H.O., Jr., 1987. Saltwater intrusion in aquifers: Development and testing of a three-dimensional finite element model, Water Resources Research, vol. 23, no. 2, pp. 293-312.

Huyakorn, P.S., Mercer, J.W., and Andersen, P.F., 1986. SWICHA: A three-dimensional finite element code for analyzing seawater intrusion in coastal aquifers, Code documentation, Version 4.0, GeoTrans, Inc., 167 pp.

Huyakorn, P.S., and White, H.O., Jr., 1990. DSTRAM: Density-dependent solute transport analysis finite element code, User's Manual, HydroGeoLogic, Inc.

Phelps, G.G., 1984. Recharge and discharge areas of the Floridan aquifer in the St. Johns River Water Management District and vicinity, Florida, U.S. Geological Survey Water-Resources Investigations Report 82-4058, 1 sheet.

Phelps, G.G., and Rohrer, K.P., 1987. Hydrogeology in the area of freshwater lens in the Floridan aquifer system, Northeast Seminole County Florida, U.S. Geological Survey Water-Resource Investigations Report 86-4078, 74 pp.

Planert, M., and Aucott, W.R., 1985. Water-supply potential of the Floridan aquifer in Osceola, eastern Orange, and Southwestern Brevard Counties, Florida, U.S. Geological Survey Water-Resources Investigations Report 84-4135, 69 pp.

Schiner, G.R., and Hayes, E.C., 1981. Potentiometric surface of the St. Johns River Water Management District and vicinity, Florida, September 1981: U.S. Geological Survey Open-File Report 82-118, 1 sheet.

Schiner, G.R., and Hayes E.C., 1982. Potentiometric surface of the Floridan aquifer in the St. Johns River Water Management District and vicinity, Florida, September 1982: U.S. Geological Survey Open-File Report 83-30, 1 sheet.

Skipp, D. Ground-Water flow model of Brevard, Indian River, Orange, Osceola, and Seminole Counties, Florida, St. Johns River Water Management District, Technical Publication no. SJ 88-2, 86 pp.

Souza, W.R. and Voss, C.I., 1989. Assessment of potable groundwater in a freshwater lens using variable-density flow and solute transport simulation, Proc. of 4th Int. Conf. on the Use of Models to Analyze and find Working Solutions to Ground Water Problems, sponsored by International Ground Water Modeling Center, Butler University, Feb. 7-9, 1989, pp. 1023-1043.

Tibbals, C.H., 1975. Recharge areas of the Floridan aquifer in Seminole County and vicinity, Florida, Florida Dept. of Nat. Resources, Bur. Geol. Map Series 68.

Tibbals, C.H., 1977. Availability of ground water in Seminole County and vicinity, Florida, U.S. Geological Survey Water-Resources Investigations Report 76-97, 15 pp.

Tibbals, C.H., 1981. Computer simulation of the steady-state flow system of the Tertiary limestone (Floridan) aquifer system in east-central Florida: U.S. Geological Survey Water-Resources Investigations Open-File Report 81-681, 31 pp. and 9 sheets.

APPENDIX A

ALLOCATION OF MATERIAL ZONES TO THE ENTIRE DOMAIN FOR THREE-DIMENSIONAL SIMULATIONS

0 = outside domain
1 = lower Avon Park units
2 = upper Avon Park units
3 = Ocala Foramation

406 elements/slice
450 nodes/slice

X =

0.00	1000.00	2000.00	3000.00	4500.00	6000.00	8000.00	10000.00
12000.00	14000.00	16000.00	18000.00	20000.00	22500.00	25000.00	27500.00
30000.00	32500.00	35000.00	37250.00	39250.00	41250.00	44000.00	46000.00
48000.00	49500.00	51000.00	52000.00	53970.00	55440.00		

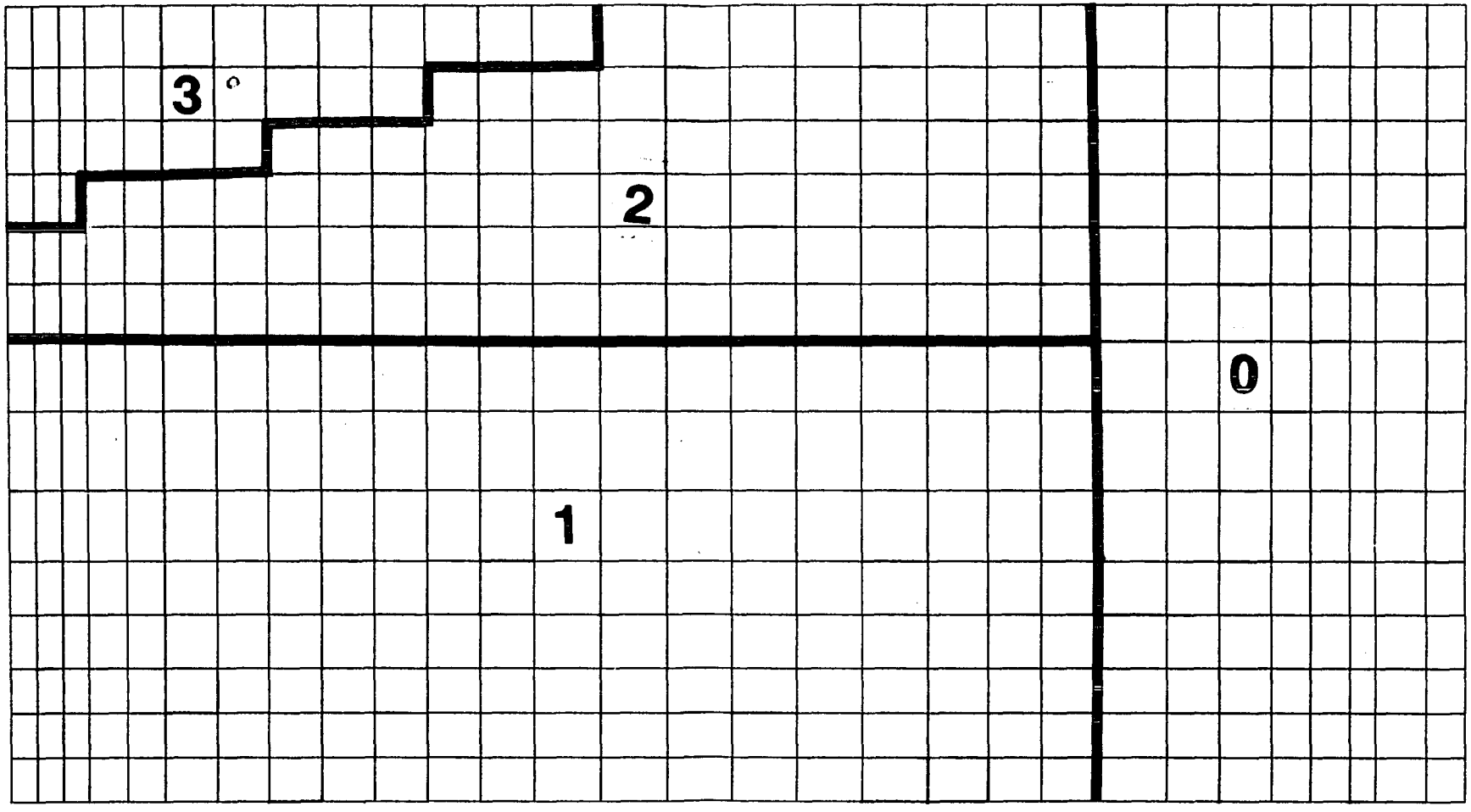

Y =

0.00	25.00	50.00	75.00	105.00	135.00	175.00	220.00
260.00	292.50	325.00	355.00	385.00	415.00	450.00	

PLANE 1, 2, and 3

406 elements/slice
450 nodes/slice

X = 0.00 1000.00 2000.00 3000.00 4500.00 6000.00 8000.00 10000.00
12000.00 14000.00 16000.00 18000.00 20000.00 22500.00 25000.00 27500.00
30000.00 32500.00 35000.00 37250.00 39250.00 41250.00 44000.00 46000.00
48000.00 49500.00 51000.00 52000.00 53970.00 55440.00

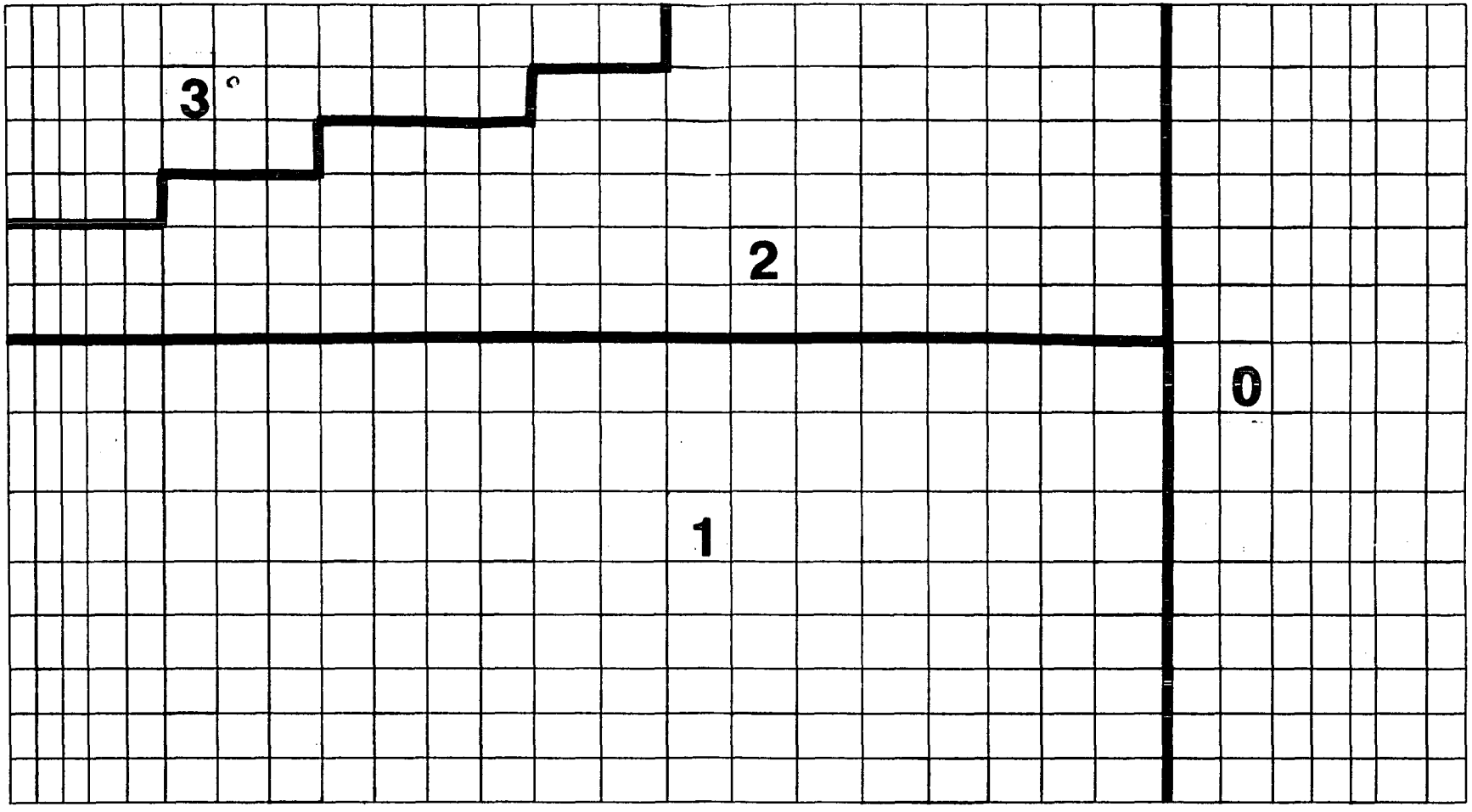

Y = 0.00 25.00 50.00 75.00 105.00 135.00 175.00 220.00
260.00 292.50 325.00 355.00 385.00 415.00 450.00

PLANE 4

406 elements/slice
450 nodes/slice

X = 0.00 1000.00 2000.00 3000.00 4500.00 6000.00 8000.00 10000.00
12000.00 14000.00 16000.00 18000.00 20000.00 22500.00 25000.00 27500.00
30000.00 32500.00 35000.00 37250.00 39250.00 41250.00 44000.00 46000.00
48000.00 49500.00 51000.00 52000.00 53970.00 55440.00

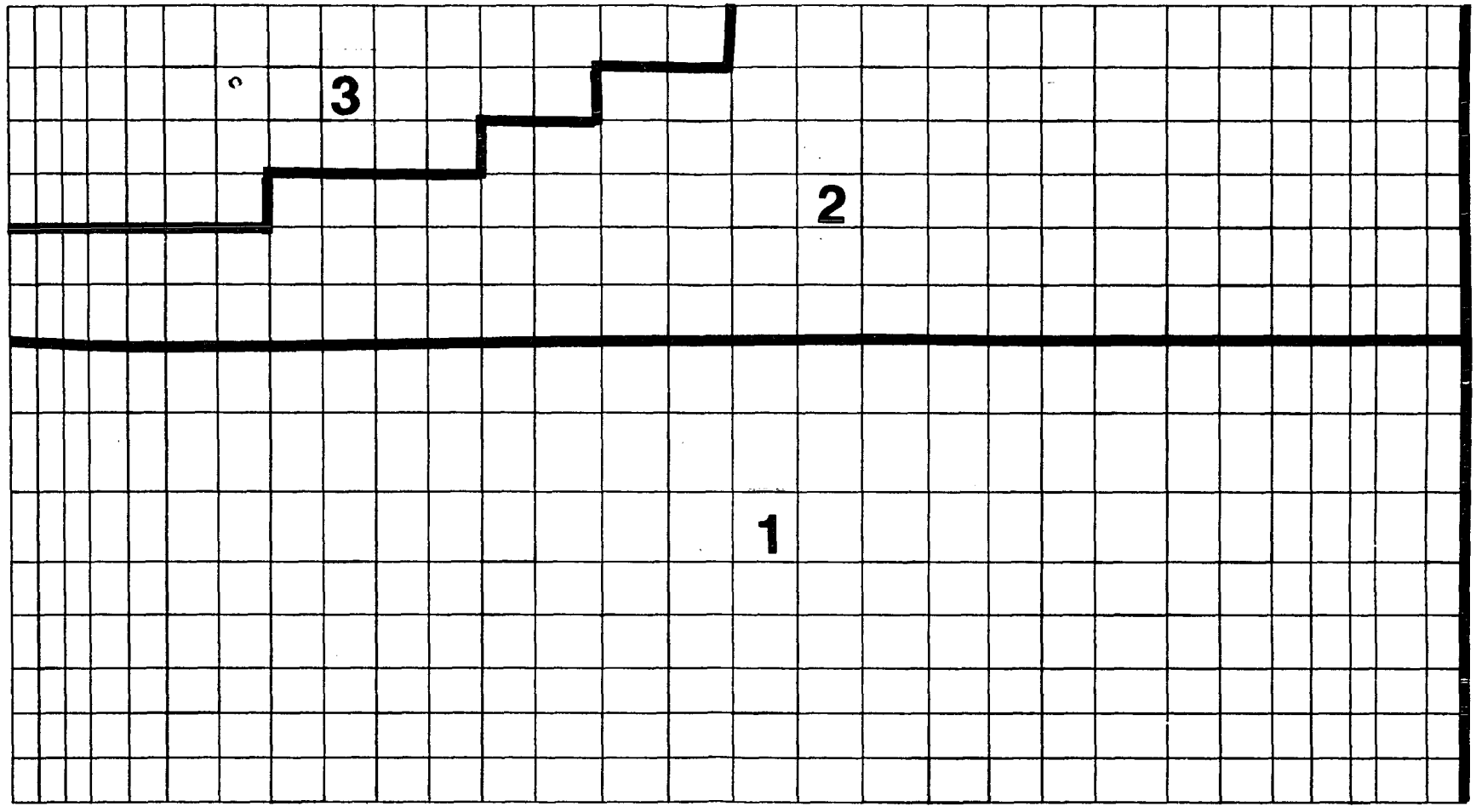

Y = 0.00 25.00 50.00 75.00 105.00 135.00 175.00 220.00
260.00 292.50 325.00 355.00 385.00 415.00 450.00

PLANE 5

X = 0.00 1000.00 2000.00 3000.00 4500.00 6000.00 8000.00 10000.00
12000.00 14000.00 16000.00 18000.00 20000.00 22500.00 25000.00 27500.00
30000.00 32500.00 35000.00 37250.00 39250.00 41250.00 44000.00 46000.00
48000.00 49500.00 51000.00 52000.00 53970.00 55440.00

406 elements/slice
450 nodes/slice

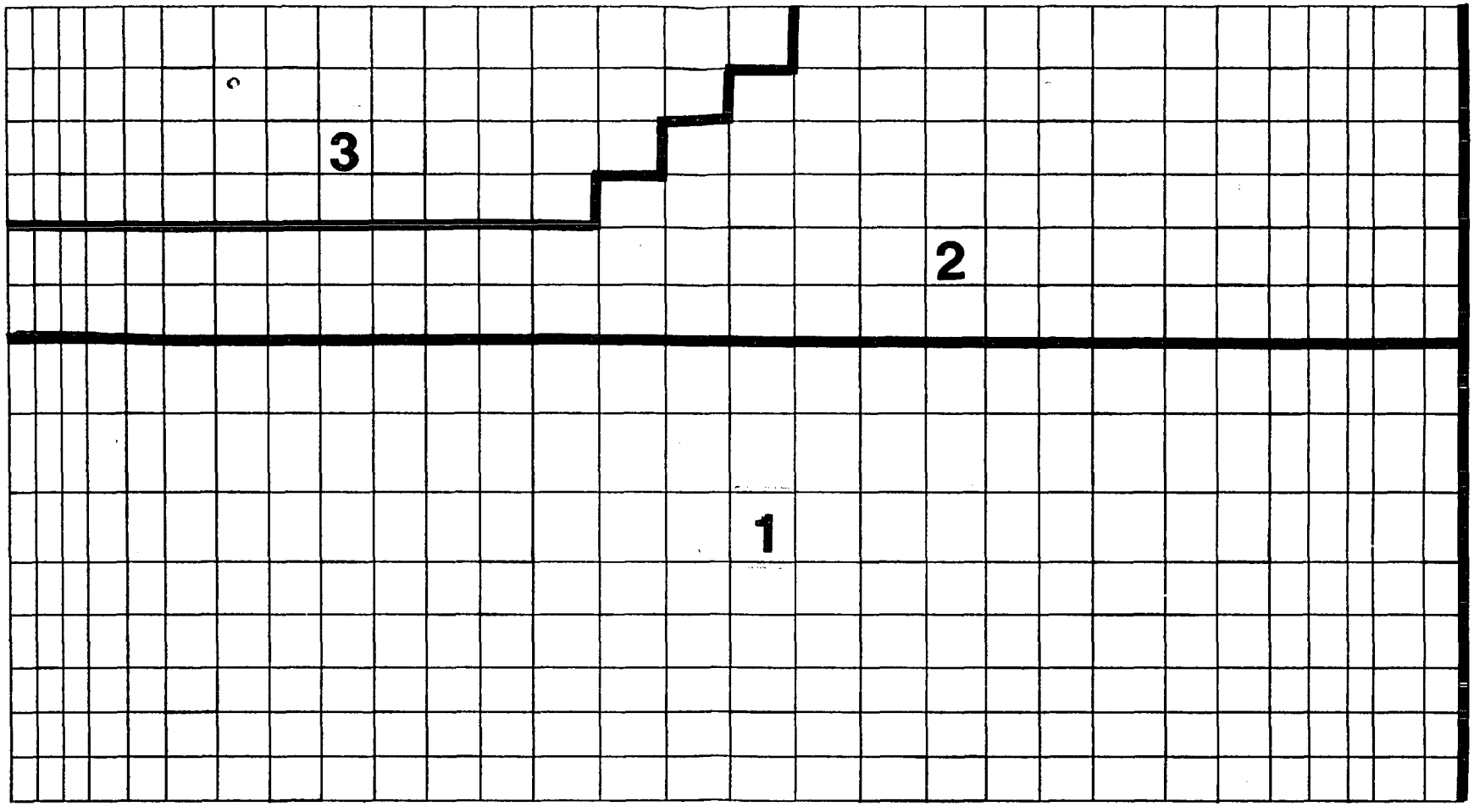

Y = 0.00 25.00 50.00 75.00 105.00 135.00 175.00 220.00
260.00 292.50 325.00 355.00 385.00 415.00 450.00

PLANE 6

406 elements/slice
450 nodes/slice

X = 0.00 1000.00 2000.00 3000.00 4500.00 6000.00 8000.00 10000.00
12000.00 14000.00 16000.00 18000.00 20000.00 22500.00 25000.00 27500.00
30000.00 32500.00 35000.00 37250.00 39250.00 41250.00 44000.00 46000.00
48000.00 49500.00 51000.00 52000.00 53970.00 55440.00

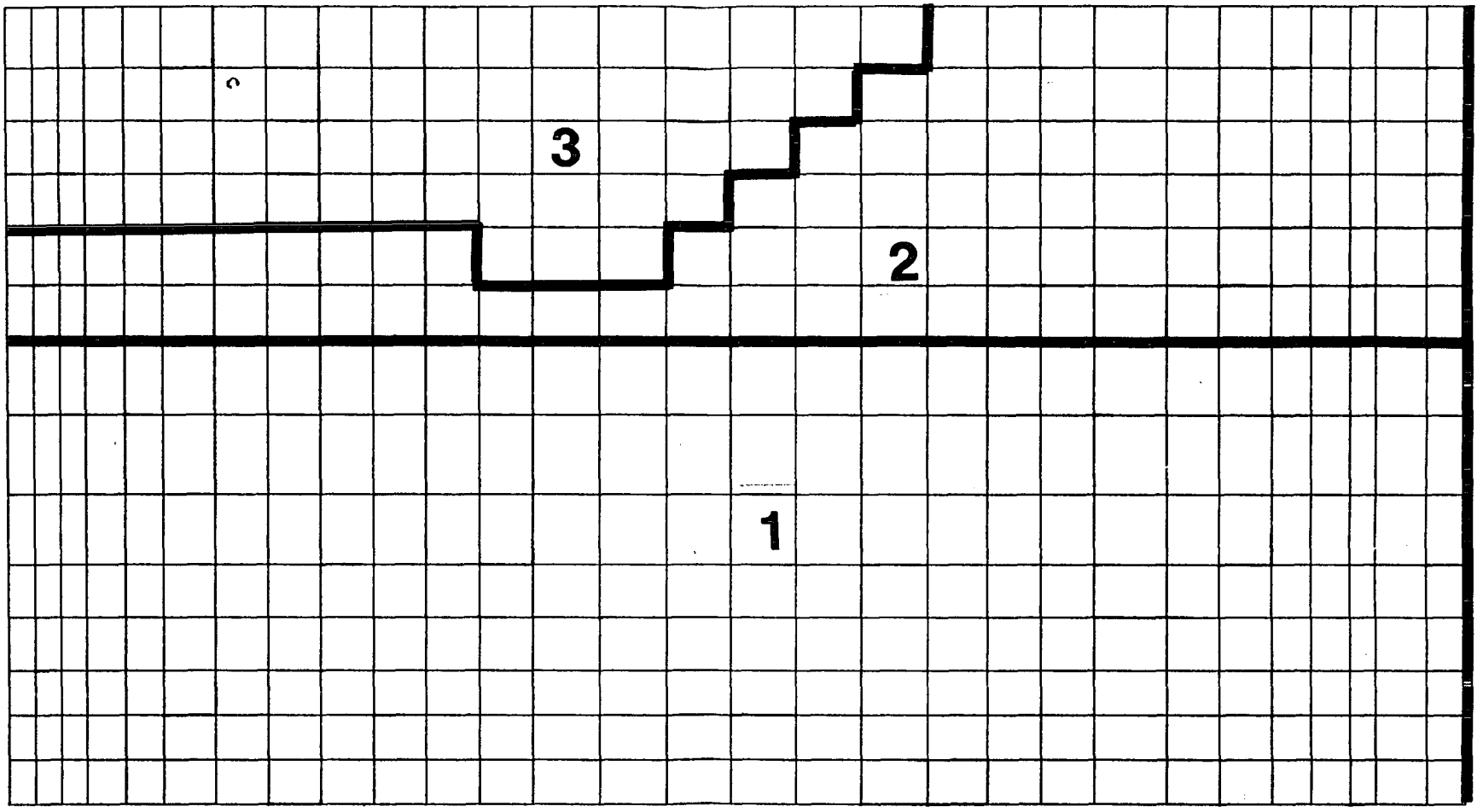

Y = 0.00 25.00 50.00 75.00 105.00 135.00 175.00 220.00
260.00 292.50 325.00 355.00 385.00 415.00 450.00

PLANE 7

406 elements/slice
450 nodes/slice

X = 0.00 1000.00 2000.00 3000.00 4500.00 6000.00 8000.00 10000.00
12000.00 14000.00 16000.00 18000.00 20000.00 22500.00 25000.00 27500.00
30000.00 32500.00 35000.00 37250.00 39250.00 41250.00 44000.00 46000.00
48000.00 49500.00 51000.00 52000.00 53970.00 55440.00

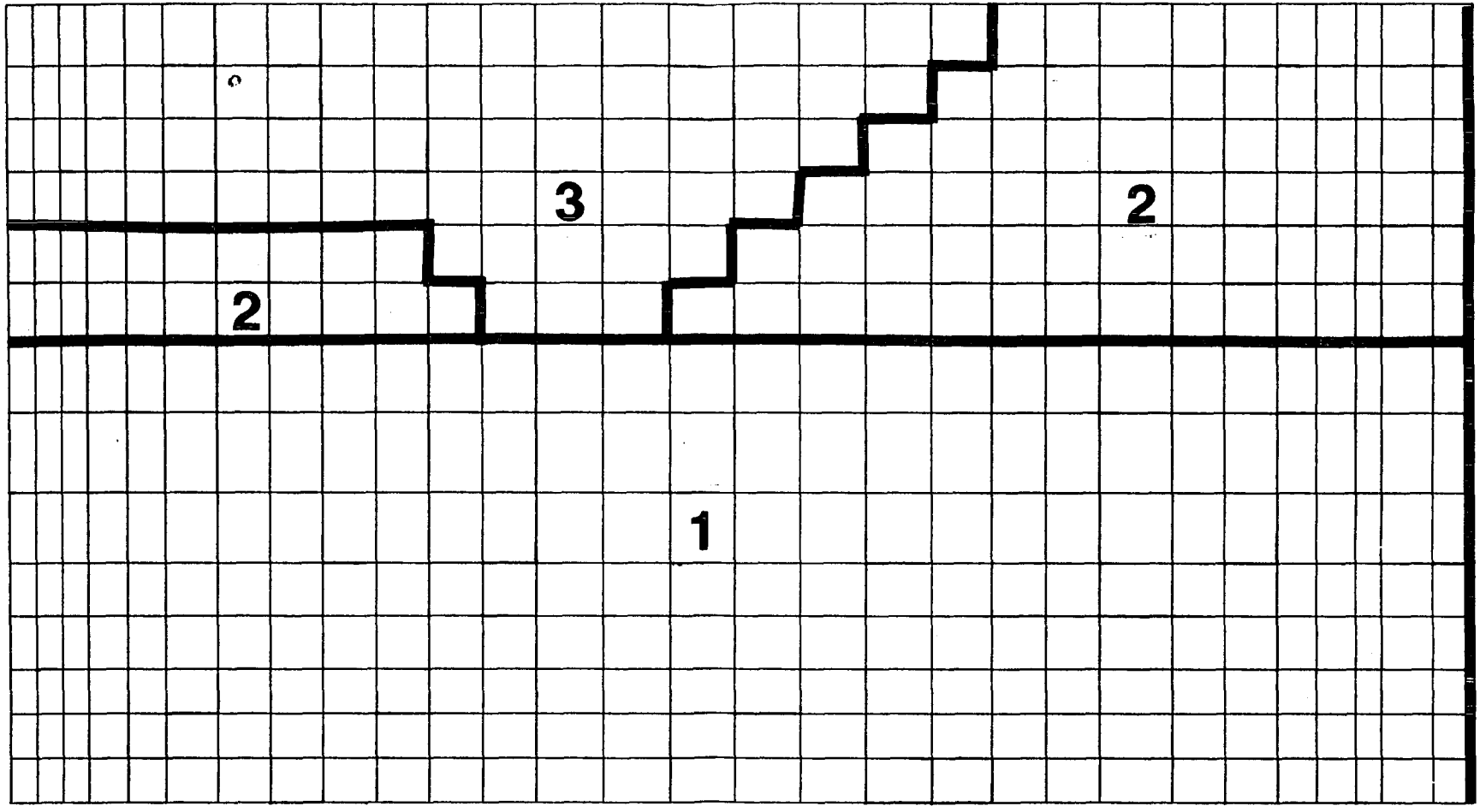

Y = 0.00 25.00 50.00 75.00 105.00 135.00 175.00 220.00
260.00 292.50 325.00 355.00 385.00 415.00 450.00

PLANE 8

406 elements/slice
450 nodes/slice

X = 0.00 1000.00 2000.00 3000.00 4500.00 6000.00 8000.00 10000.00
12000.00 14000.00 16000.00 18000.00 20000.00 22500.00 25000.00 27500.00
30000.00 32500.00 35000.00 37250.00 39250.00 41250.00 44000.00 46000.00
48000.00 49500.00 51000.00 52000.00 53970.00 55440.00

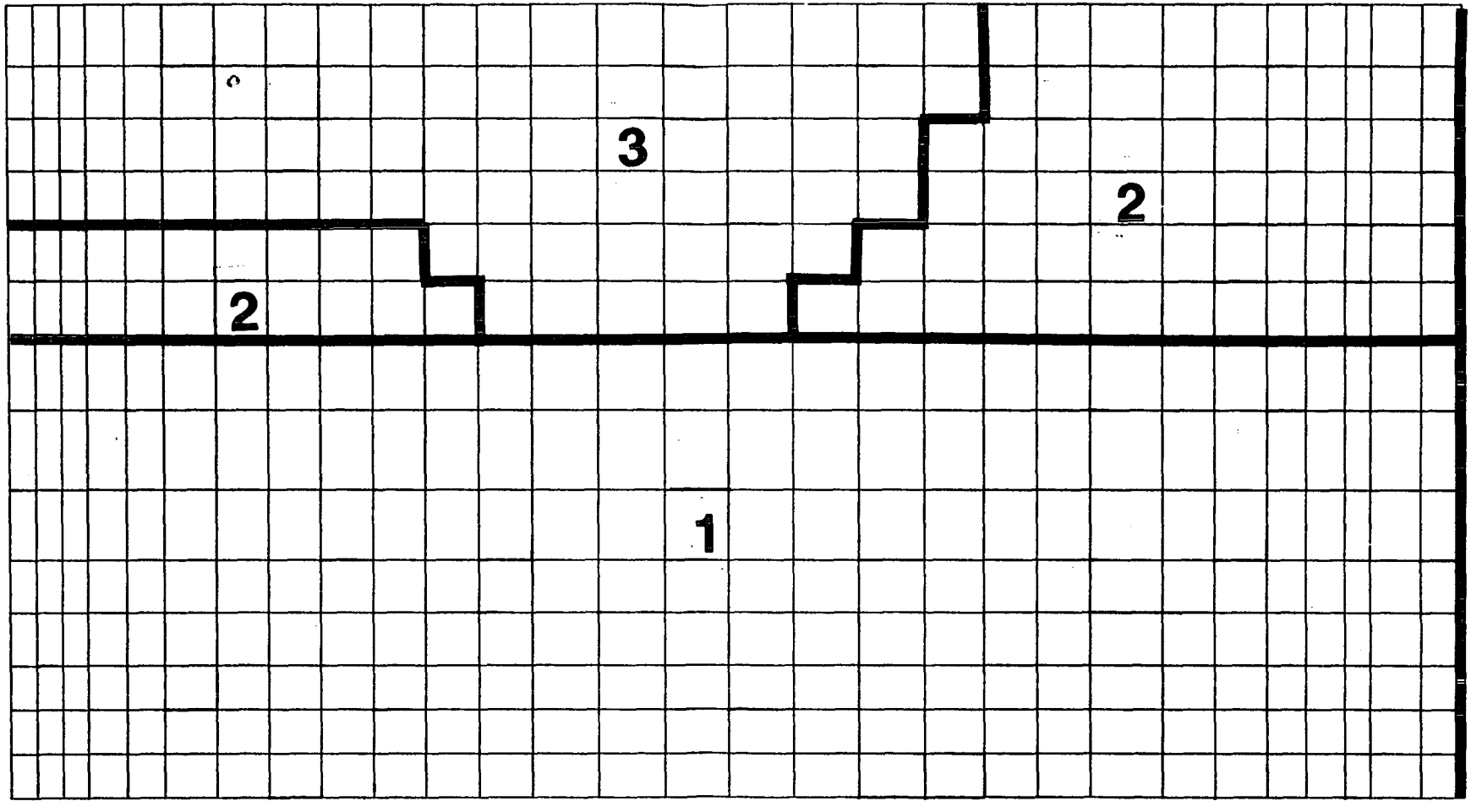

Y = 0.00 25.00 50.00 75.00 105.00 135.00 175.00 220.00
200.00 292.50 325.00 355.00 385.00 415.00 450.00

PLANE 9

406 elements/slice
450 nodes/slice

X =

0.00	1000.00	2000.00	3000.00	4500.00	6000.00	8000.00	10000.00
12000.00	14000.00	16000.00	18000.00	20000.00	22500.00	25000.00	27500.00
30000.00	32500.00	35000.00	37250.00	39250.00	41250.00	44000.00	46000.00
48000.00	49500.00	51000.00	52000.00	53970.00	55440.00		

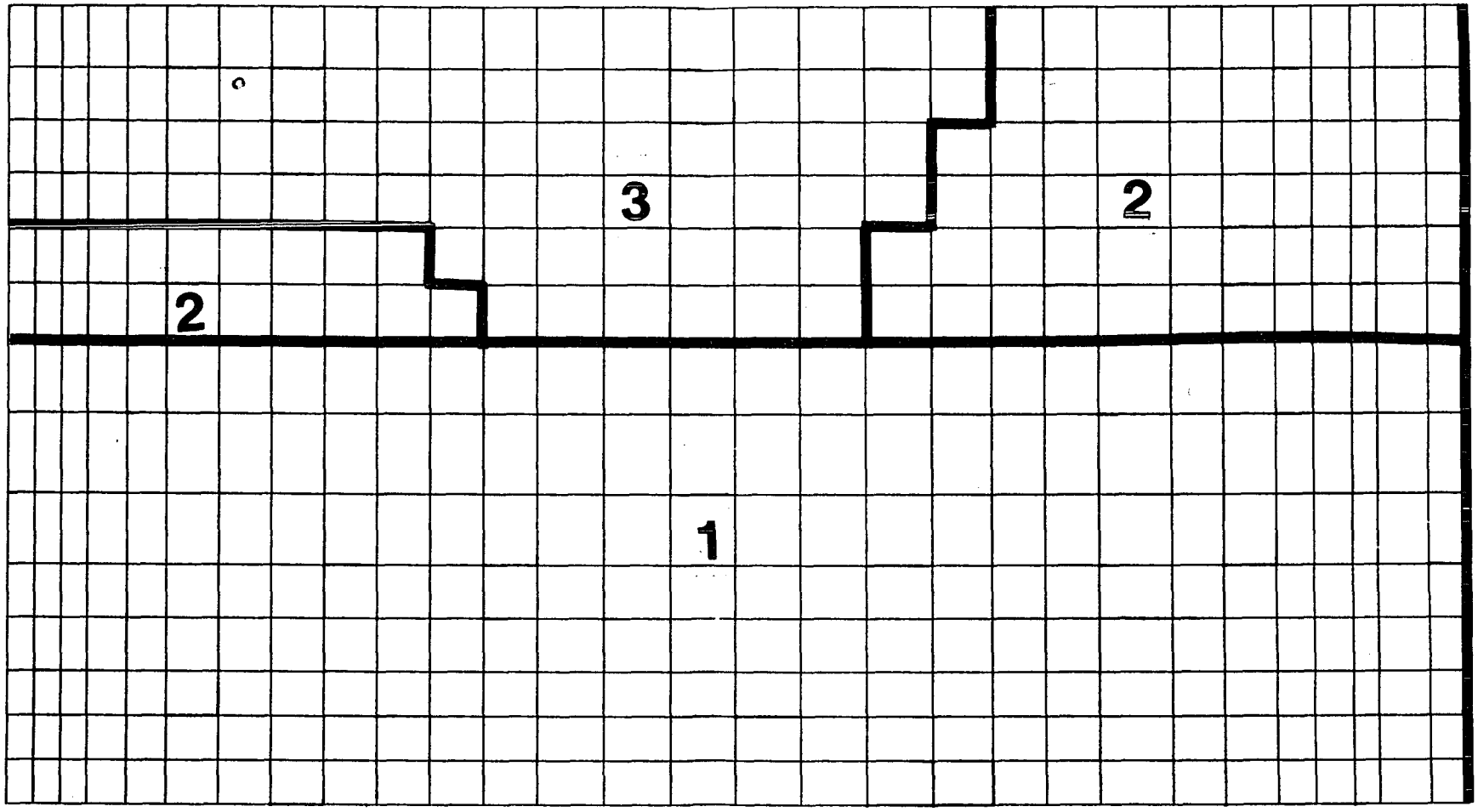

Y =

0.00	25.00	50.00	75.00	105.00	135.00	175.00	220.00
260.00	292.50	325.00	355.00	385.00	415.00	450.00	

PLANE 10

406 elements/slice
450 nodes/slice

X =

0.00	1000.00	2000.00	3000.00	4500.00	6000.00	8000.00	10000.00
12000.00	14000.00	16000.00	18000.00	20000.00	22500.00	25000.00	27500.00
30000.00	32500.00	35000.00	37250.00	39250.00	41250.00	44000.00	46000.00
48000.00	49500.00	51000.00	52000.00	53970.00	55440.00		

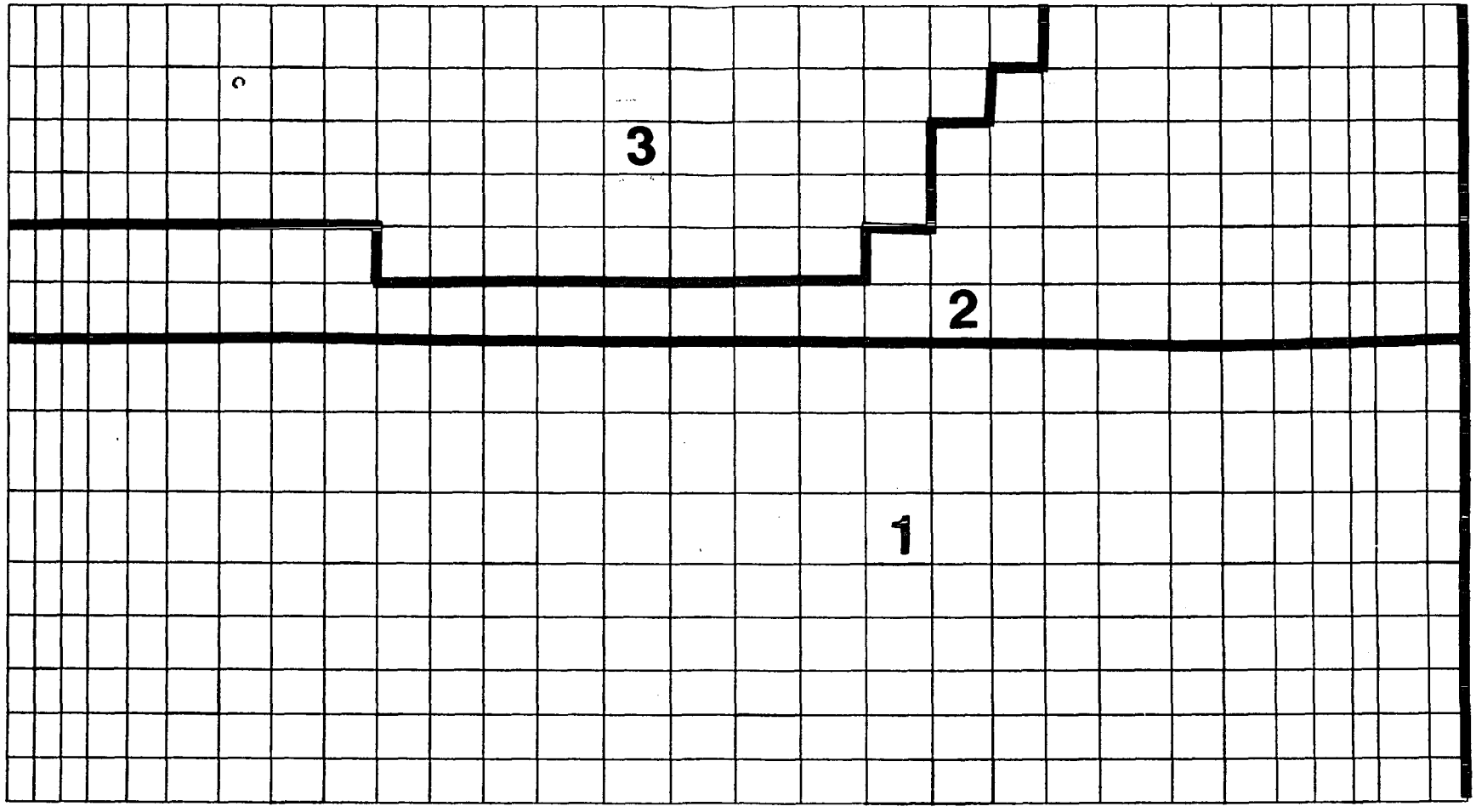

Y =

0.00	25.00	50.00	75.00	105.00	135.00	175.00	220.00
260.00	292.50	325.00	355.00	385.00	415.00	450.00	

PLANE 11

X = 0.00 1000.00 2000.00 3000.00 4500.00 6000.00 8000.00 10000.00
12000.00 14000.00 16000.00 18000.00 20000.00 22500.00 25000.00 27500.00
30000.00 32500.00 35000.00 37250.00 39250.00 41250.00 44000.00 46000.00
48000.00 49500.00 51000.00 52000.00 53970.00 55440.00

406 elements/slice
450 nodes/slice

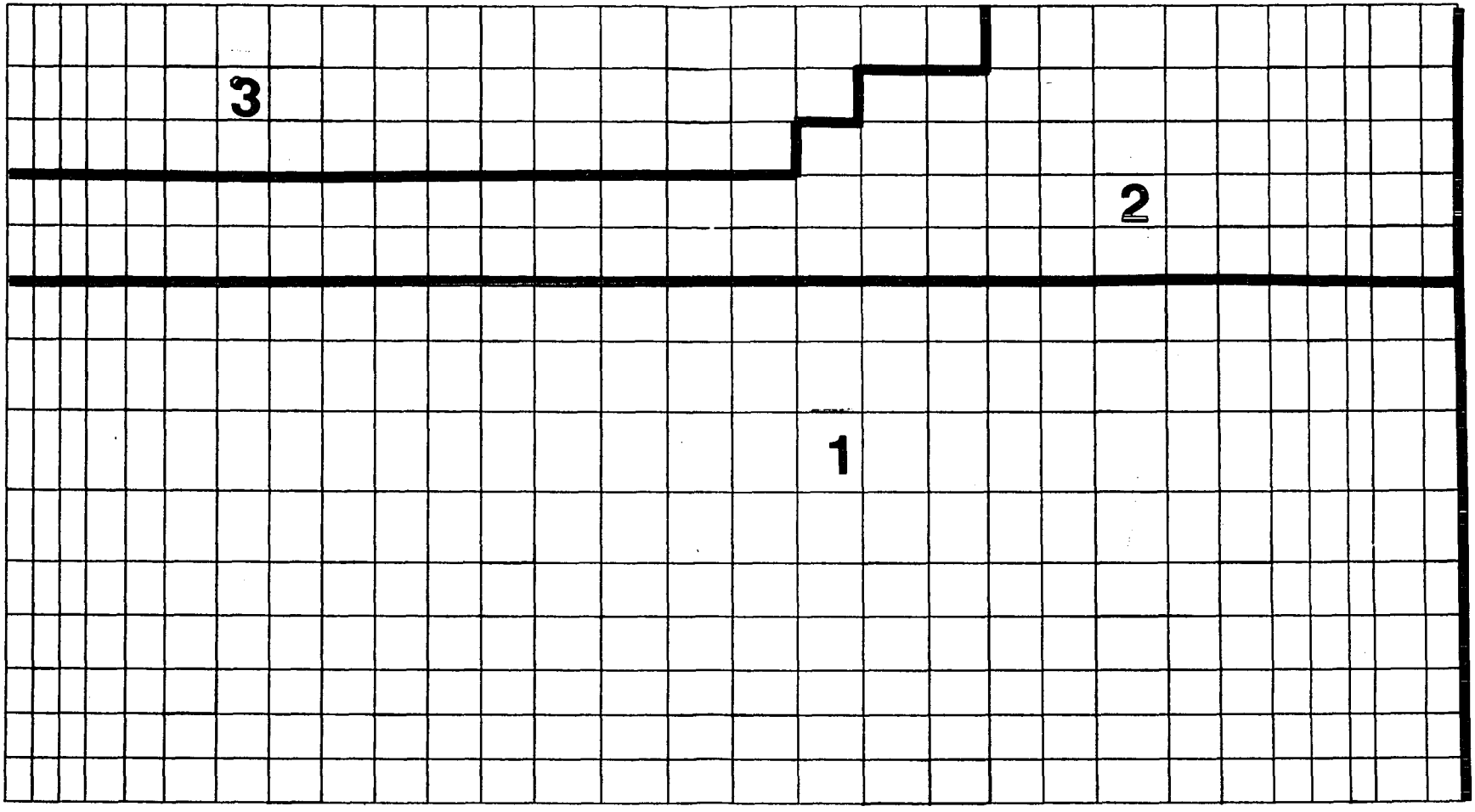

Y = 0.00 25.00 50.00 75.00 105.00 135.00 175.00 220.00
260.00 292.50 325.00 355.00 385.00 415.00 450.00

PLANE 12

406 elements/slice
450 nodes/slice

X =

0.00	1000.00	2000.00	3000.00	4500.00	6000.00	8000.00	10000.00
12000.00	14000.00	16000.00	18000.00	20000.00	22500.00	25000.00	27500.00
30000.00	32500.00	35000.00	37250.00	39250.00	41250.00	44000.00	46000.00
48000.00	49500.00	51000.00	52000.00	53970.00	55440.00		

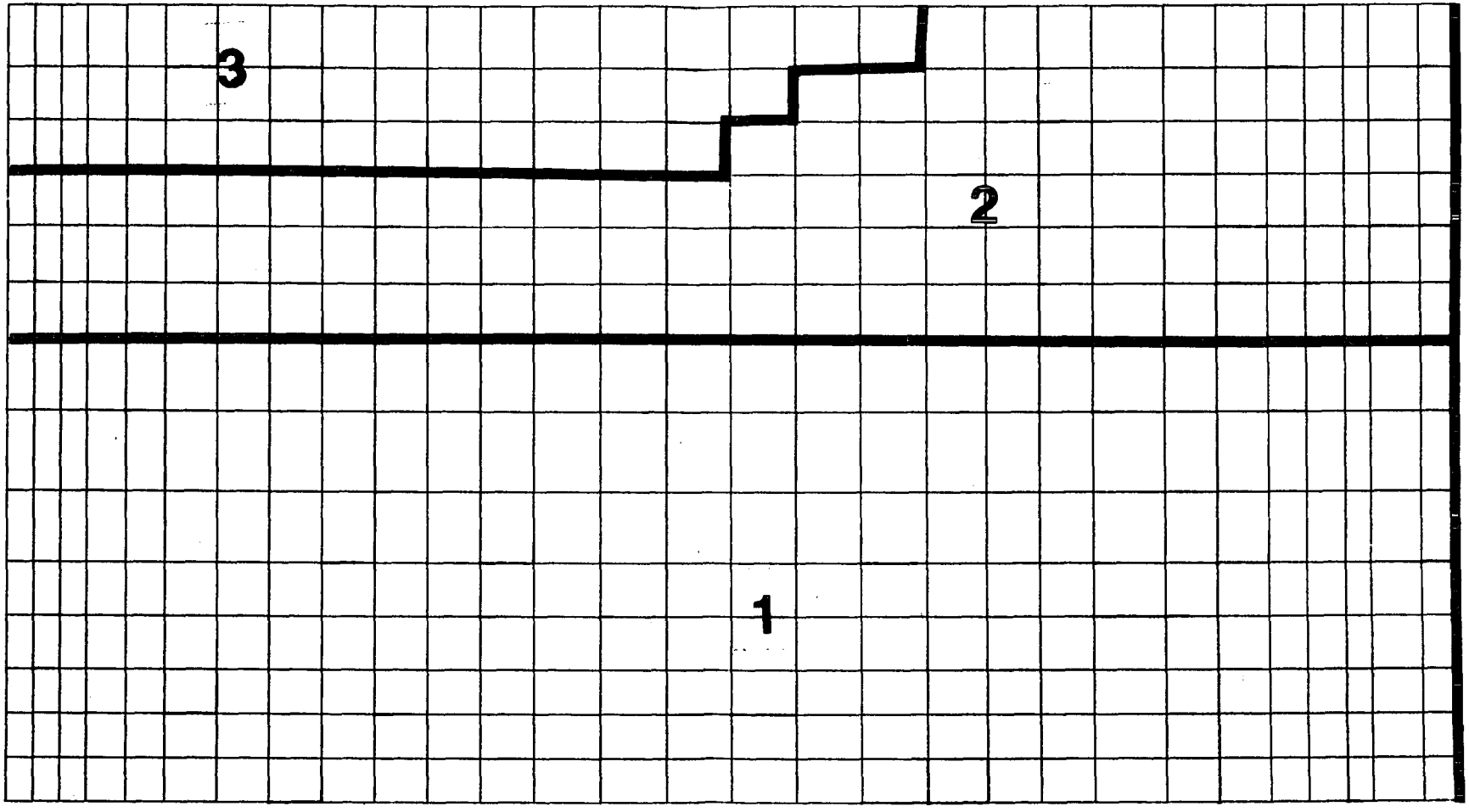

Y =

0.00	25.00	50.00	75.00	105.00	135.00	175.00	220.00
260.00	292.50	325.00	355.00	385.00	415.00	450.00	

PLANE 13

406 elements/slice
450 nodes/slice

X = 0.00 1000.00 2000.00 3000.00 4500.00 6000.00 8000.00 10000.00
12000.00 14000.00 16000.00 18000.00 20000.00 22500.00 25000.00 27500.00
30000.00 32500.00 35000.00 37250.00 39250.00 41250.00 44000.00 46000.00
48000.00 49500.00 51000.00 52000.00 53970.00 55440.00

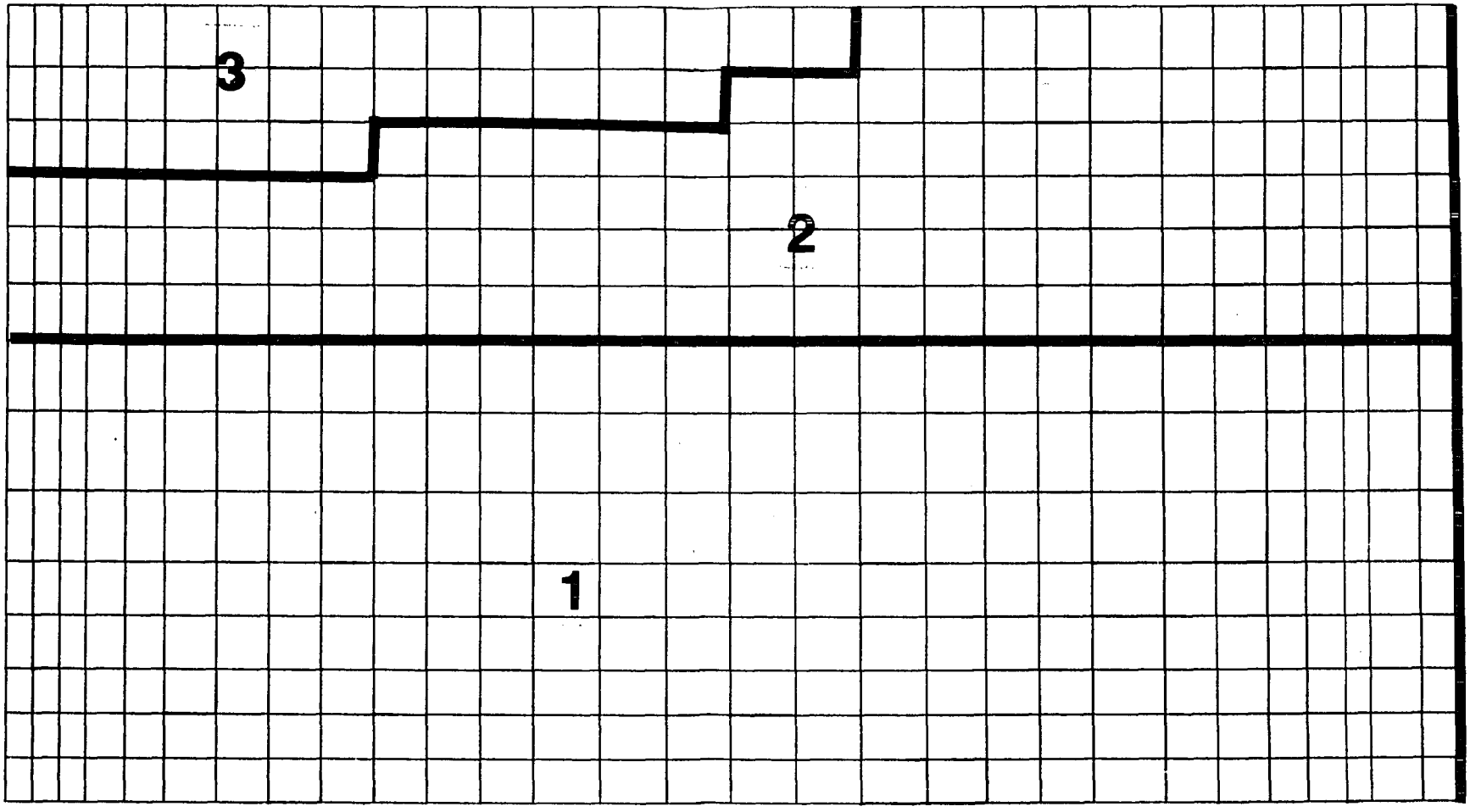

Y = 0.00 25.00 50.00 75.00 105.00 135.00 175.00 220.00
260.00 292.50 325.00 355.00 385.00 415.00 450.00

PLANE 14, 15, and 16

406 elements/slice
450 nodes/slice

X = 0.00 1000.00 2000.00 3000.00 4500.00 6000.00 8000.00 10000.00
12000.00 14000.00 16000.00 18000.00 20000.00 22500.00 25000.00 27500.00
30000.00 32500.00 35000.00 37250.00 39250.00 41250.00 44000.00 46000.00
48000.00 49500.00 51000.00 52000.00 53970.00 55440.00

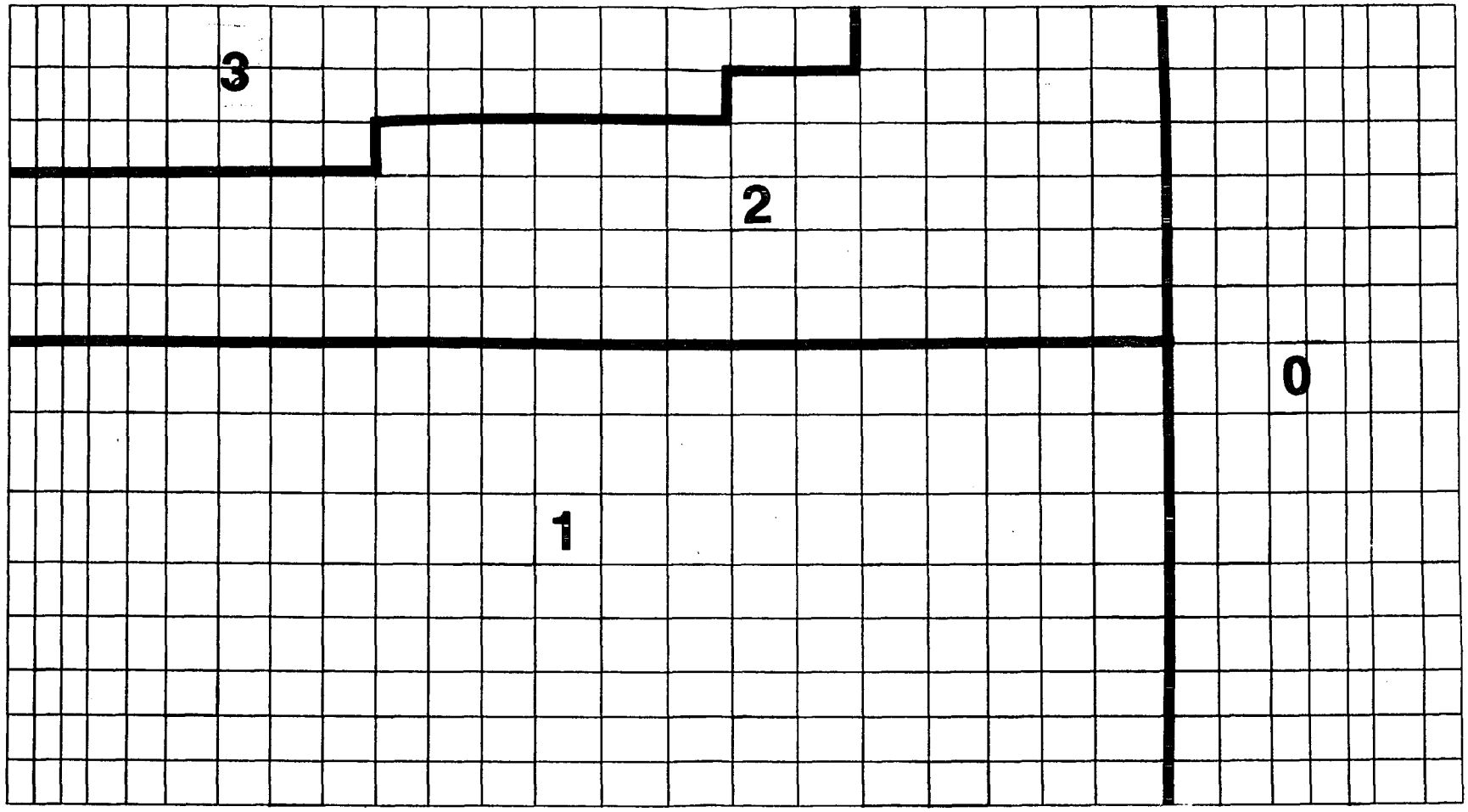

Y = 0.00 25.00 50.00 75.00 105.00 135.00 175.00 220.00
260.00 292.50 325.00 355.00 385.00 415.00 450.00

PLANE 17

406 elements/slice
450 nodes/slice

X = 0.00 1000.00 2000.00 3000.00 4500.00 6000.00 8000.00 10000.00
12000.00 14000.00 16000.00 18000.00 20000.00 22500.00 25000.00 27500.00
30000.00 32500.00 35000.00 37250.00 39250.00 41250.00 44000.00 46000.00
48000.00 49500.00 51000.00 52000.00 53970.00 55440.00

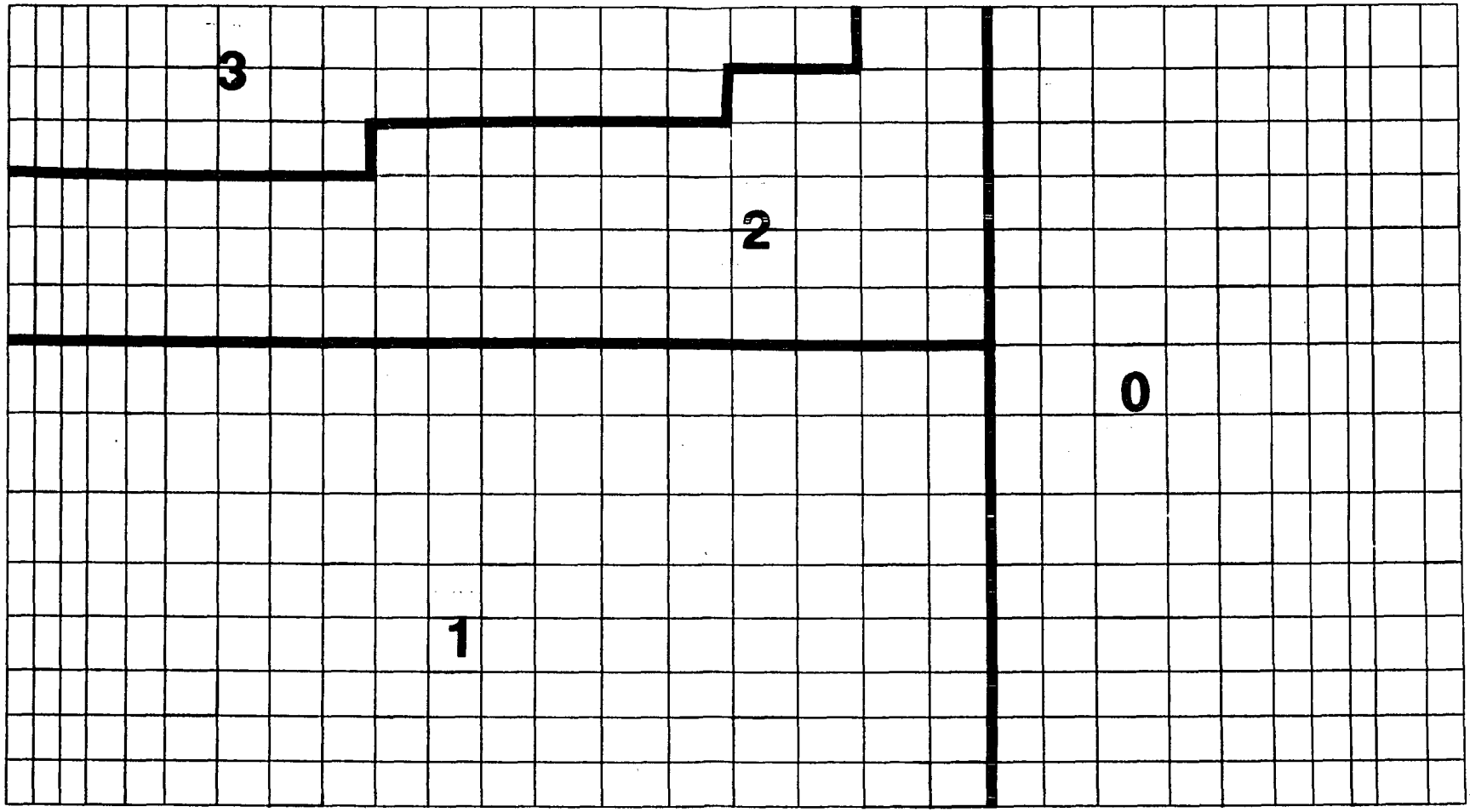

Y = 0.00 25.00 50.00 75.00 105.00 135.00 175.00 220.00
200.00 292.50 325.00 355.00 385.00 415.00 450.00

PLANE 18 and 19